# Keeyask Generation Project

## Physical Environment Monitoring Plan

# Physical Environment Monitoring Report

**PEMP-2023-01**

ᑮᔮᐢᐠ
KEEYASK

Manitoba Environment and Climate Client File 5550.00
Manitoba Environment Act Licence No. 3107

**2022 - 2023**

# KEEYASK GENERATION PROJECT

## PHYSICAL ENVIRONMENT MONITORING PLAN

REPORT #PEMP-2023-01

## 2022-2023 PHYSICAL ENVIRONMENT MONITORING REPORT: YEAR 2 OPERATION

Prepared by

Manitoba Hydro

June 2023

This report should be cited as follows:

Manitoba Hydro, 2023. 2022-2023 Physical Environment Monitoring Report: Year 2 Operation. Keeyask Generation Project Physical Environment Monitoring Plan Report #PEMP-2023-01. June 2023.

# SUMMARY

## Background

The Keeyask Generation Project (the Project) involves the construction and operation of the Keeyask Generating Station (GS) on the Nelson River at the former location of Gull Rapids and managing Gull Lake as a reservoir. To obtain a Manitoba Environment Act licence to construct the GS, and before construction began in July 2014, the Keeyask Hydropower Limited Partnership (KHLP) prepared a plan to monitor the effects of the Project on the physical environment. Monitoring results will help the KHLP, government regulators, members of the partner First Nations communities, and the general public understand how GS construction and operation affects the physical environment. Monitoring will help determine if the actual effects are consistent with predicted effects reported in the Project's environmental impact statement (EIS).

The Keeyask Physical Environment Monitoring Plan (PEMP) discusses planned monitoring during construction and operation of the Project, which includes monitoring of water and ice regimes, shoreline erosion, sedimentation, debris, and emission of greenhouse gases from the reservoir. This report describes the physical environment monitoring activities and results for the 2022/23 monitoring period.

## Water and Ice Regime

The water and ice monitoring parameters include water levels, water depth, water velocity, and ice cover. After receiving approval for the Project in the summer of 2014, six automated, continuous water level gauges were installed on the Nelson River between Clark Lake and Gull Rapids to monitor water levels during the construction of the Project.

During the reporting monitoring period, Nelson River flows gradually increased from January to May 2022, steadily rising from low flow conditions that existed in 2021, going from about 2,200 $m^3$/s in January to 3,000 $m^3$/s in early May. Flows then increased rapidly to about 6,000 $m^3$/s by the end of June due to wet conditions in the Nelson River basin and large flows coming out of Lake Winnipeg. Record daily high flows of about 6,000-6,500 $m^3$/s occurred much of the time from late June to mid-August and remained above 6,000 $m^3$/s, between the 95$^{th}$-100$^{th}$ percentile high flow, until about the middle of October. Flow decreased steadily in late fall to about 4,000-4,500 from mid-November to early March 2023, remaining in the high flow range near the 90$^{th}$ percentile. Flow dropped from about 4,000 $m^3$/s from March to the end into April before starting to rise again due to spring melt.

The open water operating range for the reservoir on Gull Lake is between 158 and 159 m asl. In the 2022/23 monitoring period water levels were held at or near 159 m on Gull Lake most of the time due to high flow conditions. In 2021, open-water levels were relatively flat from Gull Lake to Birthday Rapids due to low flow conditions, with levels flat at about 159 m between Gull Lake and Birthday Rapids and only about 1-1.5 m difference between Gull Lake and the gauge 1 km upstream of Birthday Rapids. Conditions were markedly different in 2022, with the water levels just below Birthday Rapids 1.5 m higher than Gull Lake while the level at the gauge 1 km upstream of the rapids was 3.5 m higher than Gull Lake.

In winter, ice effects increased water levels on Split and Clark lakes by about 0.6-0.7 m, which is a typical increase in winter prior to the Keeyask Project (KHLP 2012b). In addition to an increase at the start of winter, levels on Split and Clark lakes and just downstream rose during a cold period in February 2023. While Split Lake rose about 0.1-0.15 m at the time it is not evident that the increase was due to Keeyask GS effects on the ice regime. The cold conditions occurring at the time would be likely to cause increased ice constriction at both the Split Lake and Clark Lake outlets that would cause levels on these lakes to rise. During this cold spell the level on Split Lake increased to about the peak water level that occurred about a month earlier in January.


**Downstream of Clark Lake**

March 22, 2023

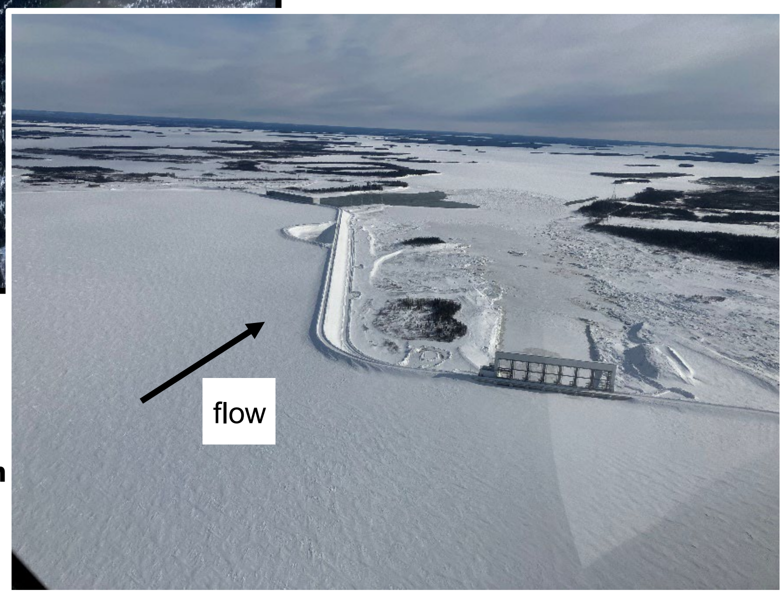


**Keeyask Dam looking downstream**

Ice monitoring is done using satellite imagery and photographs taken along the length of the study area during monthly field trips. Gull Lake developed an ice cover between November 7-11 and advanced to Birthday Rapids by December 4. Ice cover growth stalled at Birthday Rapids for a couple of months due to high flow conditions before cold weather conditions allowed it to advance through the rapids in early February. The ice cover ultimately advanced up to about 6.5 km upstream of Birthday Rapids, similar to previous years. The ice cover remained relatively intact until early May 2023 but was mostly gone by the third week of May.

Ice cover thickness was monitored at 5 locations upstream of the Keeyask GS and two downstream to verify the prediction that with the Project a smoother and thinner ice cover would form on the reservoir upstream and at the entrance to Stephens Lake, particularly where rough and thick hanging ice dams previously formed. Monitoring found greater ice thicknesses in March than April, ranging from about 1.25-1.40 m thick on Gull Lake and about 1.10-1.22 m downstream of the GS. These thicknesses were greater than the maximum thickness of about 0.7-0.9 m observed in 2022. However, it is much thinner in areas where hanging ice dams several metres thick formed before the Project at the upstream end of Gull Lake and the entrance to Stephens Lake.

Water velocity monitoring was also done at more than 54 transect locations from upstream of Birthday Rapids to the entrance of Stephens Lake just downstream of the GS. The Keeyask PEMP committed to velocity monitoring under low, average, and high flow conditions. The monitoring in 2022 obtained velocities under high flow conditions while the 2021 monitoring captured low flow conditions, which leaves average conditions to be measured. Monitoring results have shown velocities to be generally consistent with expectations based on hydraulic modeling.

### Sedimentation

Sedimentation monitoring includes studying how sediment is carried (sediment transport) in the water and where it is deposited. It involves collecting water samples to measure the amount of sediment suspended in the water (done in a laboratory), using electronic devices that continuously measure turbidity (i.e., the murkiness of the water) over time and by taking readings with a hand-held meter when visiting monitoring sites. Sediment traps are used to collect sediment from the water over time to monitor the potential for sediment to settle out (deposit) near areas of potentially important sturgeon habitat.

**Collecting Water Samples for Sedimentation Monitoring**

Winter monitoring in 2021/22 included continuous turbidity monitoring at four sites from Clark Lake to just downstream of the Keeyask GS from January to April. Results showed levels in Gull Lake and just downstream were relatively consistent between the sites and about 1-2 mg/l lower than the upstream Clark Lake sites. As in previous years, turbidity was higher in January and steadily decreased until April. Average winter turbidity was within the range observed the previous 7 winter seasons, but slightly higher than in the past several winter seasons, potentially due to higher flows. Total suspended sediment (TSS) samples were collected approximately monthly at the continuous turbidity sites and results were comparable with the 5 previous winter seasons, with a low average TSS of about 3 mg/l. Turbidity was also measured at 12 backbay sites in January and April and was generally lower than along the river main stem but showed a similar decrease between early and late winter.

In the 2022 summer period (Jun–Oct), turbidity was continuously monitored at 5 mainstem sites between Clark Lake and the Kettle GS as well as six backbay sites, including one on Stephens Lake. The four sites between Clark Lake to just downstream of Keeyask GS had similar results with little difference between them. The site near Kettle GS generally had lower turbidity, which is consistent with results seen in previous years and prior to construction due to deposition within Stephens Lake. Despite 2022 having higher flow than previous years of monitoring, the average continuous turbidity on the mainstem was lower than in 2021 under very low flows, and lower than any previous year of monitoring. Turbidity in Keeyask backbays was variable, but typically lower than along the mainstem, indicating very low levels of suspended sediment in these bays, as observed in 2021. The Stephens Lake backbay site had somewhat higher turbidity than Keeyask backbays, which is consistent with what has been seen in the past.

Four times in summer 2021, water samples were collected at mainstem and backbay sites to test for TSS concentrations. TSS was low overall and had a relatively small range of variation, at both mainstem and backbay sites. Average concentrations were somewhat higher in June and August, and lower in July and September, but overall, there was only about 2 mg/l difference between the high and low monthly averages. The 2022 summer average TSS concentration was about 4 mg/l under high flow conditions at the mainstem sites, which is the same as observed during low flow conditions in 2021, with the 2022 results displaying a smaller range of variability. TSS concentrations displayed little change from Clark Lake upstream to just downstream of the Keeyask GS, indicating no increase due to erosion of Keeyask shorelines or decrease due to deposition as water passed through the reservoir. The average mainstem concentrations are significantly lower than the overall average of about 15 mg/l prior to construction and 13 mg/l during construction. Because the very low TSS concentrations in 2021 and 2022 are observed at the Clark Lake monitoring site, the processes causing low TSS are occurring upstream limit of the Keeyask open water hydraulic zone of influence (which is located a few kilometres downstream of Clark Lake), which indicates that the processes causing low TSS are not a result of the Keeyask Project.

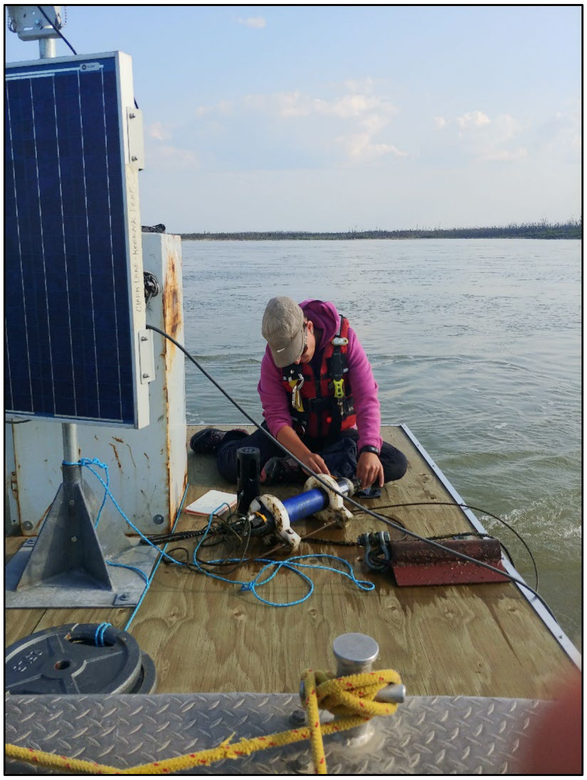

**Continuous Turbidity Monitoring Equipment – Setting Up a Turbidity Sensor**

### Dissolved Oxygen (DO)

Dissolved Oxygen (DO) monitoring was performed at four mainstem sites and 48 backbay locations in winter 2021/22 (Jan-Apr). Results showed DO to be at or near the saturation concentration (i.e., the maximum DO the water will usually hold depending on water temperature) at mainstem sites, including immediately downstream of the GS. About 70% of backbay locations had high DO concentrations, from the top to the bottom of the water. Sites where DO was low were generally shallower and further removed from the mainstem. These results were generally expected based on pre-Project modeling.

DO monitoring in the 2022 open water season included continuous monitoring at five mainstem sites and in six backbays, two mainstem sites and one backbay site were located on Stephens Lake. The backbay sites used two DO sensors with one near the water surface and one near the bottom of the water to check for differences between the top and bottom. In the backbays, bottom DO was at moderate to low concentrations more often than was predicted. There may be a couple of reasons for this result including less mixing than anticipated due to peat rising to the surface; less mixing of the water by wind: and greater decay of flooded peat and vegetation than anticipated (decay uses oxygen from the water). It was found that there was lower turbidity than expected in the backbays, which means more light was able to get into the water which could result in greater decay and removal of more DO from the water than expected. At all mainstem sites, DO was found to be at or near 100% saturation. The results also showed that increases in the amount of water going through the spillway caused when DO to increase above the saturation concentration immediately downstream of the GS. DO was not above saturation when all flow was through the powerhouse, which is what would generally be expected.

DO monitoring was also done using a probe to measure DO concentration on site at several depths between the surface and bottom of the water at 11 mainstem sites and 12 backbays sites. Up to six separate locations were sampled at each site. The on-site measurements, which were done up to four times in summer 2022, showed high DO concentrations along the mainstem, as observed with the continuous monitoring. Most of the backbay locations, about 73%, had high DO concentrations between the surface and bottom, while about 9% had high to moderate DO, 17% had high to low DO, and 2% (one location) had low DO through the entire depth. As with winter DO sampling, locations with lower DO tended to be shallower and further removed from the main flow. These results are generally consistent with expectations described in the EIS.

### Debris

In summer 2022, the woody debris management program consisted of two parts, the first being two boat patrols on the reservoir, and the second being a 20-person work crew on shore. As in 2021, the large work crew focussed its clean-up efforts in the vicinity of the Keeyask GS and the north and south dikes where quantities of woody debris accumulate on an ongoing basis. The crews removed debris near the powerhouse and upstream on the north dike that affected water flow into the powerhouse. It also worked along a few kilometres of the south dike, west of the spillway. Debris collected in 2021 that was stockpiled beside the south dike and left to dry was burned in May 2022, and debris collected in 2022 was stockpiled in the same location where it could dry before being burned in 2023.

**Woody Debris Adjacent to the South Dike**

Unlike 2021 when the boat patrols had to shuttle the work crew between the Split Lake community and Keeyask each day, the two boat patrols could focus its effort on debris management on the waterway in 2022. Patrols were conducted daily during the summer, weather permitting, and the crews removed floating woody debris each day they were out on the water. The crews also marked hazards like newly formed reefs, spoke with resource users on the waterway, and assisted waterway users when required (e.g., boat engine problems).

### Reservoir Greenhouse Gas

Reservoir greenhouse gas emissions (GHG) were monitored after reservoir impoundment from 2021 to 2022, during the water-up period in 2020, and during the pre-impoundment periods of 2009-2010, 2012 to 2014, and 2017 to 2019. GHG emissions are being measured by above ground towers and underwater sensors that continuously record carbon dioxide ($CO_2$) and methane ($CH_4$). Water samples are also taken to give point-in-time measurements of GHGs. Monitoring in the last year indicates that GHG emissions remain elevated after flooding compared to pre-impoundment levels, as predicted in the EIS. A large portion of the post-flood GHG emissions are coming from the newly flooded, shallow regions of the reservoir. The organic material in these areas is decomposing and releasing $CO_2$ and $CH_4$. The amount of emissions released from the shallow waters of the reservoir are similar to those of northern beaver ponds. As planned, monitoring will continue to be conducted to observe changes in GHG emissions over time.

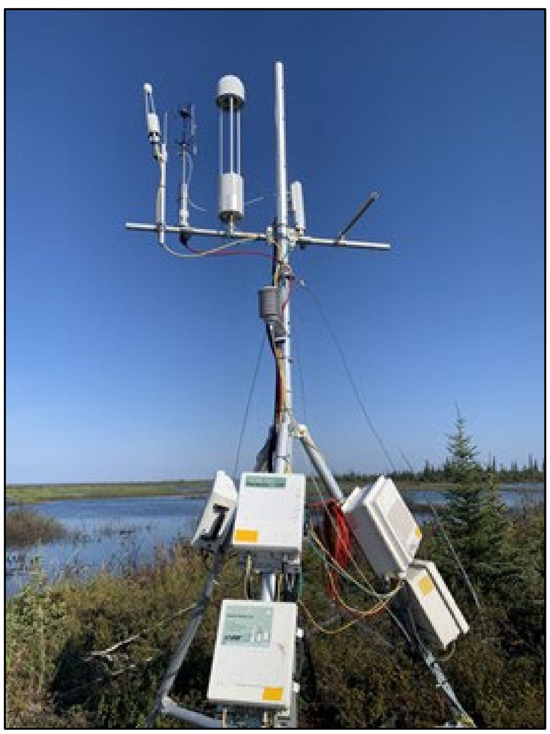

**GHG Monitoring Tower**

# ACKNOWLEDGEMENTS

We would like to thank Jo-Anne Smith and Terrence Atkinson from Manitoba Hydro for logistical support that made these monitoring studies possible.

# STUDY TEAM

**Field Team and Support**

Andrew Benger (Manitoba Hydro)

Darrel Brunet (Manitoba Hydro)

Keith Dobson (Manitoba Hydro)

Leslie Flett (Tataskweyak Cree Nation)

Leslie Gbeve (Manitoba Hydro)

Paiten Harapiak (Manitoba Hydro)

Leslie Klaassen (Manitoba Hydro)

Joseph Langan (Manitoba Hydro)

Jarod Morrison (Manitoba Hydro)

Greg Petryk (Manitoba Hydro)

Justin Pollick (Manitoba Hydro)

Tim Papakyriakou (University of Manitoba)

Ashley Soloway (University of Manitoba)

Daniel Gedig (University of Manitoba)

Bailey Baldwin (Manitoba Hydro)

Nick Decker (University of Manitoba)

Keilan Ledger (University of Manitoba)

Randy Flett (Manitoba Hydro)

Eugene Kitchekeesik (Manitoba Hydro)

Jack Kitchekeesik (Manitoba Hydro)

Bob Gill (Manitoba Hydro)

**Data Analysis, Report Preparation, and Report Review**

Wil DeWit (Manitoba Hydro)

Bob Gill (Manitoba Hydro)

Martin Hunt (Manitoba Hydro)

Danielle Kerr (Manitoba Hydro)

Michaelin Lower (Manitoba Hydro)

Tim Papakyriakou (University of Manitoba)

Russell Schmidt (Manitoba Hydro)

Ashley Soloway (University of Manitoba)

Daniel Gedig (University of Manitoba)

Marc Totte (Manitoba Hydro)

# TABLE OF CONTENTS

# LIST OF TABLES

# LIST OF FIGURES

# LIST OF MAPS



# LIST OF PHOTOS



# LIST OF APPENDICES

# 1.0 INTRODUCTION

Construction of the Keeyask Generation Project (the Project), a 695-megawatt hydroelectric generating station (GS) and associated facilities, began in July 2014. The Project is located at Gull Rapids on the lower Nelson River in northern Manitoba where Gull Lake flows into Stephens Lake, 35 km upstream of the existing Kettle GS.

The *Keeyask Generation Project: Response to EIS Guidelines* (EIS), completed in June 2012, provides a summary of predicted effects and planned mitigation for the Project (KHLP 2012a). Technical supporting information for the physical environment and a summary of proposed monitoring and follow-up programs are provided in the *Keeyask Generation Project Environmental Impact Statement: Physical Environment Supporting Volume* (PESV; KHLP 2012b). As part of the licensing process for the Project, the Keeyask Physical Environment Monitoring Plan (PEMP) was developed detailing the monitoring activities for various components of the physical environment. The PEMP was finalized in 2015 following regulatory review and approval (KHLP 2015a).

This report generally describes the physical environment monitoring performed from April 2021 to March 2022, the first full monitoring season after the reservoir was impounded by raising water levels to the full supply level of 159 m ASL in September 2020. Although construction activities continued in 2021/22 and not all generating units were yet in operation, this period is considered the first year of operation because it is the first season when the reservoir water level was controlled within its licensed operating range of 158-159 m ASL. Note that where information is not yet available or requires further review at the time of the annual report the information will be considered in the following year's report.

The physical environment is defined as the physical and chemical make-up of an ecosystem and describes the area where things live and includes the air, water, and land within the ecosystem. Monitoring and follow-up activities focus on effects to key components of the physical environment to:

- Determine if EIS predictions of Project effects on the physical environment are correct and to identify unanticipated effects.
- Support other monitoring programs (e.g., aquatic and terrestrial) that will monitor Project effects and determine the effectiveness of mitigation and offsetting measures.

The environmental components that are monitored under the PEMP include the following:

- surface water (level/depth) and ice-regimes,
- shoreline erosion and reservoir expansion,
- sedimentation (related to water quality, sediment transport and deposition),
- greenhouse gas,
- woody debris,

- surface water temperature and dissolved oxygen (related to water quality and aquatic habitat), and
- total dissolved gas pressure.

In 2022/23, physical environment monitoring included surface water and ice regime, sedimentation, dissolved oxygen, greenhouse gases, and woody debris monitoring. Monitoring for turbidity, suspended sediment, and water temperature and dissolved oxygen occurred in the 2022/23 winter period and the results will be provided in next years report. Shoreline erosion and reservoir expansion analyses using aerial imagery to map shoreline locations are to be completed based on imagery obtained in 2021. Total dissolved gas pressure monitoring will begin after the powerhouse is fully operating with all 7 turbines in service. The PEMP provides a schedule of the physical environment monitoring activities planned during the construction and operation periods of the Project. The study area generally extends from Clark Lake into Stephens Lake as far as bout 30 km downstream near the Kettle Generating Station as shown on Map 1 (detailed site maps are provided in Appendix 1).

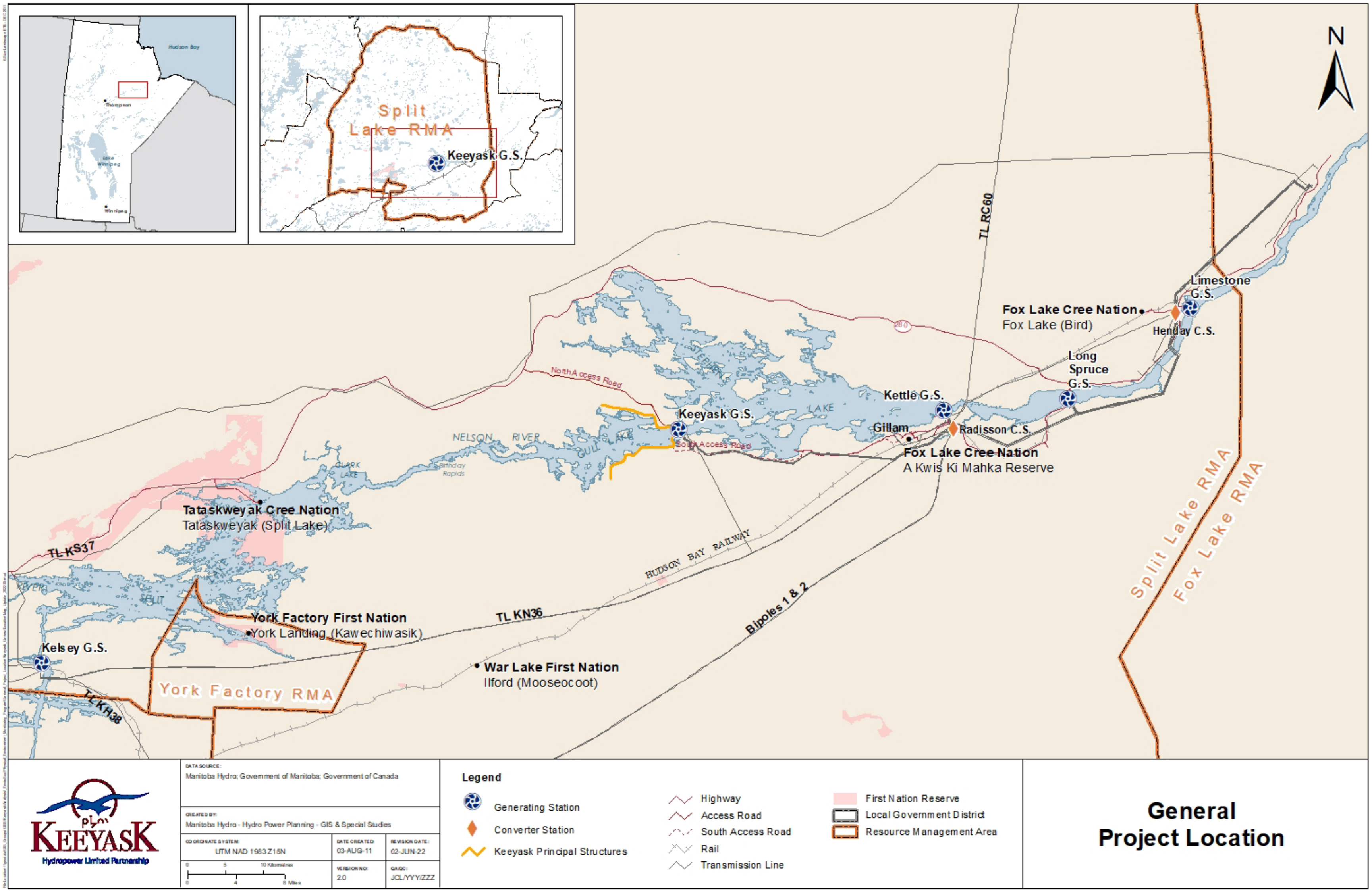


**Map 1:** **General Project location and study area**

# 2.0 SURFACE WATER AND ICE REGIMES

The water regime and ice parameters include water levels, water depth, river and lake-bottom elevation, water velocity, and ice cover. The largest changes to water and ice regimes are expected to occur once the reservoir has been impounded and include increases in water levels, reduction of velocities and development of a smoother ice cover. During the construction period, water levels are expected to increase from the construction of cofferdams used to isolate construction areas and an ice cover is expected to develop earlier from the installation of an ice boom.

The objectives of the water and ice regime monitoring include:

- determining water level regime and verifying expected changes in water levels resulting from the Project;
- confirming that there are no unanticipated Project effects on Split Lake water levels;
- determining water depth/bottom elevation and velocity information to support monitoring being performed under the Aquatic Effects Monitoring Plan (AEMP; KHLP 2015b);
- measuring ice conditions to support understanding of winter water levels, which may be affected by ice processes; and
- confirming that future ice conditions during operation are consistent with predicted effects reported in the EIS.

## 2.1 NELSON RIVER FLOW CONDITIONS

Prior to the 2021-22 monitoring report, river inflow to Gull Lake was reported as the outflow from Split Lake, which is not affected by the Keeyask Project, where this flow was calculated based on upstream inputs (e.g., Kelsey GS discharge, Burntwood River flow, and Split Lake water level changes). Small streams that flow into the monitoring area between Clark Lake and Gull Rapids typically contribute less than 3% of the total flow (KHLP 2012b) and were not included in the calculated flow. However, since Keeyask began operation, data on discharges from the generating station and spillway combined with changes in Gull Lake water levels have been used to calculate the inflow to Gull Lake. These Keeyask inflows are used for the Keeyask operating period starting in 2022.

The historical daily flow records have been analyzed to characterize flow conditions since September 1, 1977 and represent regulated flow conditions since Lake Winnipeg Regulation and Churchill River Diversion began operating. Average seasonal flows are summarized in Table 1; the summer flows are taken as May through October and winter flows from November through April.

**Table 1: Split Lake seasonal discharges since start of Keeyask construction**

| Year /Season | Minimum Daily ($m^3/s$) | Mean Daily ($m^3/s$) | Maximum Daily ($m^3/s$) |
|---|---|---|---|
| 2014 Summer | 3438 | 5245 | 5907 |
| 2014/15 Winter | 3340 | 3865 | 5057 |
| 2015 Summer | 3277 | 3694 | 4282 |
| 2015/16 Winter | 3198 | 3745 | 4050 |
| 2016 Summer | 3194 | 40343 | 4748 |
| 2016/17 Winter | 3583 | 4366 | 5007 |
| 2017 Summer | 3082 | 4838 | 6594 |
| 2017/18 Winter | 2880 | 3396 | 4093 |
| 2018 Summer | 2508 | 3060 | 3608 |
| 2018/19 Winter | 2817 | 3227 | 3735 |
| 2019 Summer | 2614 | 3259 | 3665 |
| 2019/20 Winter | 3135 | 4051 | 4390 |
| 2020 Summer | 3350 | 4913 | 5944 |
| 2020/21 Winter | 3008 | 3516 | 4111 |
| 2021 Summer | 1820 | 2585 | 3675 |
| 2021/22 Winter | 1757 | 2307 | 2744 |
| 2022 Summer | 2895 | 5763 | 6608 |
| 2022/23 Winter | 3211 | 4048 | 5383 |

The seasonal mean daily discharge (Table 1) during the 2021/22 winter season the mean flow of 2,307 $m^3/s$ was the lowest since the start of construction while the 2022 summer flow of 5,763 $m^3/s$ was the highest since 2014 due to wet conditions in the Nelson River drainage basin. High flow conditions persisted into winter 2022/23. Keeyask inflows started out low in April 2022 following the dry year in 2021 (Figure 1). In May, the flows began to increase sharply and continued to rise to up to the peak summer flow of about 6,600 $m^3/s$ on August 9. Over the two months from June 18 to August 16, the flows in 2022 represented new historical maximums. Flows decreased gradually to about 6,000 $m^3/s$ by mid-October and then decreased rapidly to about 4,000 $m^3/s$ by mid-November. New record high flows occurred on more than half the days in October. After mid-November the flows were generally steadier between about 4,000 $m^3/s$ to 4300 $m^3/s$ before beginning to decrease closer to median flows in March 2023.

Flow through the powerhouse was generally between 3,000-4,000 $m^3/s$ most of the time in 2022/23 except at the start of the monitoring period when inflows were still low. Due to the high inflow conditions, the spillway was in operation most of the time, discharging between 2,000-3,000 $m^3/s$ over most of the open water season. Spillway flow decreased to generally less than 500 $m^3/s$ during the 2022/23 winter period due to reduce inflow conditions.

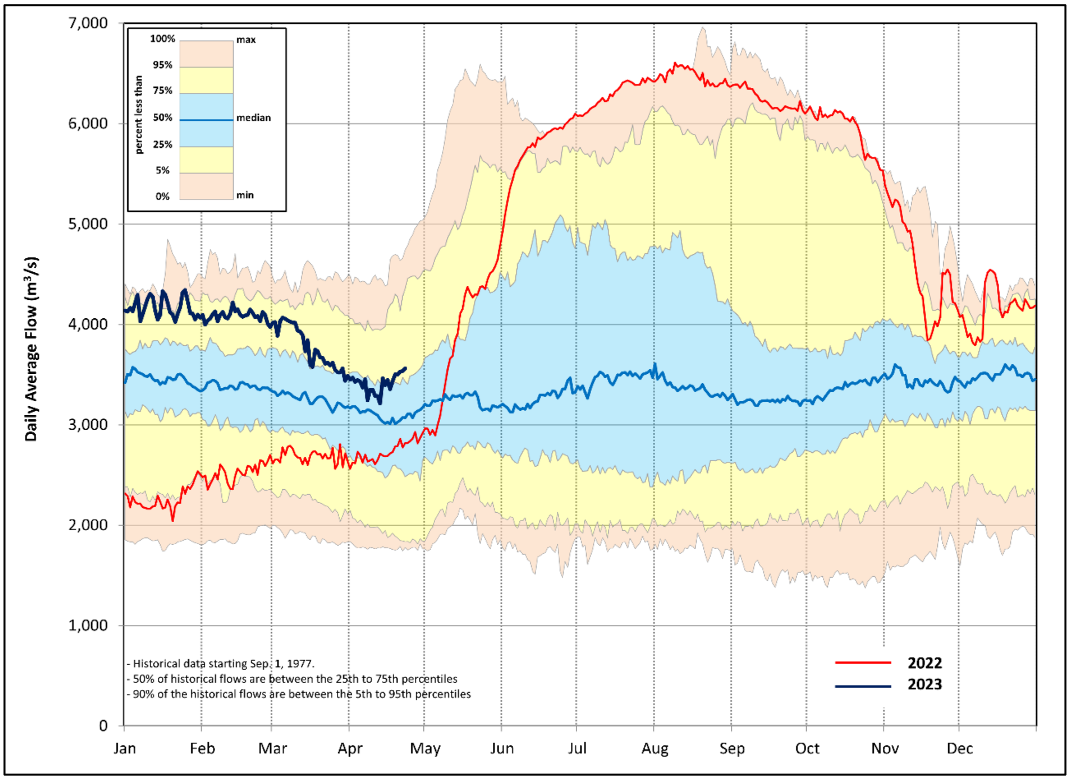


**Figure 1: 2022/2023 Keeyask Daily Average Inflow and Historical Statistics**

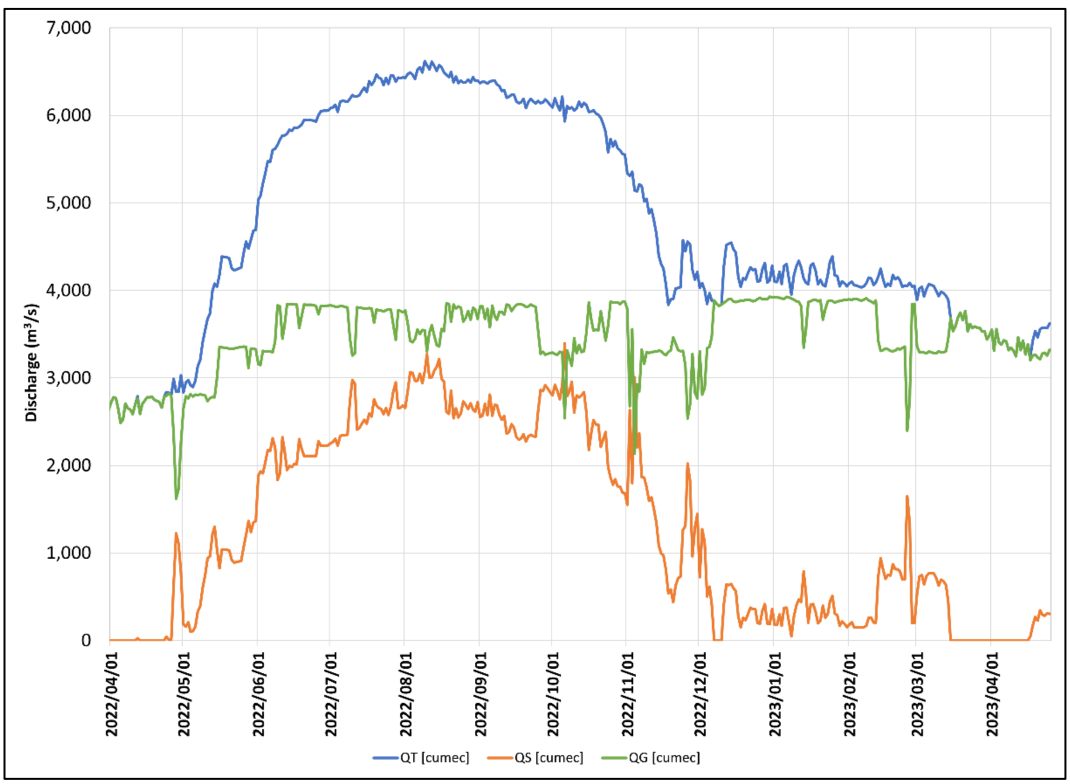


**Figure 2: 2022/2023 Keeyask Generating Station (GS) and Spillway Discharge**

## 2.2 OBSERVED WATER LEVELS

Water levels are monitored at six sites from Clark Lake to Gull Rapids (Table 2, Map 2). A typical water level gauge is shown in Photo 1. The two Clark Lake sites have been monitored regularly since 2003, while the Gull Lake gauge was installed at the start of construction in mid July 2014. The other three sites were installed after construction started, once the necessary permits and heritage surveys were complete, which were applied for and done after the Environment Act licence was received in early July 2014. The original gauge at the upstream end of Gull Lake (05UF749) was wrecked by ice and was discontinued in May 2016. The gauge was relocated about 3 km upstream to the mouth of Portage Creek and began operation in September 2016 (site 05UF587). In addition to data from the PEMP gauges, data is reported from the existing gauge on Split Lake at the community of Split Lake.

**Table 2: List of water level monitoring sites**

| Site ID | Name | Record | Notes |
|---|---|---|---|
| 05UF766 | Clark Lake | Oct. 2003 - present | 4 km above outlet |
| 05UF759 | downstream of Clark Lake | Dec. 2003 - present | 1.9 km below outlet |
| 05UF770 | upstream of Birthday Rapids | Oct. 2014 - present | 1.1 km above rapids |
| 05UF771 | downstream of Birthday Rapids | Oct. 2014 - present | 2.1 km below rapids |
| 05UF749 | upstream of Gull Lake | Oct. 2014 - May 2016 | 0.26 km above lake |
| 05UF587 | upstream of Gull Lake | Sep. 2016 - present | 3.0 km above lake |
| 05UF596 | Gull Lake | Jul. 2014 - present | 7 km above Gull Rapids |
| 05UF701 | Split Lake at Split Lake Community | Oct. 1997 - present | existing site |

**Photo 1: Water level gauging station in winter**

The 2022/23 monitoring period is the second year of Keeyask GS operation in which the levels on Gull Lake could be regulated within the operating range between 158 and 159 m asl. Through the entire period (Figure 3) water levels were held between 158.4 and 159.1 m on Gull Lake (station 05UF596).

In the late winter and spring of 2022 water levels were influenced by river ice. Even as flows increased, the levels generally decreased until the latter part May as ice effects diminished (Figure 3). Water levels then subsequently increased as flows increased to a peak of about 6,600 $m^3/s$ at the beginning of August. Water levels then began to decline as flows decreased more gradually up to mid-October and then more rapidly up to mid-November when ice began to affect levels.

Ice started forming in mid-November and water levels increased quickly at the gauge above Gull Lake and the two gauges at Birthday Rapids (Figure 3). While levels just upstream of Gull Lake peaked within about 10 days before dropping to lower levels the rest of the winter, the other upstream water level sites peaked much later in the season. The sites upstream of Birthday Rapids did not peak until after the ice front progressed through the rapids at the start of February.

After the site upstream of Birthday Rapids peaks on February 3, the levels at this location steadily decline even as flows remain relatively steady, likely due to reduced ice effects downstream (i.e., smoothing and/or thinning of the ice cover). Conversely, the levels downstream of Clark Lake continued to rise for another 3 weeks before peaking on February 23. The divergence between the gauge upstream of Birthday Rapids and the one downstream of Clark Lake suggests some constriction of the channel by ice between the two sites during this period. Levels on Clark Lake similarly peaked in late February. Water levels at the upstream sites decreased through March as the effects of ice diminish due to smoothing and thinning of the ice cover.

## 2.3 CLARK LAKE AND SPLIT LAKE WATER LEVELS

The levels on these two lakes show the same pattern of variation, differing by about 0.5-0.6 m in summer when flows were high, and about 0.4-0.5 m in winter when flow was lower (Figure 3). The water level data do not indicate a hydraulic influence of Keeyask on Split Lake during open water conditions.

In winter, ice effects typically increase water levels on Split and Clark lakes by about 0.6 m on average above open water levels (KHLP 2012b). Monitoring showed levels on these lakes increased about 0-6-0.7 m in the winter between the beginning of November and February under flows that varied about 300-400 $m^3/s$. The increase over winter is consistent with expectations and ice effects observed prior to Keeyask development. As discussed below (Section 0), levels below Clark Lake rose about 1 m during the first 3 weeks of February after the ice front moved through Birthday Rapids in response to cold weather and apparent ice accumulation between Clark Lake and Birthday Rapids. Split and Clark Lake levels also rose about 0.1 m at this time,

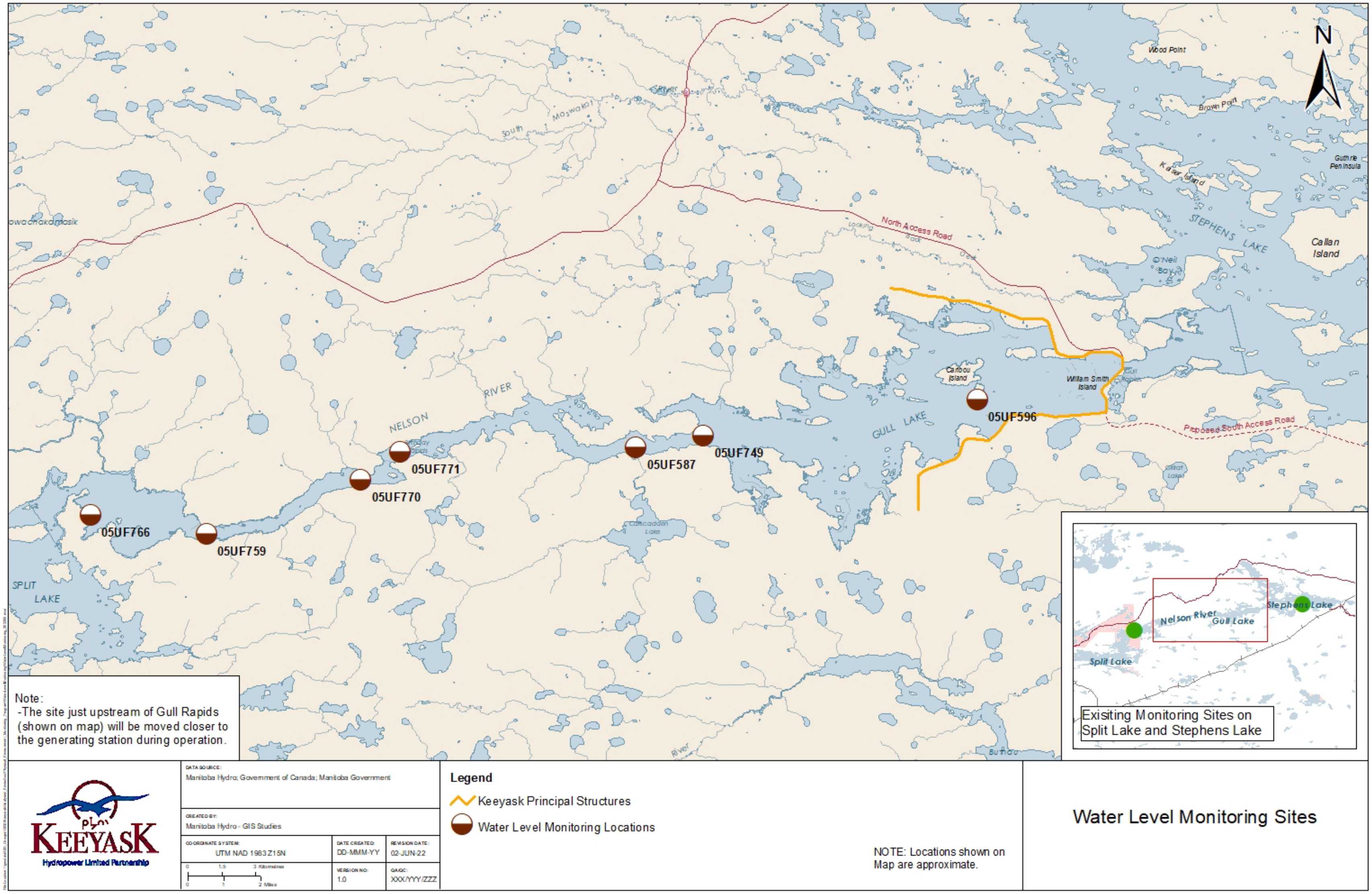


**Map 2:** **PEMP water level monitoring sites**

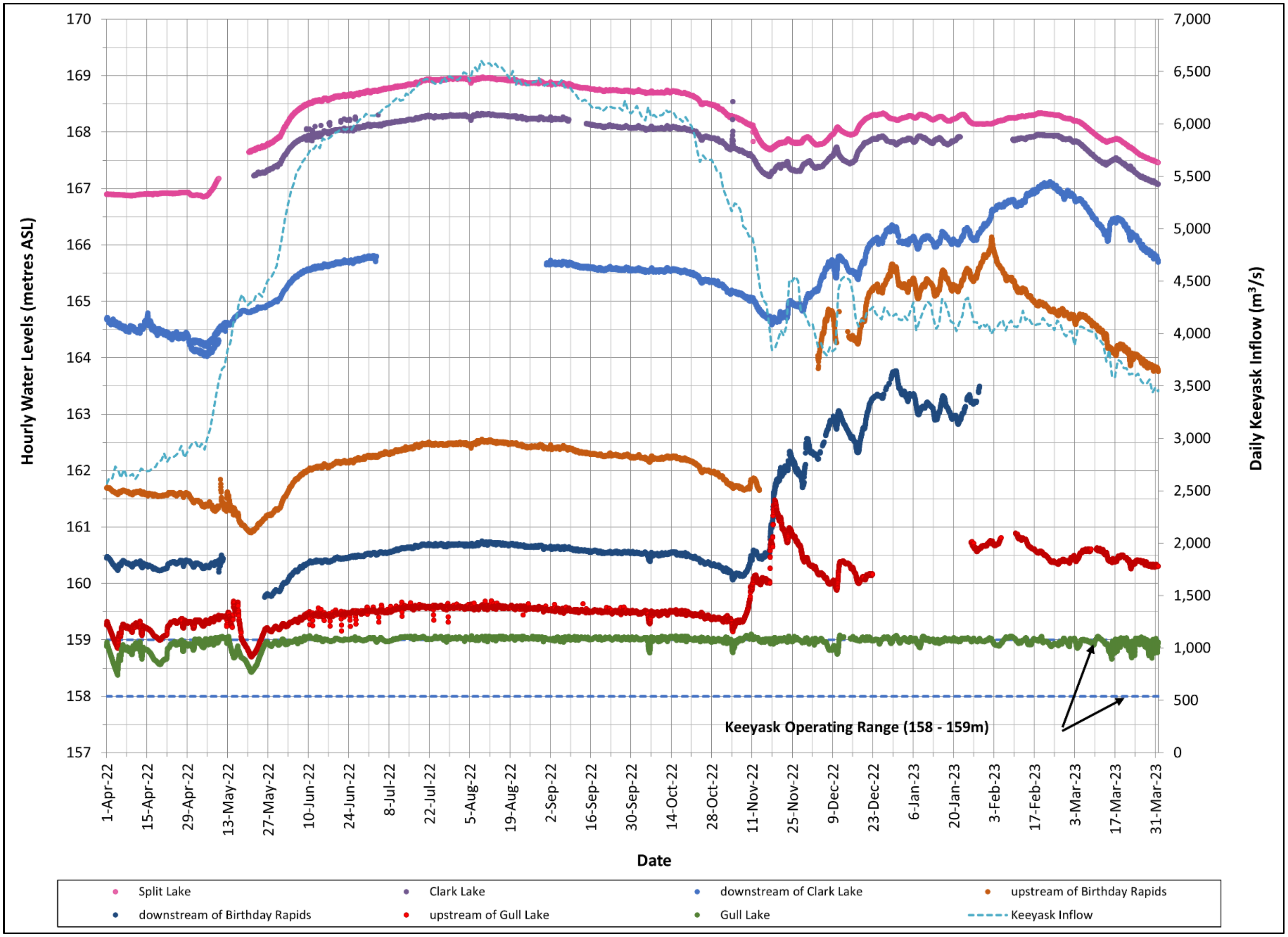


**Figure 3: Observed water levels at PEMP monitoring sites in 2022/2023**

but it is not apparent that this is due to ice accumulation downstream because of cold weather that likely caused the ice front to advance through Birthday Rapids would also tend to cause additional ice constriction at the outlets of Split and Clark lakes, which would raise water levels on those lakes. An increase of 0.1 m on these two lakes in response to cold conditions constricting the outlets is not unusual.

## 2.4 ICE REGIME

The PESV (KHLP 2012b, Section 4) discusses ice processes and the pre-Project ice regime in the vicinity of the Project. In the pre-Project environment, a complete ice cover formed most years (approximately 2 out of 3 years) on Gull Lake and the Nelson River up to Birthday Rapids, although the timing and extent varied with flow and climate conditions. A combination of higher flow and/or warmer conditions could prevent an ice bridge from forming in some years so that open water persisted in the central channel from the exit of Split Lake to the entrance of Stephens Lake. In contrast, with early cold temperatures and lower flows the ice front cover could advance upstream of Birthday Rapids. In years when bridging occurred, the date when it formed ranged from as early as November at lower flows to as late as January at higher flows.

The approximate dates for freeze up and breakup on Gull Lake since the start of construction are shown in Table 3. The 2022/2023 winter saw the initiation of an ice cover in the second week of November. Unlike winter 2021/2022, when flows were low enough for Clark Lake to freeze over almost entirely, higher flows in 2022/2023 kept the center of Clark Lake ice free, which is more typical (Photo 2). In January 2023, there was open water below both the spillway and powerhouse as both were in operation (Photo 3), but by the end of March the spillway was no longer in use and the area downstream had frozen over. Ice conditions below the dam are as expected in the Keeyask EIS.

Based on water level changes, ice formation began around November 7, 2022, and by the 14$^{th}$ Gull Lake was ice covered, with the ice front just upstream of the lake (Figure 4). The ice front progressed to the foot of Birthday Rapids by December 4 and progression stalled there until at least January 30, 2023 (Figure 5, Figure 6). About February 2$^{nd}$ or 3$^{rd}$, water levels indicate the ice front progressed through Birthday Rapids and by the 4$^{th}$ the front was about 5.5 km upstream of the rapids (Figure 7). The ice front reached about 6.5 km upstream of Birthday Rapids at its maximum extent (Figure 8). While the ice cover grew more rapidly under low flow conditions in winter 2021/22 (KHLP 2022) versus 2022/23, the maximum extent of the cover in both years was about the same. The cover remained at its maximum extent for about a month before gradually deteriorating and mainstem becoming largely ice free by May 18 (Figure 9).

**Table 3: Ice dates and cover advancement / break-up**

| Year | Initial Freeze-up on Gull Lake | Ice Cover Advancement | Gull Lake Ice Break-up |
|---|---|---|---|
| 2014/15 | Jan 23, 2015<br>Nov 9, 2014* | foot of Birthday Rapids | May 13-15, 2015 |
| 2015/16 | Nov 20, 2015 | about 4 km upstream of Birthday Rapids | May 4-9, 2016 |
| 2016/17 | Nov 19, 2016 | about 6 km upstream of Birthday Rapids | May 22-24, 2017 |
| 2017/18 | Nov 4, 2017 | about 6 km upstream of Birthday Rapids | May 19-20, 2018 |
| 2018/19 | Nov 4-6, 2018 | about 6 km upstream of Birthday Rapids | May 13-15 2019 |
| 2019/20 | Nov 5, 2019 | Birthday Rapids | May 21-25, 2020 |
| 2020/21 | Nov 2-3, 2020 | About 6 km upstream of Birthday Rapids | May 22-23, 2021 |
| 2021/22 | Nov 19-20, 2021 | About 6.5 km upstream of Birthday Rapids | May 18-21, 2022 |
| 2022/23 | Nov 7-11, 2022 | About 6.5 km upstream of Birthday Rapids | May 13-15, 2023 |

*Ice formation start date before ice boom failed



**Photo 2: Ice formation Downstream of Keeyask**

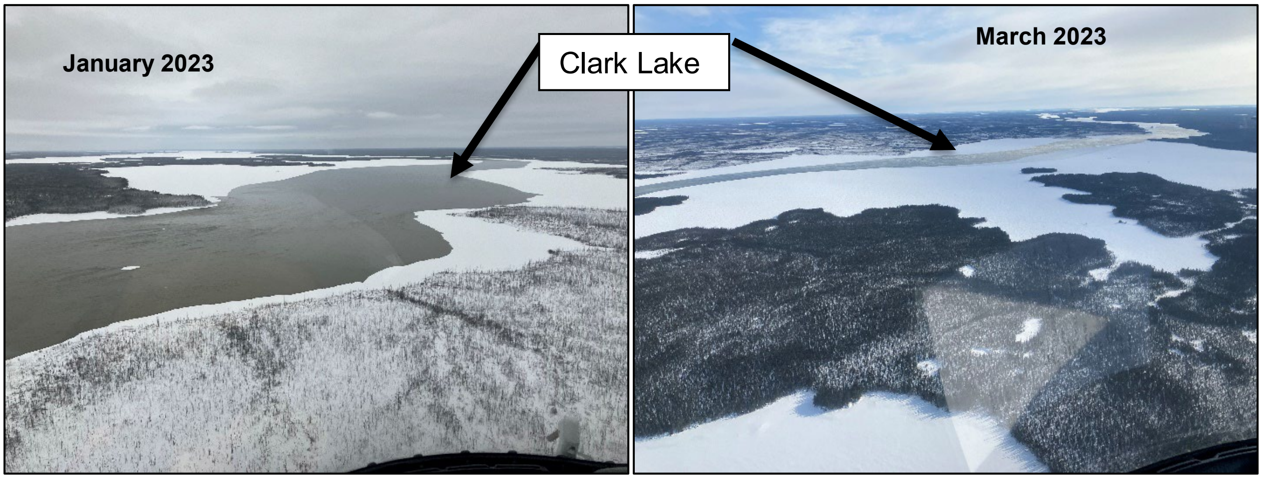


**Photo 3: Ice Cover of Clark Lake**

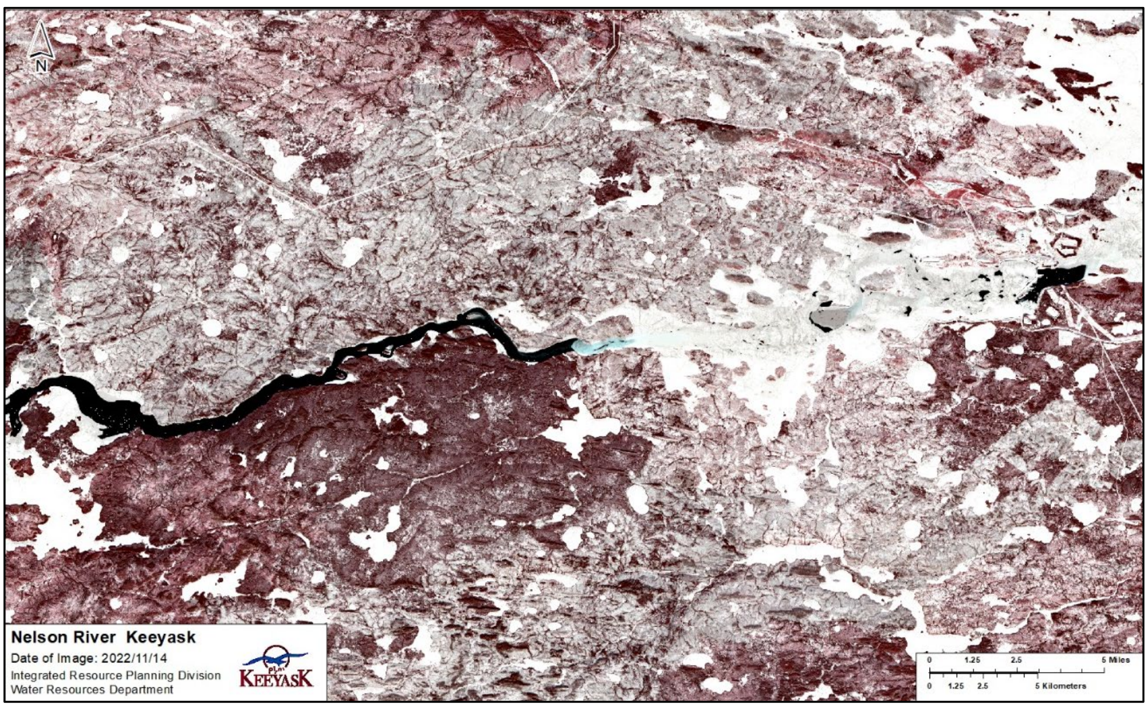


**Figure 4: Ice cover development observations from satellite images 2022/11/14**

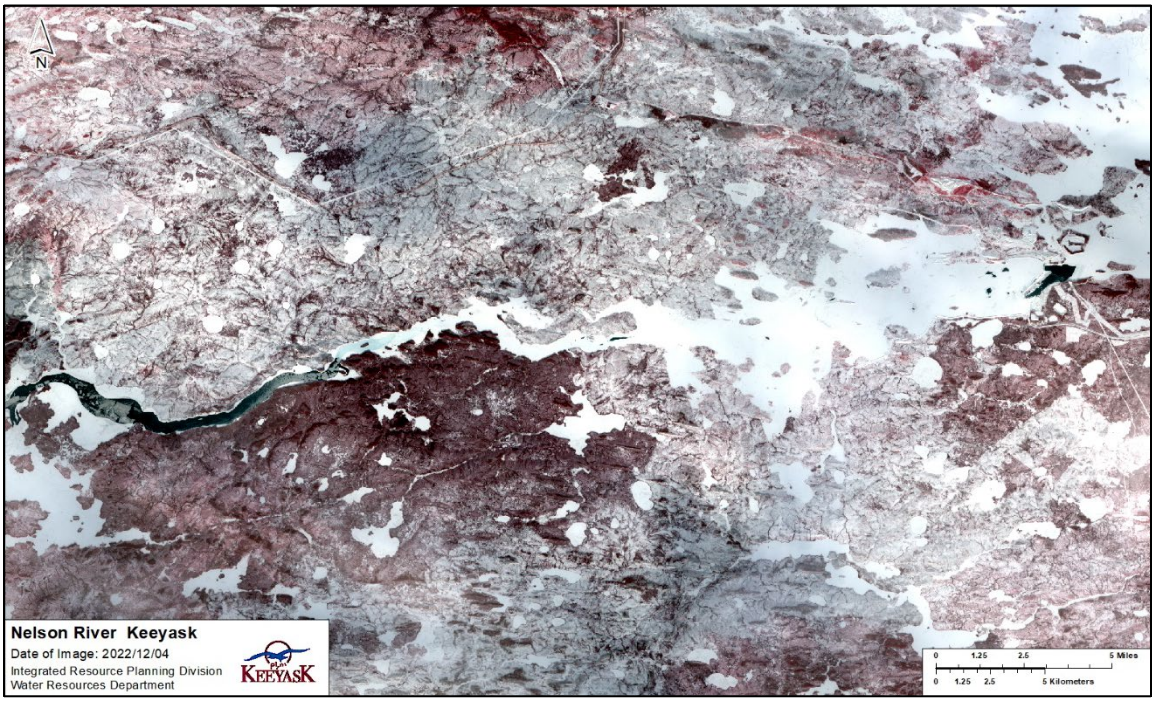


**Figure 5: Ice cover development observations from satellite images 2021/12/04**

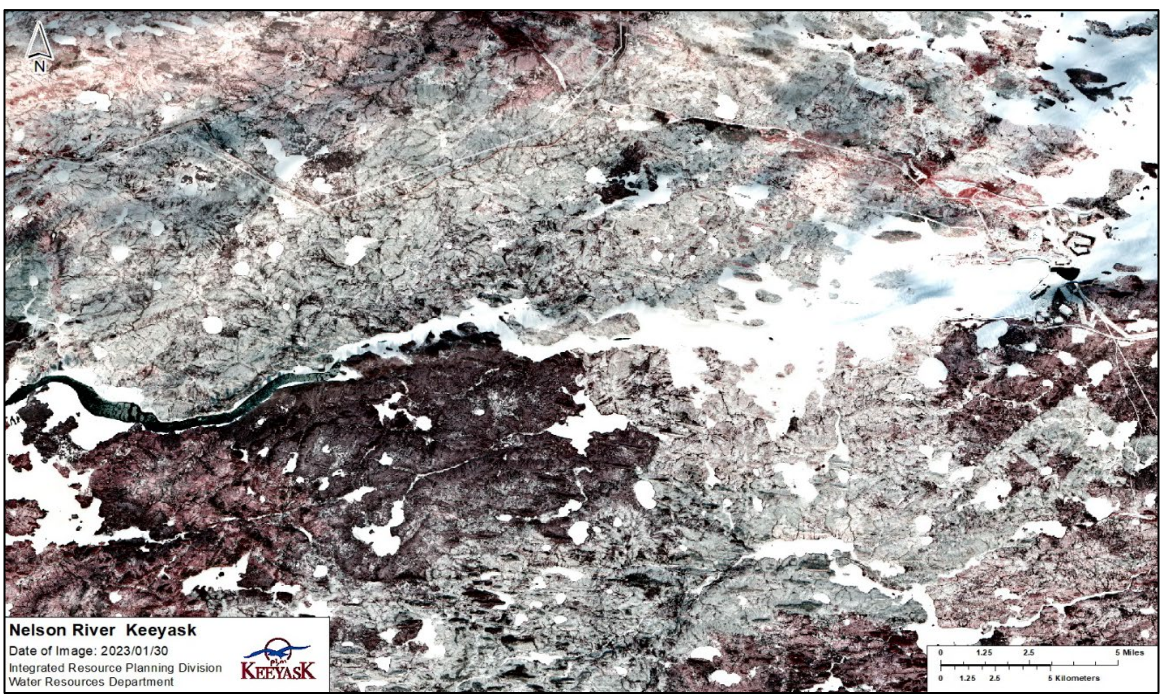


**Figure 6: Ice cover development observations from satellite images 2023/01/30**

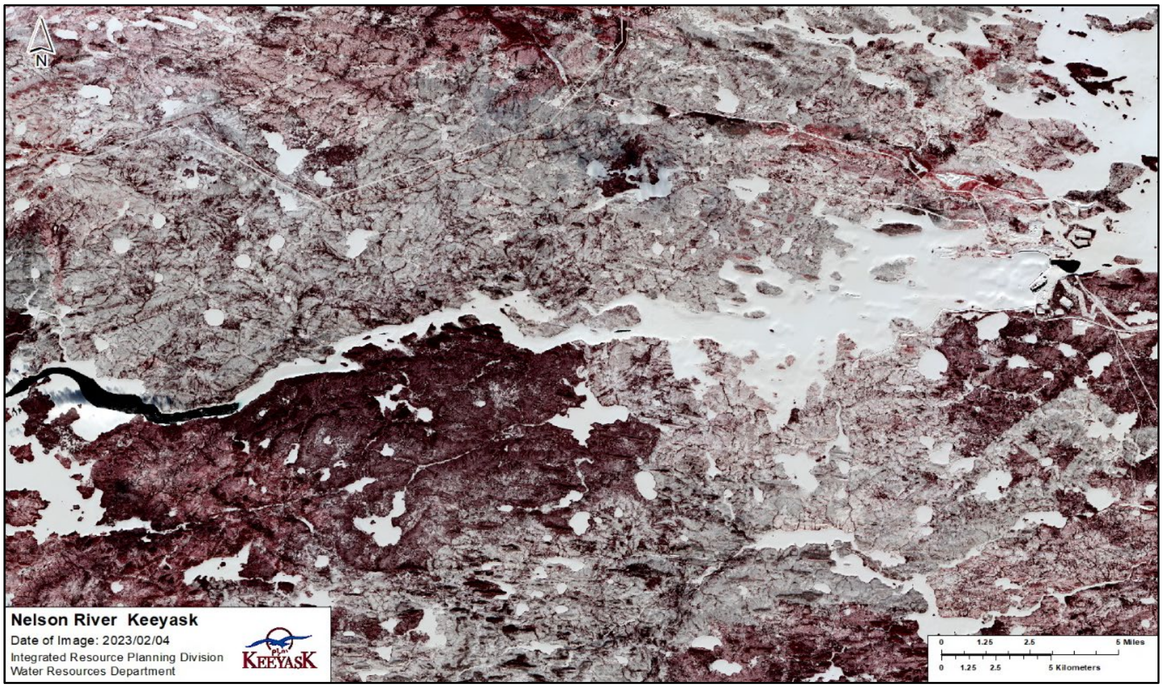


**Figure 7: Ice cover advancement observations from satellite images 2023/02/04**

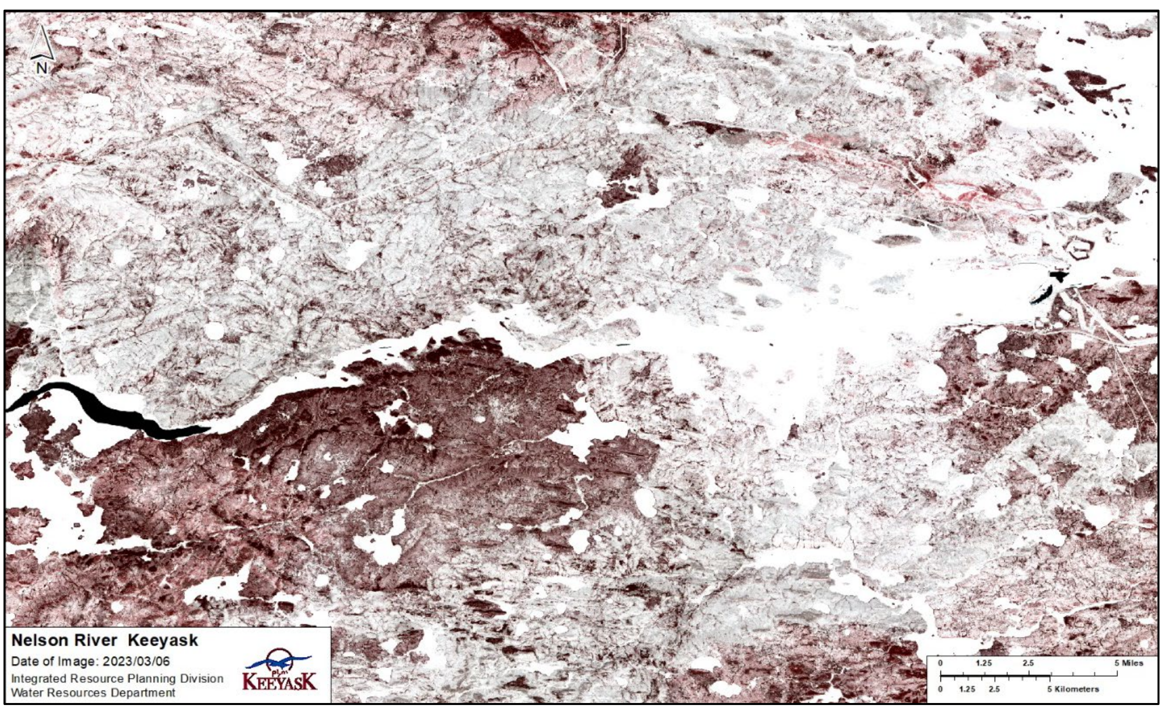


**Figure 8: Ice cover advancement observations from satellite images 2023/03/06**

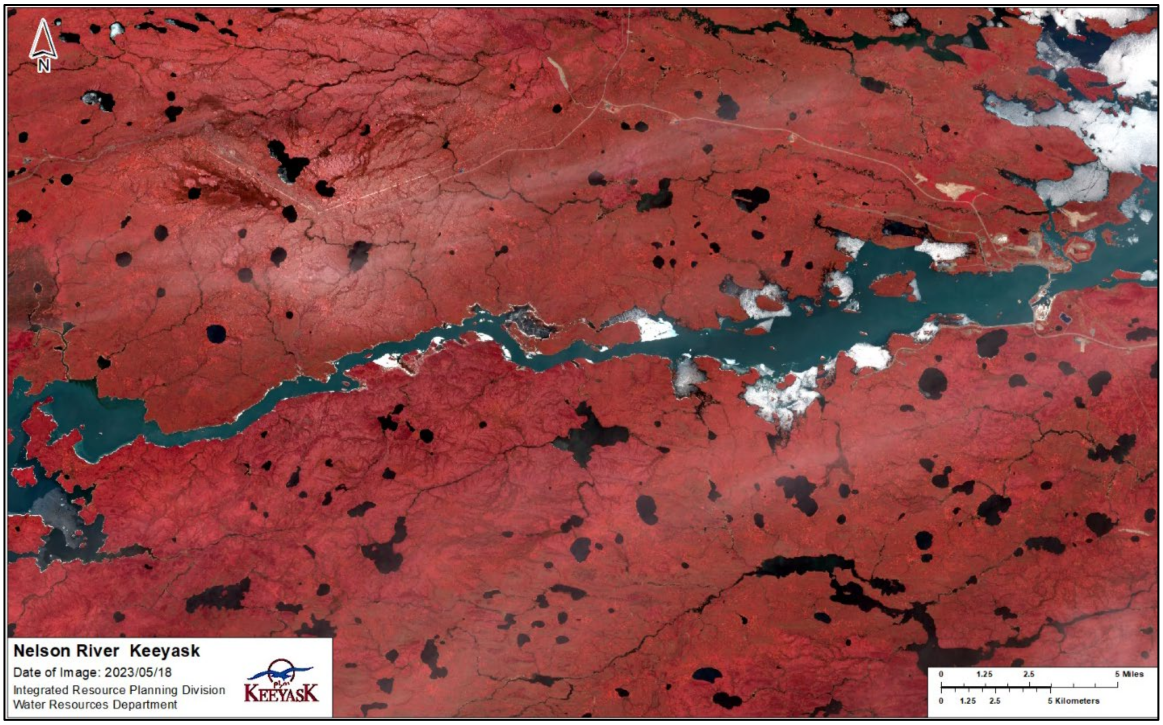


**Figure 9: Receding ice cover observations from satellite images 2023/05/18**

The Keeyask EIS (KHLP, 2012b) predicted that a generally thinner ice cover would develop upstream of the Keeyask GS, particularly at the upstream end of Gull Lake where a thick hanging ice dam would form most years. Similarly, ice within the reach about 4 km downstream of the GS was also predicted to be smoother and thinner because the Project would prevent the formation of a rough and thick hanging ice dam at the entrance to Stephens Lake. The ice cover in the reservoir reach and entrance to Stephens Lake was predicted to develop to a thickness similar to local lake areas (e.g., Split and Stephens lakes), which generally have a maximum ice thickness of about 0.8-1.2 m, depending on specific conditions each winter.

Ice thickness was monitored at 7 locations in 2022: 5 upstream spaced about 5 km apart and two approximately 2 and 4 km downstream of the GS (Figure 10). Measurements were obtained at these sites on March 4 and April 6. Upstream of the GS, ice thickness was relatively uniform and thicker in March than in April, ranging from 1.25-1.40 m and 1.02-1.08 m respectively (Figure 10). Downstream, ice thickness was also greater in March at 1.22 m and 1.10 m compared with 0.91 m and 1.04 m in April. The ice was thicker than in the same months in 2021 when the ice had a maximum thickness of 0.92 m, which is not unanticipated between years due to climate and flow differences. As predicted, the ice cover at the upstream end of Gull Lake and downstream of the GS was much smoother and thinner than occurred prior to the project because these areas no longer experience the pushing and shoving that creates a rough surface and thick hanging ice dams no longer form in these areas. The 2022 monitoring results were consistent with expectations.

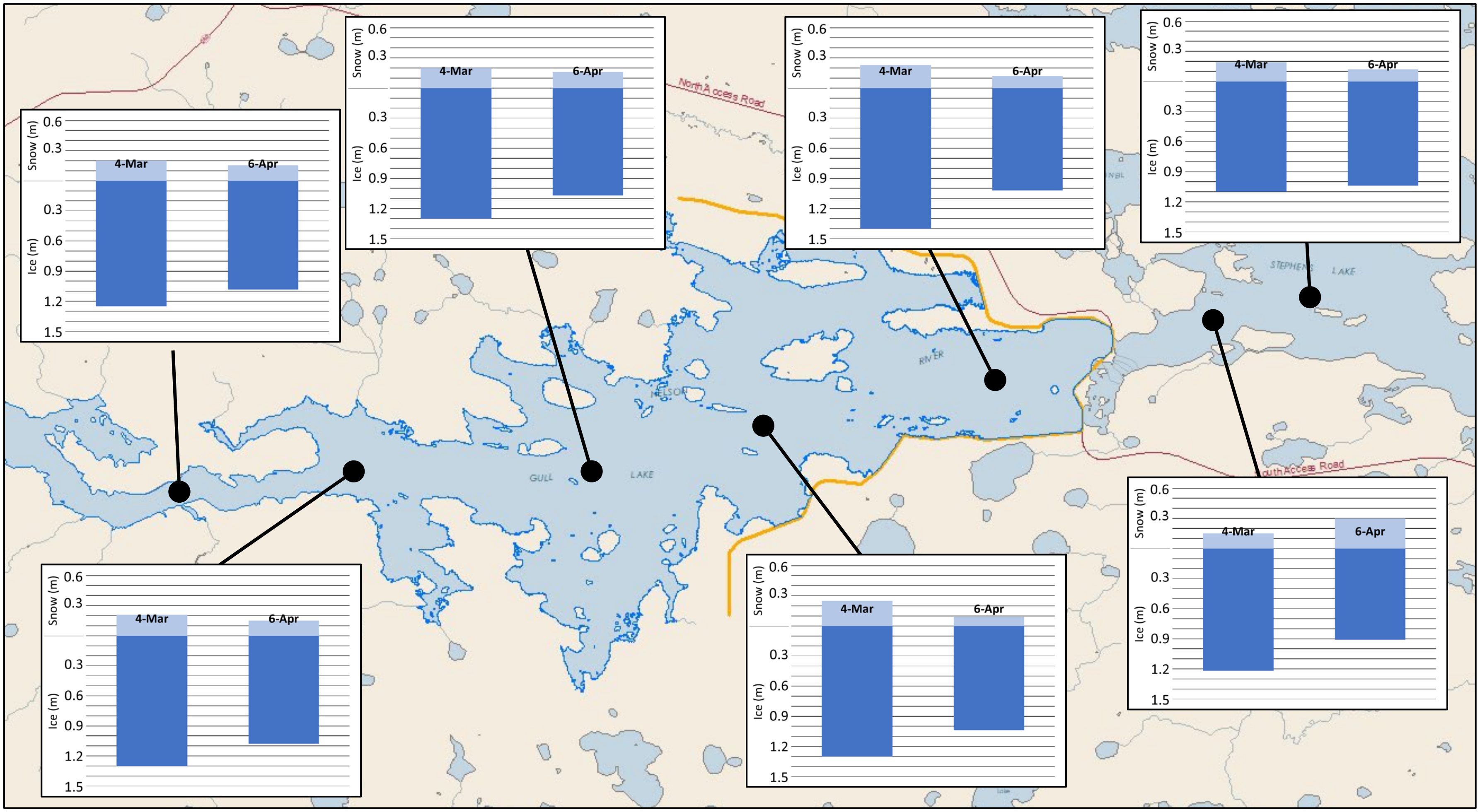


**Figure 10: 2022 ice thickness & snow depth measurements**

## 2.5 WATER VELOCITY

The Keeyask PEMP committed to measuring water velocities under low, moderate, and high flow conditions (i.e., approximately 5th, 50th, 95th percentile flows) during the operating period to identify the range of velocities occurring in various aquatic habitat areas affected by the project. Because high flows were forecast to occur in summer 2022, velocity monitoring was initiated during the open water season. The aquatic monitoring team identified several areas for velocity monitoring from upstream of Birthday Rapids to the entrance of Stephens Lake downstream of the GS. The PEMP monitoring crew measured velocities at 54 transects from August 26-31. Keeyask inflows varied between 6,370-6,450 $m^3/s$, which exceeds the $95^{th}$ percentile and is among the highest Keeyask inflows.

Because velocities at this high a flow were not modeled for the Keeyask EIS, a MIKE21 hydrodynamic model was run to predict velocities for an inflow of 6,400 $m^3/s$, with 4,000 $m^3/s$ passing through the powerhouse and the remaining 2,400 $m^3/s$ through the spillway.The measured and predicted velocities were categorized as either standing (0-.2 $m^3/s$), low (0.2-0.5 $m^3/s$), moderate (0.5-1.5 $m^3/s$), or high (>1.5 $m^3/s$) and results were mapped together for comparison (Figure 11, Figure 12, Figure 13, Figure 14, Figure 15).

Measured and predicted velocities generally compared well for transects upstream of Birthday Rapids and downstream of the Keeyask GS (Figure 11, Figure 15). At the other transect locations there are several transects where the modeled and measured velocities compare favourably. However, a larger number of transects show higher measured velocities than predicted, particularly in central areas of the flow channel: for example the three most eastern transects at locations below Birthday Rapids and the entrance of Gull Lake (Figure 12, Figure 13) and various transects around Caribou Island (Figure 14). Additionally, at various transects in these same locations, the modeled velocities are higher than measured in some areas, particularly towards the ends of the transects. While the categories of the predicted and measured velocities of the measured data points matched most of the time (approx. 62%), modeled values were one category higher or lower than the measured category about 13% and 22% of the time respectively, with a difference of more than one category at the remaining 2.5% of data points (approx. 51,200 measured data points).

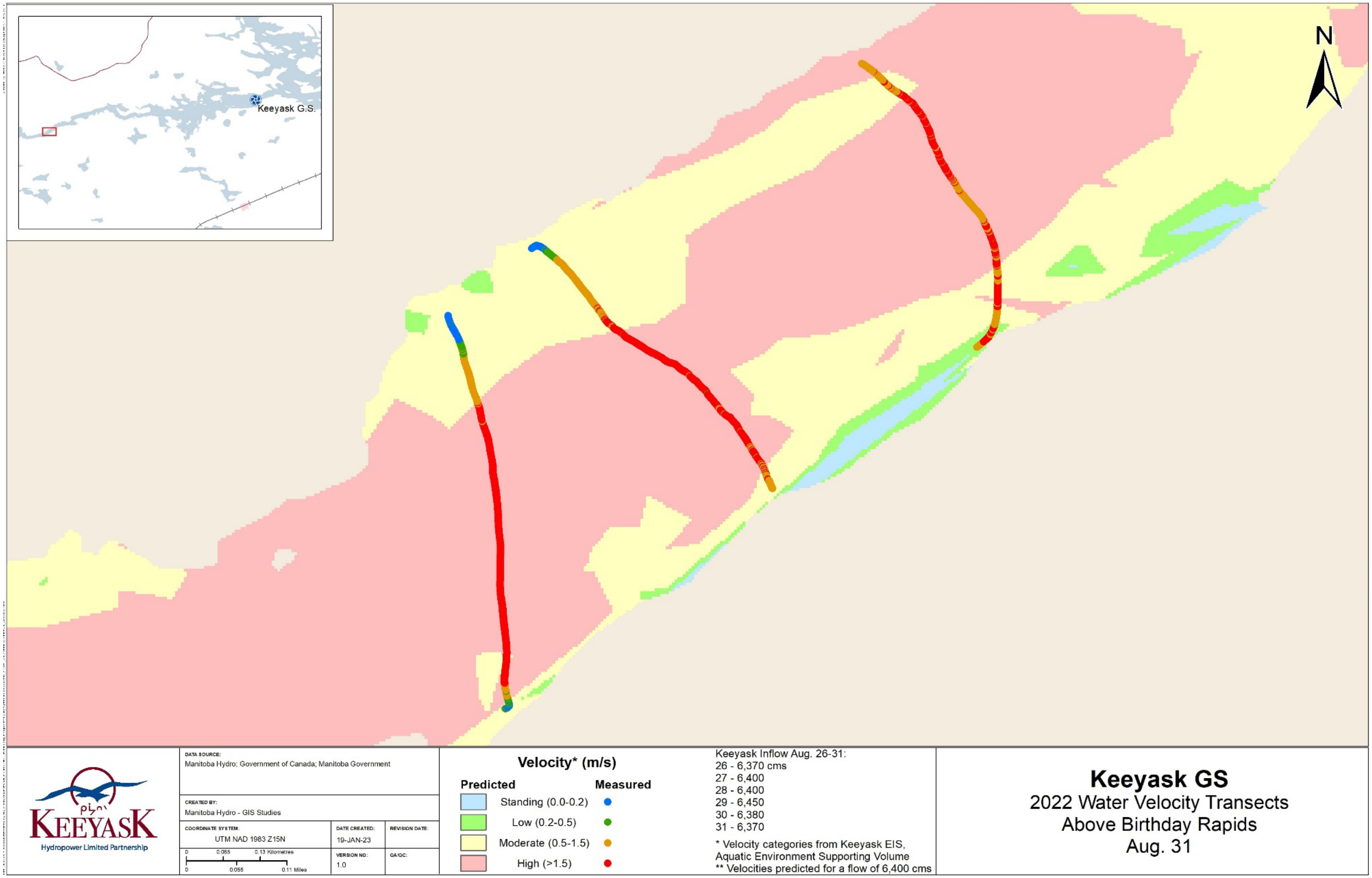


**Figure 11: Velocity transects above Birthday Rapids**

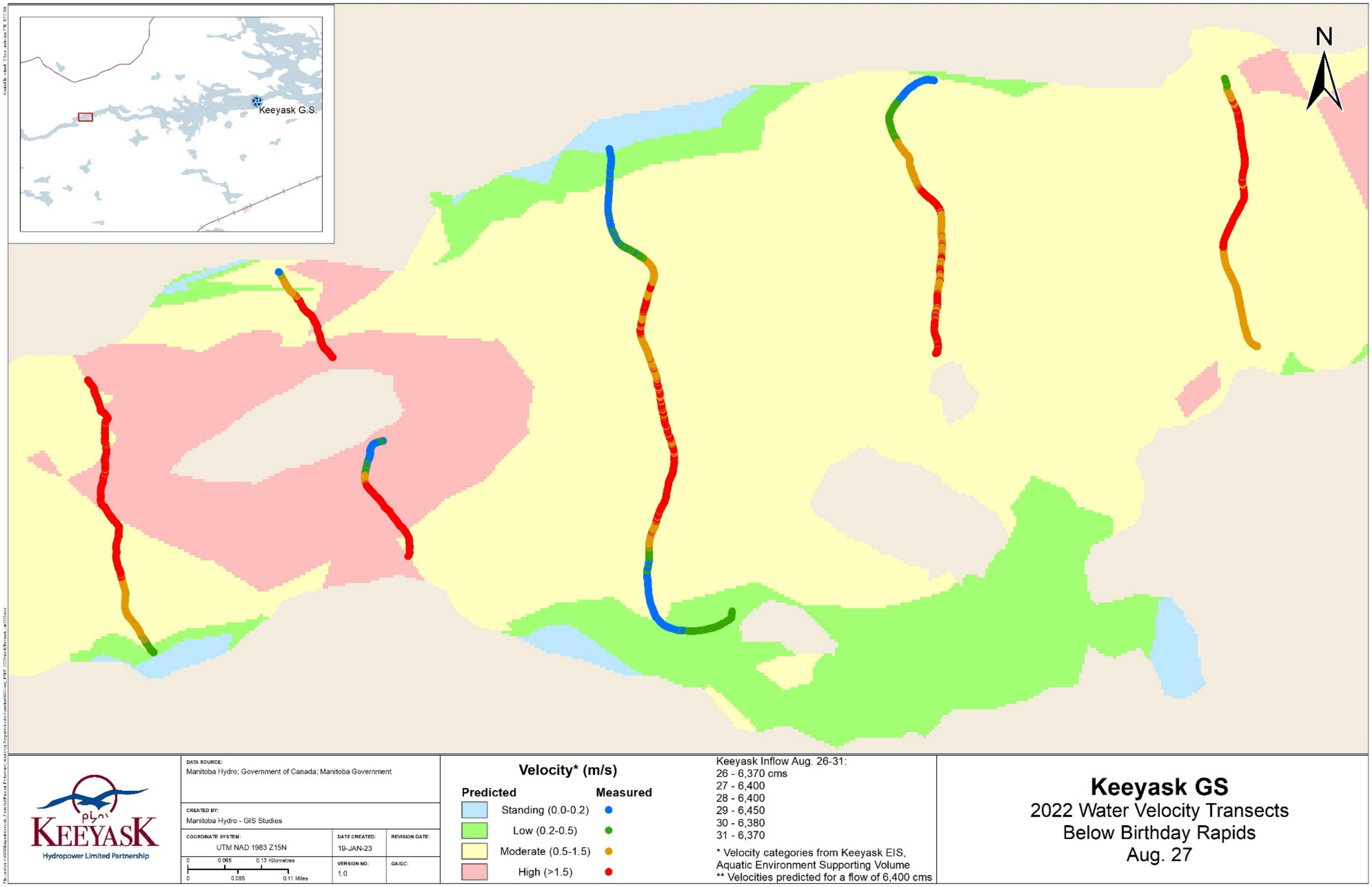


**Figure 12: Velocity transects below Birthday Rapids**

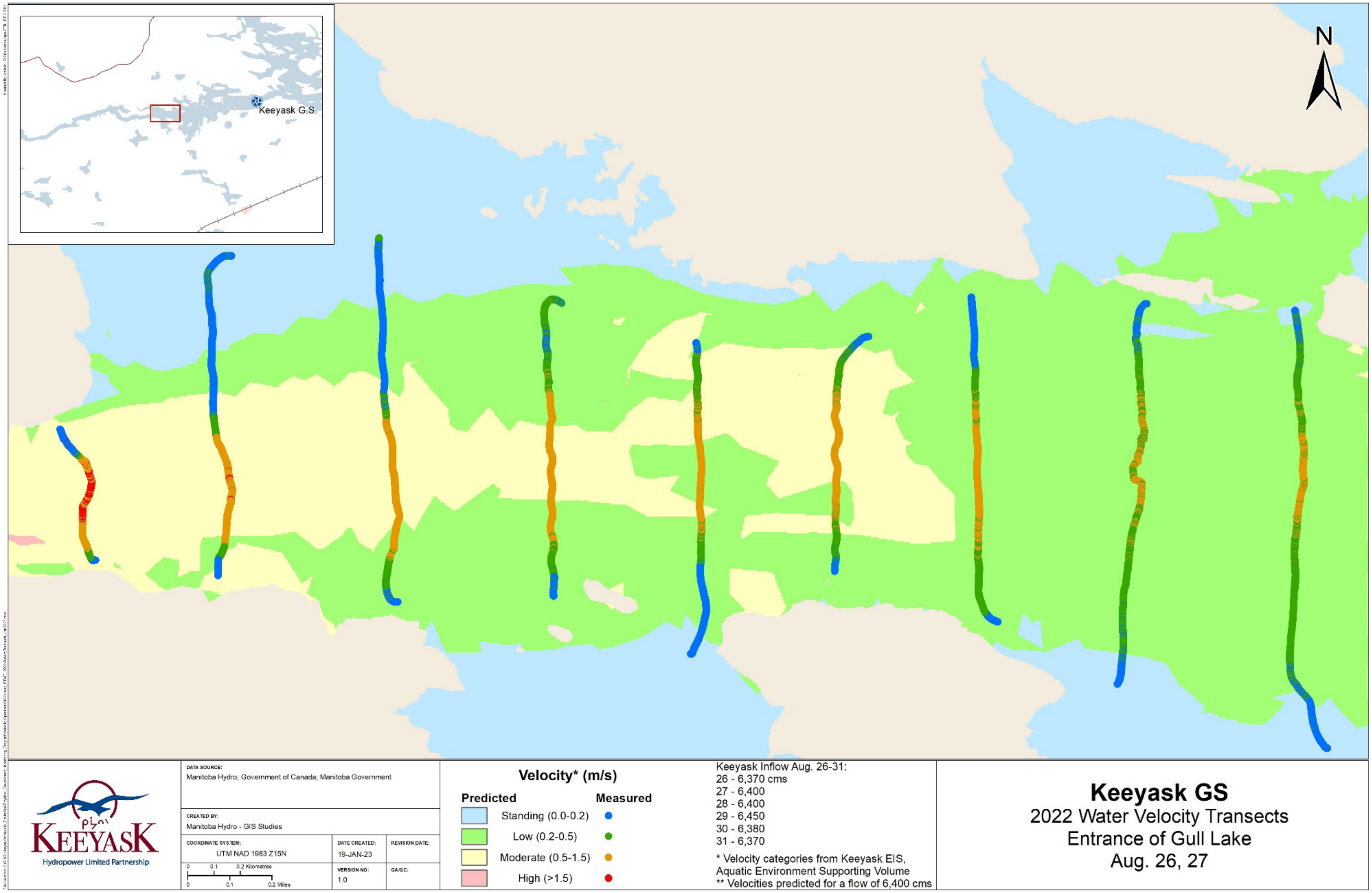


**Figure 13: Velocity transects at entrance to Gull Lake**

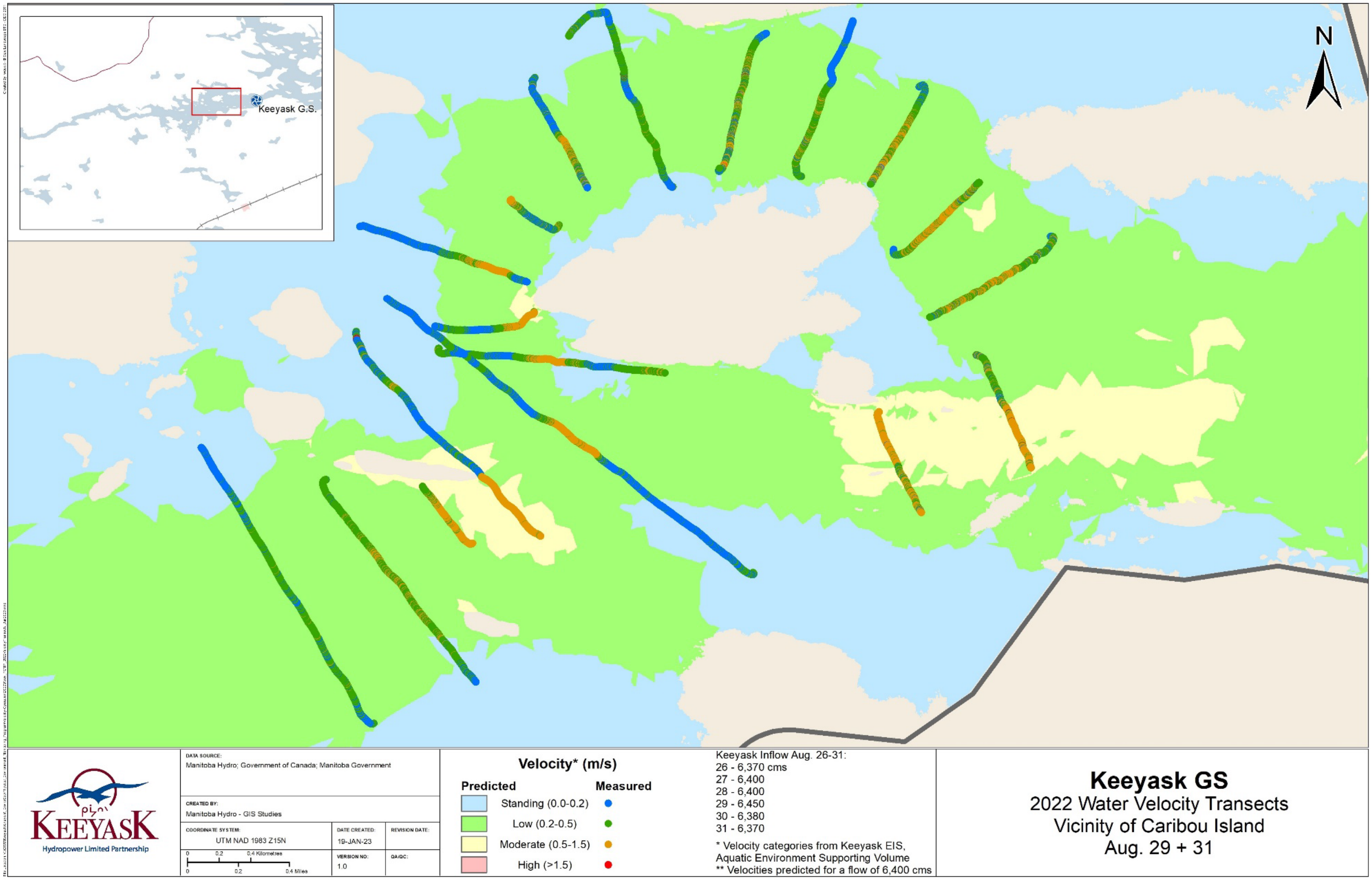


**Figure 14: Velocity transects around Caribou Island**

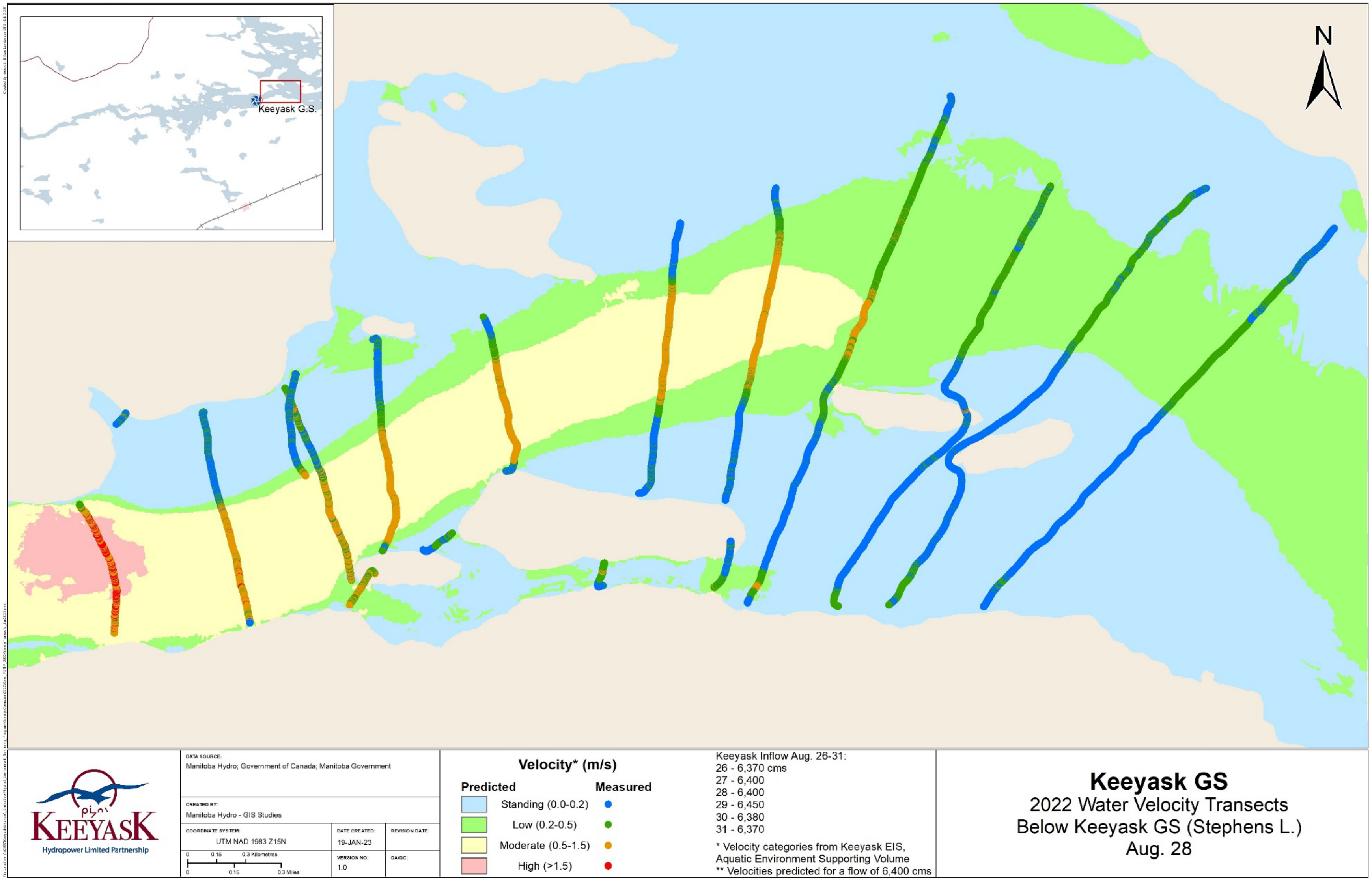


**Figure 15: Velocity transects downstream of Keeyask GS (Stephens Lake)**

# 3.0 SHORELINE EROSION

Shoreline erosion monitoring during construction consists of mapping the shoreline position prior to full impoundment of the reservoir. In 2014 a high-resolution satellite imagery was collected at the start of the construction period. In 2019 another similar satellite image was collected to represent the conditions prior to impoundment that occurred in 2020, and another set of images was obtained in late summer 2021. The shorelines at the start and end of construction will be compared to see if any substantive shoreline erosion occurred during construction. Images collected after impoundment will be used to determine the actual extent of flooding and reservoir expansion over time.

# 4.0 SEDIMENTATION

Sedimentation monitoring includes monitoring the transport and deposition of sediment; the objectives of the sedimentation monitoring include:

- confirming sediment transport and deposition predictions; and
- supporting water quality and aquatic habitat monitoring components of the AEMP (KHLP 2015b).

The largest overall effects of the Project on sedimentation are predicted to occur during operation after impoundment of the reservoir with the highest total sediment loading predicted to occur in the first year after impoundment. During the construction period prior to reservoir impoundment the PEMP sedimentation monitoring was generally done to collect data that will support conclusions of the effects of the Project on sediment transport and deposition after impoundment.

Sediment transport monitoring is done through the collection of discrete water samples, continuous turbidity monitoring and sediment traps at locations shown in Map 3 (detailed site maps are provided in Appendix 1). Discrete sampling involves the collection of water samples and in-situ measurements by field personnel at certain times (e.g., monthly) while continuous turbidity monitoring involves the installation of automated equipment that remains in place to take readings much more frequently. The continuous turbidity sites are periodically visited for maintenance checks; typically completed while discrete monitoring is performed. Sediment loading is estimated from the continuous turbidity data.

## 4.1 WINTER 2021-2022

In each annual report the winter sedimentation data is reported from the previous winter (i.e. one year delay) to allow time after the end of the field season for all data to be reviewed and analyzed before reporting. This report presents the 2021-22 winter sedimentation data.

### 4.1.1 CONTINUOUS AND DISCRETE TURBIDITY AND TSS

Winter discrete monitoring in 2021-22 was conducted monthly at four continuous turbidity sites (Table 4), upstream of the Project area in Clark Lake, upstream and downstream ends of Gull Lake, and downstream of the Project in the entrance to Stephens Lake (seep maps Appx. 1). Equipment was installed in January after suitable ice conditions developed at all the sites and was removed in early April before ice break up. The data collected at each of the monitoring sites was reviewed to identify and remove poor quality data from factors such ice, dead batteries, and

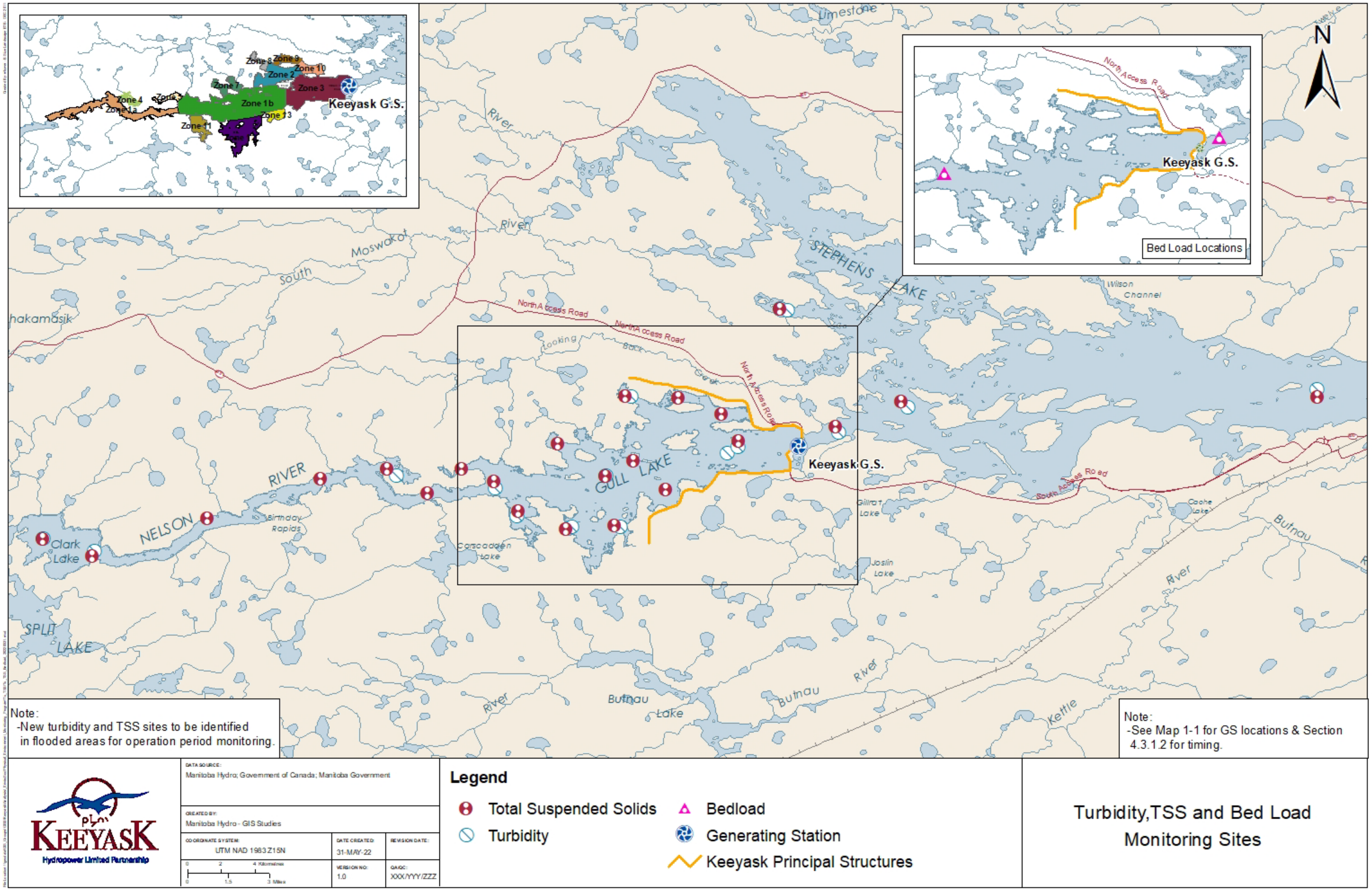


**Map 3: Turbidity, total suspended solids and bed load monitoring sites**

equipment malfunction. The continuous data were also compared with the discrete readings obtained on each maintenance site visit and adjustments made for any sensor drift.

**Table 4: 2021-2022 winter continuous TU & discrete TSS monitoring locations**

| Site ID | Dates |
|---|---|
| CL-1 (Clark Lake) | 19-Jan-2022 to 11-Apr-2022 |
| KE-4-b (Gull Lake upstream) | 19-Jan-2022 to 11-Apr-2022 |
| KE-9 (Gull Lake downstream) | 20-Jan-2022 to 11-Apr-2022 |
| STL-4 (entrance to Stephens L) | 20-Jan-2022 to 12-Apr-2022 |

Turbidity levels at the two Gull Lake sites and just downstream (KE-5, KE-10-c, STL-4) were all generally within about 1 FNU of each other and turbidity steadily decreased from about 18-19 FNU at the start of monitoring to about 10 FNU at the end (Figure 16). Turbidity at the Clark Lake site (CL-1) was generally lower than the downstream sites by about 1-2 FNU, and steadily decreased from about 16 FNU to 9 FNU from January to April. While the turbidity in January was somewhat higher than observed the last several winter seasons, the pattern of winter decrease and the low values at the end are similar to past observations.

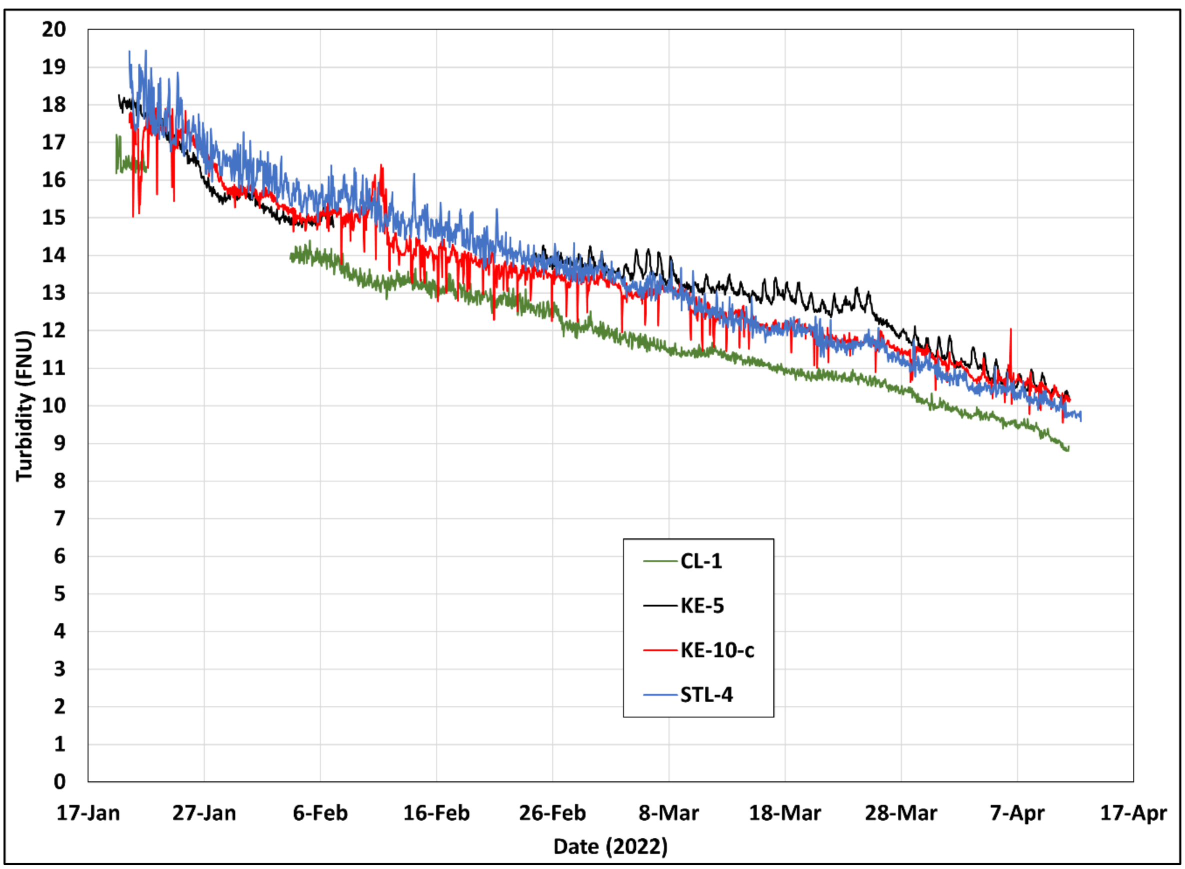


**Figure 16: 2021-2022 winter continuous TU**

The range and average of continuous turbidity was summarized and compared with continuous turbidity observed prior to and during construction (Figure 17). In 2022, as in the years since 2016, the turbidity levels in Stephens Lake downstream of the Keeyask GS have been generally lower than observed prior to construction, with much narrower and range and lower peak levels. This is consistent with the Keeyask EIS prediction that the Project would “significantly reduce erosion potential” downstream of the Project after construction, which would result in lower turbidity downstream. Prior to the project a large hanging ice dam formed each winter at the entrance to Stephens Lake and would cause water levels to rise and flows to be redirected along erodible shorelines, which would add sediment to the river. With the Keeyask GS in operation, this hanging ice dam does not form, which mitigates the entrainment of sediment from eroding shorelines.

Discrete TSS and turbidity data show consistent results with the continuous data (Figure 18, Figure 19). With the ice boom working to produce a stable ice cover upstream of the Project the downstream TSS and turbidity are lower than compared with pre-project conditions. Results from both years of operation are similar and generally slightly lower than conditions observed in the previous years during construction. The average TSS in 2022 was low at about 3 mg/l, or about the same as in 2021, and lower than the averages of about 4-5 mg/l in the previous years of construction. While average TSS concentrations in 2022 were about the same as 2021 and lower than previous years of construction, the turbidity in 2022 was slightly higher but still low like previous years of construction.

In addition to turbidity monitoring at the four mainstem sites (Figure 16), discrete monitoring was performed twice, once early in winter in December/January and again in April, at 11 backbays upstream of the project and in a backbay on Stephens Lake that is unaffected by the project (Figure 20). At each site the turbidity levels in Dec/Jan are generally higher than in April. With a few exceptions, KE-Z9-1 had lower turbidity across its 4 sampling locations (a to d) than observed at other sites, with three of four locations below 8 FNU in Dec/Jan while April levels were 4-5 FNU. For the remaining locations, the Dec/Jan turbidities largely varied from about 10-16 FNU except for a few locations that were lower. As in 2021, turbidity averaged about 5 FNU lower in April, and in 2022 generally ranged from about 6-9 FNU. This is consistent with the decline in turbidity over the course of winter that was observed from the continuous data.

At the backbay sampling sites, the four separate sampling locations (a-d, or 1-4 at site KE-Z8) are ordered with the first location (a or 1) furthest from the main channel and the last (d or 4) closest to the main channel. In the Dec/Jan round of monitoring many of the sites sampled had lower turbidity at the location furthest from the main channel and higher levels closer to the channel: for example, KE-Z10-1-a is about 3 FNU lower than KE-Z10-1-d. This likely results from sites closer to the mainstem being influenced more by the turbidity of the flow in the mainstem of the river. This effect is less prevalent in the April round of sampling when turbidity is less variable at the monitoring sites.

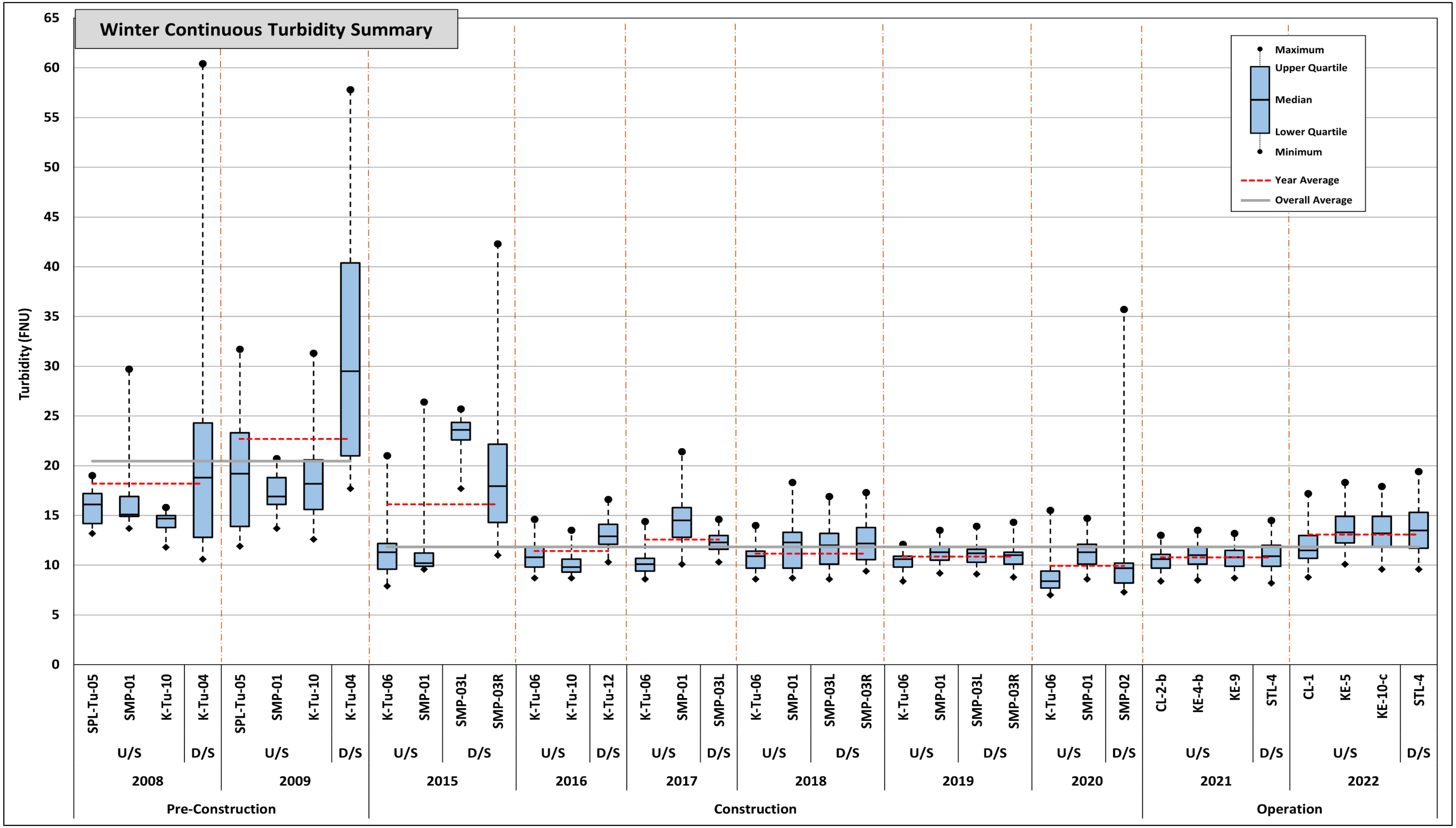


**Figure 17: Summary of winter continuous TU (2008-2022)**

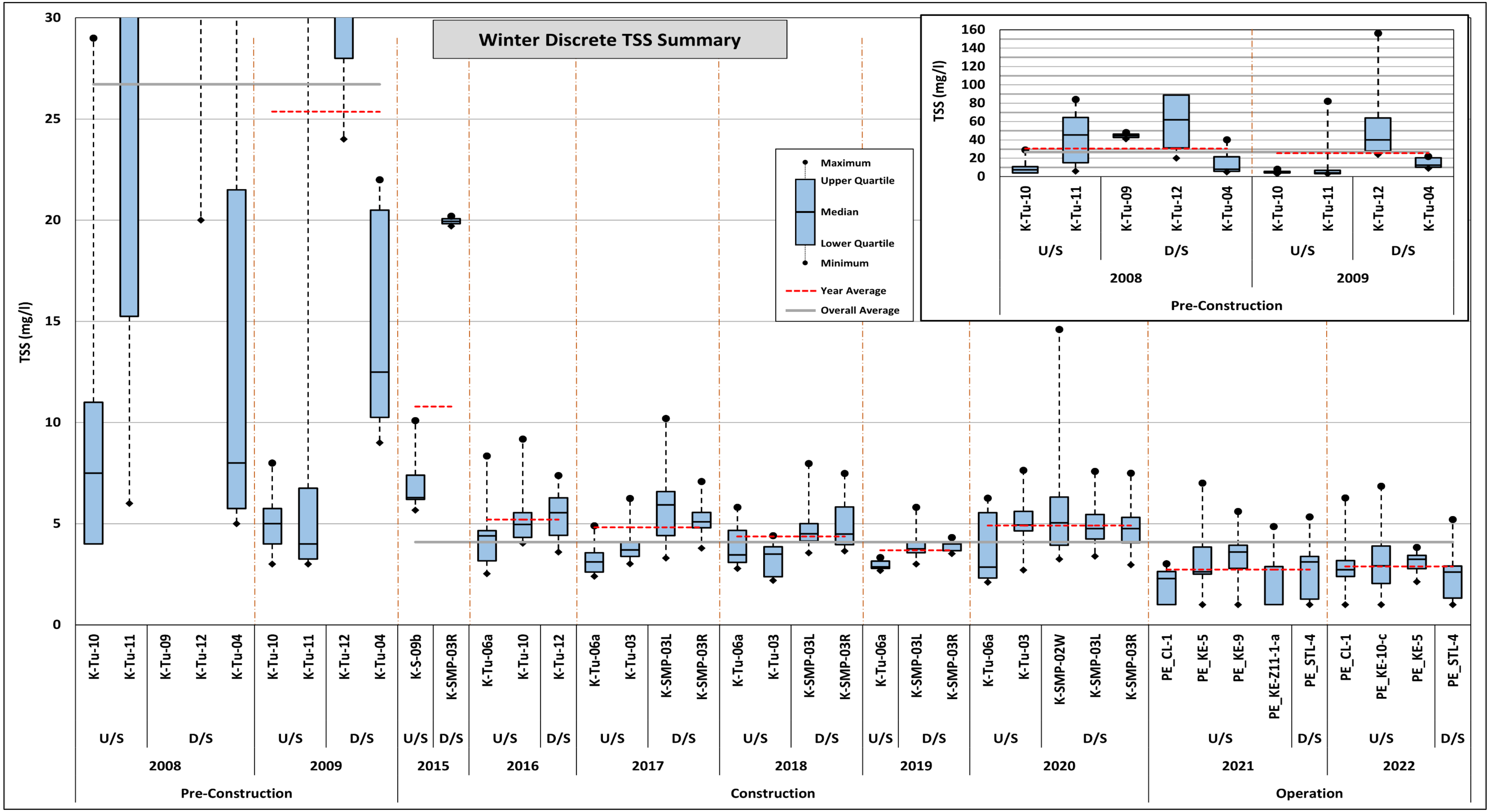


**Figure 18: Summary of mainstem winter discrete TSS (2008-2022)**

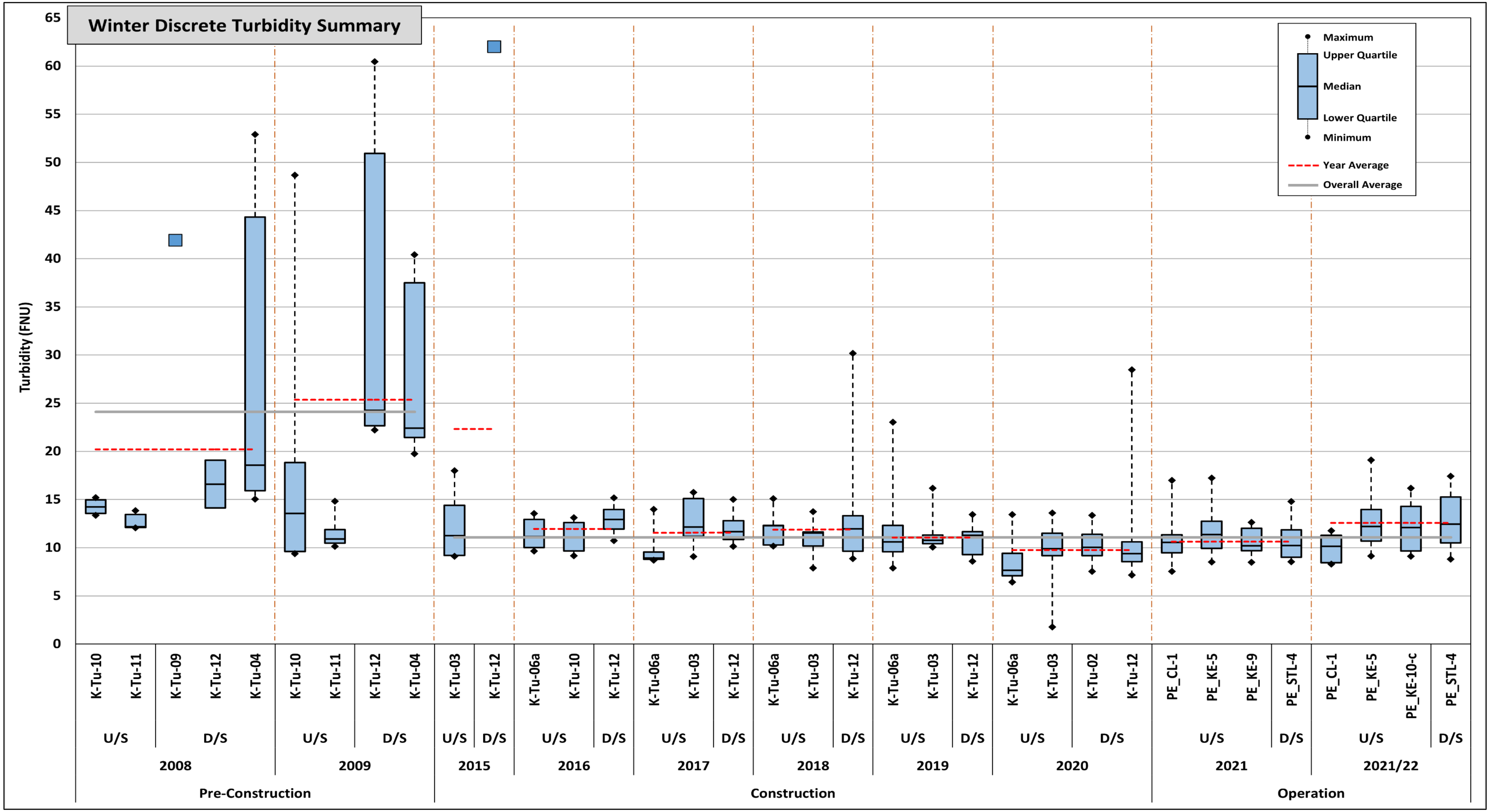


**Figure 19: Summary of mainstem winter discrete TU (2008-2022)**

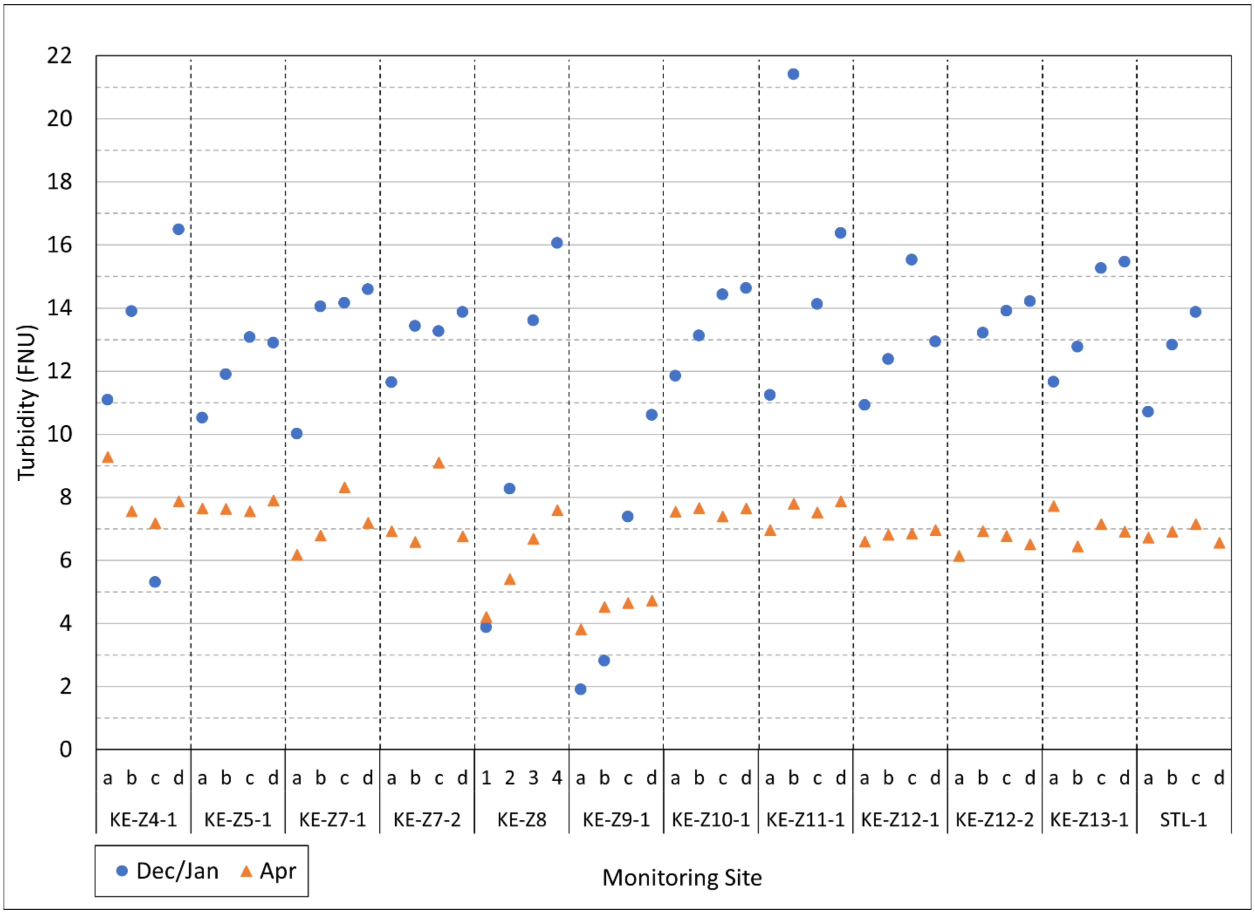


**Figure 20: Discrete TU at backbay sites (winter 2021-2022)**

## 4.1.2 ESTIMATED SUSPENDED SEDIMENT LOAD

The winter suspended sediment loads (Figure 21) are estimated based on the average daily turbidity and discharge. Turbidity was converted to TSS concentrations using a Turbidity-TSS relationship developed for the Sediment Management Plan (KHLP 2014) based on pre-project discrete monitoring.

The estimated daily sediment load at Clark Lake (sites SPL-Tu-05 & K-Tu-06 before operation, and CL-1 & CL-2-b during operation) upstream of expected hydraulic effects due to Keeyask indicates that the winter average was higher during the two pre-construction years than the winters monitored since 2015. In 2022, the sediment loads at sites downstream of Clark Lake were about 20% greater than at Clark Lake, which is consistent with previous years during construction when the downstream loadings have generally been about 10-30% greater (Figure 21). The overall average load in 2022 was about 1,650 t/d, which is comparable with previous years during construction when loads have ranged from roughly 1,600-2,000 t/d with the exception of 2017, which was about 2,700 t/d.

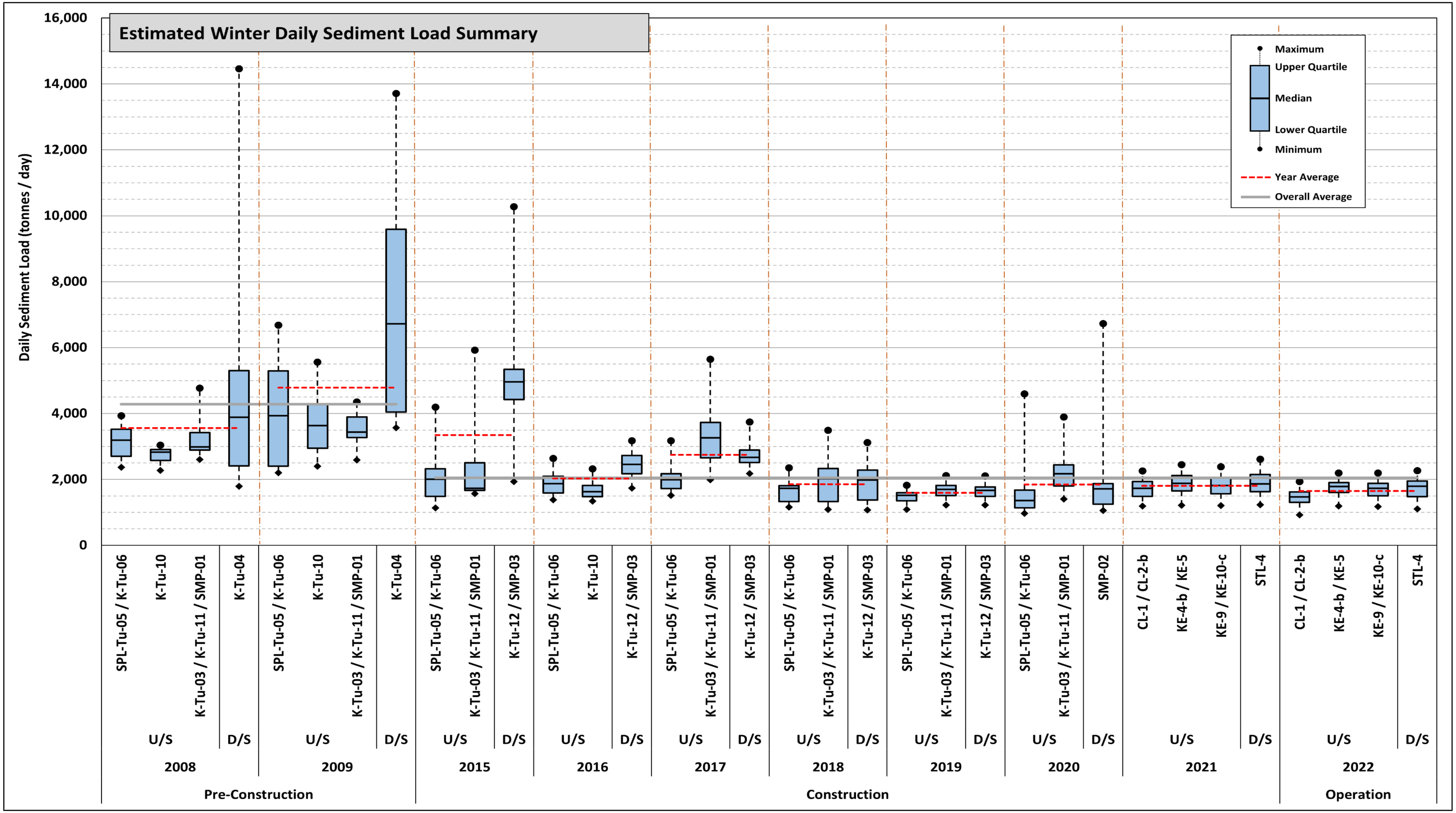


**Figure 21: Summary of winter daily suspended sediment load (2008-2022)**

As noted above, a downstream reduction in turbidity (suspended sediment) has resulted in a reduced sediment load entering Stephens Lake since 2016 as compared with the pre-construction period and in 2014-15 when the ice boom failed. Loads are reduced because a hanging ice dam no longer forms at the entrance to Stephens Lake, as verified by downstream ice measurements (see Sec. 2.4), which reduces scour of the bed and banks in this area. This change results in less sediment being transported into Stephens Lake and downstream along the Nelson River to Hudson Bay, which was an expected effect of the project.

## 4.2 SUMMER 2022

The summer monitoring period extends from the time ice has melted and equipment can be safely placed in the water (typically in June) until equipment can be safely removed before winter conditions and freeze up starts (typically late September to early October).

### 4.2.1 CONTINUOUS TURBIDITY

Eleven continuous turbidity sites were monitored in summer 2022. This included 5 sites on the Nelson River mainstem between Clark Lake upstream of project effects to 30 km downstream of the Keeyask GS in Stephens Lake near Kettle GS, as well as 5 flooded backbays upstream of Keeyask and a bay on Stephens Lake (Table 5; location maps in Appendix 1).

**Table 5: 2022 summer continuous turbidity monitoring locations**

| Site ID / Location | Dates |
|---|---|
| Mainstem Sites | |
| CL-2-b (Clark Lake) | Jun 24 – Sep 28 |
| KE-4-b (entrance Gull Lake) | Jun 20 – Sep 26 |
| KE-10-c (just upstream Keeyask GS) | Jun 20 – Sep 7 |
| STL-2-d (entrance Stephens Lake) | Jun 19 – Sep 6 |
| STL-5 (Stephens Lake near Kettle GS) | Jun 19 – Sep 26 |
| Backbay Sites | |
| KE-Z4-1-a | Jun 14 – Sep 27 |
| KE-Z8-2 | Jun 14 – Sep 28 |
| KE-Z11-1-a | Jun 15 – Sep 27 |
| KE-Z12-1-b | Jun 16 – Sep 28 |
| KE-Z12-2-b | Jun 16 – Oct 3 |
| STL-1-c (Stephens Lake) | Jun 17 – Sep 26 |

The continuous turbidity monitoring stations consist of either a catamaran equipped for satellite data transmission (Photo 4) or a stand-alone buoy system requiring manual downloading of data. Both systems were equipped with a YSI multi-parameter sonde (6600 series) suspended two metres below the surface of the water.

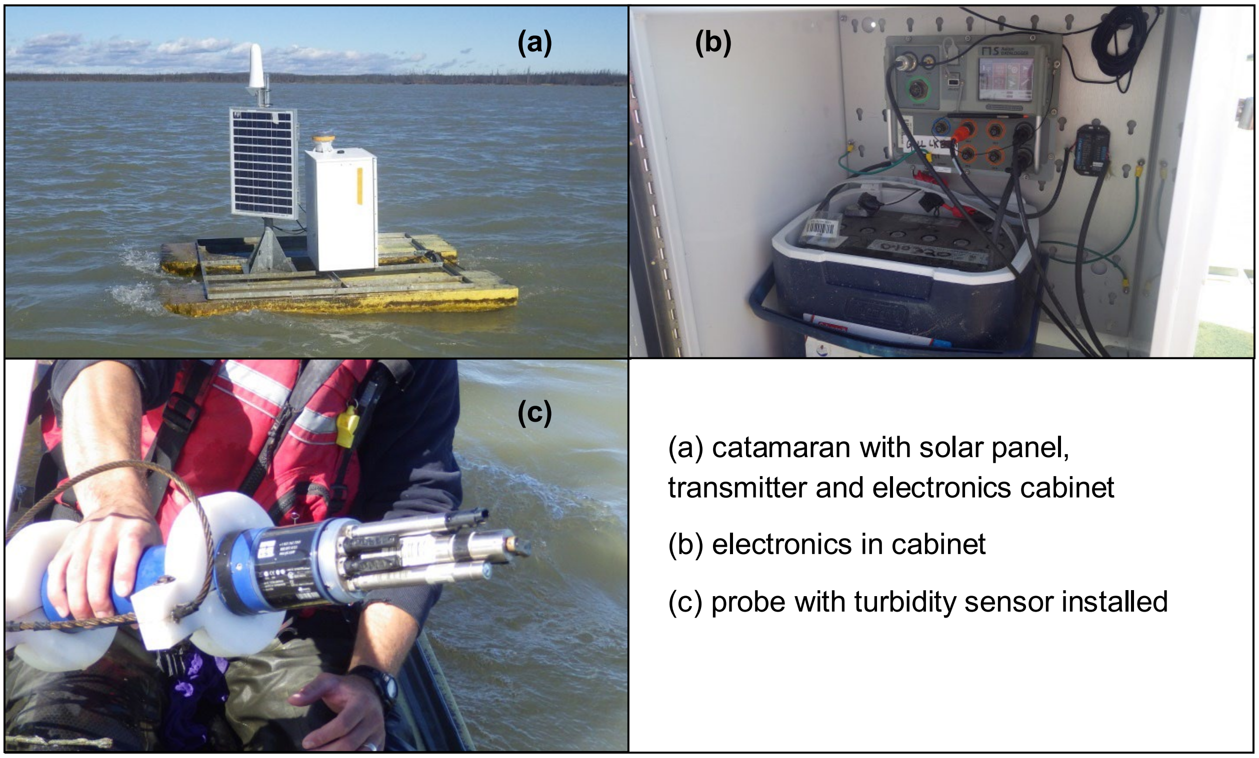


**Photo 4: Continuous turbidity monitoring equipment**

The data collected at each of the monitoring sites was reviewed to identify and remove poor quality data that may result due to factors such as algae growth and vegetation on probes, dead batteries, and equipment malfunction. The continuous data were also compared with the discrete readings obtained on each maintenance site visit and adjustments made for any sensor drift. As a result of the review some data was excluded at several sites and, except for site KE-4-b, it was not necessary to remove extended periods of poor-quality data so there are no large gaps in these 2022 summer records. Equipment failures at site KE-4-b resulting in the exclusion of data from mid-June to mid-July and the last 3 weeks of August.

As observed in 2021 and during construction, the turbidity at each of the 3 mainstem sites upstream of the Keeyask GS and at STL-2-d just downstream followed each other closely, generally within about 1-2 FNU (Figure 22). Site STL-5 near Kettle GS followed the same general trend but was typically 1-2 FNU lower than the other sites, which is consistent with past observations that turbidity (and suspended sediment) generally deceases due to deposition in Stephens Lake. There are several intermittent peaks at monitoring sites that may be associated with periods of higher winds that cause sediment to enter the water. All sites saw turbidity increase about 2-4 NTU over several days in the week of August 6 before declining to lower levels. This may have been partly caused by higher winds, although winds were not elevated during the entire event. The increase is driven by higher turbidity water from Split Lake, so it appears an upstream condition unrelated to Keeyask caused these higher turbidity levels. The mainstem turbidity results do not indicate any significant change in turbidity due to the Keeyask reservoir: i.e., no notable increase due to erosion of flooded shorelines or decreases resulting from deposition due to lower velocities in the reservoir.

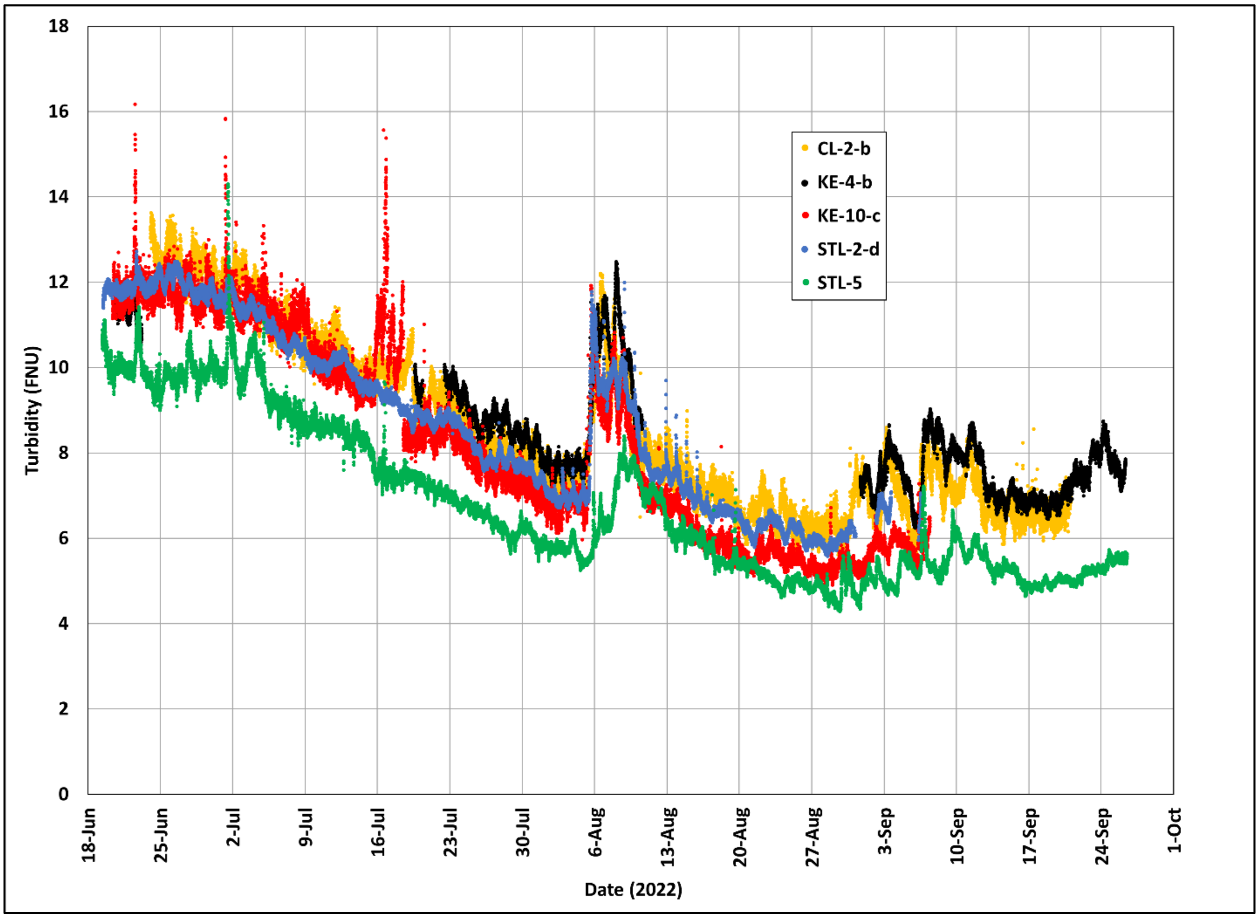


**Figure 22: 2022 summer continuous TU – mainstem sites**

Continuous turbidity monitoring was also conducted in 5 backbay locations forming part of the Keeyask reservoir, plus one site downstream on Stephens Lake, which forms the Kettle GS reservoir, and each site has a good record over the entire summer (Figure 23). At 4 of the 5 sites upstream of Keeyask, turbidity levels are typically less than 7 FNU. The two sites on the north side of the reservoir, KE-Z4-1-a and KE-Z8-2, had the lowest overall turbidity with 95% and 100% of readings below 7 FNU respectively, while sites KE-Z11-1-b and KE-Z12-1-b had 85% of reading below 7 FNU. Site KE-8-2 was particularly low with about 80% of readings between 1-2 FNU, indicative of almost no sediment in the water. Upstream site KE-Z12-2-b had somewhat higher turbidity with only 44% of readings below 7 FNU while downstream site STL-1-c had the highest overall turbidity as more than 95% of readings exceeded 7 FNU. STL-1-c typically has higher turbidity than the other sites every year.

The sites on the south side of the reservoir and site STL-1-c also had higher peak levels than sites on the north side. Higher turbidity levels at sites KE-Z11-1-b and KE-Z12-1-b, and particularly at KE-Z12-2-b and STL-1-c, are likely a result of greater exposure to the more predominant north to northeast winds that tend to occur in the region. As in 2021, turbidity levels at 4 of the upstream backbays were generally lower than observed on the mainstem with the magnitude of difference depending on the site considered. Turbidity at KE-Z12-2-b was in the same range and followed a similar pattern of variation as the mainstem sites, suggesting that in addition to wind, this site may be influenced by conditions on the mainstem of the river.

The 2022 mainstem continuous turbidity data was summarized to show the overall ranges of turbidity as well as quartile and median values and results were plotted along with summary data from 2007-2021 (Figure 24). The 2022 results show average turbidity levels for each site were the lowest observed among the 12 years that have been monitored, including 2021, which had been the lowest observed to date. Overall average turbidity in 2022 was about 8 FNU while in 2021 it was 12.5 FNU. From 2007 to 2020, the annual averages ranged from about 17-30 FNU. Average overall turbidity in the pre-construction (2007-2009) and construction (2014-2020) periods both exceeded 20 FNU at 25 FNU and 23 FNU respectively. The overall average during operation has been less than half those levels at only 10 FNU. In addition, at about 10 FNU difference between minimum and maximum levels, the overall ranges of turbidity variation in 2022 (and 2021) are much narrower than previously observed where the ranges may be 20-30 FNU.

The low turbidity levels observed in 2021 were thought to be a result of low flow conditions on the Nelson River that summer: average summer flow (Jun-Sep) was about 2,600 $m^3/s$ (near $5^{th}$ percentile low-flow) in 2021 versus average flows ranging from 3,100-5,500 $m^3/s$ in the previous years. However, because 2022 turbidity was about 33% lower than 2021, the data suggest another cause: low turbidity occurred despite 2022 having a very high average summer flow of about 6,500 $m^3/s$ (near $95^{th}$ percentile high flow), the highest among the 12 years of continuous turbidity monitoring. While the low turbidity levels in 2021-2022 are coincident with the start of Keeyask operation, the fact turbidity is low at Clark Lake (CL-2-b) indicates the reduced turbidity levels are not caused by the Keeyask project. This is because the upstream limit of Keeyask's open-water hydraulic zone of influence is downstream of Clark Lake (see Sec. 2.3): therefore, there are no project impacts on the Split Lake water regime (level, flow) that would cause lower turbidity due to sediment deposition as compared with previous years. Because the apparent decline in turbidity from upstream sources is not caused by the Keeyask project, investigation of the cause of the decline is beyond the scope of the PEMP monitoring.

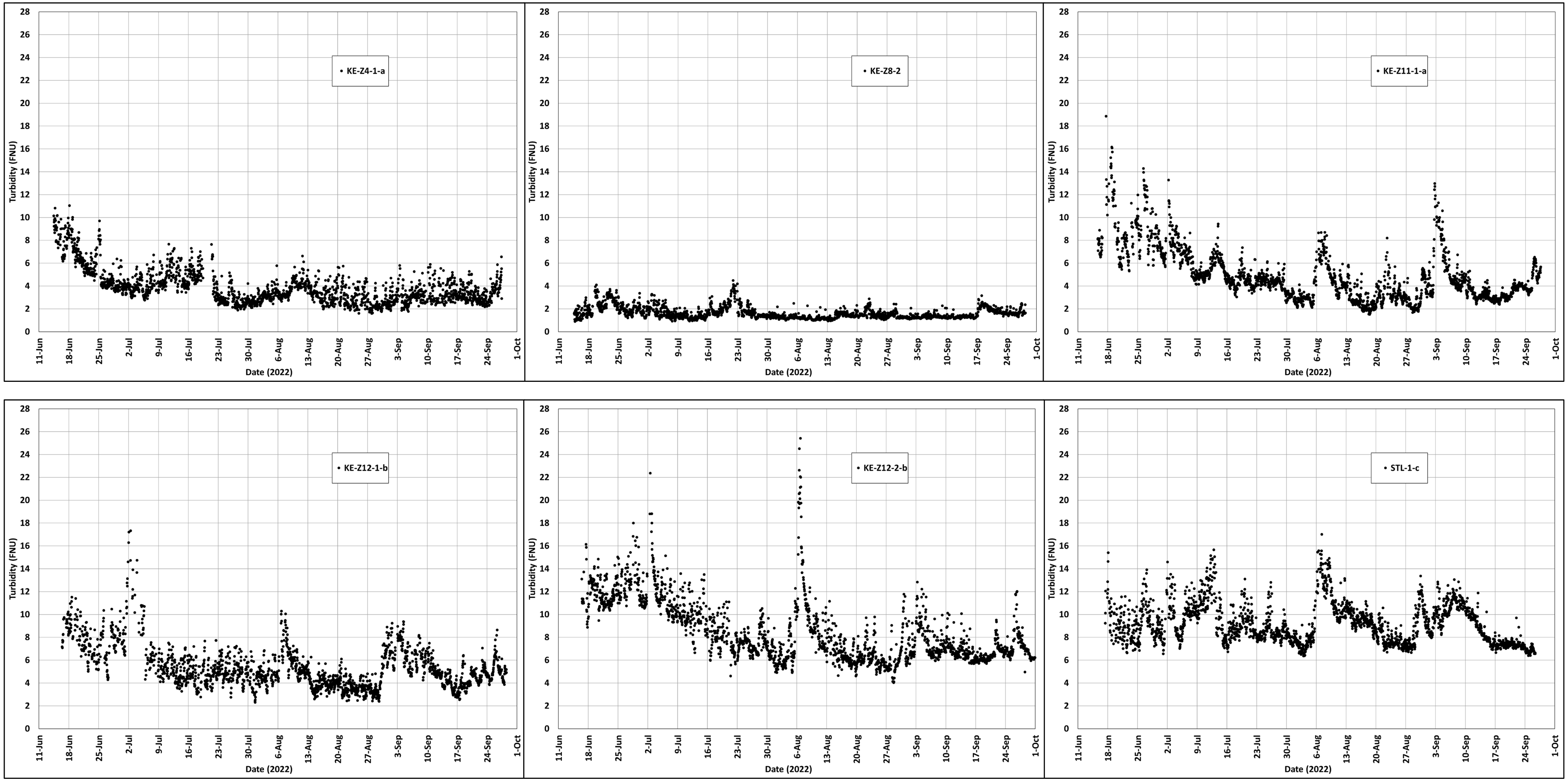


**Figure 23: 2022 summer continuous TU – backbay sites**

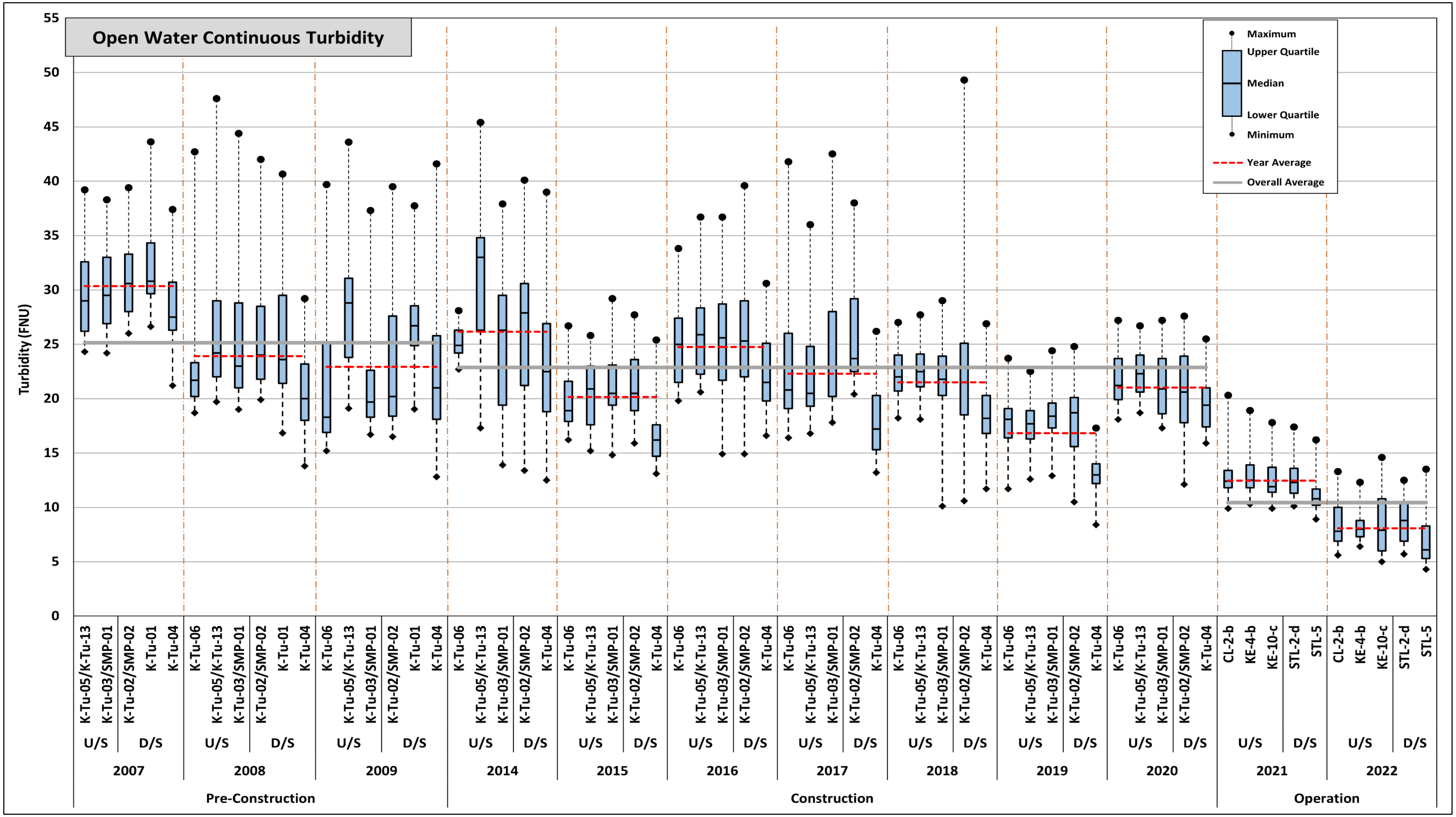


**Figure 24: Summary of mainstem annual summer continuous TU (2007-2022)**

## 4.2.2 DISCRETE TOTAL SUSPENDED SEDIMENT

During the summer period, site visits were performed at both the discrete monitoring sites and at the continuous turbidity sites between Clark Lake and a site in Stephens Lake just upstream of Kettle GS, about 30 km downstream of Keeyask GS (see maps in Appendix 1). Visits were performed to obtain water samples for total suspended sediment (TSS) and in-situ turbidity (TU) readings. The sites were visited 4 times, approximately monthly in June, July, August, and September, typically coinciding with the scheduled monthly maintenance visits at the continuous turbidity sites. Discrete water samples were collected from 35 locations across 11 monitoring sites (1-6 locations sampled per site) along the mainstem and at 14 locations at 12 backbay sites. Two water samples for TSS testing were typically collected at each location at 20% and 80% of site depth. Turbidity measurements were obtained at each of the mainstem water sampling sites and at 46 locations across the 12 backbay sites (up to 4 locations at each site). Turbidity was measured at multiple depths at the monitoring locations. The discrete readings are used to verify the continuous readings, identify variability over depth of the site, and to correlate TSS and TU. Monitoring results were reviewed for vertical variation at the sites but, since values did not have notable vertical variation, the results were summarized considering depth averaged values.

The 2022 TSS concentrations (Figure 25) generally ranged between 1 and 6 mg/l at mainstem and backbay locations. Note that the TSS laboratory detection limit is 2 mg/l and any reported results below 2 mg/l were assumed to be 1 mg/l for reporting purposes (i.e., half the detection limit): therefore, an average TSS less than 2 mg/l indicates it includes results below the detection limit. TSS was generally higher in June than the other months at mainstem and backbay sites, varying from about 3-6 mg/l and 2-6 mg/l respectively. Mainstem TSS was lower in July and August, ranging from about 2-5 mg/l both months, and lower still in September, ranging from about 1-4 mg/l. At backbay sites, TSS was lower in August, ranging from about 2-4 mg/l and, excluding a high value of 5.4 mg/l at site KE-Z9-1-a in September, TSS was lower still in July and September, ranging from 1-3 mg/l both months.

The results do not suggest a consistent pattern of TSS change at mainstem sites from site CL-2 upstream of the Keeysk hydraulic zone of influence to site STL-2 just downstream of Keeyask: neither increasing due to sediment from erosion in the Keeyask reservoir nor decreasing due to deposition as flow passes through the reservoir. site STL-5 typically has lower TSS than the other mainstem sites, consistent with pre-project observations that sediment deposits in Stephens Lake (KHLP 2012b).

Summer 2022 average TSS at the mainstem sites was compared with average concentrations observed previously at sites along the mainstem in 6 years prior to Keeyask construction from 2005-2010, in 7 years of construction from 2014-2020, and in 2 years of operation (Figure 26). Prior to operation, the bulk of the measurements varied from about 10-25 mg/l. Periods of somewhat lower TSS occurred in 2010 prior to construction as well as 2019 and 2020 during construction, each of these years averaging about 10 mg/l. The overall average TSS prior to

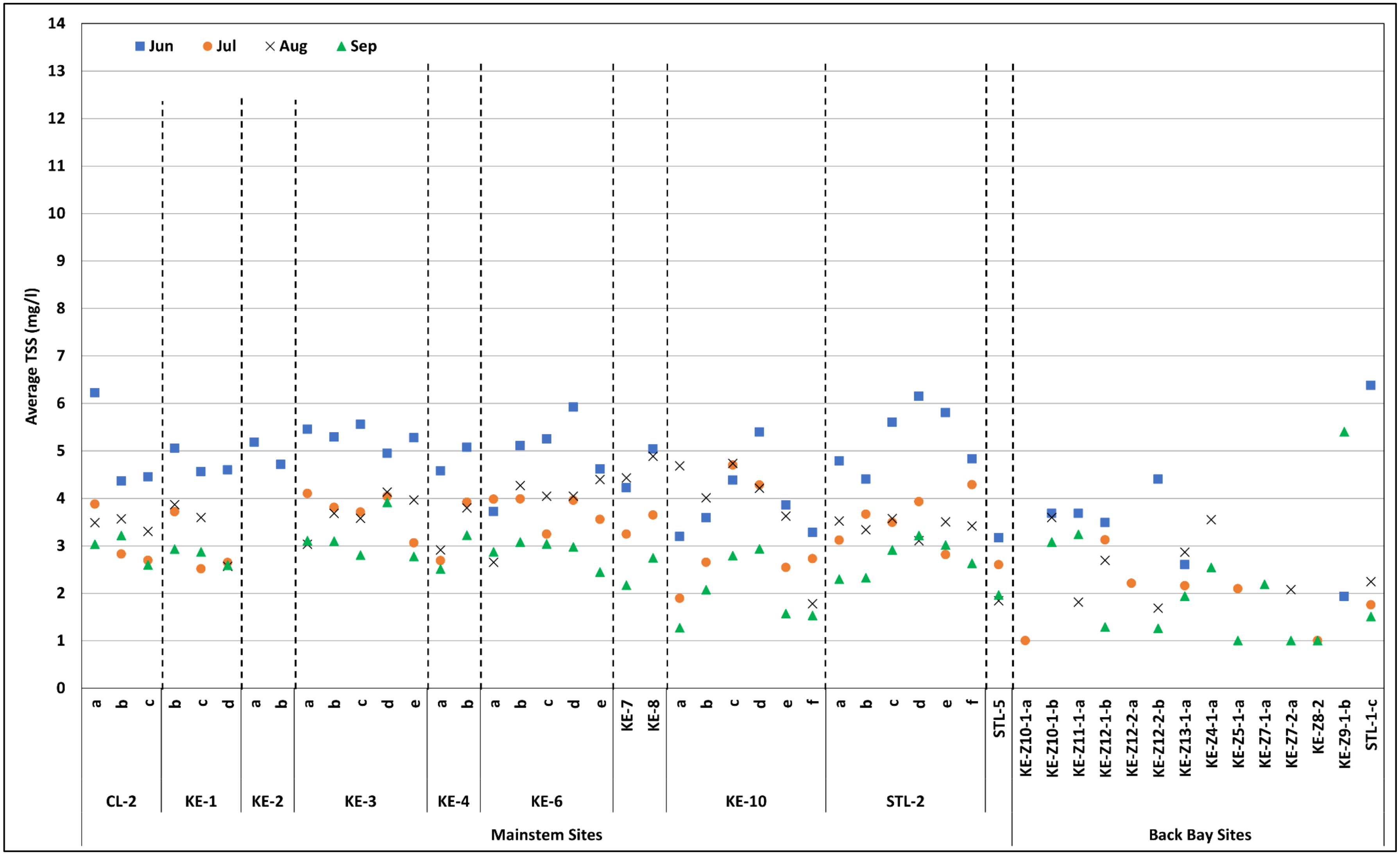


**Figure 25: 2022 summer discrete TSS**

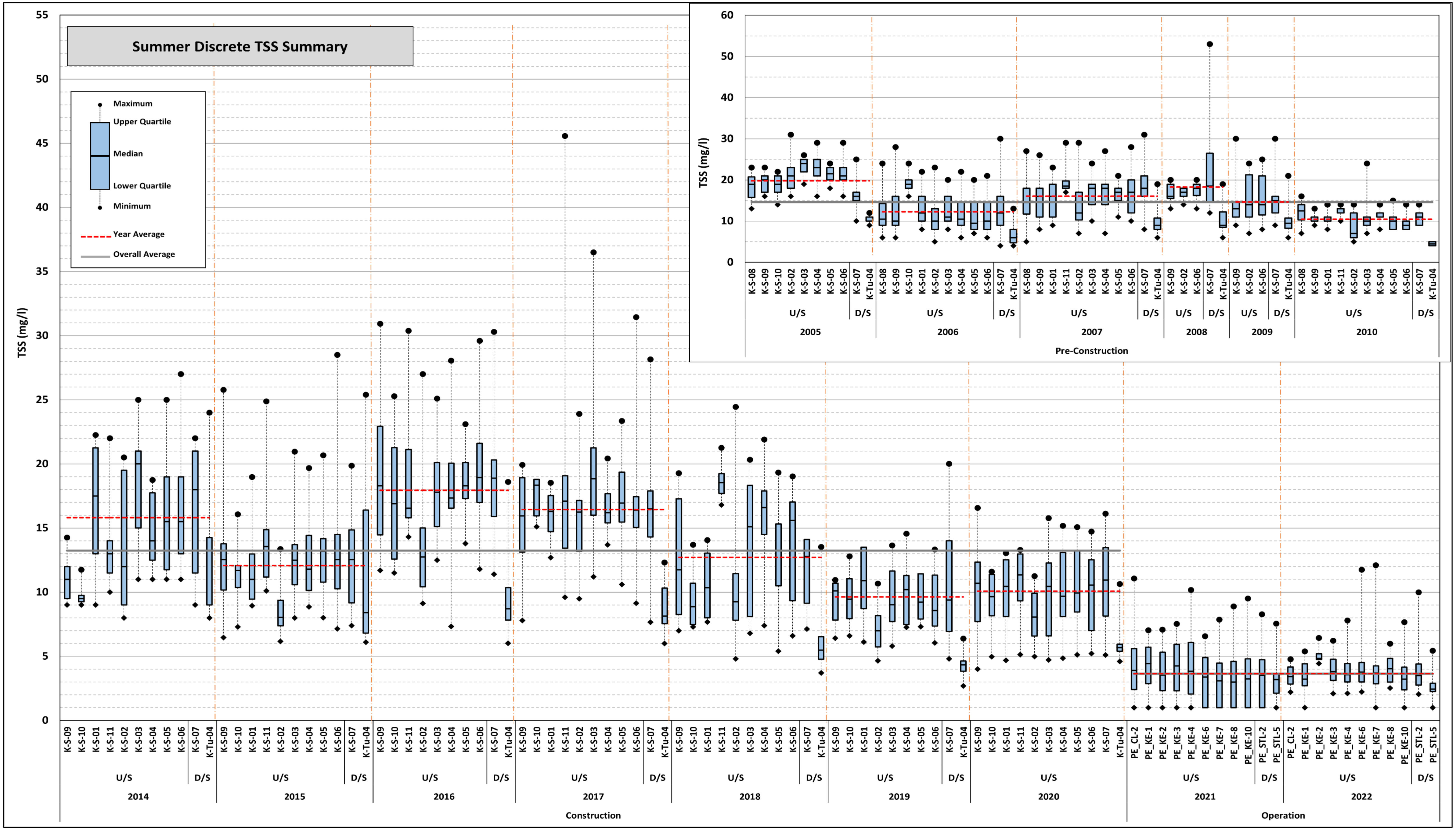


**Figure 26: Summary of annual summer discrete TSS at mainstem sites (2005-2022)**

construction (2005-2010) was about 15 mg/l while the average during construction (2014-2020) was about 13 mg/l (Figure 26). The averages during operation in both 2022 and 2021 were about 3.6 mg/l both years, significantly lower than the previous monitoring periods. The 2022 TSS results were generally less varied (smaller range between 25th to 75th percentiles) but did have a couple of higher TSS values. In both 2021 and 2022 few peak TSS concentrations exceeded 10 mg/l, which is quite different than previous years when the majority of TSS concentrations exceeded that level. The TSS results for 2022 (and 2021) do not display either a significant increasing or decreasing trend through the reservoir between the upstream site at CL-2 to site STL-2 just downstream. This indicates that the TSS is not increasing due to erosion of newly flooded shorelines or decreasing due to deposition of sediment in the reservoir.

The Keeyask EIS (KHLP 2012b) predicted that TSS would decrease about 2-5 mg/l relative to pre-project conditions due to the reservoir, but the results indicate the concentrations in the first two years of operation were more about 10-12 mg/l lower than observed prior to the project and during construction. However, as noted in the preceding section for continuous turbidity, the large decrease in TSS is also observed at the Clark Lake monitoring site (CL-2), upstream of the Keeyask's hydraulic zone of influence. This indicates the large decrease in TSS in 2021-2022 is not caused by the Keeyask project but rather is due to some other upstream process.

### 4.2.3 DISCRETE TURBIDITY

Turbidity monitoring shows a marked difference between mainstem and backbay sampling sites (Figure 27). Generally, turbidity declined over the summer at mainstem and backbay sites: decreasing from about 11 FNU in June to about 9 FNU in July/August and 8 FNU in September at mainstem sites; and, decreasing from about 9 FNU in June to 6 FNU in July and then 5 FNU in August/September at backbay sites. This is consistent with generally decreasing TSS over the summer as noted in the preceding section. Average turbidity each month was higher at the mainstem sites than in the backbays by about 2-4 FNU depending on the month. Turbidity values along the mainstem were above 6 FNU at all sites except for a reading at KE-10-e all results for site KE-10-f, where both locations are near the south dike over flooded peat. The mainstem sites largely varied from about 6-12 FNU. Turbidity levels were more varied at the backbay sites, largely ranging from about 2-11 FNU.

Site STL-1 tended to have higher turbidity than other backbay sites in Jun-Aug, which is not unexpected as the west side of Stephens Lake has previously been observed to have higher levels of sediment. Remote sensing data from Sentinel 2 satellite imagery was used to estimate TSS in the study area from Clark Lake to Stephens Lake. The results highlight the spatial variation of TSS between areas upstream of Keeyask and the west side of Stephens Lake (Figure 28). Images from June 17, August 13, and September 5, 2022, show higher levels of turbidity along the west side of Stephens Lake north of Keeyask GS as compared with areas upstream of the GS. Generally, the high TSS on Stephens Lake is due to wind effects, particularly strong north and east winds. The variability observed in the satellite imagery is consistent with discrete TU and TSS observations.

The backbay sampling locations are labeled in order with the ‘a’ locations (or 1 for site KE-Z8) being deeper in the bay, further from the main stem flow, while locations b, c and d (or 2, 3, 4 for KE-Z8) are progressively nearer the mainstem. It is interesting to note that for almost each site in each month of sampling, turbidity is lowest at the ‘a’ (or 1) location furthest from the mainstem and incrementally increases to the ‘d’ or ‘4’ location closest to the mainstem (Figure 27). This may indicate a diminishing influence of mixing from the mainstem flow into the far ends of the backbays. Note this pattern is not observed for site KE-Z9-1 due to its relative isolation from the main body of the reservoir and STL-1, which is not near the main flow. This pattern is also consistent with the spatial variability observed in the satellite imagery (Figure 28).

The 2022 discrete turbidity data at the mainstem sites was summarized and compared with turbidity levels observed in 5 years prior to Keeyask construction from 2006-2010, in 7 years of construction from 2014-2020, and in 2 years of operation (Figure 29). As observed with TSS results in the previous section, the average mainstem TU for the summer 2022 operating period was significantly lower than turbidity levels observed before and during construction. The overall average in 2022 was about 9 FNU, which is about 5 FNU lower than the 14 FNU average observed in 2021. The bulk of discrete turbidity readings in 2022 were less than about 12 FNU, which is markedly different than observations from 2006-2020 when few readings were below 12 FNU. The average in 2021-2022 during operation is about 11.6 FNU, which is approximately half the overall turbidity of 22 FNU during construction and less than half the 26.2 FNU average prior to construction. As noted for continuous TU and discrete TSS, the decrease in discrete turbidity during operation is not related to Keeyask operation since the changes are also observed at Clark Lake site CL-2, which is upstream of Keeyask’s hydraulic effects.

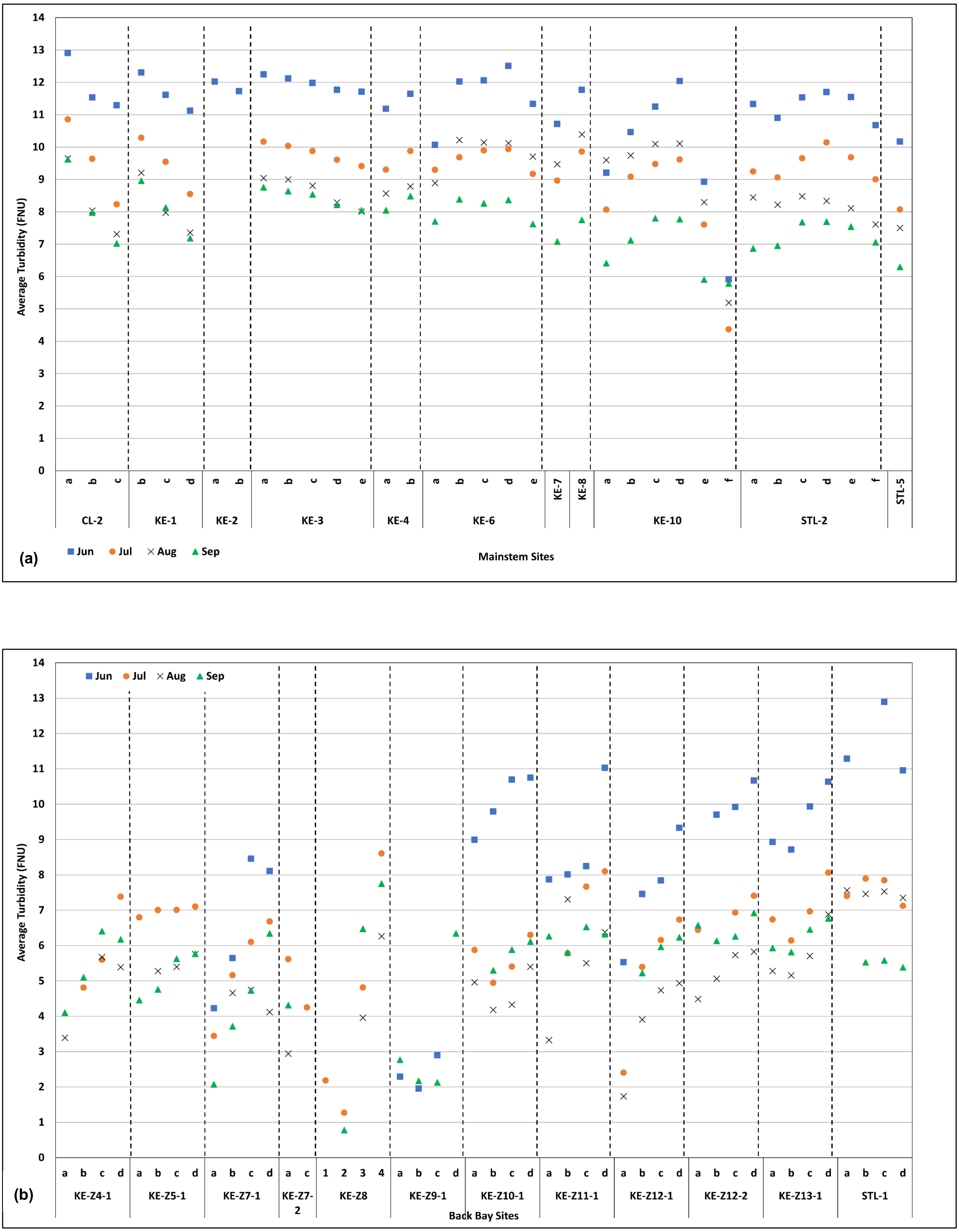


**Figure 27:** **2022 summer discrete TU at (a) mainstem sites, (b) backbay sites**

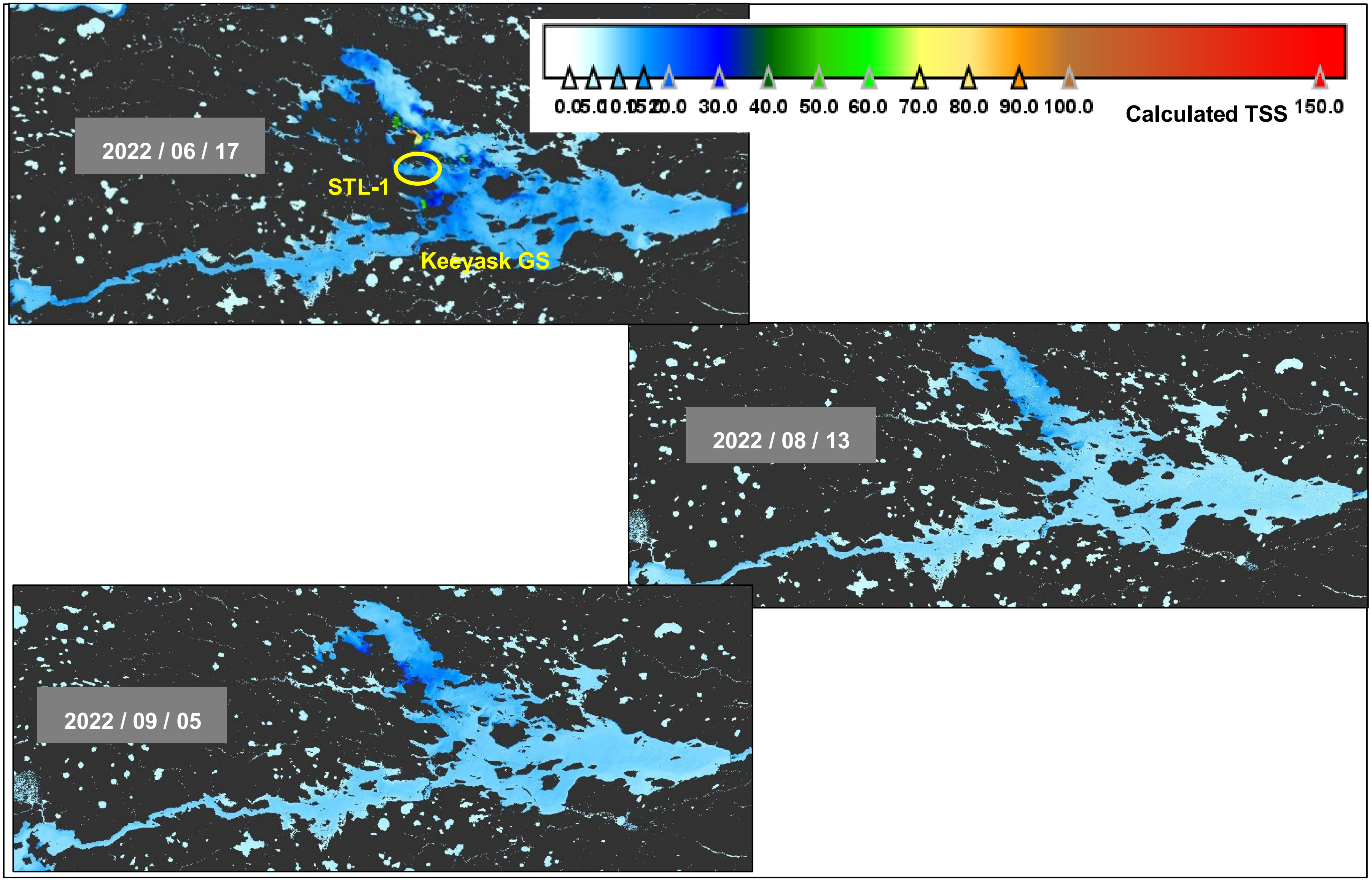


**Figure 28: Spatial variation of TSS calculated from Sentinel 2 satellite data**

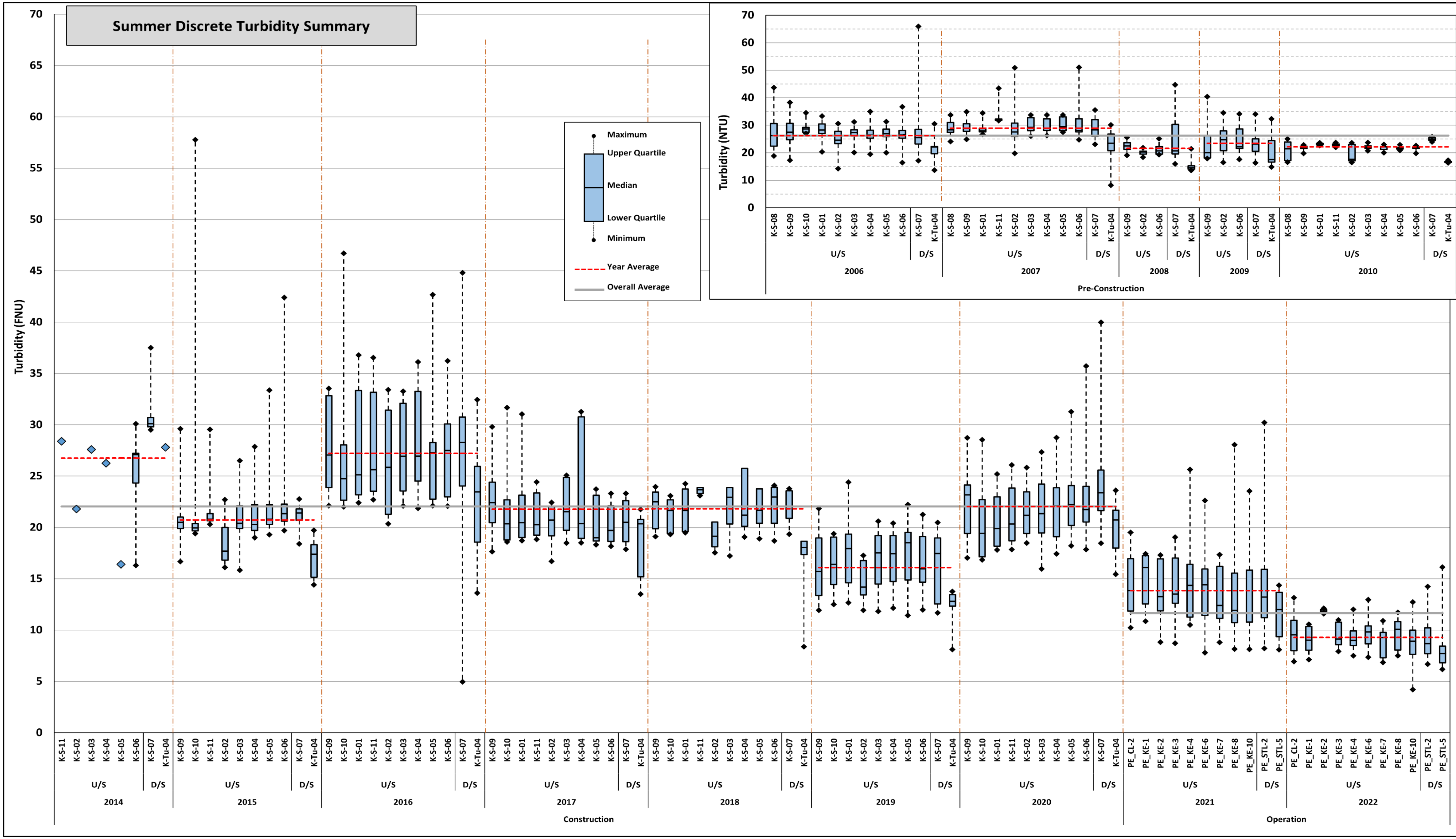


**Figure 29: Summary of annual summer discrete TU at mainstem sites (2006-2022)**

### 4.2.4 ESTIMATED SUSPENDED SEDIMENT LOAD

The summer suspended sediment loads (Figure 30) were estimated based on the average daily turbidity calculated from the continuous monitoring data and the calculated Keeyask inflow. Turbidity was converted to TSS concentrations using based on TSS-TU relationships derived from discrete data obtained each monitoring year prior to operation and using a relationship derived from the combined discrete data for the operating years.

The 2022 average summer suspended sediment load was approximately 1,500 t/d, which is about 600 t/d greater than observed in 2021 despite the average continuous TU being lower in 2022: the load is higher because the flow is much greater in 2022.These sediment loads are much lower than observed prior to and during construction when average annual loads ranged from 6,250-7,650 t/d and 2,750-8,350 t/d respectively. The average sediment load during the two years of operation is about 1,150 t/d, which is less than on quarter the loading of about 4,900 t/d during construction and about a sixth of the 6,850 t/d loading prior to construction. Again, as noted in previous sections, the marked decrease in loading during operation is not due to Keeyask since the change is also observed at the upstream Clark Lake site CL-2, indicating the effect is due to processes upstream of Clark Lake and the hydraulic influence of the Keeyask project.

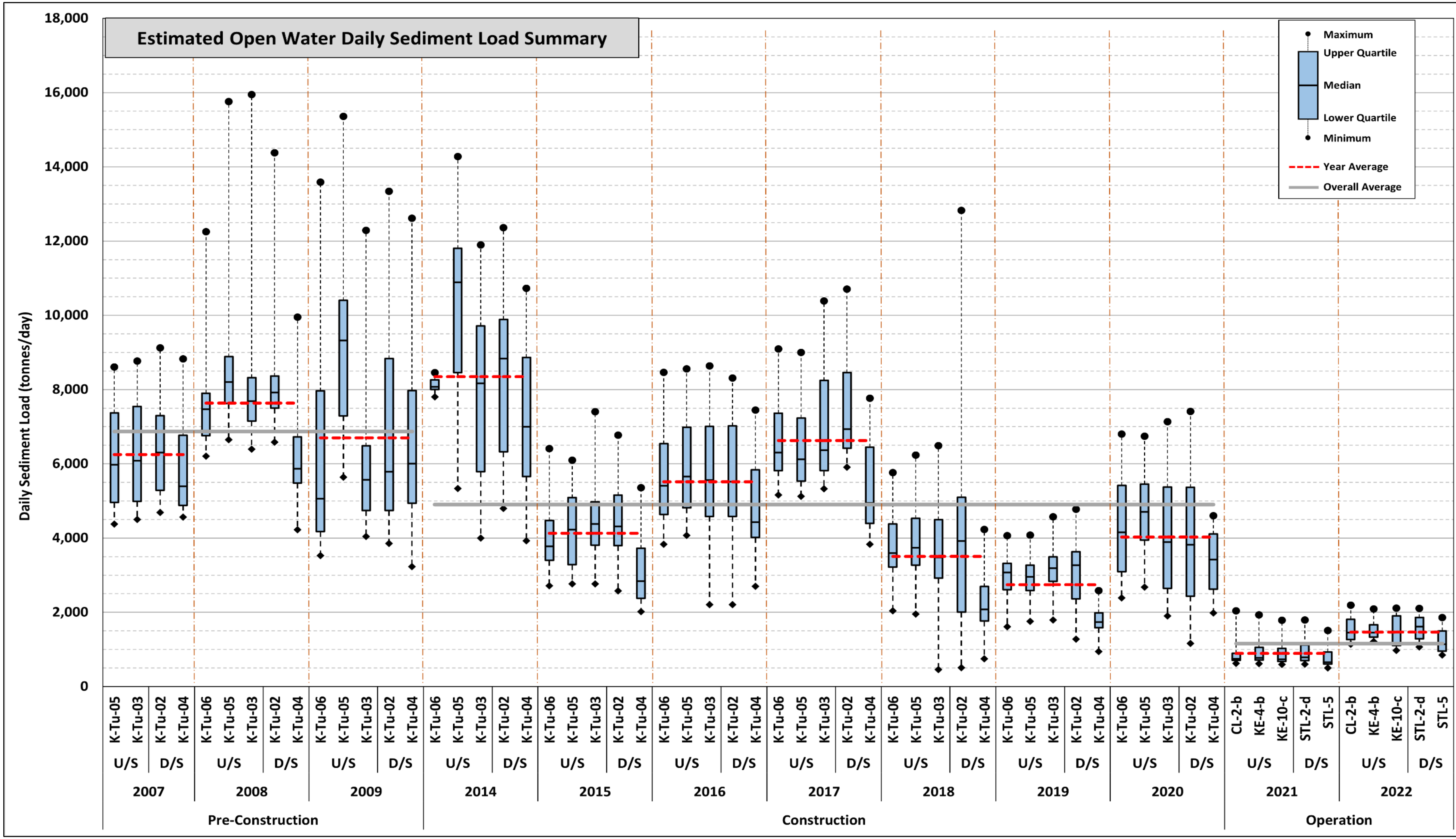


**Figure 30: Summary of estimated summer daily sediment load**

### 4.2.5 DEPOSITION

Sediment traps with two vertical tubes (Photo 5) were installed in Gull Lake and Stephens Lake to monitor the sediment accumulation rate over the 2021/22 winter and the 2022 summer periods. One tube is a settling trap that is open at the top and the second tube is a flow through trap that has holes in the side to allow water and sediment to flow into it. Sediment trap data from 2022/23 and previous years are under combined review that will need to consider data from 2023/24 and reporting will therefor be deferred to subsequent annual report.

**Photo 5: Sediment traps - 2 tube design**

# 5.0 ORGANIC CARBON

## 5.1 PREDICTED PROJECT EFFECTS ON ORGANIC CARBON

Organic carbon (total, dissolved and particulate) in the water was not expected to be affected by construction prior to impoundment of the reservoir but was measured during construction to provide baseline data. Although changes to organic carbon were not specifically predicted, the Keeyask EIS did estimate the potential increase in organic sediment concentration (i.e. peat, of which carbon is but one of the component elements) in the mainstem areas of Gull Lake (zones 1-3) and the flooded backbays (PESV Vol. 7, Table 7.4-5). The analysis was based on estimated volumes of broken-down peat being suspended in the different peat transport zones in Gull Lake and its flooded backbays during open water conditions. It considered the increase for year 1, the first year after impoundment when the greatest amount of breakdown was predicted, and years 2 and 5 which were predicted to have progressively less peat breakdown. Conditions in 2021 represent year 1, the first year of operating conditions after impoundment in 2020.

In the mainstem areas (zones 1-3) peak estimated increases in suspended organic sediment concentration were low, ranging from 0-2 mg/l (PESV Vol. 7, Table 7.4-5). Among backbay zones, the predicted peak increases in zones 5, 10 and 13 were low, ranging from 2-4 mg/l. More moderate peak increases of 8-10 mg/l were predicted for zones 7, 9 and 12, although this would represent a large overall increase in suspended material considering typical TSS concentrations. Large peak increases of 15 and 21 mg/l were predicted for zones 11 and 8 respectively due to the large amount of peat predicted to break down in these areas and their small overall volumes. Although changes in organic carbon concentrations were not directly predicted in Keeyask EIS, the estimates of peak suspended organic sediment effects may suggest which areas are more or less likely to experience larger or smaller effects on organic carbon concentrations.

## 5.2 WINTER 2022

Discrete water samples were obtained at up to 4 sites once a month from January to April 2022 between Clark Lake and the entrance to Stephens Lake along the mainstem of the river: backbays were not sampled. These water samples were tested to measure the concentrations of Dissolved Organic Carbon (DOC) and Total Organic Carbon (TOC). These results are used to calculate the amount of Particulate Organic Carbon (POC), since POC is equal to TOC minus DOC. Note that in some cases the lab reported DOC is greater than the reported TOC, although the two values tend to be relatively close (1-2 mg/l difference), suggesting POC is likely limited.

Typically, water samples were obtained at two or three depths in the water column (e.g., 20% & 80% depth) on each sampling visit. For purposes of the organic carbon analysis, the respective TOC or DOC results obtained from multiple depths at a site for each sampling day were averaged to get a single concentration value for the site and the results for each month were plotted (Figure 31). Where the average TOC exceeds DOC the plot shows the calculated POC, but where DOC exceeds TOC only the DOC is plotted: thus the plot shows the maximum organic average organic carbon concentration. The results do not suggest any apparent trend during the winter period, nor do they indicate trend from upstream to downstream.

The organic carbon concentration varied from about 7-10 mg/l, although most values were above 8 mg/l, while the overall average was about 8.6 mg/l (

Table 6). The range and average of TOC in winter 2022 was similar to conditions observed in previous winter periods. The results do not suggest any significant change in winter resulting from reservoir impoundment and project operation.

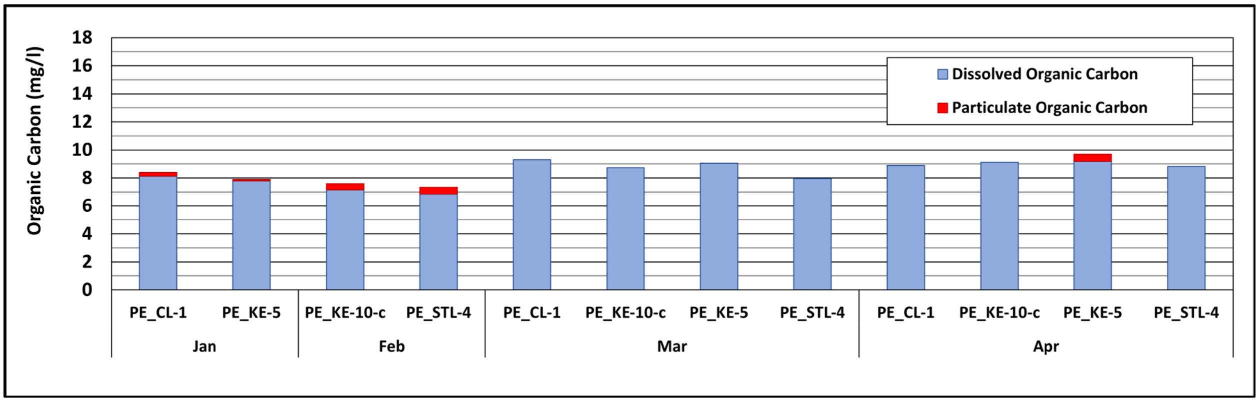


**Figure 31: DOC, POC and TOC in winter 2022**

**Table 6: Summary of maximum average organic carbon (DOC or TOC) concentration during construction and operation**

| Year | Open Water (Jun-Sep) | | | | Winter (Jan-Apr) | |
|---|---|---|---|---|---|---|
| | Mainstem | | Backbays | | Mainstem | |
| | Range | Avg | Range | Avg | Range | Avg |
| 2015 | 8-9 | 8.4 | | | | |
| 2016 | 7.5-9.5 | 8.3 | | | | |
| 2017 | 8-10 | 8.4 | | | 8-10 | 9.5 |
| 2018 | 9-10 | 9.5 | | | 9-10 | 9 |
| 2019 | 7.5-8.5 | 8.2 | | | 8-11 | 9 |
| 2020 | 8.5-10 | 9 | | | 7-9 | 8 |
| 2021 | 7.5-10.5 | 8.8 | 8-16 | 10.3 | 6-10 | 8.6 |
| 2022 | 7-13 | 8.6 | 6.1-13.5 | 8.6 | 7-10 | 8.6 |

## 5.3 SUMMER 2022

Discrete water samples were obtained at up to 48 separate sampling locations at up to 23 sampling sites: e.g., sampling site STL-2 has 5 sampling locations a-f across the width of the river. Samples were obtained once a month from June to September 2022, between Clark Lake and Stephens Lake near Kettle GS. This included up to 38 locations along the mainstem of the river and up to 12 sites in flooded backbays. As was the case for winter organic carbon, the POC was calculated as the difference between lab measured TOC and DOC, but in many of the results for June, July and September, DOC exceeds TOC but, because the difference between the two is typically less than 1 mg/l, the TOC is assumed to be equal to DOC where the DOC is larger for the purposes of analysis and plotting. Results for August 2022 were notably different than the other three months, with DOC exceeding TOC by 3-6 mg/l at most sampling locations. The cause of this larger discrepancy in August is uncertain, but for the purposes of reporting the larger value between DOC or TOC is considered to represent the total concentration to avoid under-representing conditions.

The averaged organic carbon concentrations were plotted for each sampling location for the mainstem and backbay sites in each month (Figure 32). The results do not suggest any trend in organic carbon concentrations along the mainstem from upstream to downstream, indicating no increases occurring due to the reservoir. An upstream to downstream trend would not be expected for the backbay sites. Unlike 2021 (KHLP 2022), when higher organic carbon concentrations tended to occur in backbays, the results from 2022 show organic carbon concentrations are generally within similar ranges in the mainstem and backbays in each month. While conditions were similar in June, July, and September, suggesting no strong seasonal trends, some higher concentrations were measured in August as noted above but it is not clear that this indicates a seasonal effect.

In June, July and September, the organic carbon concentrations generally varied from 7-9 mg/l in both the mainstem and backbay areas (Figure 32). Two exceptions that stand out were at the backbay locations KE-Z9-1-b and KE-Z8-2 which had organic carbon concentrations up to 12 mg/l and 13 mg/l respectively. August differs from the other three months with generally higher concentrations. However, higher values exceeding about 10 mg/l are more prevalent for the upstream mainstem locations at sites KE-CL-2, KE-1, KE-3 and KE 4 (Figure 32). At the more downstream mainstem sites and backbay sites the concentrations are more typically in the range of 8-10 mg/l with only four of these locations exceeding 10 mg/l. It is not entirely clear why organic carbon might be elevated in August at the more upstream sites. However, sampling was done on August 10 when inflow was at its 2022 peak of about 6,600 $m^3/s$, which is among the historic high flows into Gull Lake. It may be that high flows and water levels from upstream resulted in greater amounts of organic carbon in the water, but it is not clear why higher DOC would primarily occur at the upstream sites but not downstream since the dissolved component would not be subject to deposition in the reservoir that would result in a concentration decrease, as may occur with particulate material.

Overall, the results from 2022 are consistent with previous observations and do not suggest any significant effect of the project on organic carbon concentrations along the mainstem from Clark Lake to the Keeyask GS, nor in the water discharged downstream.

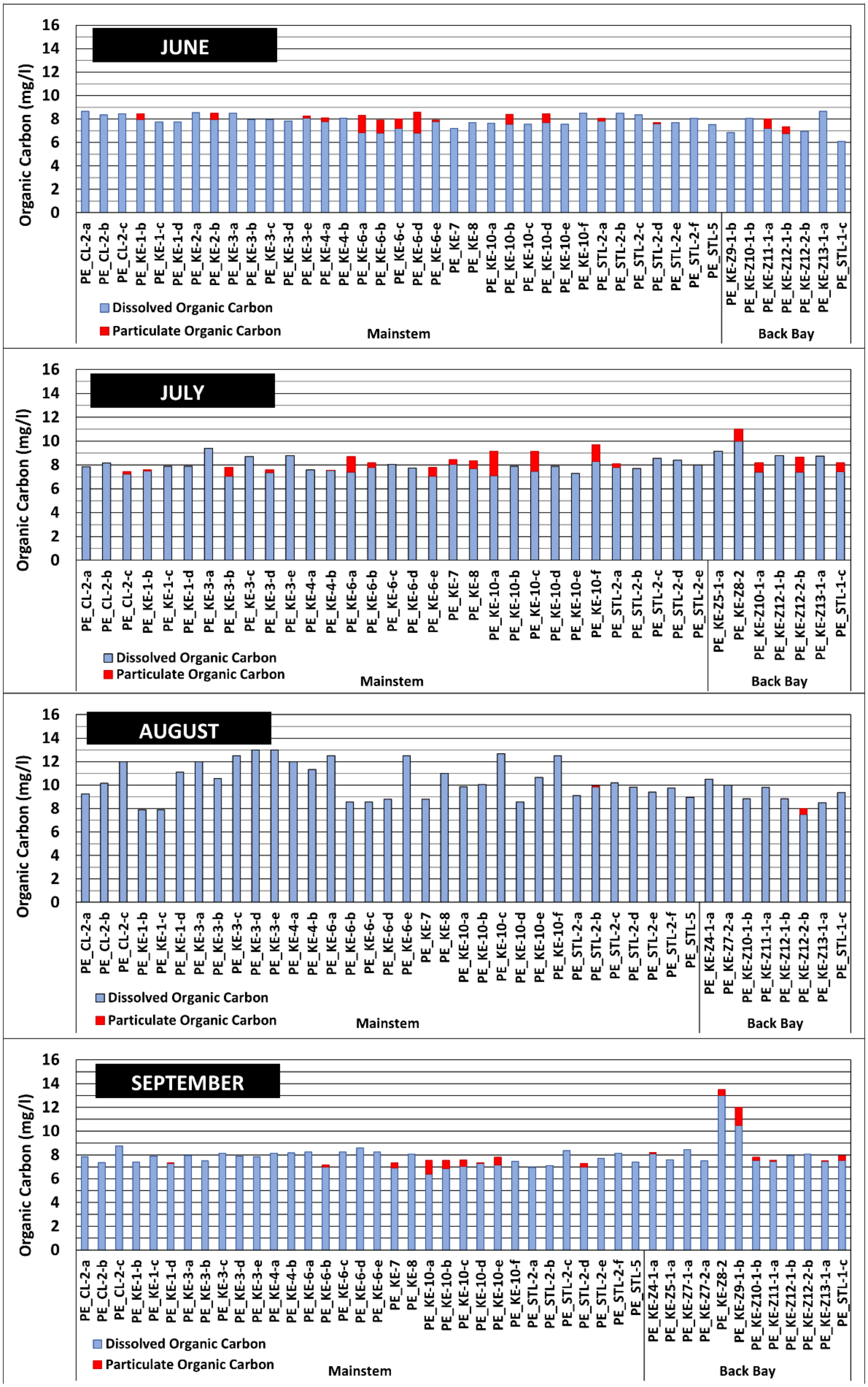


**Figure 32: DOC, POC and TOC in summer 2022**

# 6.0 DISSOLVED OXYGEN

Dissolved oxygen (DO) and water temperature (T) monitoring was performed using electronic sondes to collect in-situ measurements of these parameters along with percent saturation calculated based on ambient conditions. The monitoring included collection of discrete measurements in both winter (Dec 2021 – Apr 2022) and summer open water period (Jun-Sep), as well as continuous monitoring at several sites in both seasons. Discrete monitoring involved obtaining measurements through the depth of the water column to identify vertical variability, particularly to see if DO is reduced near the bottom in water overlying flooded peat. Continuous monitoring involved placing one or two sondes at each monitoring site for several months. Two sondes were used at some locations, with one sonde placed near the water surface and the other just above the bed, to identify if DO concentrations differ between the surface and bottom. The discrete and continuous data sets were reviewed for data quality and erroneous and inconsistent data were filtered out. For the continuous data sets, the review tended to err on the side of leaving data in rather than remove potentially suspect data.

## 6.1 2022 WINTER DISCRETE & CONTINUOUS DO

### 6.1.1 WINTER DISCRETE DO

In winter 2021/22 (Dec-Apr), discrete DO and T monitoring was performed at 4 sites along the mainstem of the Nelson River from Clark L upstream (site CL-1) to just downstream of Keeyask GS in Stephens Lake (site STL-4), 11 sites in backbays flooded by the project and a backbay in Stephens L. At the mainstem sites only one location was sampled. In backbays, measurements were obtained at four sampling locations at each site. The sites and locations monitored were (see Appx. 1 for locations):

- Mainstem sites
  - CL-1; KE-5; KE-9; and STL-4
- Backbay sites (four locations measured at each identified as a, b, c, d, except KE-Z8 which has locations 1, 2, 3, 4)
  - KE-Z4-1; KE-Z5-1; KE-Z7-1; KE-Z7-2; KE-Z8; KE-Z9-1; KE-Z10-1; KE-Z11-1; KE-Z12-1; KE-Z12-2; KE-Z13-1; and STL-1

Charts showing the measured depth profiles of DO concentration, % saturation[1] and T are provided in Appendix 2.

[1] Saturation concentration is the DO concentration that water at a given temperature will tend to maintain in the absence of bio-chemical DO consumption, which reduces DO, or addition of excess DO from turbulent flow, which causes supersaturation.

Monitoring results for the mainstem sites showed that DO was high through the winter at these locations and T was just above 0°C (Appx. 2). At each site, the DO was about 14-15 mg/l with a percent saturation between 95%-100%. The same results were observed for the sites upstream of the GS (CL-1, KE-5, and KE-9) in the winter 2021 (Jan-Apr) monitoring. At site STL-4, the concentrations were somewhat higher in 2021 when elevated DO concentrations were observed because the spillway was operating, which caused entrainment of additional oxygen, leading to super-saturated conditions (Manitoba Hydro, 2022).

To generally summarize discrete DO concentrations observed at the backbay monitoring sites, the DO conditions were identified as being either low, moderate, or high depending on the range of concentrations observed during the winter period. These classifications are defined based on consideration of the minimum 7-day average and instantaneous DO objectives when water temperatures are below 5°C for cool and cold aquatic species (Manitoba Water Stewardship, 2011). The 7-day average DO objectives for cool and cold-water species are 4 mg/l and 9.5 mg/l respectively while the respective instantaneous objectives are 3 mg/l and 8 mg/l. Based on these objectives, the following classifications were used to describe the DO variation between the surface and bottom for the 48 backbay sampling locations (Table 7):

- Low < 4 mg/l < Moderate < 9.5 mg/l < High.

**Table 7: Summary of winter discrete DO conditions at backbay sites**

| Site/ Location[1] | a or 1 | b or 2 | c or 3 | d or 4 |
|---|---|---|---|---|
| KE-Z4-1 | H / M[2, 3] | H / M | H | H |
| KE-Z5-1 | H | H | H | H |
| KE-Z7-1 | H / M | H | H | H |
| KE-Z7-2 | H | H | H | H |
| KE-Z8 | M / L | M / L | H / M | H |
| KE-Z9-1 | H / M | H / M | H / M | H / M |
| KE-Z10-1 | H | H | H | H |
| KE-Z11-1 | H / M | H | H | H |
| KE-Z12-1 | H | H | H | H / M |
| KE-Z12-2 | H | H | H / M | H / M |
| KE-Z13-1 | H | H | H | H |
| STL-1 | H | H | H | H |

Notes:

1. Site locations are designated by a, b, c or d (e.g., KE-Z4-1-a, KE-Z9-1-c, etc., except for KE-Z8 which is designated by 1, 2, 3, or 4 (i.e., KE-Z8-1, KE-Z8-2, etc.)
2. DO classified based on concentration where: low (L) < 4 mg/l < moderate (M) < 9.5 mg/l < high (H)
3. Single L, H or M indicates condition through depth of water column while combinations indicate variation from surface to bottom (e.g., H / L, high near surface low near bottom)

The results show that for most monitoring locations, 34 of 48, the discrete DO concentrations were classified as high through the depth of the water column. At 12 of the monitoring locations, the DO varied from high near the surface to moderate near the bottom. Only 2 of the monitoring sites had low DO. At both locations, the DO was moderate near the surface while the low DO concentrations were only observed right at the bottom. This is notably different from 2021 when low DO was observed at 12 locations. Most of the sites, 10 of 14, where moderate or low DO was observed also had reduced DO in 2021.

The majority of backbay sites, including those identified as having high DO concentrations, showed some vertical variation in DO concentration with generally higher levels near the surface and lower concentrations near the bottom (Figure 34, Appx. 2). In most cases the variation occurs within the lower 1-2 m of the water column. Similarly, some variation in T is also observed at the backbay monitoring sites, typically with lower temperatures at the surface and higher temperatures near the bottom (Appx. 2). Although temperatures remain below 1°C through the water column at most of the sites, a couple of locations have water temperatures up to 2-3°C, including each site in zone KE-Z9.

Overall, the winter DO results are generally consistent with expectations for winter DO in the Keeyask EIS (KHLP 2012b). Concentrations at monitoring sites KE-Z7-1, KE-Z7-2, KE-Z10-1 and KE-Z-11-1 may be somewhat higher than expected for backbay areas. It was expected that very low DO would be likely to develop in KE-Z9-1 because it is cut off from the reservoir in winter.

### 6.1.2 WINTER CONTINUOUS DO

Continuous DO sensors were placed near the surface below the ice at 4 mainstem locations between mid-January to mid-April at monitoring sites CL-1, KE-5, KE-10-c and STL-4. Monitoring results showed DO concentrations along the mainstem remained high, with all 4 sites having DO concentrations between 14-15 mg/l throughout the winter (Figure 33). These DO concentrations were at or near 100% saturation during the monitoring period. Although the spillway did pass flow for a couple of weeks during the monitoring period, elevated DO concentrations were not observed at STL-4, likely due to the spill volumes being small relative to the total flow.

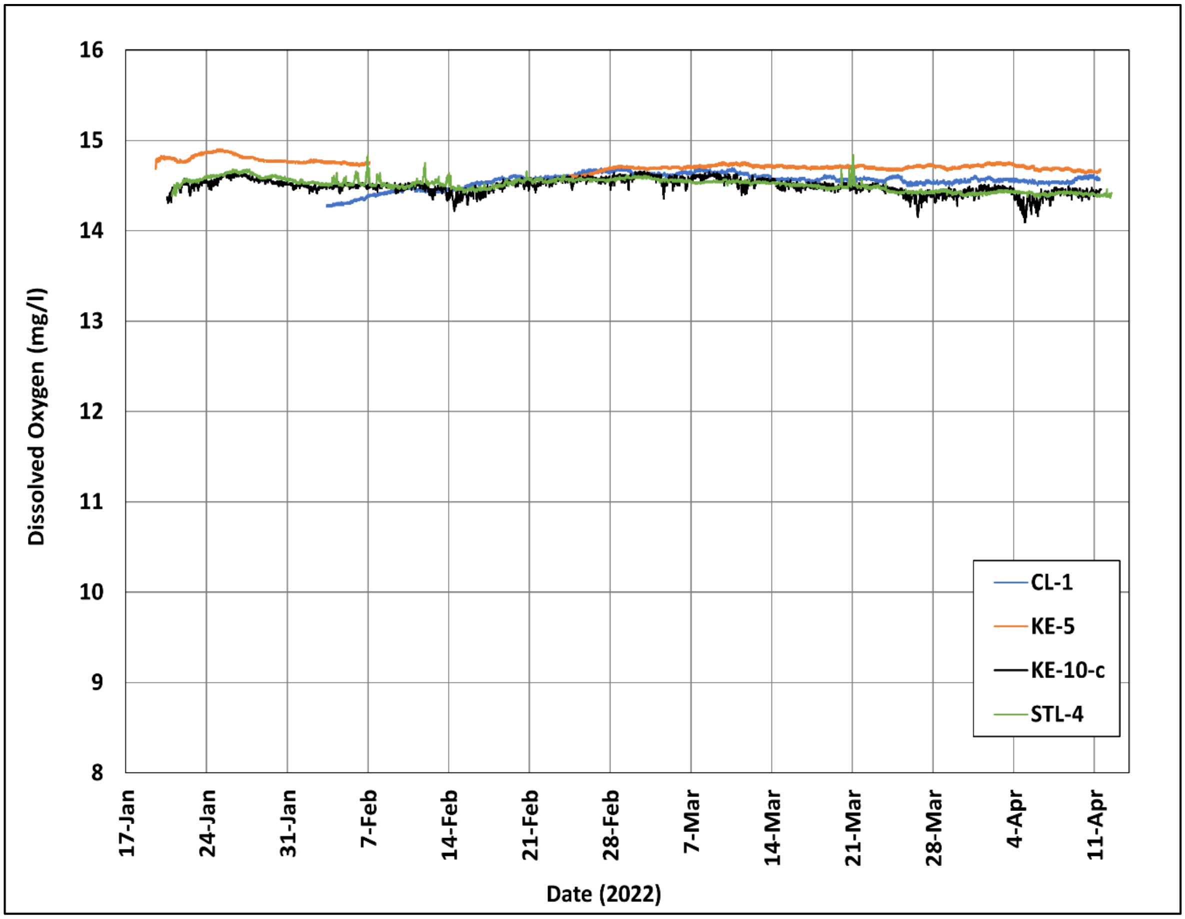


**Figure 33: Winter Continuous DO at mainstem sites**

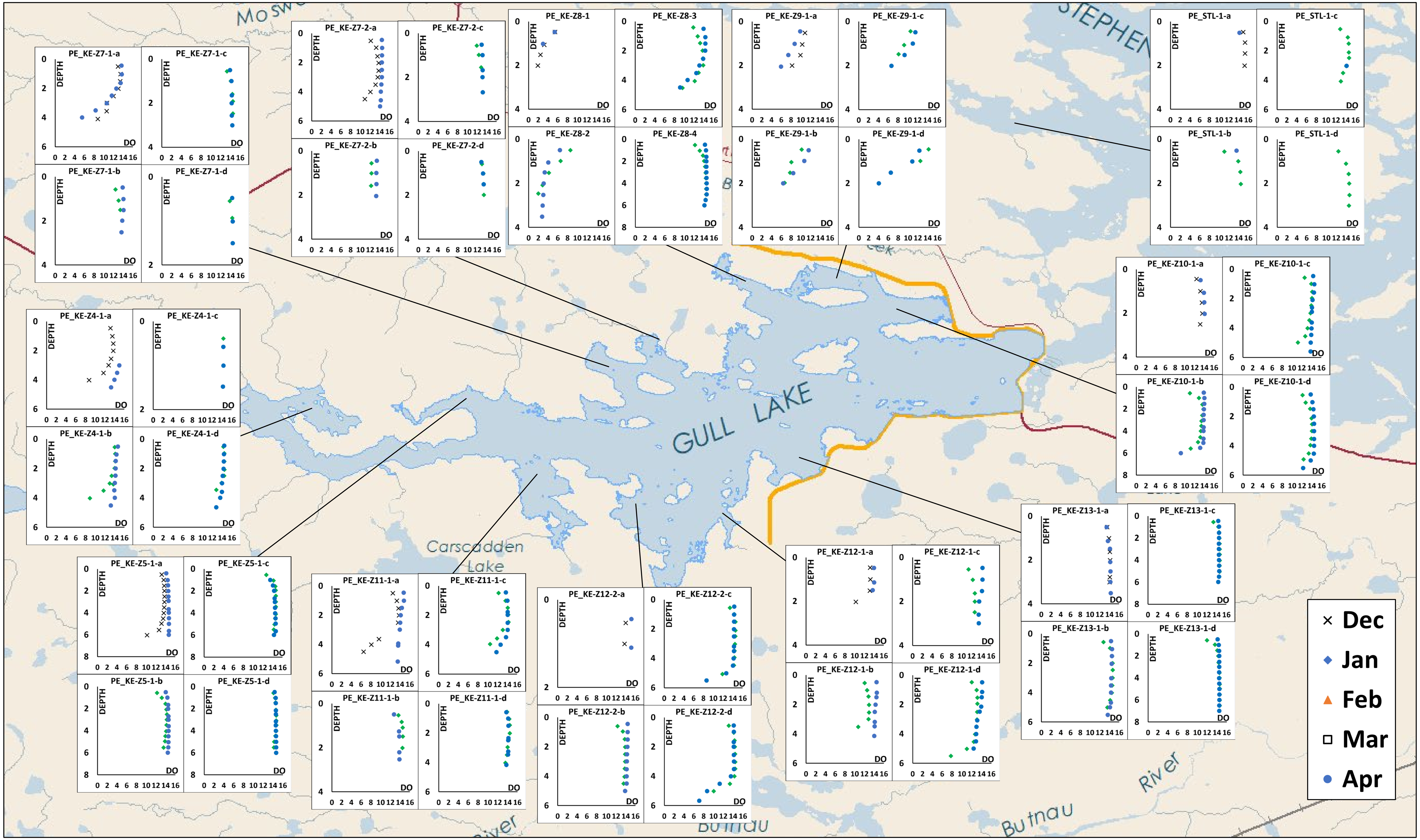


**Figure 34: Winter DO depth profiles in backbays**

# 6.2 2021 SUMMER DISCRETE & CONTINUOUS DO

## 6.2.1 SUMMER DISCRETE DO

In summer 202s (Jun-Sep), discrete DO and T monitoring was performed at 11 sites along the mainstem of the Nelson River from Clark L upstream (site CL-2) to about 30 km downstream of the Keeyask GS in Stephens Lake (site STL-5), plus 11 sites in backbays flooded by the project and a backbay in Stephens L. Up to six sampling locations were monitored across the width of the river at the mainstem sites. In backbays, measurements were obtained at four sampling locations at each site. The sites and locations monitored were (see Appx. 1 for locations):

- Mainstem sites
  - CL-2-a to c (i.e., PE_CL-2-a, PE_CL-2-b, PE_CL-2-c); KE-1-b to d; KE-2-a & b; KE-3-a to e; KE-4-a and b; KE-6-a to e; KE-7; KE-8; KE-10-a to f; and STL-2-a to f; and STL-5
- Backbay sites (four locations measured at each identified as a, b, c, d, except KE-Z8 which has locations 1, 2, 3, 4)
  - KE-Z4-1; KE-Z5-1; KE-Z7-1; KE-Z7-2 (excluding b & d); KE-Z8; KE-Z9-1; KE-Z10-1; KE-Z11-1; KE-Z12-1; KE-Z12-2; KE-Z13-1; and STL-1

Sampling was generally done at each site in June, July August, and September, although some locations were sampled only 1-3 times. Sample locations KE-Z7-2-b and KE-Z7-2-d were not sampled because floating peat mats covered these locations. Charts showing the measured depth profiles of DO concentration, % saturation and T for each monitoring site are provided in Appendix 3. Depth profiles of backbay DO concentrations are also displayed together for comparison between the different monitoring sites (Figure 36).

Since the study area is aligned in a general west-east direction, the average concentrations at each location and date of sampling were plotted based on the planned easting of each sample location to identify any upstream to downstream trends that may be due to the project (Figure 35). Monitoring results showed that DO was high at all mainstem sites. Except for a few locations on particular, the DO concentrations at mainstem sites were typically in the range of 8.5-10 mg/l, with a degree of saturation between about 95%-100%. This was for conditions where water temperature ranged from a low of about 14°C in June and September to 20°C in July. DO concentrations was typically uniform through the water column depth at each sampling location.

The results show relatively uniform DO conditions from upstream to downstream along the mainstem, with some more variation at location KE-10 immediately upstream of the dam and at STL-2 immediately downstream. Some lower DO values were observed at location KE-10-f, which is in shallower water over flooded land near the south shore. Elevated DO concentrations were observed at sites STL-2-e and STL-2-f closer to the south shore, which resulted due to operation of the spillway, which causes excess oxygen to be entrained in the water. DO saturation level was about 85% for the low DO concentrations at KE-10-f and up to 118% for peak levels at STL-2-f.

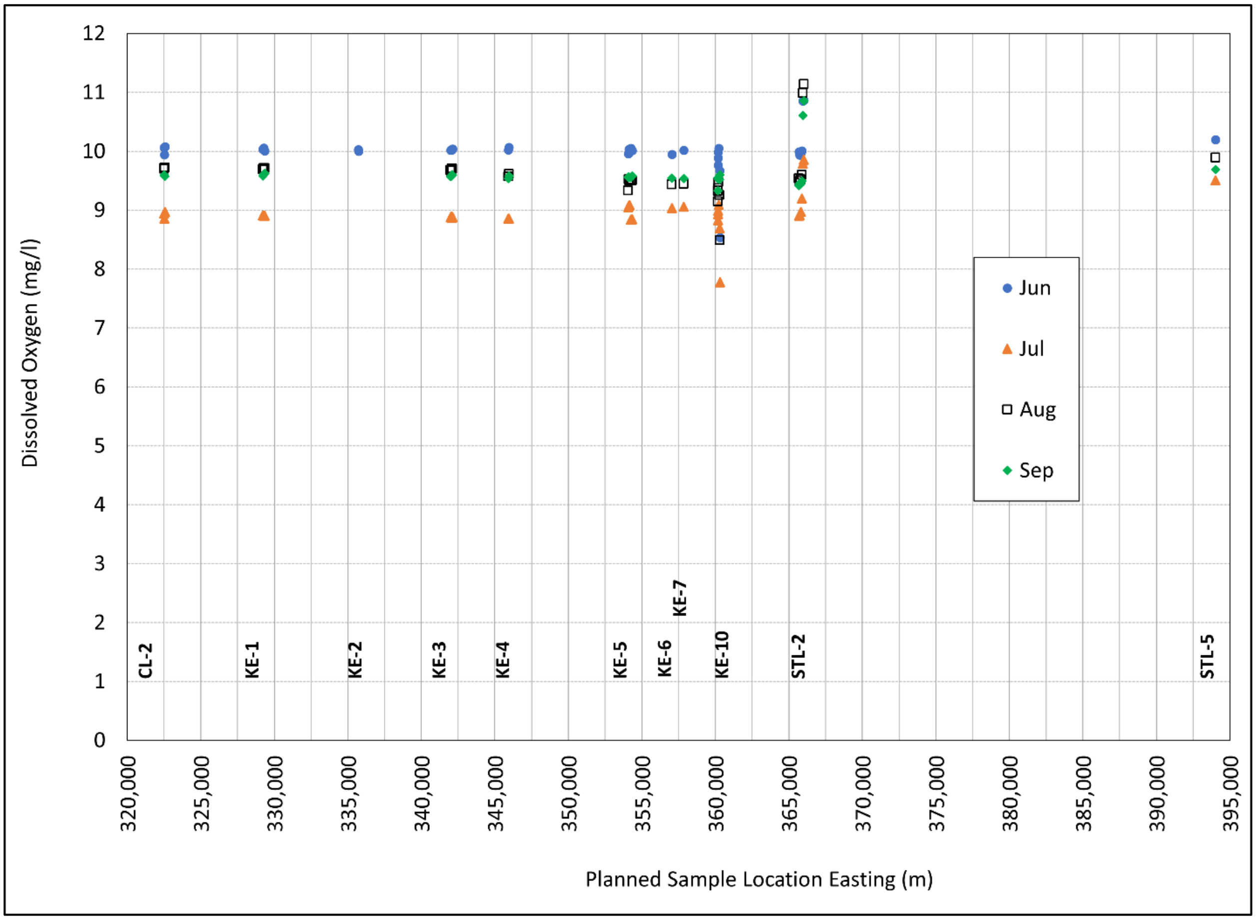


**Figure 35: Average DO at mainstem sites, summer 2022**

DO concentrations observed in backbays varied over a much wider range than along the mainstem (Figure 36, Appx 3). To generally summarize discrete DO concentrations observed at these sites, the DO conditions were identified as being either low, moderate, or high depending on the range of concentrations observed during the summer period. These classifications are defined based on consideration of the minimum 7-day average and instantaneous DO objectives when water temperatures are above 5°C for cool and cold aquatic species (Manitoba Water Stewardship, 2011). The 7-day average DO objectives for cool and cold-water species are 6 mg/l and 5 mg/l respectively, while the respective instantaneous minimum objectives are 5 mg/l and 4 mg/l. Based on these values, the following classifications were selected to describe the DO variation between the surface and bottom for the 48 backbay sampling locations (Table 8):

- Low < 4 mg/l < Moderate < 6 mg/l < High.

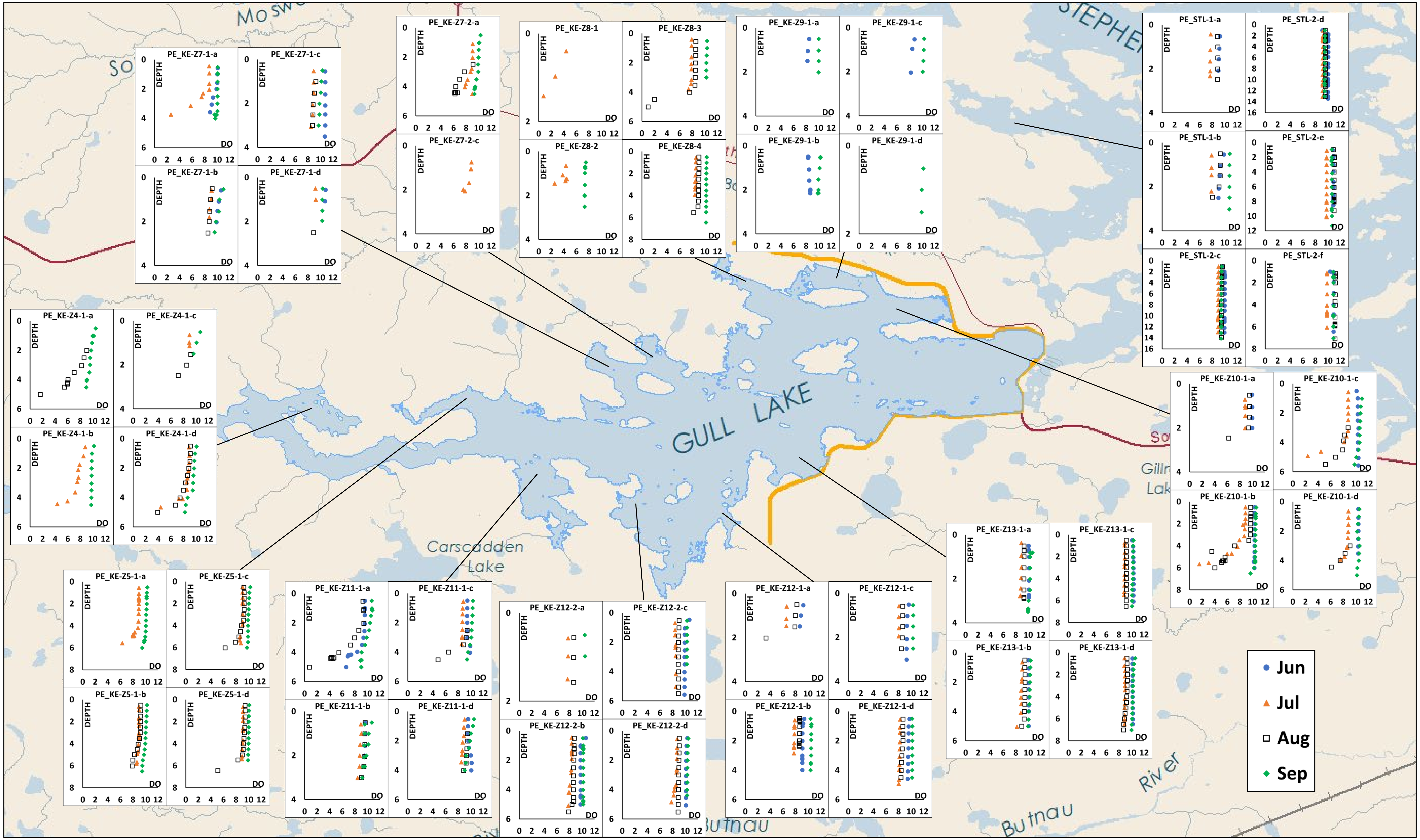


**Figure 36: Summer DO depth profiles in backbays**

Based on these criteria, 33 of the 46 discrete sampling sites were classified as having high DO, with concentrations that exceeded 6 mg/l (Table 8) at all depths for each sampling period. While DO concentration may have varied between about 6-10 mg/l at these locations, many locations exceeded about 8 mg/l and had DO saturation of about 80-100%. Many of these sites showed some vertical differentiation with a lower DO concentration near the bottom, even if it was only a small difference of less than 1 mg/l (Figure 36).

**Table 8: Summary of summer discrete DO conditions at backbay sites**

| Site/ Location[1] | a or 1 | b or 2 | c or 3 | d or 4 |
|---|---|---|---|---|
| KE-Z4-1 | H / L[2, 3] | H / M | H | H / L |
| KE-Z5-1 | H | H | H | H / M |
| KE-Z7-1 | H / L | H | H | H |
| KE-Z7-2 | H | n/a | H | n/a |
| KE-Z8 | L | H / L | H / L | H |
| KE-Z9-1 | H | H | H | H |
| KE-Z10-1 | H | H / L | H / M | H |
| KE-Z11-1 | H / L | H | H / M | H |
| KE-Z12-1 | H / L | H | H | H |
| KE-Z12-2 | H | H | H | H |
| KE-Z13-1 | H | H | H | H |
| STL-1 | H | H | H | H |

Notes:

1. Site locations are designated by a, b, c or d (e.g., KE-Z4-1-a, KE-Z9-1-c, etc., except for KE-Z8 which is designated by 1, 2, 3, or 4 (i.e., KE-Z8-1, KE-Z8-2, etc.)
2. DO classified based on concentration where: low (L) < 4 mg/l < moderate (M) < 6 mg/l < high (H)
3. Single L, H or M indicates condition through depth of water column while combinations indicate variation from surface to bottom (e.g., H / L, high near surface low near bottom)

Four of the backbay sampling locations had high DO near the surface that decrease to moderate DO near the bottom, while another 8 had high surface DO that dropped to low DO at the bottom (Table 8). In the most extreme case, at location KE-Z11-a, the DO drops from about 9.3 mg/l near the surface to less than 1 mg/l at the bottom. While these locations may have had high DO near the surface (i.e., >6 mg/l), they frequently had somewhat lower DO through much of the water column as compared with other less affected sites in the same month. Note that since the classifications in Table 8 consider the range over the summer, some locations my be moderate or low DO through the entire water column in a particular month. In Table 8, location KE-Z8-1 was classified as low because DO was below 4 mg/l through the entire depth: However, this location was only sampled in July and my have had higher DO at other times, as occurred at location

KE-Z8-2, which also had low DO in July but high DO in September. Aside from KE-Z8-1 and KE Z8-2, no other locations had DO concentrations that were entirely moderate or low through the full water column in a particular sampling period: i.e., all other locations and sampling dates had high DO concentrations at some point in the water column.

For each backbay monitoring location and sampling date, the average DO concentration was calculated from the measurements obtained through the depth of the water column. For plotting purposes, depth averaged DO was plotted based on the planned easting the sample locations so that results are shown according to their relative position along the monitoring area, which has a west-east alignment (Figure 37). Unlike the mainstem sites, there would be no expectation that

there could be an upstream to downstream trend in the results (e.g., between KE-Z11-1 and KE-Z12-2) since flow does not travel directly between them – they are independent. For clarity, the north and south backbays are plotted separately. Results show depth averaged DO is generally high, exceeding 7 mg/l at all but a few locations at certain times during the monitoring period. As expected based on Figure 36, the only locations with depth average DO less than 6 mg/l were sites KE-Z8-1 and KE-Z8-2 in July when the average concentrations were about 2.6 mg/l and 4 mg/l respectively. Depth averaged DO concentrations at the Stephens Lake back-bay site (STL-1a to f), which is unaffected by the project, were generally greater than the backbays upstream of Keeyask. This may be due to less biological activity at the STL-1 site as compared with the upstream sites in newly flooded areas with organic substrates.

The discrete monitoring results are generally consistent with expectations from the Keeyask EIS that DO would typically remain relatively high (>6 mg/l), even in flooded backbays. Reduced DO was expected to occur in some backbays, notably in association with periods of reduced winds when reaeration is decreased. Low DO observed in some locations near the bottom or through the depth of the water column was not necessarily associated with low wind conditions. These low DO levels may indicate less mixing due to wind and flow and/or higher oxygen demand from organic decay than assumed in the Keeyask EIS assessment of effects on DO.

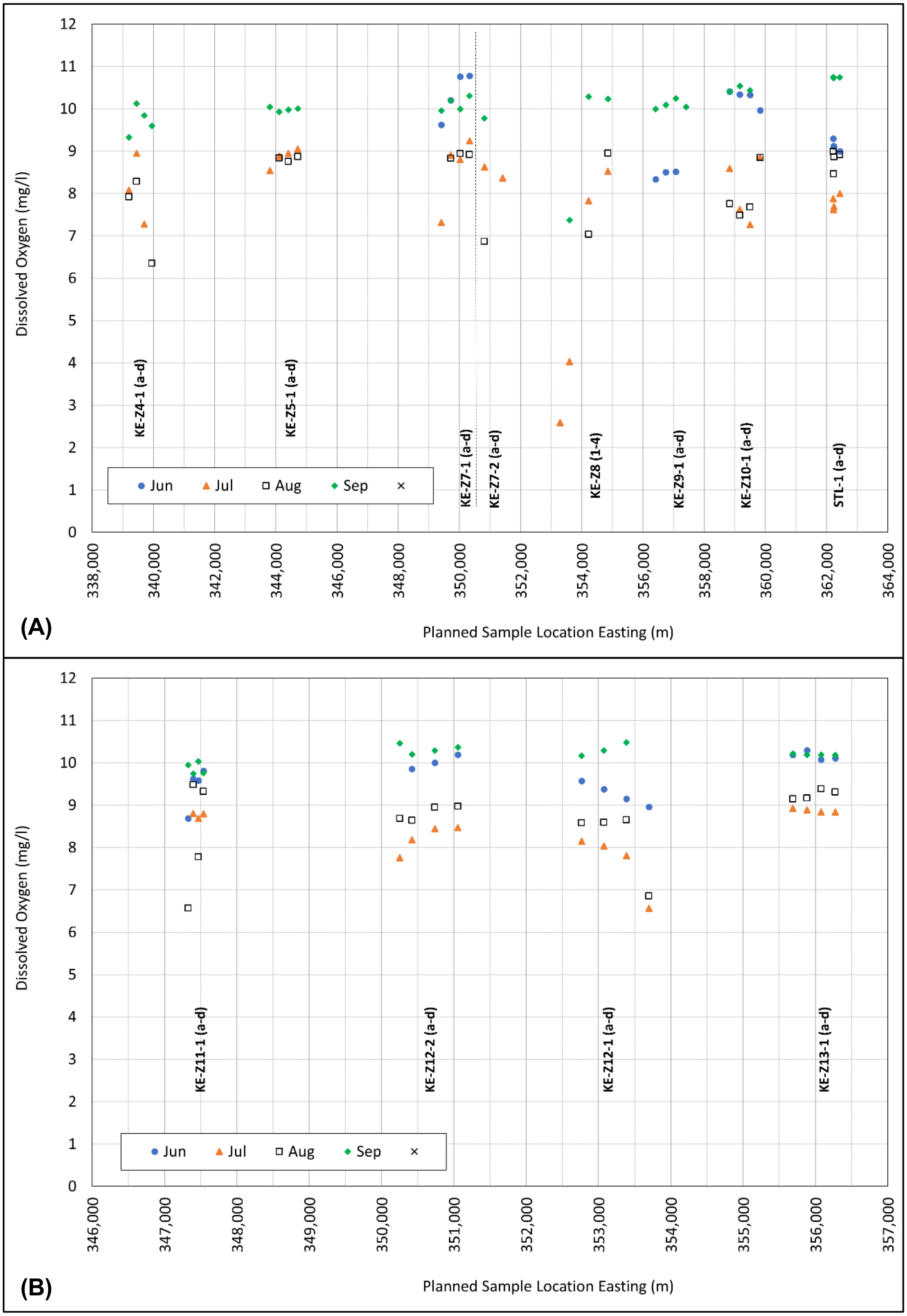


**Figure 37: Average DO at north (A) and south (B) backbay sites, summer 2022**

### 6.2.2 SUMMER CONTINUOUS DO

Continuous DO sensors were placed either near the surface (~2 m below) and bottom (~ 1m above) at the following 5 mainstem and 6 backbay locations between mid-June to the end of September:

- Mainstem:
  - CL-2-b surface
  - KE-4-b surface
  - KE-10-c surface and bottom
  - STL-2-d surface
  - STL-5 surface
- Backbay:
  - KE-Z4-1-a surface and bottom
  - KE-Z8-2 surface and bottom
  - KE-Z11-1-a surface and bottom
  - KE-Z12-1-b surface and bottom
  - KE-Z12-2-b surface and bottom
  - STL-1-c surface and bottom

Continuous DO results were reviewed to remove erroneous data and apply corrections were applied based on discrete measurements. While some erroneous data was removed, the review generally erred on the side of leaving data in so that in some cases the results show individual or short increases or decreases of a couple milligrams-per-litre.

Continuous monitoring results showed high levels of DO exceeding about 8.8 mg/l for the mainstem sites from CL-2-b upstream, which is upstream project effects on levels, through to site STL-5 in Stephens Lake about 30 km downstream of the Keeyask GS (Figure 38). DO concentrations were typically within about 1 mg/l of each other, except for some peaks at location STL-2-d, as discussed below. DO saturation levels were typically near 100%, ranging from about 95-110%.

DO concentrations at site STL-2 were generally similar to the KE-10 concentrations, which might be expected since the two sites are close together, being immediately downstream and upstream of the Keeyask GS respectively (Figure 38). However, the STL-2 site displays several periods where DO concentration spike up from the trend, increasing as little as about 0.2 mg/l (e.g., late July and late August) to as much as 1-2 mg/l in the first 3 weeks of August. As observed in 2021, these spikes correspond with periods of higher discharge from the Keeyask spillway (Figure 38). During these periods the turbulent spillway flow entrains more oxygen in the water, raising DO to the point that the water is supersaturated, with DO saturation levels reaching almost 130%.Figure 38 shows that the effect of Spillway discharge is larger the greater the proportion of flow through the Spillway, although the effect may reach a maximum over about 60% flow through the Spillway. This is likely because the monitoring site is in the middle of the channel, so the full effect of DO supersaturation in the Spillway flow does not reach the mid-point of the channel until the Spillway flow is more than 50% of the total flow.

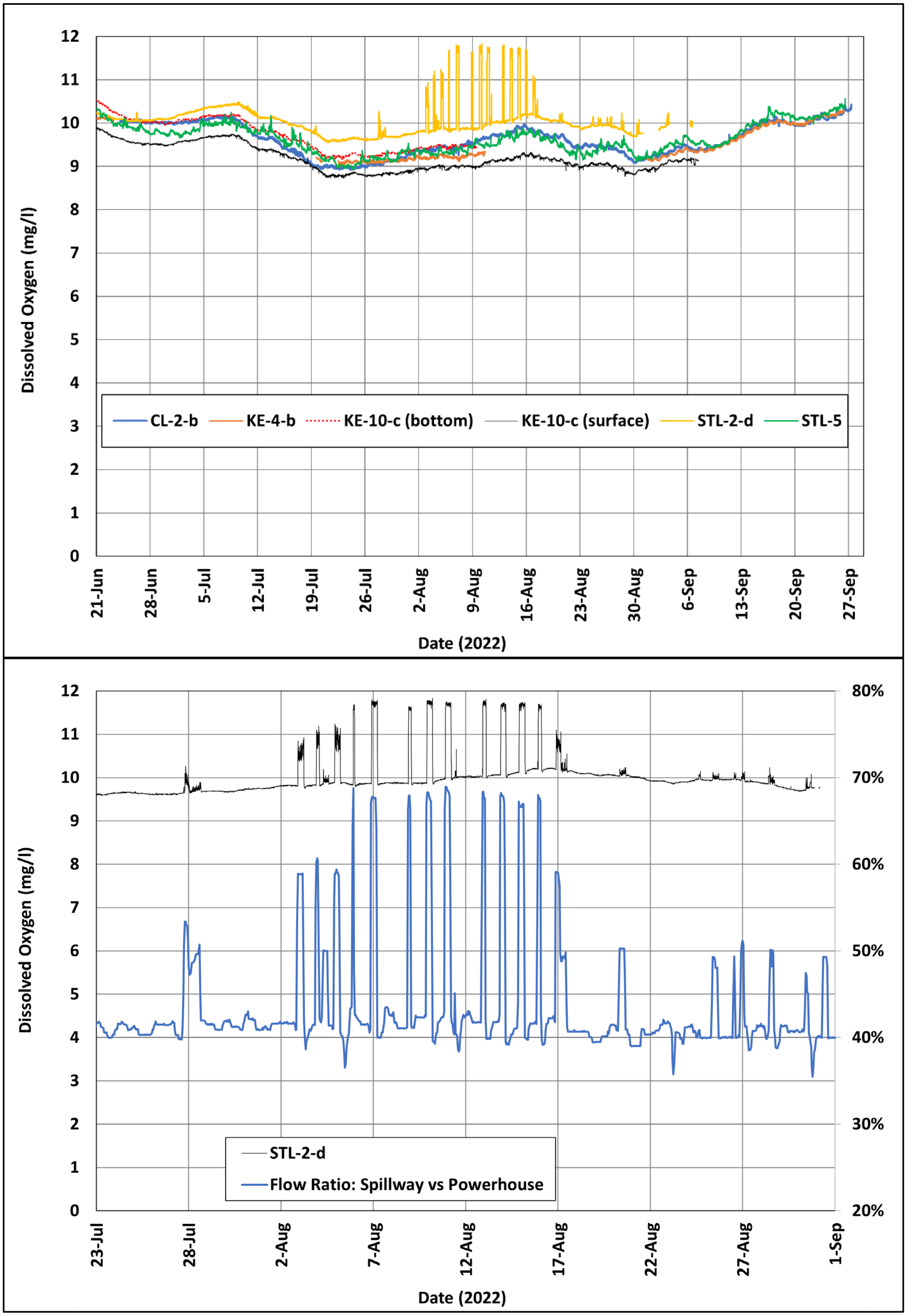


**Figure 38: Continuous DO at mainstem sites (A) and site STL-2 (B)**

At the six back-bay monitoring sites, DO probes were deployed at surface and bottom positions during the summer of 2023. However, due to equipment issues, surface DO was only recorded over about the first month of monitoring at sites KE-Z12-1-b, and KE-Z12-2-b, while at the reference site on Stephens Lake, STL-1-c, the surface DO was not properly recorded during the entire season. Bottom DO was generally recorded properly over the entire monitoring period at each of the sites.

Continuous DO concentrations at sites KE-12-1-b, KE-12-2-b and STL-1-c were above 6 mg/l most of the summer with a few short periods when bottom DO dropped below that level for up to a few days (Figure 39, Figure 42, Figure 43). Some DO concentrations below 4 mg/l were recorded at KE-12-1-b and KE-12-2-b sites, but not over any extended time.

At sites KE-Z4-1-a and KE-Z11-1-a, the surface DO concentrations were generally high, exceeding 7 mg/l over almost the entire period at both sites with few readings just below that level (Figure 40, Figure 41). Unlike sites KE-12-1-b, KE-12-2-b and STL-1-c, bottom DO at these two sites drops below 6 mg/l for extended periods of up to about 2 weeks, and below 4 mg/l for a week or more. Two extended periods of low DO occur at these two sites in mid-July and mid-August when reduced DO was noted at KE-12-1-b, KE-12-2-b and STL-1-c. Sites KE-Z4-1-a and KE-Z11-1-a also show some decreasing DO patterns in June, early August, and mid-September.

The periods of reduced and low DO noted at the five sites discussed above (KE-12-1-b, KE-12-2-b, STL-1-c, KE-Z4-1-a, and KE-Z11-1-a) correspond with periods when low wind conditions occurred. This is demonstrated in a plot of the bottom DO at site KE-Z11-1-a along with the moving 24-hour average wind speed during the summer (Figure 45). When the average wind speed drops below about 15 km/h, the bottom DO concentrations start to decrease. If the average wind is sustained below about 12 km/h the DO concentration may continue to drop and may approach 0 mg/l, as occurs at sites KE-4-1-a and KE-11-1-a (Figure 40, Figure 41). Note that each site experiences site specific conditions that determine how the DO responds, reflecting the varied effects of local demands on DO due to decay of organic matter, circulation and flow patterns, water temperature, and effects of wind direction. These patterns of low DO during periods of low winds were observed in the 2021 continuous monitoring results and during pre-project monitoring at the reference site in STL-1-c. As such, these results were anticipated based on pre-project monitoring and modeling reported in the Keeyask EIS (KHLP 2012b).

The final continuous monitoring site to consider is KE-Z8-2, where both surface and bottom DO concentrations were below 6 mg/l for most of the monitoring period, and below 4 mg/l most of the time in July and August (Figure 44). Although this site is relatively shallow (2.5-3.7 m), it does not appear that winds are able to mix the full depth of the water column to the point that high DO levels are restored, as occurs at other locations. These results are similar to conditions observed at this site in 2021 and likely reflect poor flow and circulation mixing combined with a low response to wind effects along with elevated oxygen demands.

Overall, the continuous DO monitoring results for summer 2022 are consistent with expectations from predicted effects in the Keeyask EIS (KHLP 2012b).

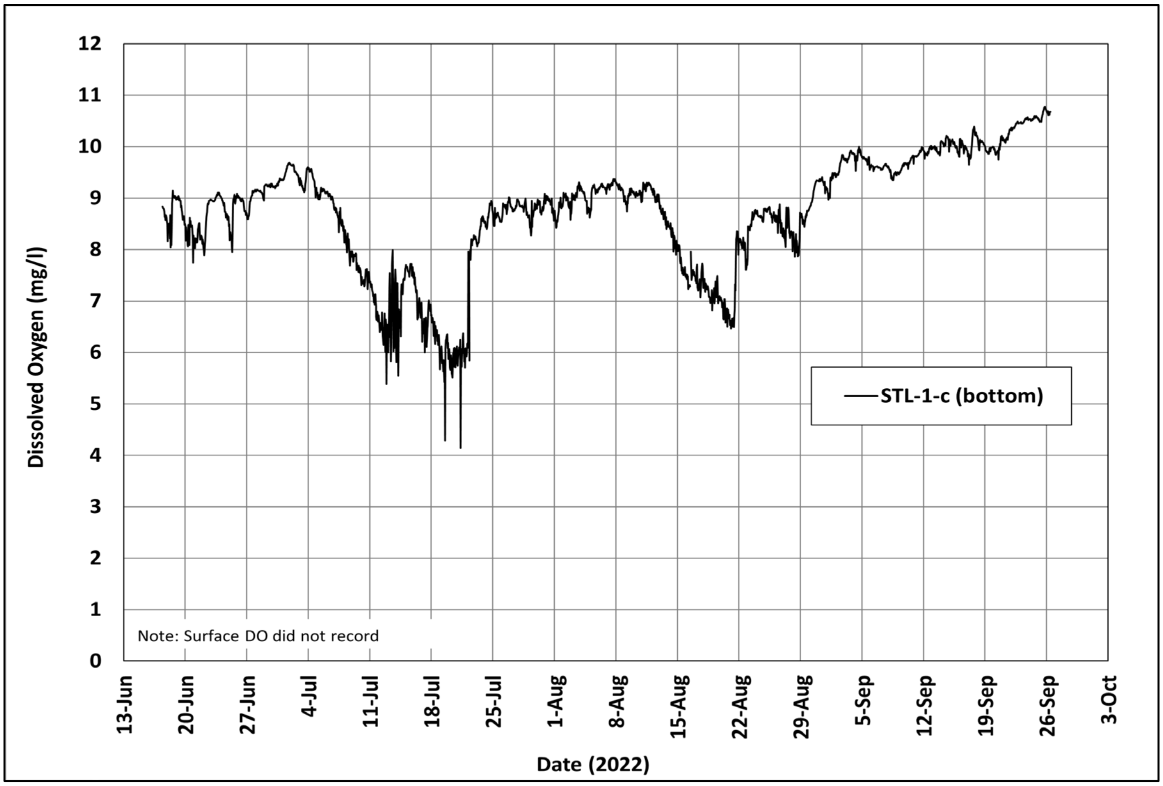


**Figure 39: Continuous DO at site STL-1**

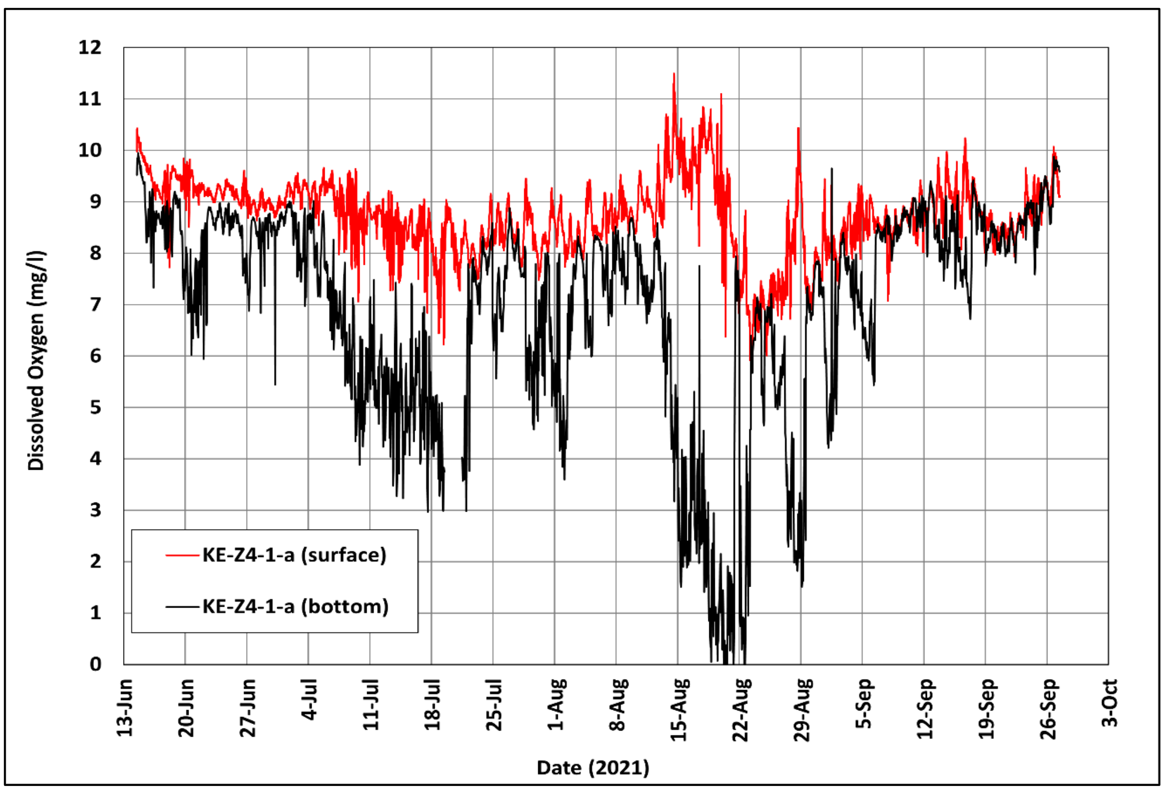


**Figure 40: Continuous DO at site KE-Z4-1-a**

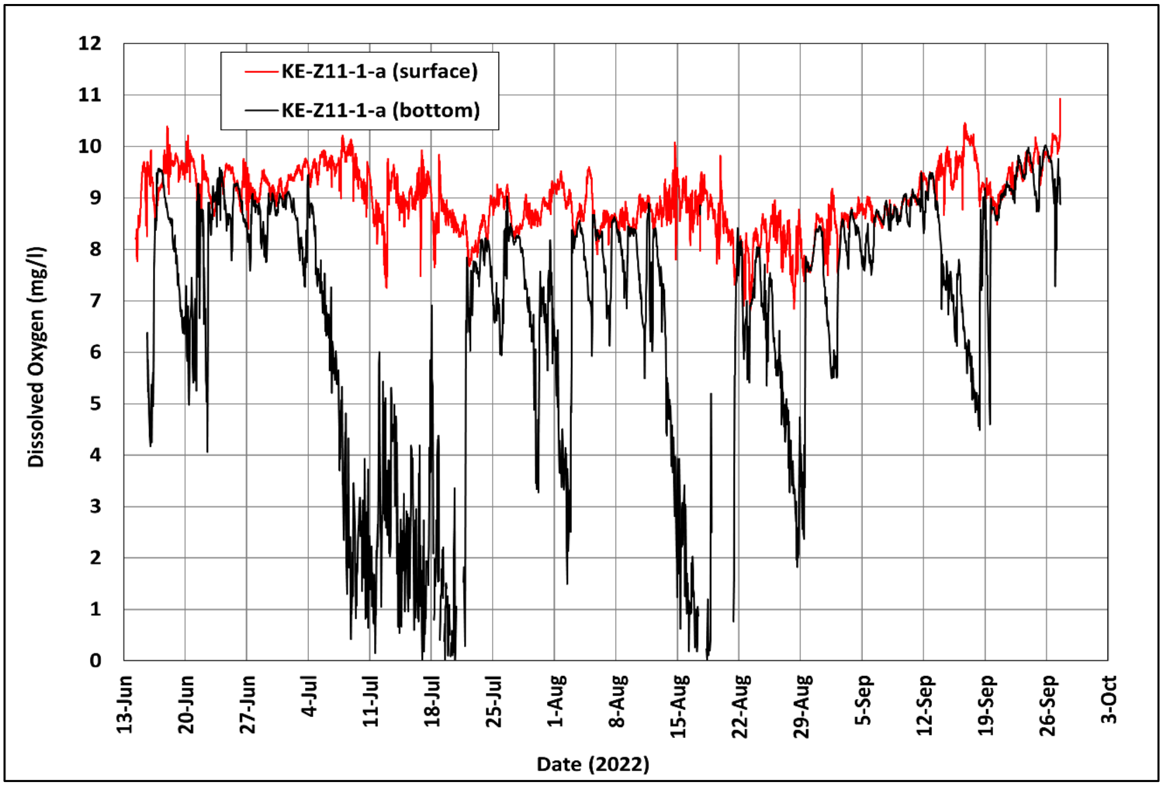


**Figure 41: Continuous DO at site KE-Z11-1-a**

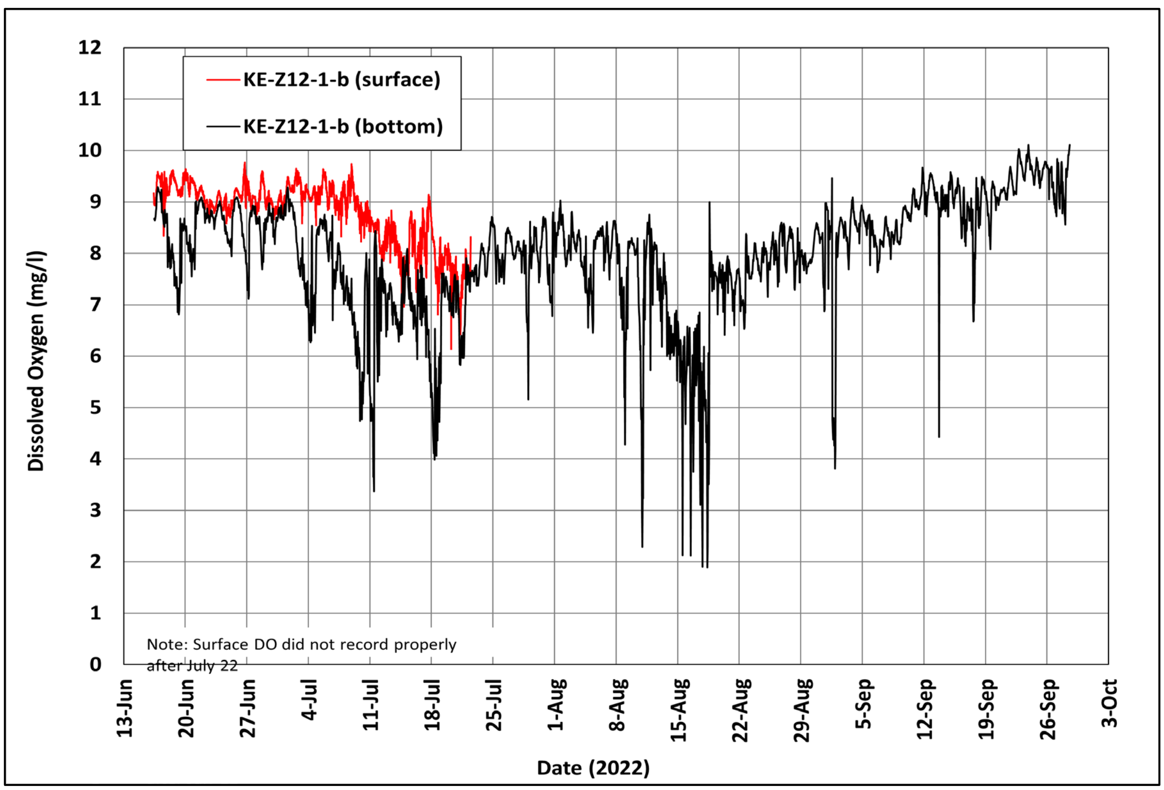


**Figure 42: Continuous DO at site KE-Z12-1-b**

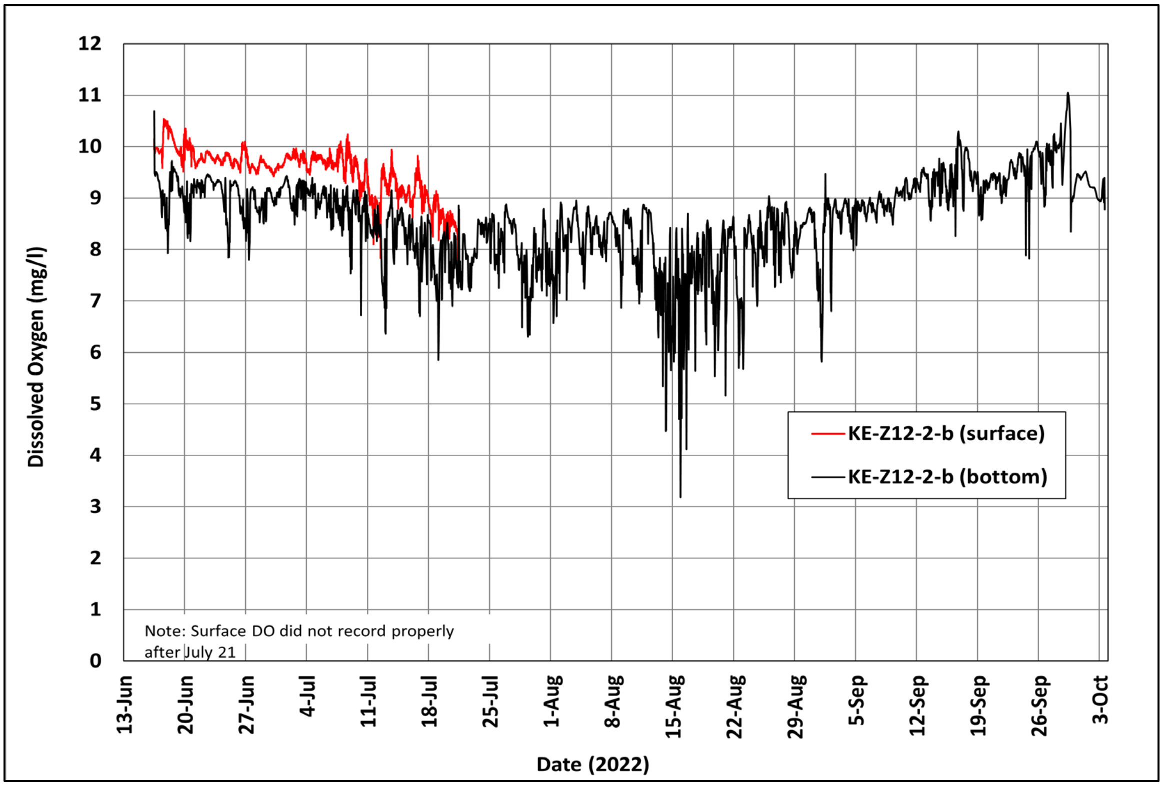


**Figure 43: Continuous DO at site KE-Z12-2-b**

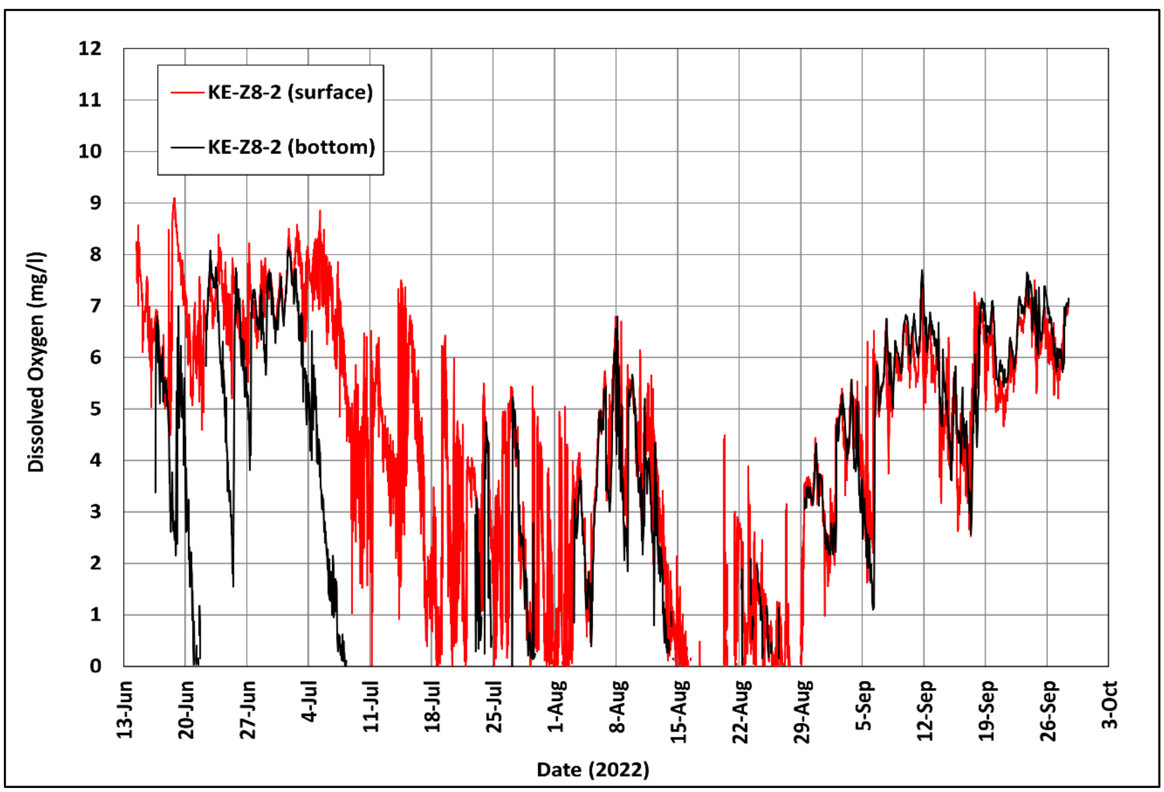


**Figure 44: Continuous DO at site KE-Z8-2**

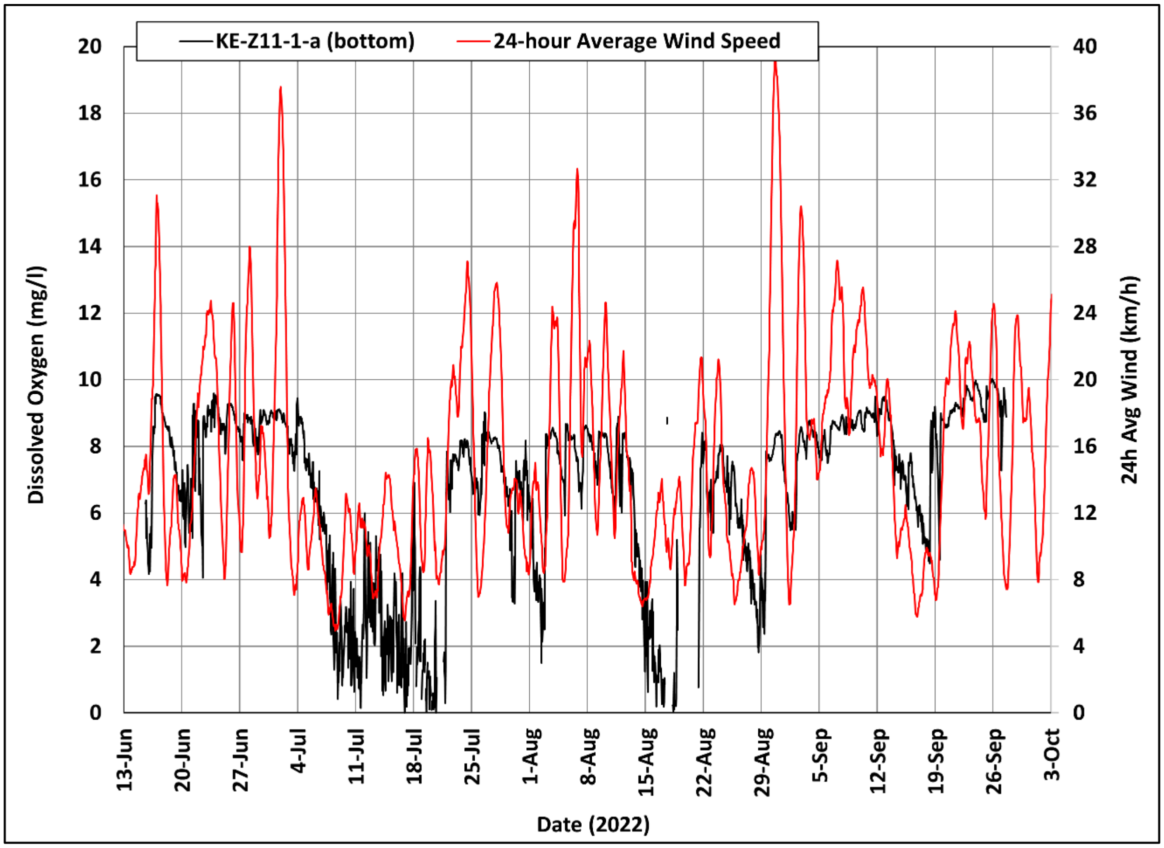


**Figure 45: 24-hour average continuous DO at site KE-Z11-1-b and wind speed**

# 6.3 LITTLE GULL LAKE AERATION SYSTEM – 2021/2022 MONITORING SUMMARY

## 6.3.1 BACKGROUND

Little Gull Lake was a small lake developed within peat bogs approximately 900 m to the north of Gull Lake (Figure 46). After impoundment of the Keeyask reservoir in fall 2020, Little Gull Lake was incorporated into the overall reservoir. Dissolved oxygen (DO) modeling conducted during the Keeyask environmental assessment indicated that this area would become anoxic during winter, due to restricted flows and the high oxygen demand from organic substrate. It was also identified that the water depth between the former Little Gull Lake and Gull Lake within the reservoir would be very shallow and could freeze to the bottom in the winter. This could restrict the movement of fish to areas of higher DO creating the risk of winterkill.

To mitigate the risk of winterkill an aeration system was installed on the North Shore of the former Little Gull Lake. The aeration system is comprised of four Keeton Industries SolAer aeration units. Each unit operates independently and is comprised of a solar power system (solar panel, batteries, and controller) and air supply system (compressor, manifold, air filter, self-sinking supply line, and two in-water diffusers). The on-land components are housed within a weatherproof insulated cabinet. Pumped air is introduced to the lake via Keeton Duraplate self-cleaning, non-clogging, membrane diffusers. There are eight diffusers in total, two per system.

## 6.3.2 AERATION SYSTEM MONITORING

During the 2020/21 winter, discrete DO readings were collected monthly along transects outside aeration field at the limit of safe ice (~5-10 m outside of the aeration field). Due to dangerous ice conditions, it is not possible to collect discrete samples within the aeration field. That data indicated that the system was elevating DO above background levels, however there is a limited increase of DO outside of the immediate area of aeration field and DO levels quickly dropped to background levels a short distance away from the field.

As 2020/21 monitoring indicated that the aeration system has a limited influence on DO levels outside of the aeration field it was determined that for the 2021/22 winter season discrete monitoring would be discontinued. Monitoring of DO for the 2021/22 season focused on the collection of continuous DO data at a location within the aeration field. Two continuous HOBO DO (U26-001) loggers were deployed within the aeration field between the internal and external ring of aeration heads. Figure 47 presents a diagram of the aeration field layout and the approximate location (**Error! Reference source not found.**) of the monitoring equipment. The HOBO DO loggers were attached to a metal rod that was driven through the aqueous 'muck layer' of the lake substrate into the underlying firm substrate. The loggers were placed at approximately 0.33 and 0.66 metres above the lakebed in the Northwest corner of the field. The equipment recoded DO and water temperature from October 22, 2021 to May 22, 2022.

DO and water temperature data from the HOBO loggers is presented in Figure 48. The data demonstrates a declining trend of DO, with DO levels starting around 13 mg/l and dropping down to 0 mg/l by mid-January. The decline in DO levels to 0 mg/l corresponds to the formation of a stable ice cover over the portion of the aeration field where the loggers were installed. It is unknown why this portion of the field froze over while other areas remained open, this could potentially be caused by one or more of the air supply lines being partially or completely plugged by ice. Field observations have indicated that the northwest portion of the aeration field is often the first to freeze over. The low DO levels are also likely influenced by the proximity of the loggers to the lakebed. The loggers were installed at 0.33 and 0.66 metres from the bed (to ensure that they would not be damaged by ice), however at this depth they may have been unable to record the influence of the aeration system.


**Figure 46: Location of Little Gull Lake**

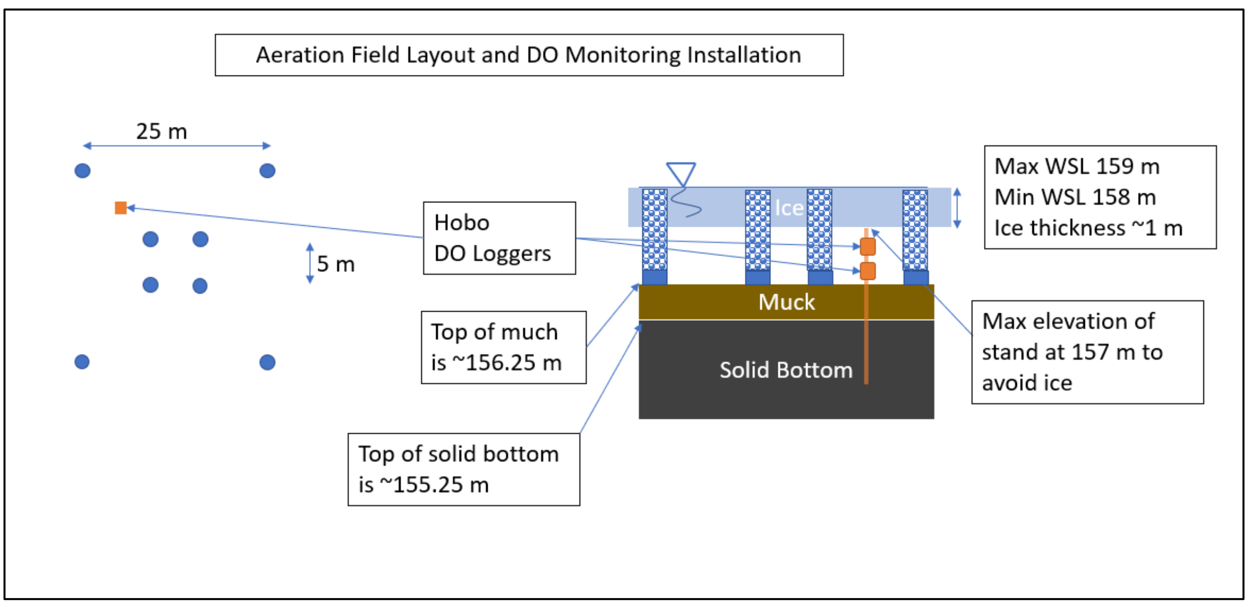


**Figure 47: Layout of aeration heads and DO monitoring location**

**Photo 6: Typical ice conditions and approximate location of DO logger installation (image from March 2022 looking north)**

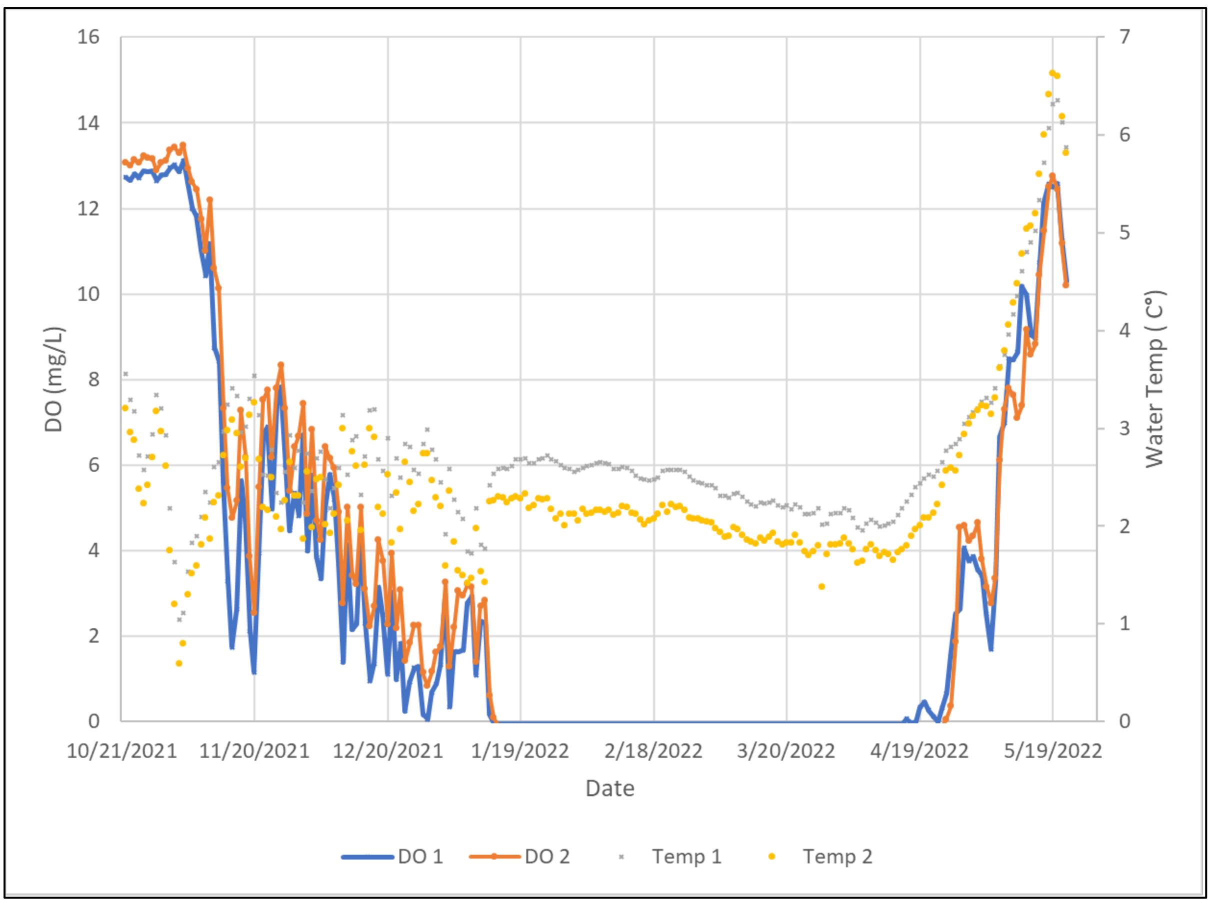


**Figure 48: Little Gull Lake DO and temperature monitoring data for winter 2021/2022**

# 7.0 DEBRIS MANAGEMENT

As part of the Keeyask GS Project, in accordance with the Joint Keeyask Development Agreement (JKDA; TCN et.al. 2009), a waterways management program was started in 2015 for the Project area from Clark Lake to Gull Rapids. The JKDA indicated that up to 25 workers configured as two two-person boat patrols plus supplementary work crews would operate in the Keeyask area. One boat patrol would operate downstream to implement safety measures and inform resource users of altered water conditions due to the Project while the other would operate upstream to implement safety measures, manage hazardous debris and assist the work crews.

Boat patrols identify and remove floating woody debris (Photo 7) that may pose a safety hazard to navigation. The boat patrol typically records the amount of debris removed each season, classifying it as either small (<1m length) or large (>1m length), and the large material is further classified as either new or old debris (generally with or without bark) or if it came from beaver activity.

Prior to 2015, this area was only visited about once each week (20% of the time) by the crew that also patrolled Split Lake and the amount of debris collected in the Clark Lake to Gull Rapids area was estimated to be 20% of the total amount of debris collected by this crew. Starting in 2018 a new data collection program was initiated allowing for tracking of the location of floating debris and accounting for debris in the Keeyask area. In 2018 and 2019, 10 or fewer pieces of debris were removed each year (Table 9). While the patrol operated in the area in 2020 - 2023, they did not record the removal of any debris. Except for 2003, the quantities removed after 2014 were much less than the estimated amounts of debris removed up to 2014. This suggests that the amounts removed from the Project prior to 2015 were likely much lower than estimated by the simple assumption it was 20% of the total amount collected by the Split Lake boat patrol.

In 2022, a 20-person work crew continued to focus its efforts on debris clean-up in the vicinity of the Keeyask dam, as it did in 2021 (Figure 49). The work crew was primarily engaged in the collection of woody debris along the south dike that accumulated between the end of the 2021 work season and the start of the 2022 season or continued to accumulate during the clean-up season. Debris collected from the south dike in 2021 was piled adjacent to the east end of the dike where it was left to dry and was subsequently burned in May 2022, at the start of the work season. Likewise, debris removed in 2022 was piled in the same area to dry before being burned at the start of the 2023 debris clean-up season. While work focussed on the south dike area, the clean-up crew also engaged in the removal of woody debris that accumulated against the upstream side of the powerhouse and the adjacent north dike area. This debris was piled nearby to dry before being burned in 2023.

Two boat patrols operated in the Keeyask area between Clark Lake and the Keeyask GS in summer 2022. Unlike the 2021 season when the boat patrol had to focus on supporting the debris clean-up crews, the crews could focus its efforts on waterway management activities. Boat patrols marked navigation hazards like newly formed reefs created by reservoir impoundment. Weather and equipment permitting, they conducted daily patrols of the waterway to locate and remove floating woody debris. The crews were able to remove a large quantity of floating woody debris from the waterway and dispose of it on shore or in piles that could be burned in winter: however, the total quantity and type of debris removed was unavailable. The amount removed was more than previously encountered prior to Keeyask operation due to woody debris that entered the waterway when the reservoir was impounded. The boat patrols also spoke with resource users on the waterway to answer people's questions let them know the patrols are around to provide assistance if needed, and patrols did assist boaters when necessary (e.g., dead engine).

**Table 9: Debris removed from the Keeyask area**

| Year | Small (<1 m) | Large (> 1m) | | | |
|---|---|---|---|---|---|
| | | New | Old | Beaver | Total |
| 2003 | 3 | 4 | 7 | 0 | 11 |
| 2004 | 36 | 1 | 140 | 0 | 141 |
| 2005 | 2 | 6 | 103 | 0 | 109 |
| 2006 | 11 | 1 | 65 | 0 | 66 |
| 2007 | 0 | 3 | 81 | 0 | 84 |
| 2008 | 1 | 0 | 49 | 1 | 49 |
| 2012 | 0 | 1 | 30 | 1 | 32 |
| 2014 | 2 | 1 | 59 | 0 | 60 |
| 2015 | 4 | 0 | 6 | 0 | 10 |
| 2016 | 3 | 1 | 2 | 0 | 6 |
| 2017 | Not available | | | | |
| 2018 | 5 | 0 | 4 | 1 | 10 |
| 2019 | 1 | 4 | 3 | | 8 |
| 2020 | Not available | | | | |
| 2021 | Not available | | | | |
| 2022 | Not available | | | | |

**Photo 7: Large floating debris is removed from the water by the boat patrol team**

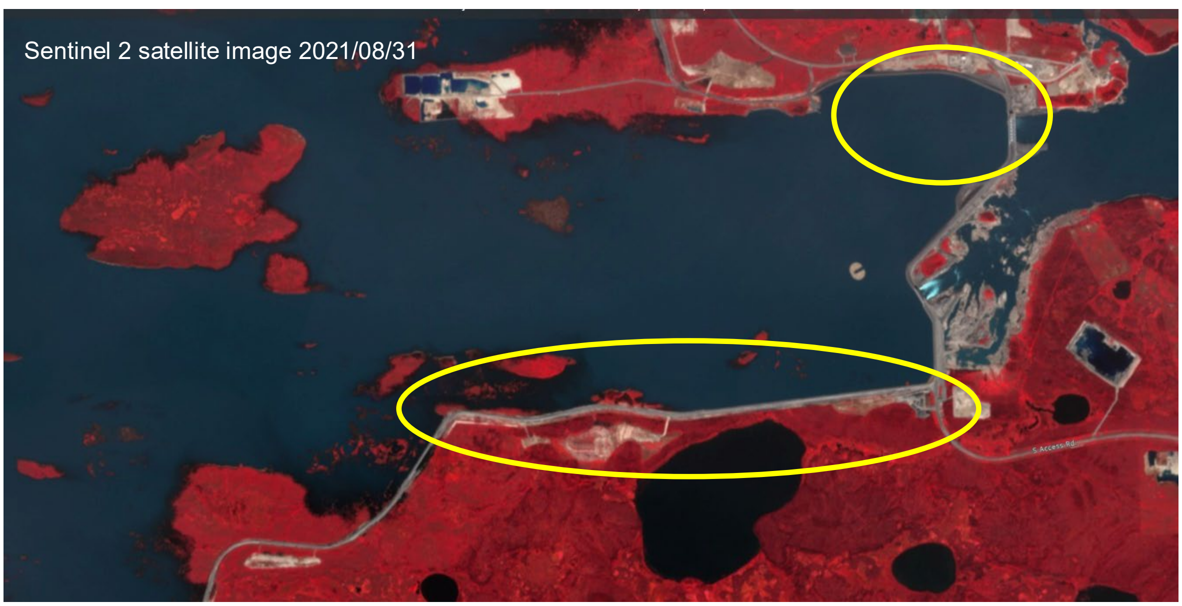


**Figure 49: General work areas for work crew debris removal activities**

# 8.0 RESERVOIR GREENHOUSE GAS

The purpose of Keeyask reservoir greenhouse gas monitoring program is to enable the comparison of aquatic greenhouse gas (GHG) concentrations and emissions before and after flooding and reservoir creation. The GHG monitoring program is implemented by Manitoba Hydro in conjunction with the Centre for Earth Observation Science at the University of Manitoba.

Studies have shown that GHG emissions from hydroelectric reservoirs in boreal ecosystems increase shortly after flooding (Teodoru et al. 2012). The size and duration of the change in GHG emissions (“reservoir effect”) is influenced by many factors including reservoir size, type and amount of biomass flooded, location, water residence time, temperature, etc. (Demarty and Tremblay 2017; Goldenfum 2012). The Keeyask Physical Environment Supporting Volume (KHLP 2012b) predicted that carbon dioxide ($CO_2$) emissions would approach background levels by approximately 10 years after impoundment and that methane ($CH_4$) emissions would remain elevated throughout the 100-year life of the Keeyask Generation Project. These predictions were based on IPCC (2006) guidance at that time. Since then, reservoir GHG science has continued to evolve (Delsontro et al. 2018, Prairie et al 2018). Studies have focussed on GHG processes and emission pathways, and how GHG emissions may relate to reservoir characteristics and location. Similarly, the methods used to study GHGs at the Keeyask reservoir have evolved and are described in this report.

The main boreal reservoir GHG emission pathways include (1) diffusion from the water to the atmosphere, (2) ebullition or GHG bubbles originated from sediments, (3) emission of gases from newly released floating peat areas, (4) degassing emissions as forebay water exits the powerhouse and spillway. The GHGs released from these environments are variable in space and time so can be difficult to measure. There is not one method that can measure all the GHG emission pathways and accurately represent the spatial and temporal variability of the reservoir.

The 2022 Keeyask reservoir GHG monitoring program included:

- two above ground micrometeorological towers (eddy covariance towers) that continuously measure the exchange of $CO_2$ and $CH_4$ between the reservoir and atmosphere along the reservoir forebay and at a representative, shallow flooded backbay;
- two sets of underwater, submersible sensors deployed on floating rafts, that continuously measure the dissolved concentrations of $CO_2$ and $CH_4$ in the main Nelson River channel and a representative, shallow flooded backbay during the open water season (June to September);
- a third submersible sensor deployed to monitor concentrations of $CO_2$ on a raft in Clark Lake upstream of the reservoir influence;
- point-in-time (discrete) water samples collected throughout the year at multiple locations upstream of, within, and downstream of the reservoir to provide a sampling plan that represents the heterogeneous nature of the reservoir, plus measurements of GHG concentrations within water entering and exiting the reservoir.

It is important to understand the inputs of carbon (sources of GHGs) that are brought into the reservoir from locations not related to Keeyask flooding, cycling of carbon (and production of GHGs) within the reservoir, and the downstream export of carbon (GHGs) leaving the reservoir.

## 8.1 MONITORING ACTIVITIES AND ANALYSIS METHODS

The locations of sites for submersible sensors, water samples and eddy covariance (EC) monitoring in 2022 (and in previous years) are shown in Figure 50. The monitoring sites were selected to provide a valid representation of the reservoir and included: the main Nelson River channel, shallow forebay waters, and shallow flooded tributaries to the reservoir (backbays), and upstream and downstream locations. The location of the sampling sites are provided in Appendix 4, Table A4. A description of the activities follows.

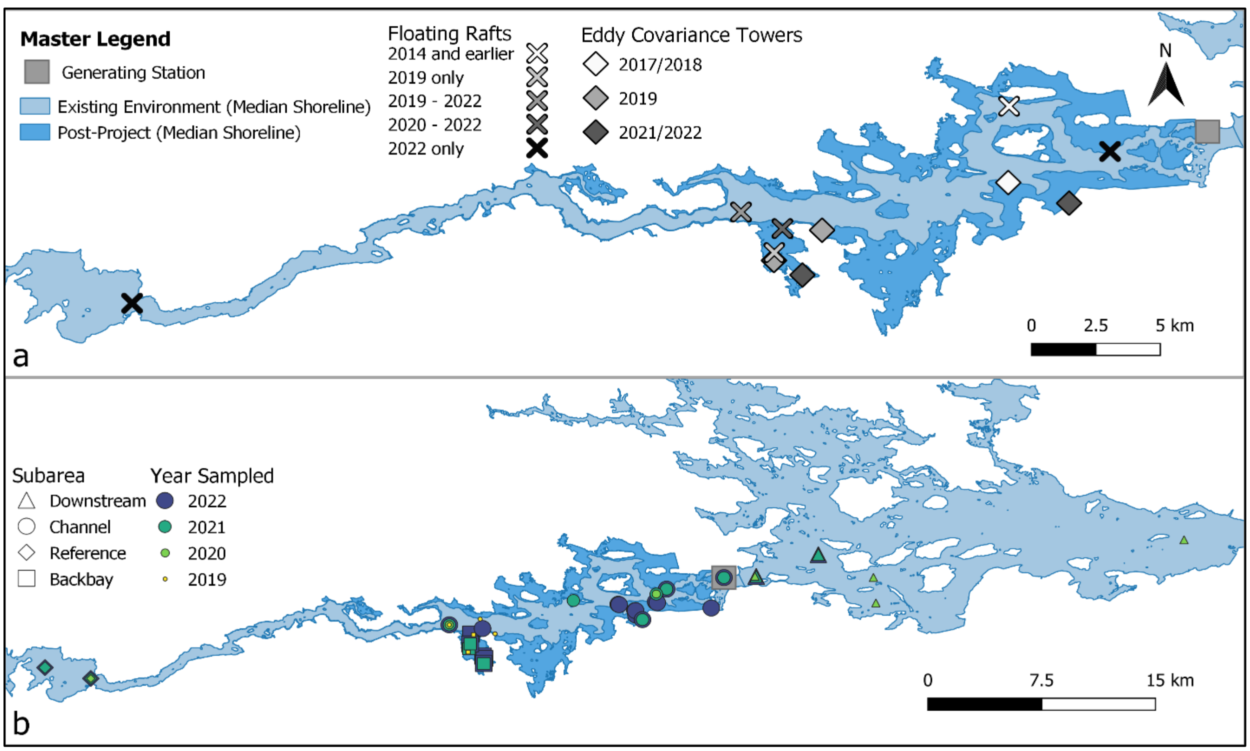


**Figure 50: Summary of eddy covariance tower locations, floating raft operations (a) and discrete sampling locations (b) for the Keeyask greenhouse gas monitoring project from inception to present (2017-2022)**

## 8.1.1 RESERVOIR-WIDE AIR-WATER GHG EXCHANGE

The GHG fluxes from the newly created reservoir include fluxes from deeper water associated with the original Nelson River channel – the central areas of the reservoir post-impoundment termed the **non-littoral zone**, and fluxes from the shallow water zone associated with the newly inundated peatland, termed the **littoral zone**. The littoral zone is considered that part of the reservoir less than 3 m in depth.

The approximate delineation between the two zones is shown in Figure 50 as the 'existing' and 'post project' median shorelines, and areal proportions are provided above.

GHG fluxes from the non-littoral zone were calculated using the diffusion-limited stagnant film model (Liss and Slater, 1974, Wanninkhof et al., 2009) requiring measurements of windspeed, water temperature, the partial pressures of $CO_2$ and $CH_4$ in the waterside of the air-water interface (i.e., $pCO_2$ and $pCH_4$, respectively), and in the lower atmosphere. The dissolved GHG concentrations were measured by the underwater, submersible sensors and from analyses of point-in-time water sampling. The transfer velocity required to estimate the diffusive fluxes in this study is attributed to Vachon and Prairie (2013). The diffusive flux estimates do not include contributions to the total emissions through ebullition, however past studies have shown that the contribution of ebullition fluxes are small in water depths in excess of 3 m (DelSontro et al., 2016).

Emission pathways resulting from the littoral zone include diffusive flux from the water surface, emissions emanating directly from partially submerged/floating peat and from methane bubbles originating in the flooded sediments and subsequently released at the water surface (hereafter ebullition flux). Fluxes resulting from these processes in the littoral zone (shallow water), were directly measured during 2021 and 2022 using the above ground micrometeorological towers (eddy covariance technique) deployed on the south dike road of the reservoir, and in a backbay system (Figure 50).

To facilitate a comparison across years both pre- and post-impoundment, the necessary data to estimate reservoir-wide fluxes resulted from measurement programs in 2022, 2021, 2019, and from baseline studies undertaken between 2009 and 2014 (Marchand et al., 2013, Marchand et al., 2015) is considered in this report.

## 8.1.2 FLUXES IN THE LITTORAL ZONE

An EC tower was deployed at the same location in the 2021 & 2022 seasons along the south dike road (South Dike Road Tower) near the Keeyask spillway, approximately 4.5-5km upstream.

The South Dike Road EC tower was deployed May 6th, 2021 and ran continuously until November 22$^{nd}$, 2022 with the full complement of eddy covariance instrumentation (56°19'20.54"N, 95°17'15.24"W, Figure 50, Photo 8, Photo 9). In November, a reduced selection of instruments remained in use to monitor over winter fluxes ($CO_2$ and associated meteorological data), with the full complement of sensors redeployed in April, 2022. The tower remains in operation.

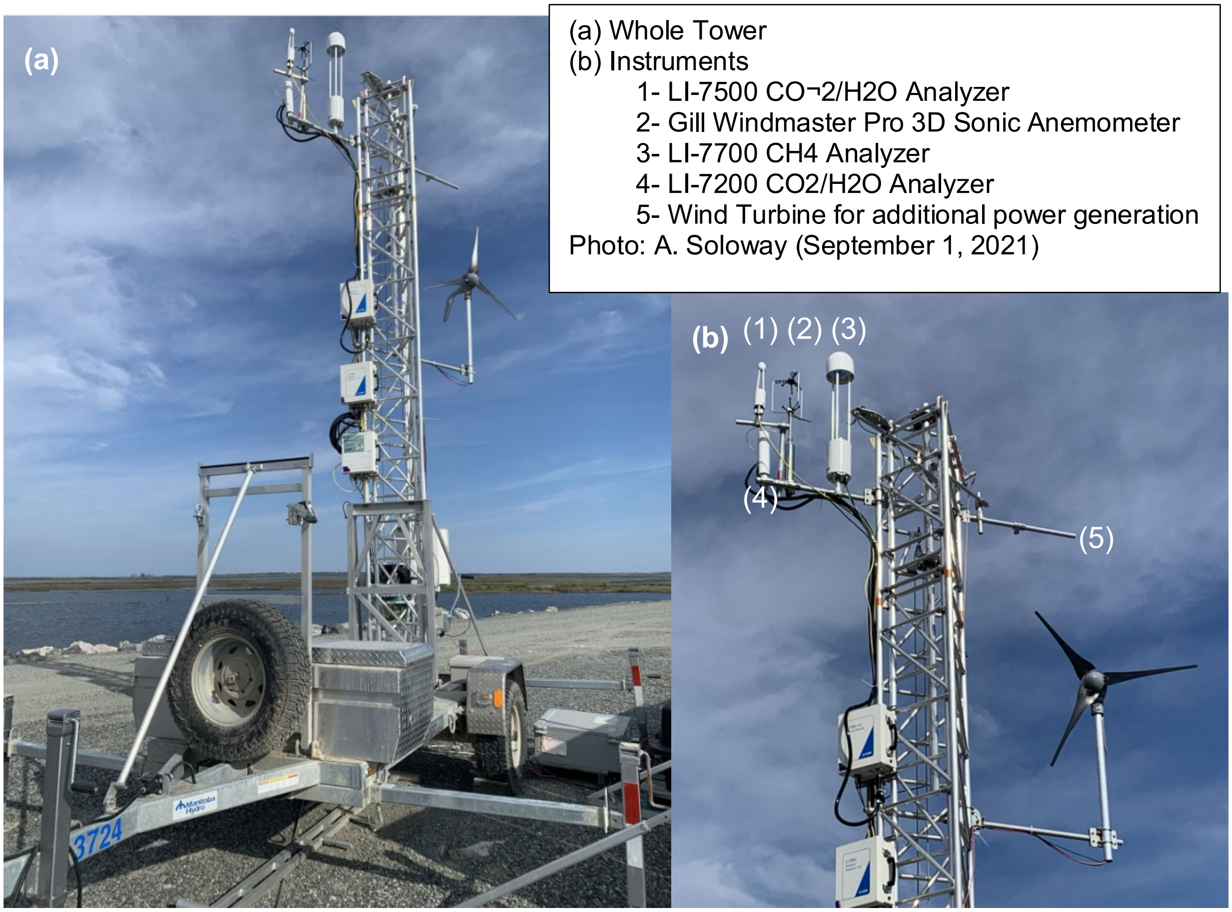


(a) Whole Tower
(b) Instruments
1- LI-7500 CO¬2/H2O Analyzer
2- Gill Windmaster Pro 3D Sonic Anemometer
3- LI-7700 CH4 Analyzer
4- LI-7200 CO2/H2O Analyzer
5- Wind Turbine for additional power generation
Photo: A. Soloway (September 1, 2021)

**Photo 8: South Dike Road Eddy Covariance Tower**

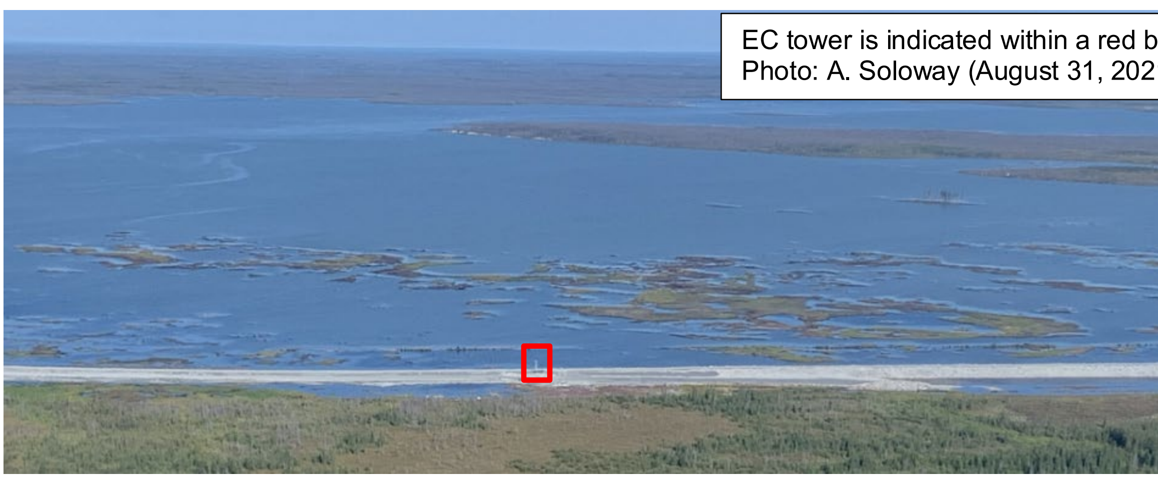

EC tower is indicated within a red box
Photo: A. Soloway (August 31, 2021)

**Photo 9: Aerial view of the Dike Road tower site showing emerging peat, peat islands and vegetation**

The Backbay tower (56°17'31.56"N, 95°27'17.29"W, Figure 50, Photo 10,Photo 11) was deployed during the ice-free season in both 2021 and 2022. It is located in the flooded Rabbit Creek wetland complex connected to the Nelson River that is approximately 15-15.5km upstream of the Keeyask axis. In 2021 the tower was operational between May 3rd and November 9th, and in 2022 between April 5 and November 22.

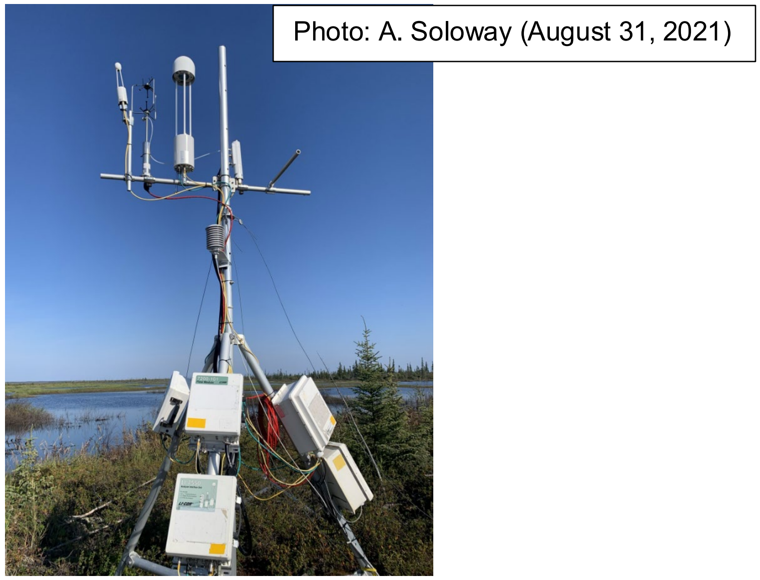


**Photo 10: Backbay tower looking towards north**

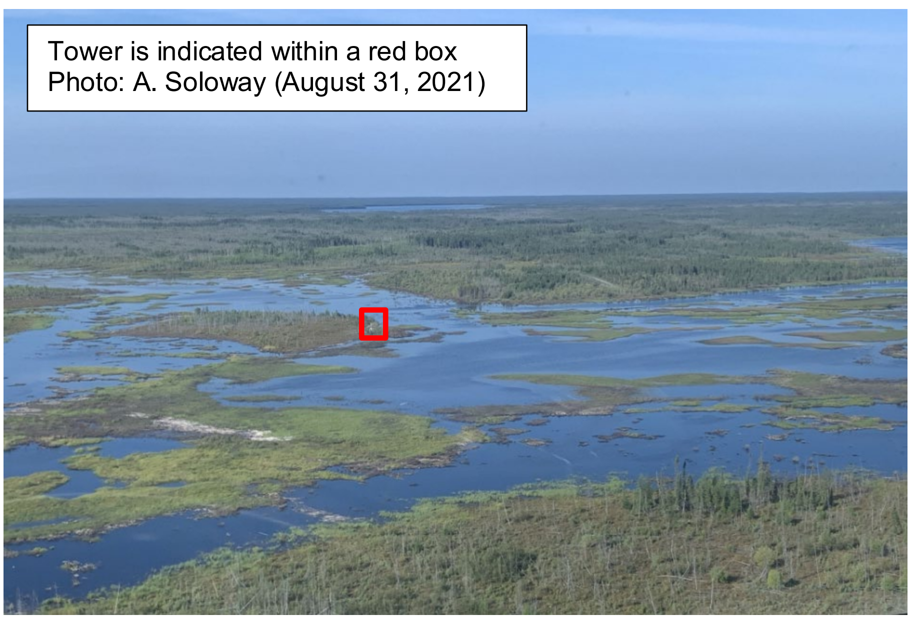


**Photo 11: Aerial view of the Backbay site showing heterogeneity after impoundment**

The GHG fluxes are representative of an area upwind of the EC tower (the flux footprint), the size of which depends on the height of the instruments, and weather conditions in the lower atmosphere. The flux footprints were calculated, and fluxes are representative of the upwind distances of approximately 600 m and 335 m for the south dike road and backbay sites. For both towers the upwind area contributing to the measured fluxes is from shallow water zones (largely less than 3 m depth) and is representative of the newly flooded shoreline of the Keeyask reservoir, including partially submerged vegetation-topped peat and floating peat islands. In the backbay the flux footprint also includes emergent vegetation that surrounded Rabbit Creek, in addition to the original Rabbit Creek channel (note aerial photographs – Photo 9, Photo 11).

### 8.1.3 AQUATIC SUBMERSIBLE GHG SENSORS

Sensors for the measurement of dissolved $CO_2$ and $CH_4$ (as gas partial pressures) were secured to two rafts in the 2021 and three rafts in 2022. Sensors were deployed between June to September, 2021 and 2022. A raft located mid-channel (PE_KE-4-B), and a raft located within the backbay (PE_KE_Z11-1-A, see Figure 50 for raft locations) were equipped with a submersible $pCO_2$ sensor ($CO_2$-Pro CV, Pro-Oceanus, Halifax, NS) and a submersible $pCH_4$ sensor (CONTROS HydroC-$CH_4$, 4H Jena Engineering, Jena, Germany). A submersible $pCO_2$ sensor was installed on the third raft (PE_CL-2-b) in Clark Lake ($CO_2$-Pro CV, Pro-Oceanus, Halifax, NS) in 2022. Data provide insights into high frequency changes in the dissolved GHG concentrations that serve both to underpin the calculation of non-littoral zone fluxes, and provide insight into temporal variability into both dissolved gas concentration, and associated air-river/reservoir GHG exchange.

Photo: A. Soloway (August 31, 2021)

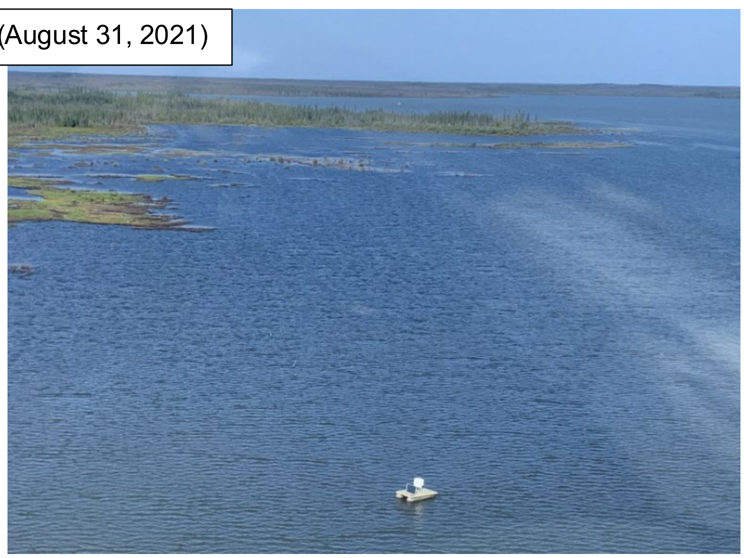

**Photo 12: Aerial view of the Backbay raft site: PE-KE-Z11-1-A where point-in-time samples were taken and submersible sensors were deployed**

### 8.1.4 POINT-IN-TIME WATER SAMPLE PROGRAM

Discrete water samples were taken at locations spanning from Clark Lake to the Kettle Generating Station forebay throughout the 2021 and 2022 season, including environments upstream, within and downstream of the Keeyask complex (Figure 50, Table 10 and Appendix 4 Table A4). In

2020, 2021 and 2022, sampling conformed to the PEMP protocol for stations with water depths greater than approximately 3 m, with samples taken at 20% of the total water column depth, and additionally at 80% depth when possible. Only surface samples were taken within the littoral zone. Parameters analyzed, as well as analysis and sampling details are included in Table 11.

**Table 10: Summary of monthly (1 to 12) discrete sampling locations throughout 2021 and 2022.**

| Site Name | 1 | 2 | 3 | 4 | 5 | 6 | 7 | 8 | 9 | 10 | 11 | 12 | Subarea |
|---|---|---|---|---|---|---|---|---|---|---|---|---|---|
| Generating Station | Y | Y | | X Y | X Y | X Y | X Y | X Y | X Y | X Y | X Y | X Y | GS |
| Dike Road Tower | | | | | Y | X Y | X Y | Y | X | X Y | X | | N/A |
| Backbay Tower | | | | Y | | X Y | Y | X Y | | X Y | X | | N/A |
| PE_CL-1 | X Y | X | X Y | X Y | | | | | | | | | Reference |
| PE_CL-2-B | | | | | | X Y | X Y | X Y | X Y | | | | Reference |
| PE_KE-10-C | | Y | Y | Y | | X Y | X Y | X Y | X Y | | | | New |
| PE_KE-4-B | | | | | | X Y | X Y | X Y | X Y | | | | Channel |
| PE_KE-6-A | X | X | X | X | | | | | | | | | New |
| PE_KE-9(-C) | X | X | X | X | | | | | | | | | Channel |
| PE_KE_Z11-1-A | X | X | X | X | | | | | | | | | Backbay |
| PE_KE-Z11-1-B | | Y | Y | Y | | Y | X Y | X Y | X Y | | | | Backbay |
| PE_STL-2-D | | | | | | X Y | X Y | X Y | X Y | | | | Downstream |
| PE_STL-3 (PE_STL_4) | X | X Y | X Y | X Y | | | | | | | | | Downstream |
| PE_STL-5 | | | | | | Y | X Y | X Y | X Y | | | | Downstream |
| PE_KE-5 | Y | | Y | Y | | | | | | | | | Channel |

Note:
An "X" and "Y" indicates that a site was sampled for that month in respectively 2021 and 2022. Site locations are provided in Appendix 4 , Table A4. The stations corresponding to subareas are also indicated in the table.

**Table 11: Water analyses for 2021 and 2022 Keeyask water sampling program**

| Variable | Units | Location of Analysis | SubSampling Glassware | Detection limit |
|---|---|---|---|---|
| Suspended nitrogen (SuspN) | mg L-1 | FWI | N/A | 0.7 mg N |
| Total dissolved nitrogen (TDN) | mg L-1 | FWI | N/A | 8 mg L-1 |
| Suspended phosphorus (SuspP) | mg L-1 | FWI | N/A | 0.4 mg L-1 |
| Total dissolved phosphorus (TDP) | mg L-1 | FWI | N/A | 0.4 mg L-1 |
| Suspended organic carbon (SuspC) | mg L-1 | FWI | N/A | 7.06 mg C |
| Dissolved organic carbon (DOC) | mmol L-1 | FWI | N/A | 13.1 mmol L-1 |
| Chlorophyll a (Chla) | mg L-1 | FWI | N/A | 0.52 mg L-1 |
| Total suspended sediment (TSS) | mg L-1 | UM | N/A | 2.5 mg L-1 |
| pH | pH units | UM | N/A | ± 0.01* |
| Conductivity | mS cm-1 | UM | N/A | 0.1 mS cm-1 |
| Dissolved inorganic carbon (DIC) | mmol kg-1 | UM | 12mL Exetainer | 7 mmol kg-1 |
| Total alkalinity (TA) | mmol kg-1 | UM | 12mL Exetainer | 20 mmol kg-1 |
| Dissolved methane concentration | nmol L-1 | UBC | 60mL serum vial | 0.4 nmol L-1 |

*Relative Accuracy; Detection Limit Not Applicable

NOTE:
Locations include the Freshwater Institute, Department of Fisheries and Oceans (FWI), University of Manitoba (UM) and University of British Columbia (UBC)

# 8.2 RESULTS

Detailed analyses of discrete water sampling, continuous measurements of dissolved $CO_2$ and $CH_4$ were conducted. The partial pressures of $CO_2$ and $CH_4$ ($pCO_2$ and $pCH_4$) are used to represent the dissolved GHG concentrations. Results for the reservoir-wide integrated fluxes for $CO_2$ and $CH_4$ are presented below. In this report, statistical differences were assessed using ANOVA and t-test analyses, based on 90% level of significance (p-value<0.1). Fluxes reported in this report are $gm^{-2}d^{-1}$ of $CO_2$ and $mgm^{-2}d^{-1}$ of $CH_4$ and a positive flux is directed toward the atmosphere.

## 8.2.1 DISSOLVED GREENHOUSE GASES

Dissolved GHGs underpin air-water gas exchange. The partial pressures for $CO_2$ and $CH_4$ resulting from the discrete sampling program for 2020 (pre-flood), 2021 and 2022 (post-flood) are shown in Figure 51 and Figure 52 for subareas within the reservoir: backbay, main channel (preexisting channel prior to flooding), downstream of the reservoir, generating station, over newly inundated terrain, and reference stations that are upstream of the reservoir influence (in Clark Lake).

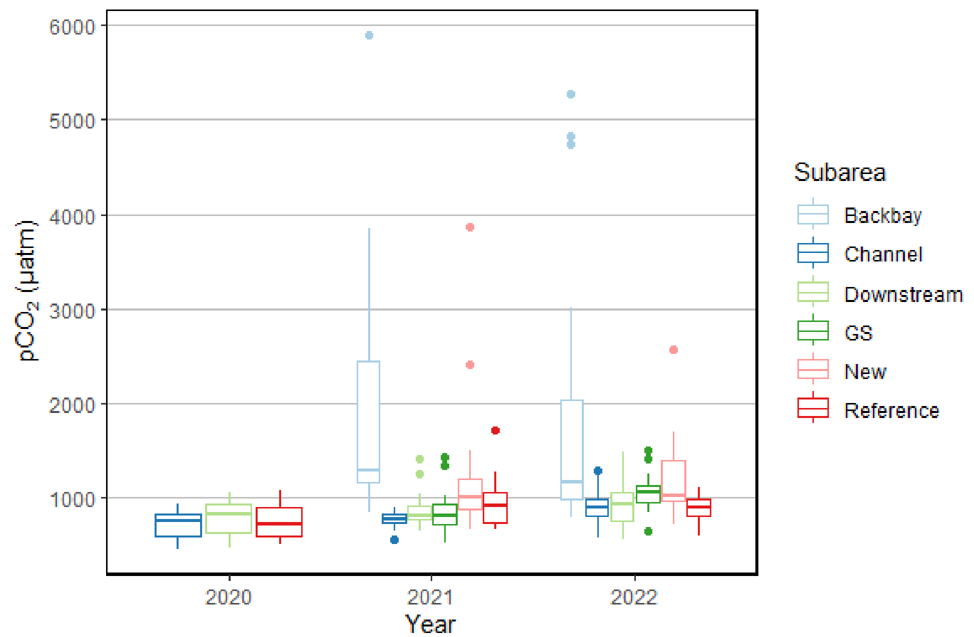


Subareas GS and New represent the generating station, and the newly inundated littoral zone, respectively. Channel represents sites within the existing river channel prior to impoundment. The reference subarea corresponds to measurements at Clark Lake, upstream of the influence of impoundment. Sub-areas are shown in Figure 50.

**Figure 51: Box and whisker plots depicting $pCO_2$ (calculated) from 2020 (water-up), 2021 and 2022 (both post flooding)**

The means (and medians) of $pCO_2$ and $pCH_4$ from all subareas were above atmospheric values (approximately 400 µatm and 2 µatm for $pCO_2$ and $pCH_4$ respectively) indicating that the systems served as a source of GHGs to the atmosphere between 2020 to 2022. During pre-flood (2020) there was little difference in $pCO_2$ among the three subareas – channel, downstream and reference. The means associated with these subareas could not be statistically differentiated. In 2021 and 2022 the $pCO_2$ within backbay and newly inundated areas were greater than in the main channel, and relative to the reference stations. In 2022 the mean $pCO_2$ in the channel could not be discriminated from values at the reference station.

In 2020 mean $pCH_4$ was also not significantly different among the three subareas. In 2021 mean $pCH_4$ was higher in the newly inundated samples relative to the other subareas, including the backbay. Mean $pCH_4$ in the channel could not be discriminated from the $pCH_4$ in the reference samples. Both the backbay and newly inundated samples showed the largest range of measured

$pCH_4$ (583 µatm and 413 µatm) among subareas. The variability may be evidence of ebullition/bubbling fluxes of $CH_4$, that could constitute a large part of $CH_4$ emissions discussed in Section 8.2.2.

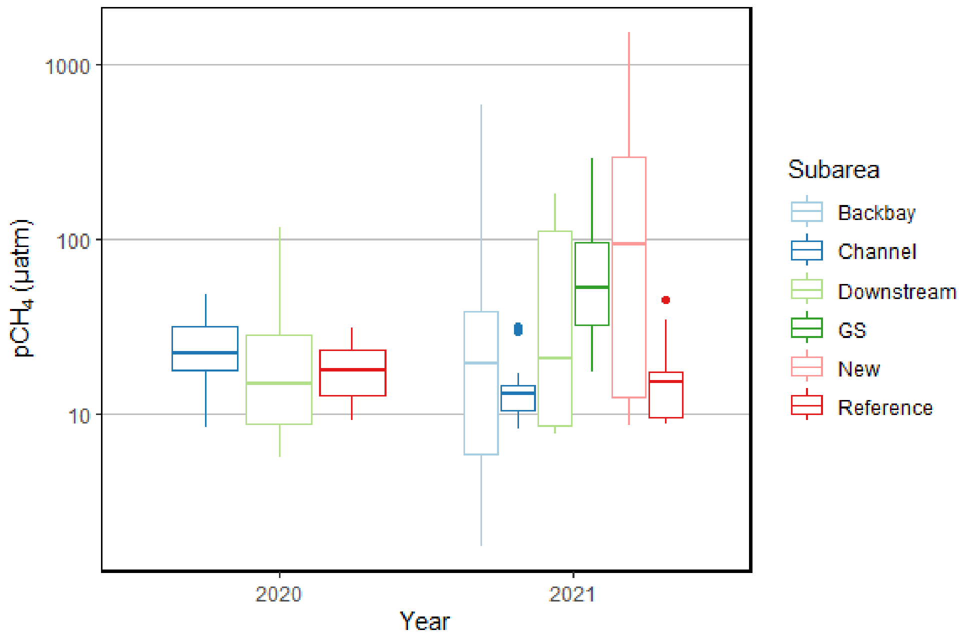


Information on subareas is provided in the caption for Figure 51. Note, data on $pCH_4$ for 2022 from discrete water samples was not available prior to the writing of this report.

**Figure 52. Box and whisker plots depicting $pCH_4$ from 2020 (water up), 2021 and 2022 (both post flooding)**

The time series of dissolved GHGs resulting from the submersible sensor program at the backbay site are shown in Figure 53 for the post-flood years 2021 and 2022. Pronounced short-term variation is observed in the $CH_4$ time series post impoundment. ` Episodic peaks were observed in the backbay data series for both 2021 and 2022, intermittently raising $pCH_4$ by several factors. These short-term peaks in $pCH_4$ may be evidence of ebullition/bubbling events and contributed to observed over-all variability in measured $pCH_4$ from the discrete water samples (Figure 54). Another key observation is that $pCH_4$ measured by the submersible sensors (averaging $129.98 \pm 85.33$ µatm and $403.28 \pm 268.63$ µatm in 2021 and 2022) where larger than values reported for the discrete sampling program in 2021 ($72.64 \pm 153.45$ µatm) suggesting that discrete sampling for $pCH_4$ is missing a considerable influence of episodic peaks on $pCH_4$ levels. The large standard deviations resulting from $pCH_4$ associated with both the point in time sampling and submersible sensor programs indicates that dissolved $CH_4$ concentrations are highly variable in space and time.

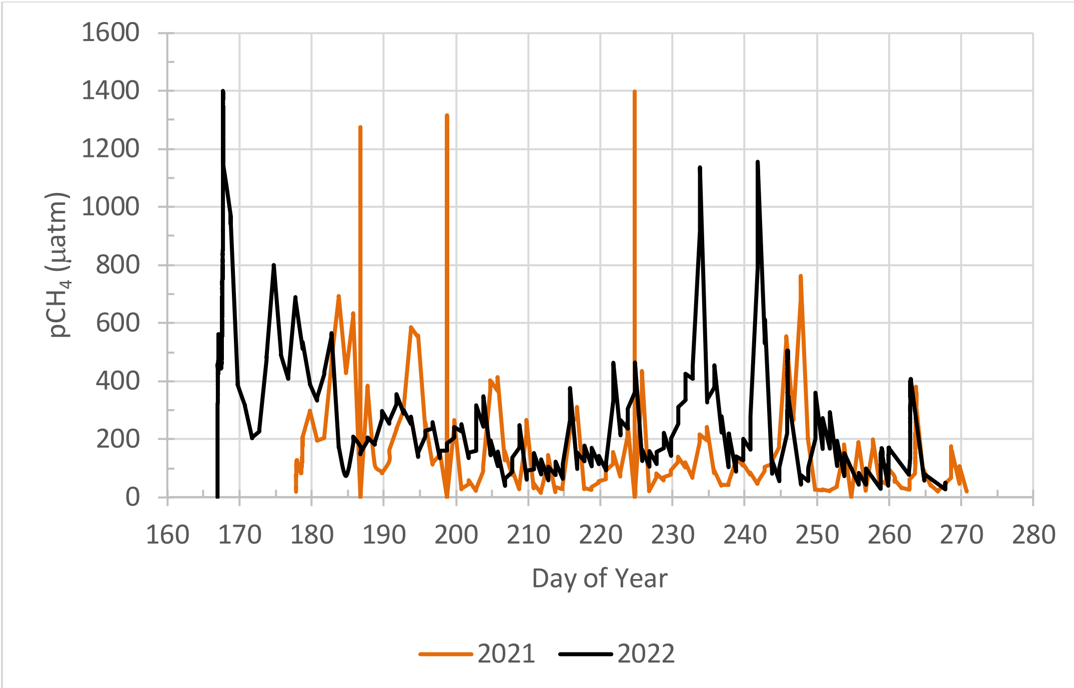


**Figure 53: Time series of $pCH_4$ measurements (in µatm) using a submersible sensor between 2021 and 2022 at the backbay raft (PE-KE-Z11-1-A).**

### 8.2.2 RESERVOIR WIDE AIR-WATER GHG EXCHANGE

Preliminary estimates for the reservoir-wide integrated fluxes for $CO_2$ and $CH_4$ were calculated daily using both EC fluxes representative of the littoral zone, and bulk diffusive fluxes for the non-littoral zone. Littoral and non-littoral zone fluxes were areally averaged assuming the littoral zone represents 22.3% of the reservoir's surface area, which is consistent with 2012 estimates of post-impoundment water depths that will be 3 metres or less over the flooded land (ECOSTEM Inc., 2012). Summertime data (June-September) were used in the calculations for the periods: 2009-2014 (baseline and construction phase), 2017-2019 (construction) and 2020 (water-up), and 2021 and 2022 (post-impoundment). Emission characteristics for pre- and post-impoundment are shown in Figure 54 and Figure 55 (Table 12 and Table 13). Reservoir-wide fluxes are shown in Figure 56 and Figure 57 (Table 14 and Table 15).

In the post-flood years $CO_2$ emissions from the littoral zone were far greater than the non-littoral zone, with emissions averaging 3.6±2.1 $gm^{-2}d^{-1}$ and 3.18±2.24 $gm^{-2}d^{-1}$ of $CO_2$ respectively in 2021 and 2022, compared to 1.47±0.69 and 2.25±0.97 $gm^{-2}d^{-1}$ for those same years in the non-littoral zone (Figure 54 and Table 12). While the average and median emission rates in the non-littoral zone were similar between periods, only fluxes in 2021 and 2017-2019 were not statistically different from one another. Fluxes during the baseline and construction period were statistically lower than fluxes in other periods, and fluxes of $CO_2$ in the littoral zone between 2021 and 2022 were statistically similar.

The difference between emission rates between the littoral and non-littoral zones in the post-flood periods are far more pronounced for $CH_4$ relative to observations for $CO_2$ (Figure 55 and Table 13). Average emissions in 2021 and 2022 ranged between 121.98±65.66 $mgm^{-2}d^{-1}$ and 93.73±40.54 $mgm^{-2}d^{-1}$, within the littoral zone while emissions in the non-littoral zone were orders of magnitude lower, rarely exceeding 3.5 $mgm^{-2}d^{-1}$. However, $CH_4$ flux rates were (statistically) not different between the baseline and construction period (2009-2014), 2020 (water-up phase). $CH_4$ emission rates observed in the non-littoral zones for both post-flood years (2021 and 2022) were also not statistically different from pre-flood measurements (2009-2014, and 2020). $CH_4$ emission rates observed in the littoral zones for both post-flood years (2021 and 2022) were (statistically) different from pre-flood measurements (2009-2014, and 2020).

EC flux measurements for $CH_4$ were close to zero, and in many instances not above the detection limit of the EC system for $CH_4$ between 2017 and 2019. This was discussed in previous reports (Manitoba Hydro 2019; 2020). For this reason, we exclude $CH_4$ results in Figure 55 and Figure 57, and correspondingly Table 13 and Table 15.

Reservoir-wide average $CO_2$ emission rates ranged between 1.95±0.79 $gm^{-2}d^{-1}$, and 2.45±0.84 $gm^{-2}d^{-1}$ in 2021 and 2022, respectively (Figure 56; Table 14). Post-flood rates are higher relative to previous periods. Flooding resulted in very large differences in $CH_4$ emissions (Figure 57) based on this preliminary analysis. Reservoir-wide average $CH_4$ emission rates ranged between 28.90±14.9 $mgm^{-2}d^{-1}$ and 22.84 ±9.10 $mgm^{-2}d^{-1}$ in 2021 and 2022, while emission rates prior to flooding rarely exceeded 2 $mgm^{-2}d^{-1}$.

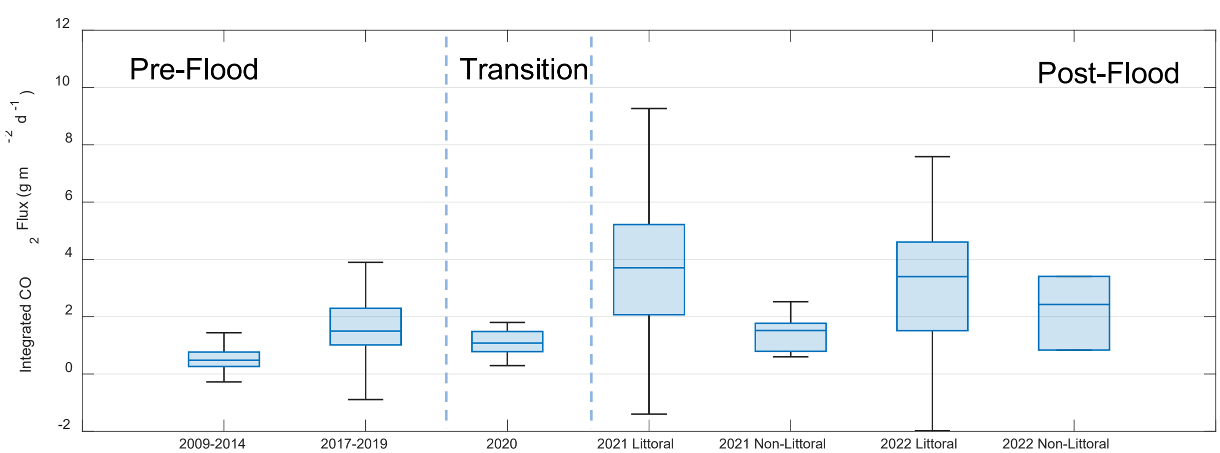


**Figure 54: Summary of open water fluxes (June to September) of $CO_2$ for the Keeyask region pre-flood (2009-2014 and 2017-2019), during water-up (2020) and post flooding shown for 2021 and 2022 littoral and non-littoral zones.**

**Table 12: Statistics describing the CO2 fluxes (g·m-2·d-1) from Keeyask area prior to/during construction (2009-2014), during construction (2017-2019), through water-up (2020), and from impounded reservoir (2021-2022).**

| | 2009-2014 | 2017-2019 | 2020 | 2021 Littoral | 2021 Non-Littoral | 2022 Littoral | 2022 Non-Littoral |
|---|---|---|---|---|---|---|---|
| Q1 | 0.26 | 1.01 | 0.78 | 2.07 | 0.79 | 1.51 | 0.84 |
| Median | 0.48 | 1.50 | 1.08 | 3.71 | 1.52 | 3.40 | 2.43 |
| Mean | 0.54 | 1.69 | 1.10 | 3.60 | 1.47 | 3.18 | 2.25 |
| Q3 | 0.77 | 2.29 | 1.48 | 5.22 | 1.77 | 4.61 | 3.40 |
| SD | 0.41 | 1.22 | 0.49 | 2.11 | 0.69 | 2.24 | 0.97 |
| n | 542 | 163 | 122 | 148 | 148 | 92 | 92 |

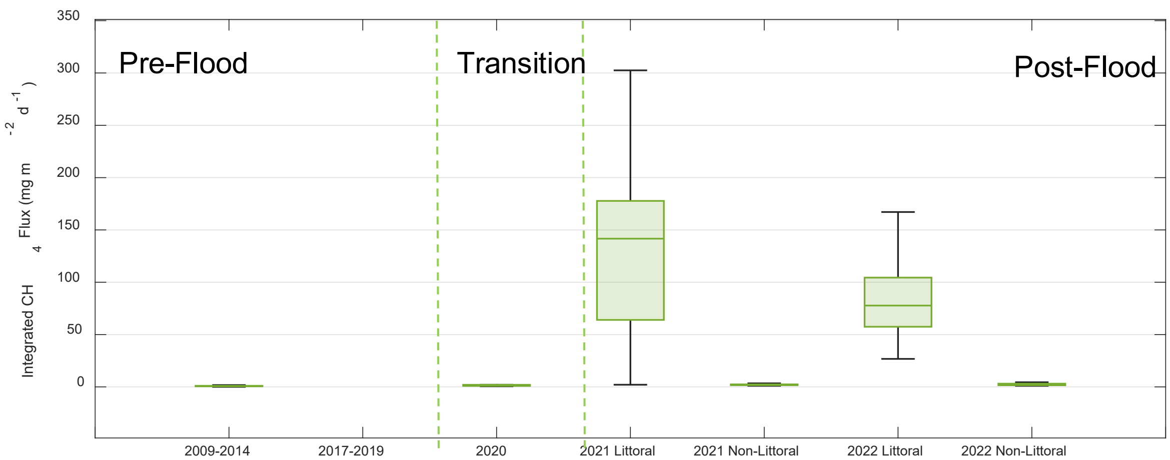


**Figure 55: Summary of open water fluxes (June to September) of $CH_4$ for the Keeyask region pre-flood (2009-2014 and 2017-2019), during water-up (2020) and post flooding shown for 2021 and 2022 littoral and non-littoral zones.**

**Table 13: Statistics describing the CH4 fluxes (mg·m-2·d-1) from Keeyask area prior to/during construction (2009-2014), during construction (2017-2019), through water-up (2020), and from impounded reservoir (2021-2022).**

| | 2009-2014 | 2017-2019 | 2020 | 2021 Littoral | 2021 Non-Littoral | 2022 Littoral | 2022 Non-Littoral |
|---|---|---|---|---|---|---|---|
| Q1 | 0.51 | | 0.78 | 64.00 | 1.60 | 65.45 | 1.59 |
| Median | 0.75 | | 1.08 | 141.66 | 2.25 | 81.30 | 2.18 |
| Mean | 0.79 | | 1.10 | 121.98 | 2.24 | 93.73 | 2.53 |
| Q3 | 1.02 | | 1.48 | 117.74 | 2.41 | 117.71 | 3.09 |
| SD | 0.39 | | 0.49 | 65.66 | 0.95 | 40.54 | 1.40 |
| n | 363 | | 122 | 117 | 117 | 75 | 75 |

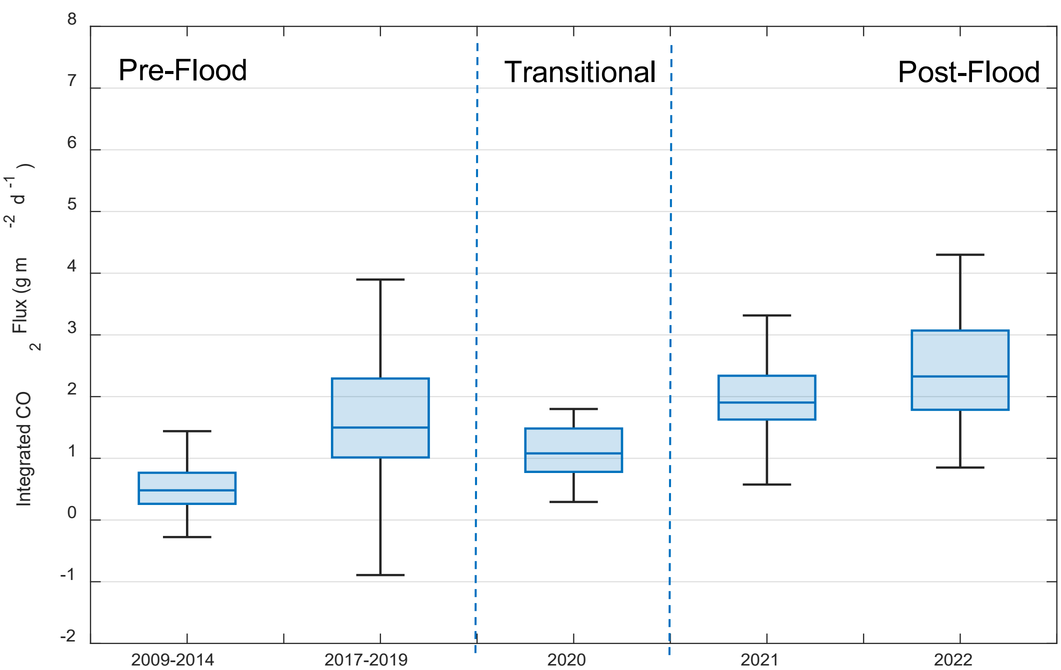


**Figure 56: Summary of the reservoir-wide integrated open water $CO_2$ flux (June to September) for the Keeyask region pre-flood (2009-2014 and 2017-2019), during water-up (2020) and post flooding shown for 2021 and 2022.**

**Table 14: Statistics describing the integrated CO2 flux (g·m-2·d-1) from Keeyask area prior to/during construction (2009-2014), during construction (2017-2019), through water-up (2020), and from impounded reservoir (2021-2022).**

| | 2009-2014 | 2017-2019 | 2020 | 2021 | 2022 |
|---|---|---|---|---|---|
| Q1 | 0.26 | 1.01 | 0.78 | 1.63 | 1.79 |
| Median | 0.48 | 1.50 | 1.08 | 1.90 | 2.33 |
| Mean | 0.54 | 1.69 | 1.10 | 1.95 | 2.45 |
| Q3 | 0.77 | 2.29 | 1.48 | 2.34 | 3.07 |
| SD | 0.41 | 1.22 | 0.49 | 0.79 | 0.84 |
| n | 542 | 163 | 122 | 148 | 92 |

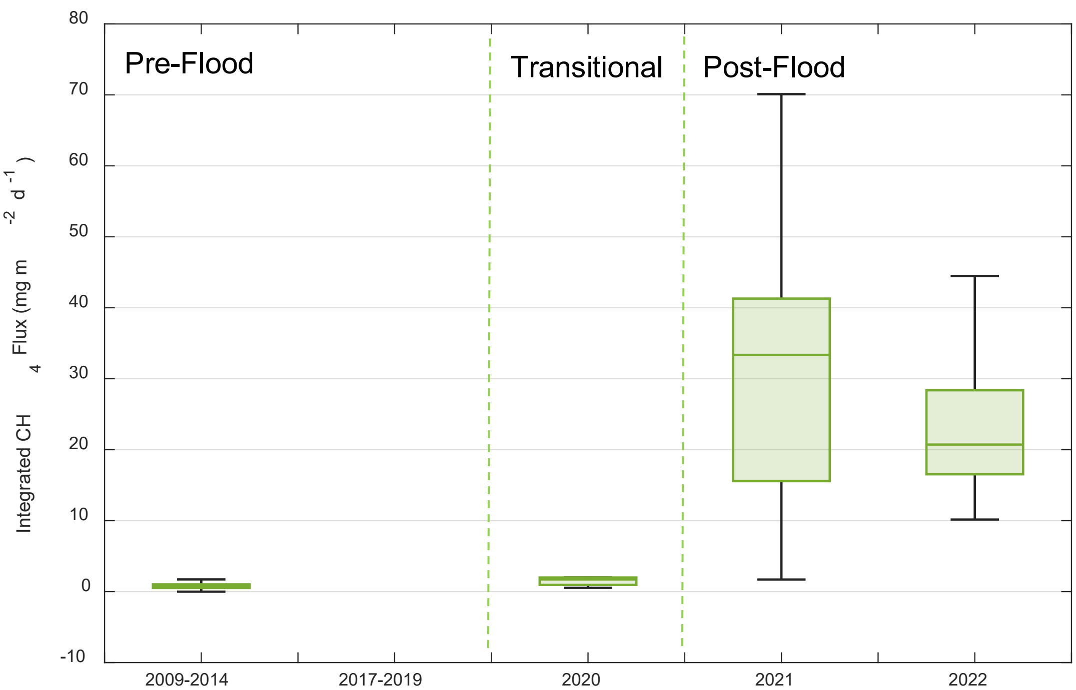


**Figure 57: Summary of the reservoir-wide integrated open water $CH_4$ flux (June to September) for the Keeyask region pre-flood (2009-2014 and 2017-2019), during water-up (2020) and post flooding shown for 2021 and 2022.**

**Table 15: Statistics describing the reservoir-wide integrated CH4 flux (mg·m-2·d-1) from Keeyask area prior to/during construction (2009-2014), during construction (2017-2019), through water up (2020), and from impounded reservoir (2021-2022).**

| | 2009-2014 | 2017-2019 | 2020 | 2021 | 2022 |
|---|---|---|---|---|---|
| Q1 | 0.51 | | 0.94 | 15.57 | 16.54 |
| Median | 0.75 | | 1.71 | 33.36 | 20.72 |
| Mean | 0.79 | | 1.30 | 28.90 | 22.84 |
| Q3 | 1.02 | | 1.99 | 41.29 | 28.37 |
| SD | 0.39 | | 0.59 | 14.90 | 9.10 |
| n | 363 | | 122 | 117 | 75 |

# 8.3 DISCUSSION

Measurements indicate that dissolved GHGs for the pre-impounded Nelson River upstream of the Keeyask generating station, and post-impoundment reservoir and associated subareas were in excess of atmospheric levels consistent with the prevailing view that inland aquatic systems are predominantly sources of GHGs ($CO_2$ and $CH_4$) to the atmosphere (e.g., Cole et al., 2007; Regnier et al., 2022).

Impoundment resulted in measurable increases in $pCO_2$ and $pCH_4$ within newly inundated areas that constitute the reservoir's littoral zone, including backbays. Impoundment also resulted in enhanced variation in dissolved GHG concentrations across the sub environments of the reservoir complex. Higher $pCO_2$ and $pCH_4$ were observed in the shallow recently inundated areas of the former river shore relative to the deeper water of the existing channel. An increase in dissolved GHGs resulting from water impoundment for hydroelectric production has been widely reported in boreal reservoirs (e.g., Teoduro et al., 2012; Deemer et al., 2016; Demarty and Tremblay, 2017), and was anticipated for the Keeyask development (Keeyask Hydropower Limited Partnership, 2012). The $pCH_4$ in particular showed pronounced variability likely resulting from the influence of episodic release of methane from submerged sediments, which is known to be spatiotemporally variable (e.g., DelSontro et al., 2016; 2018).

Impoundment did not result in an appreciable difference in $CH_4$ fluxes in the deep waters of the existing channel (non-littoral zone) relative to pre-flood years. Impound did however cause measurable increases in both the $CO_2$ and $CH_4$ fluxes in the shallow water zones associated with recent inundation, relative to the pre-flood years. Reservoir-wide estimates of GHG emissions were higher post-impoundment relative to pre-impoundment emissions, resulting largely from increased emissions in the recently inundated littoral zone of the reservoir complex. It is assumed that flux measurements from the sampling sites within the littoral zone are representative of the entire littoral zone contained within the Keeyask reservoir complex, and that the areal proportion of littoral zone is consistent with 2012 estimates of post-impoundment water depths that will be 3 metres or less over the flooded land (ECOSTEM Inc., 2012).

The littoral zone of the Keeyask reservoir complex is driving the increase in reservoir emissions, and littoral zone $CH_4$ fluxes ($93.73\pm 40.54$ $mgm^{-2}d^{-1}$ to $121.98\pm65.66$ $mgm^{-2}d^{-1}$) are close to values reported for boreal beaver ponds. For example, Roulet et al. (1997) reported beaver pond $CH_4$ emission rates of between 108.86 $mgm^{-2}d^{-1}$ and 161.57 $mgm^{-2}d^{-1}$ during the ice-free season. Both the beaver pond and the littoral zone of the Keeyask reservoir complex are underlain by carbon rich soils, and hence on impoundment the similarity in $CH_4$ emissions should not be surprising. These early observations suggest that the Keeyask reservoir may have created a new environment, at least short term, that is favourable for producing $CH_4$.

Given the disproportionate influence of the fluxes in the littoral zone, it is important that its areal proportion is well constrained to facilitate accurate reservoir estimates, that future monitoring has an emphasis on both characterizing variation in the flux, and variability in dissolved gas concentrations that underpin measured fluxes for a representative sample of littoral environments.

The emissions reported in this report are gross emissions. A next step is to develop estimates for net change in emissions by considering the carbon sinks and sources from the terrestrial and natural aquatic ecosystems that existed prior to flooding and have since been inundated through flooding.

# 8.4 SUMMARY

- Dissolved GHGs for the pre-impounded Nelson River upstream of the Keeyask generating station, and post-impoundment reservoir and associated subareas were in excess of atmospheric levels and therefore are sources of the GHGs $CO_2$ and $CH_4$ to the atmosphere;
- Consistent with Project predictions, reservoir-wide estimates of GHG emissions were higher after flooding relative to pre-impoundment emissions;
- Impoundment resulted in increases in both $pCO_2$ and $pCH_4$ within newly inundated areas that constitute the reservoir's littoral zone, including backbays;
- An increase in emissions of both $CO_2$ and $CH_4$ were observed in the recently inundated littoral zone of the reservoir complex;
- The impact of flooding appears to have affected rates of $CH_4$ emissions to a greater extent than emissions of $CO_2$. The reasons that underpin this observation require more study, but may be related to the naturally high water alkalinity of the Nelson River. The littoral zone of the Keeyask reservoir complex is driving reservoir emissions, and in the case of $CH_4$ emissions are similar to values reported for boreal beaver ponds. These early observations suggest that the Keeyask reservoir may have created, at least short term, a new environment that is favourable for producing $CH_4$;
- The shallow water/littoral zone emits a large proportion of the reservoir emissions. It is important to continue to monitor GHG concentrations in the water and emissions to the air in these regions.

# 9.0 LITERATURE CITED

Barros, N., J. J. Cole, L. J. Tranvik, Y. T. Prairie, D. Bastviken, V. L. M. Huszar, P. del Giorgio, F. Roland, 2011. Carbon emission from hydroelectric reservoirs linked to reservoir age and latitude, Nature Geoscience, Letters, http://www.nature.com/doifinder/10.1038/ngeo1211.

Bastien, J., M. Demarty, A. Tremblay, 2011. $CO_2$ and $CH_4$ diffusive and degassing emissions from 2003 to 2009 at Eastmain 1 hydroelectric reservoir, Québec, Canada, Inland Waters 1, pp. 113--123.

Cole, J.J., Y.T. Prairie, N.F. Caraco, W.H. McDowell, L.J. Tranvik, R.G. Striegl, C.M. Duarte, P. Kortelainen, J.A. Downing, J.J. Middelburg, & J. Melack, (2007). Plumbing the global carbon cycle: integrating inland waters into the terrestrial carbon budget. Ecosystems, pp. 10, 172–185.

Deemer, B.R., J.A. Harrison, S. Li, (2016). Greenhouse gas emissions from reservoir water surfaces: a new global synthesis. *Bioscience*, 66(11), 949–964. https://doi.org/10.1093/biosci/biw117.

DelSontro, T., L. Boutet, A. St-Pierre, P. A. del Giorgio, Y. Prairie, (2016). Methane ebullition and diffusion from northern ponds and lakes regulated by the interaction between temperature and system productivity, Limnol. Oceanogr., 61, S62-S77, doi: 10.1002/Lno.10335.

DelSontro, T., J. J. Beaulieu, J. A. Downing, 2018. Greenhouse gas emissions from lakes and impoundments: Upscaling in the face of global change, Limnology and Oceanography Letters 3, pp. 64–75, doi: 10.1002/lol2.10073.

Demarty, M. and A. Tremblay, (2017). Long term follow-up of $pCO_2$, $pCH_4$ and emissions from Eastmain 1 boreal reservoir, and the Rupert diversion bays, Canada, Ecohydrology & Hydrobiology, 19(4), 529-540.

ECOSTEM Inc., (2012). Keeyask Generation Project, Stage IV Studies – Physical Environment: Peatland Disintegration In the Proposed Keeyask Reservoir Area: Model Development and Post-Project Predictions – GN 9.2.7. December 2012.

Goldenfum, J.A., 2012. Challenges and solutions for assessing the impact of freshwater reservoirs on natural GHG emissions, Ecohydrology Hydrobiology, Volume 12, No. 12, pp. 115-122.

IPCC, (2019). 2019 Refinement to the 2006 IPCC Guidelines for National Greenhouse Gas Inventories: Chapter 7 Wetlands, C.E. Lovelock, C. Evans, N. Barros, Y. Prairie, J. Alm, D. Bastviken, J.J. Beaulieu, M. Garneau, A. Harby, J. Harrison, D. Pare, H. Lerche Raadal, B. Sherman, C. Zhang, S.O. Ogle, Published: IPCC, Switzerland.

Keeyask Hydropower Limited Partnership (KHLP). 2012a. Keeyask Generation Project: Response to EIS Guidelines. June 2012. Winnipeg, Manitoba.

Keeyask Hydropower Limited Partnership (KHLP). 2012b. Keeyask Generation Project: Physical Environment Supporting Volume. June 2012. Winnipeg, Manitoba

Keeyask Hydropower Limited Partnership (KHLP). 2012c. Keeyask Generation Project: Aquatic Environment Supporting Volume. June 2012. Winnipeg, Manitoba

Keeyask Hydropower Limited Partnership (KHLP). 2015a. Keeyask Generation Project: Physical Environment Monitoring Plan. October 2015. Winnipeg, Manitoba.

Keeyask Hydropower Limited Partnership (KHLP). 2015b. Keeyask Generation Project: Aquatic Effects Monitoring Plan. June 2015. Winnipeg, Manitoba.

Keeyask Hydropower Limited Partnership (KHLP). 2015c. Keeyask Generation Project: Reservoir Clearing Plan. April 2015. Winnipeg, Manitoba.

Keeyask Hydropower Limited Partnership (KHLP). 2014. Keeyask Generation Project: Sediment Management Plan for In-stream Construction. July 2014. Winnipeg, Manitoba.

KGS Acres Ltd. 2011. Keeyask Generating Station, Stage IV Studies: Existing Environment Sedimentation (Memorandum GN9.2.3, Mb Hydro File No. 00195-11100-0154_03). June 2011. Winnipeg, Manitoba.

Liss, P. and P. Slater, (1974). Flux of Gases across the Air-Sea Interface. Nature 247, 181–184.

Manitoba Hydro. 2015. 2014–2015 Physical Environment Monitoring Report: Year 1 Construction. June 2016. Winnipeg, Manitoba.

Manitoba Hydro. 2016. 2015–2016 Physical Environment Monitoring Report: Year 2 Construction. June 2016. Winnipeg, Manitoba.

Manitoba Hydro. 2017. 2016–2017 Physical Environment Monitoring Report: Year 3 Construction. June 2017. Winnipeg, Manitoba.

Manitoba Hydro. 2018. 2017–2018 Physical Environment Monitoring Report: Year 4 Construction. June 2018. Winnipeg, Manitoba.

Manitoba Hydro. 2019. 2018–2019 Physical Environment Monitoring Report: Year 5 Construction. June 2019. Winnipeg, Manitoba.

Manitoba Hydro. 2020. 2019–2020 Physical Environment Monitoring Report: Year 6 Construction. June 2020. Winnipeg, Manitoba.

Manitoba Hydro. 2021. 2020–2021 Physical Environment Monitoring Report: Year 7 Construction. June 2021. Winnipeg, Manitoba.

Manitoba Hydro. 2022. 2021–2022 Physical Environment Monitoring Report: Year 1 Operation. June 2022. Winnipeg, Manitoba.

Manitoba Hydro. 2020. Sediment Management Plan for In-Stream Construction Annual Report April 2019 – March 2020. June 2020. Winnipeg, Manitoba.

Marchand D., M. Demarty and R. Gill, (2013). Reservoir Greenhouse Gas Monitoring Report – 2013. Report prepared by Environnement Illimité inc. for Manitoba Hydro, Tier 1: 46 p. and 3 appendices. Tier 2: 47 p. and 1 appendix.

Marchand D., M. Demarty, and R. Gill, (2015). Keeyask Technical Summary – 2014. Summary prepared by Environnement Illimité for Manitoba Hydro, 11 p.

Pierrot, D., E. Lewis, and D.W.R. Wallace, (2006). MS Excel Program Developed for CO2 System Calculations.

Prairie YT, J. Alm, A. Harby, S. Mercier-Blais, and R. Nahas, (2017). The GHG Reservoir Tool (Gres) Technical documentation. Updated version 3.2 (2022-12-19). UNESCO/IHA research project on the GHG status of freshwater reservoirs. Joint publication of the UNESCO Chair in Global Environmental Change and the International Hydropower Association. 75 pages.

Prairie, Y.T., J. Alm, J. Beaulieu, N. Barros, T. Battin, J. Cole, P. del Giorigio, T. Delsontro, F. Guérin, A. Harby, J. Harrison, S. Mercier-Blais, D. Serçra, S. Sobek, and D. Vachon, (2018). Greenhouse gas emissions from freshwater reservoirs: what does the atmosphere see?, Ecosystems, 21, 1058-1071.

Prairie, Y.T., S. Mercier-Blais, J.A. Harrison, C. Soued, P. del Giorgio, A. Harby, J. Alm, V. Chanudet, and R. Nahas, (2021). A new modelling framework to assess biogenic GHG emissions from reservoirs: The G-res tool, Environmental Modelling & Software, Volume 143, 105117, ISSN 1364-8152, https://doi.org/10.1016/j.envsoft.2021.105117.

Regnier, P., L. Resplandy, R. G. Najjar, and P. Ciais, (2022). The land-to-ocean loops of the global carbon cycle. Nature, 603, https://doi.org/10.1038/s41586-021-04339-9.

Rosa, E., J. Gaillardet, C. Hillaire-Marcel, J.F. Hélie, and L.F. Richard, (2012). Rock denudation rates and organic carbon exports along a latitudinal gradient in the Hudson, James, and Ungava bays watershed. Canadian Journal of Earth Sciences, 49, 742–757. https://doi.org/10.1139/e2012-021.

Roulet, N.T., P.M. Crill, N.T. Comer, A. Dove and R.A Boubonniere, (1997). CO2 and CH4 flux between a boreal beaver pond and the atmosphere, J. Geophys. Res., 102, D24, 29,313-29,319. doi:10.1029/97JD01237.

Tank S.E., P.A. Raymond, R.G. Striegl, J.W. McClelland, R.M. Holmes, G.J. Fiske and B.J. Peterson, (2012). A land-to-ocean perspective on the magnitude, source and implication of DIC flux from major Arctic rivers to the Arctic Ocean. Global Biogeochemical Cycles, 26, GB4018.

Teodoru, C.R., J. Bastien, M.C. Bonneville, P.A. del Giorgio, M. Demarty, M. Gameau, J.F. Hélie, L. Pelletier, Y.T. Prairie, N.T. Roulet, J.B. Strachan, and A. Tremblay, (2012). The net carbon footprint of a newly created boreal hydroelectric reservoir. Global Biogeochemical Cycles, 26, 1-14.

TetrES Consultants Inc., 2011. Water Temperature & Dissolved Oxygen Study – Project Effects. Keeyask Project Environmental Studies Program Report prepared for Manitoba Hydro. 100 pp.

Tremblay, A., J. Bastien, M. Demarty, and C. Demers, (2010). Measuring Greenhouse Gas Emissions from a Canadian Reservoir. Hydro Review, Volume 29, No. 5, pages 22-29.

TCN, WLFN, YFFN, FLCN and the Manitoba Hydro-Electric Board. 2009. Joint Keeyask Development Agreement. May 2009. Winnipeg, Manitoba.

United States Environmental Protection Agency (USEPA), 1985. Rates, Constants, and Kinetics Formulations in Surface Water Quality Modeling. Second Edition (EPA/600/3-85/040). Environmental Research Laboratory, Office of Research and Development. June 1985. Athens, GA.

Vachon, D. and Y.T. Prairie, (2013). The ecosystem size and shape dependence of gas transfer velocity versus wind speed relationships in lakes. Canadian Journal of Fisheries and Aquatic Sciences 70(12):1-8.

Wanninkhof, R., W.E. Asher, D.T. Ho, C. Sweeney, and W.R. McGillis, (2009). Advances in Quantifying Air-Sea Gas Exchange and Environmental Forcing. Annual Review of Marine Science 1:1, 213-244.

# APPENDIX 1:
# DETAILED MAPS OF PEMP MONITORING SITES

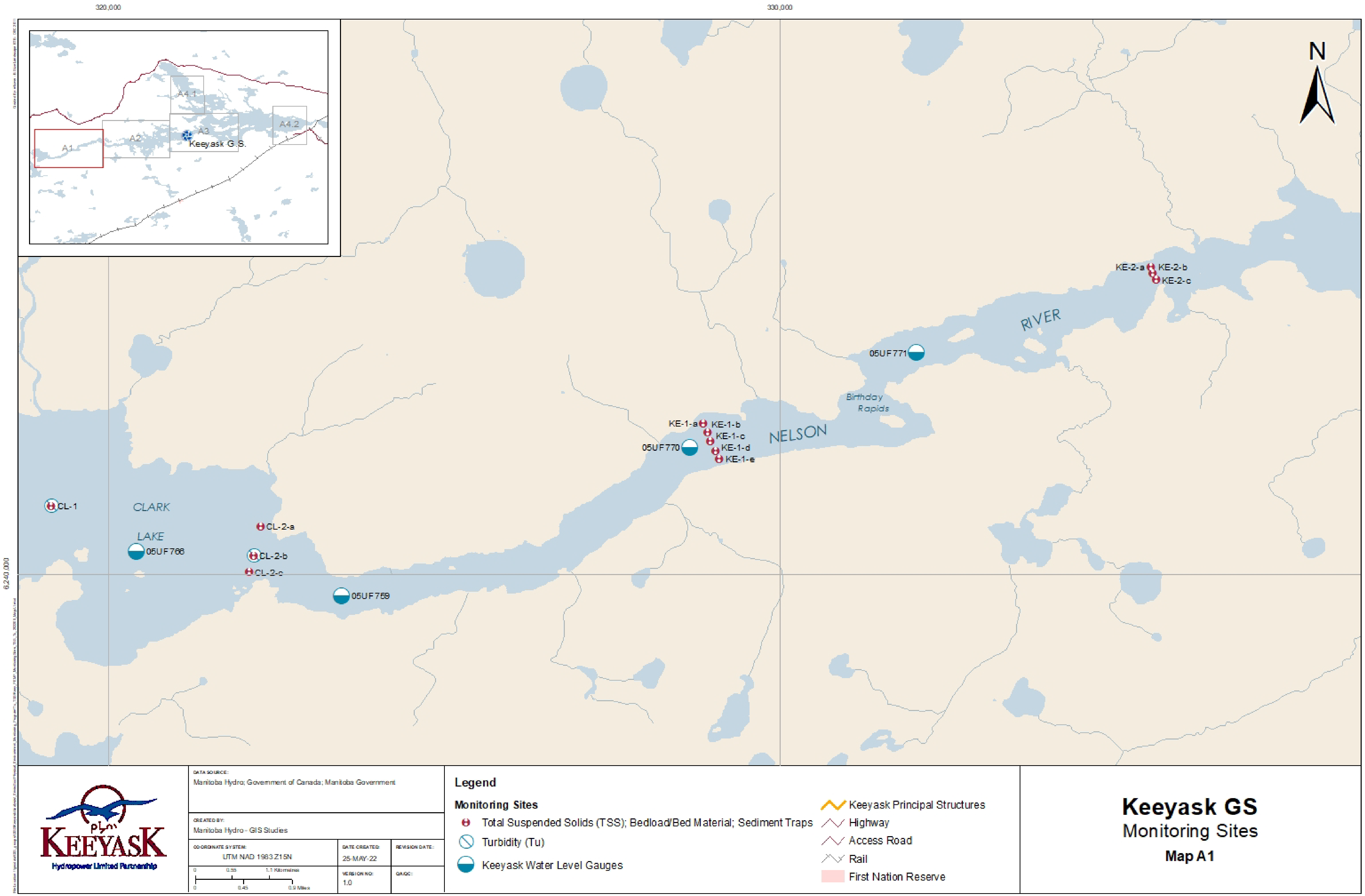
320,000
330,000
6,240,000
N
A4-1
A4-2
A3
A2
A1
Keeyask G.S.
KE-2-a
KE-2-b
KE-2-c
RIVER
05UF771
Birthday Rapids
NELSON
KE-1-a
KE-1-b
KE-1-c
KE-1-d
KE-1-e
05UF770
CL-1
CLARK
LAKE
05UF766
CL-2-a
CL-2-b
CL-2-c
05UF769
DATA SOURCE:
Manitoba Hydro; Government of Canada; Manitoba Government
CREATED BY:
Manitoba Hydro - GIS Studies
COORDINATE SYSTEM:
UTM NAD 1983 Z15N
DATE CREATED:
25-MAY-22
REVISION DATE:
VERSION NO:
1.0
QA/QC:
KEEYASK
Hydropower Limited Partnership
Legend
Monitoring Sites
Total Suspended Solids (TSS); Bedload/Bed Material; Sediment Traps
Turbidity (Tu)
Keeyask Water Level Gauges
Keeyask Principal Structures
Highway
Access Road
Rail
First Nation Reserve
Keeyask GS
Monitoring Sites
Map A1

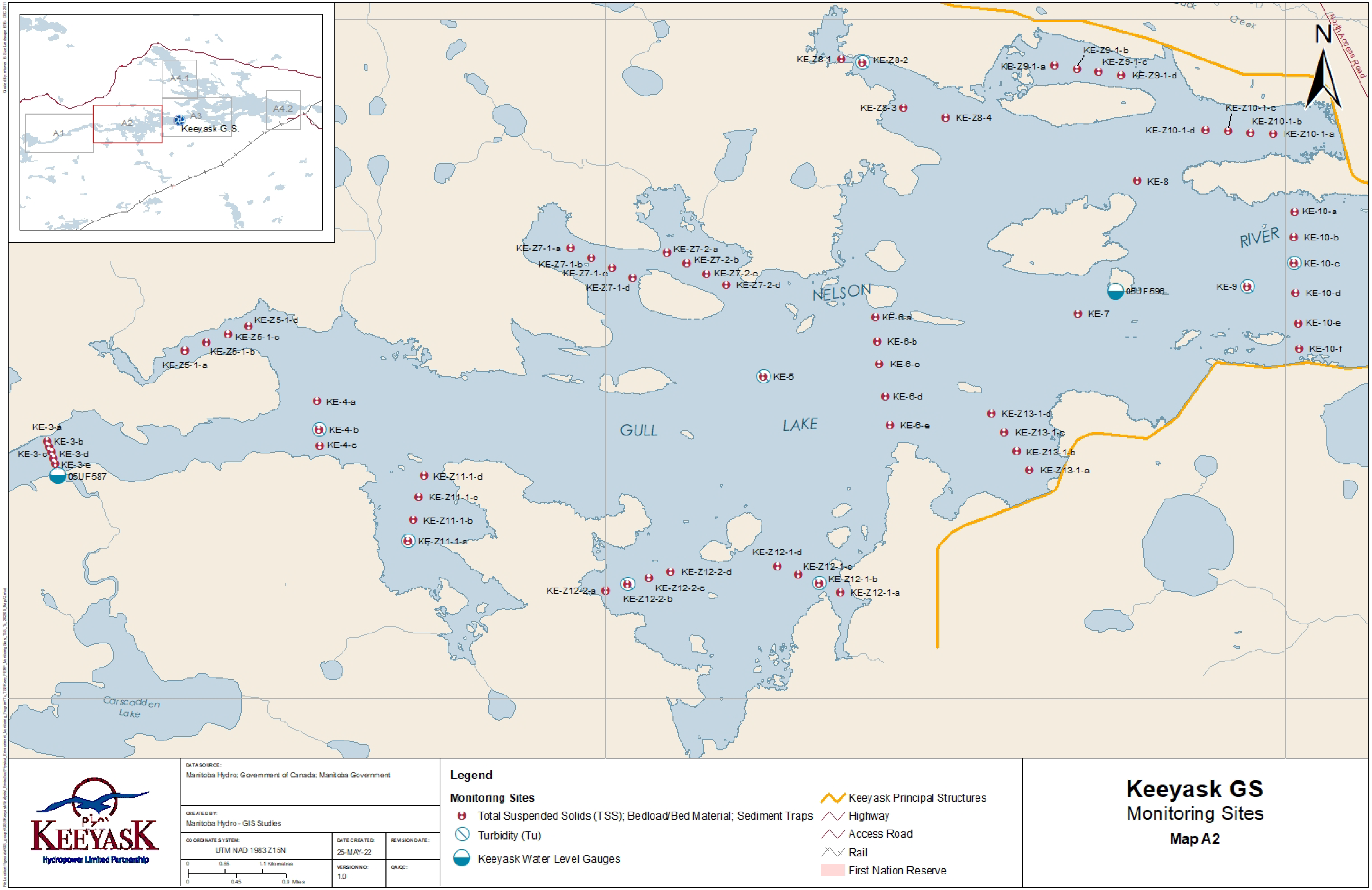
350,000
360,000
6,250,000
6,240,000
N
KE-Z8-1
KE-Z8-2
KE-Z8-3
KE-Z8-4
KE-Z9-1-a
KE-Z9-1-b
KE-Z9-1-c
KE-Z9-1-d
KE-Z10-1-a
KE-Z10-1-b
KE-Z10-1-c
KE-Z10-1-d
KE-8
KE-10-a
KE-10-b
KE-10-c
KE-10-d
KE-10-e
KE-10-f
KE-9
05UF596
KE-7
RIVER
NELSON
GULL
LAKE
KE-Z7-1-a
KE-Z7-1-b
KE-Z7-1-c
KE-Z7-1-d
KE-Z7-2-a
KE-Z7-2-b
KE-Z7-2-c
KE-Z7-2-d
KE-6-a
KE-6-b
KE-6-c
KE-6-d
KE-6-e
KE-5
KE-Z5-1-a
KE-Z5-1-b
KE-Z5-1-c
KE-Z5-1-d
KE-4-a
KE-4-b
KE-4-c
KE-3-a
KE-3-b
KE-3-c
KE-3-d
KE-3-e
05UF587
KE-Z11-1-a
KE-Z11-1-b
KE-Z11-1-c
KE-Z11-1-d
KE-Z12-1-a
KE-Z12-1-b
KE-Z12-1-c
KE-Z12-1-d
KE-Z12-2-a
KE-Z12-2-b
KE-Z12-2-c
KE-Z12-2-d
KE-Z13-1-a
KE-Z13-1-b
KE-Z13-1-c
KE-Z13-1-d
Carscadden Lake
A1
A2
A3
A4.1
A4.2
Keeyask G.S.
DATA SOURCE:
Manitoba Hydro; Government of Canada; Manitoba Government
CREATED BY:
Manitoba Hydro - GIS Studies
COORDINATE SYSTEM:
UTM NAD 1983 Z15N
DATE CREATED:
25-MAY-22
REVISION DATE:
VERSION NO:
1.0
QA/QC:
Legend
Monitoring Sites
Total Suspended Solids (TSS); Bedload/Bed Material; Sediment Traps
Turbidity (Tu)
Keeyask Water Level Gauges
Keeyask Principal Structures
Highway
Access Road
Rail
First Nation Reserve
Keeyask GS
Monitoring Sites
Map A2

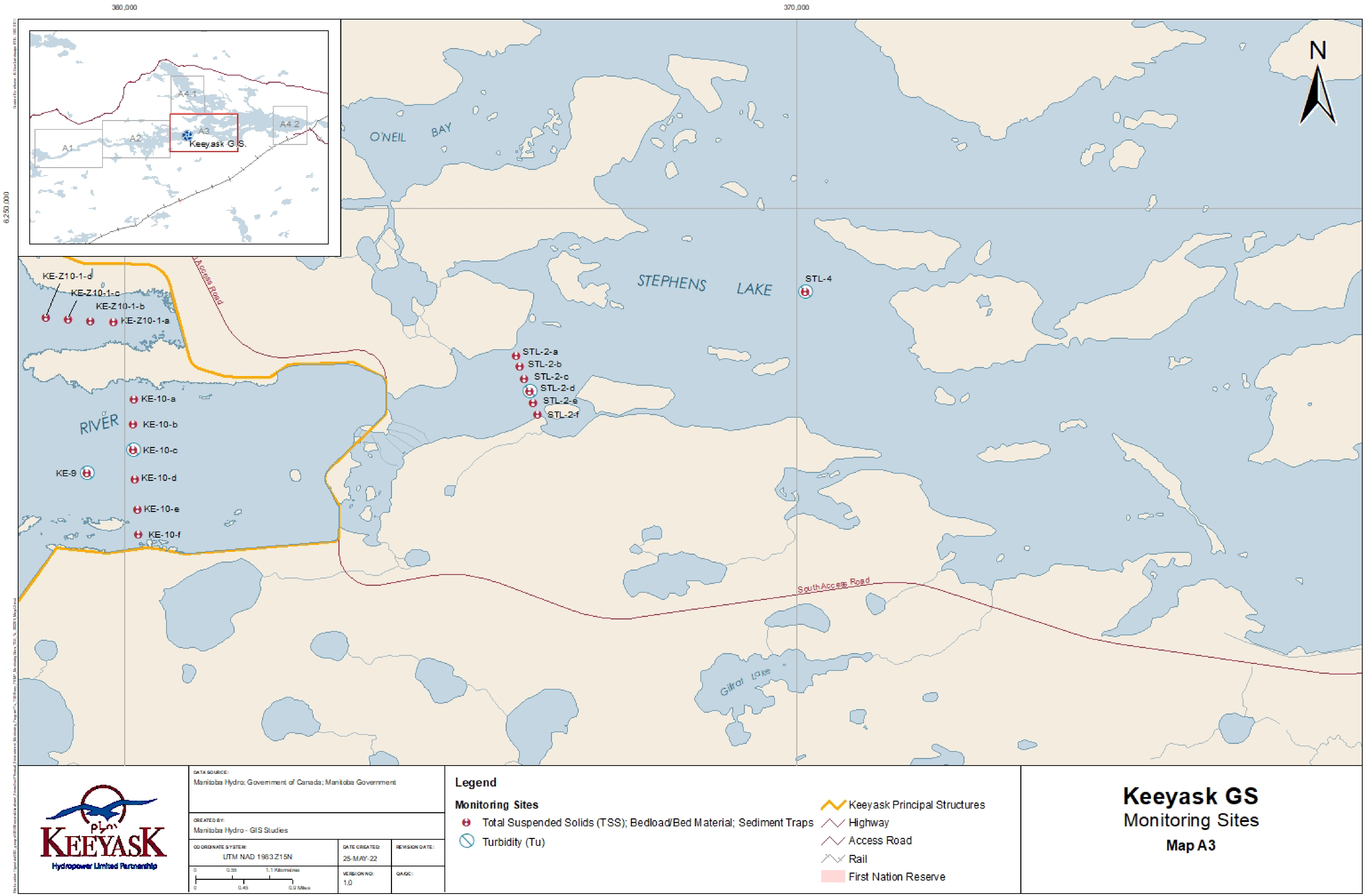
360,000
370,000
6,250,000
6,250,000
N
A1
A2
A3
A4.1
A4.2
Keeyask G.S.
O'NEIL BAY
STEPHENS LAKE
RIVER
Access Road
South Access Road
Gillrat Lake
KE-Z10-1-d
KE-Z10-1-c
KE-Z10-1-b
KE-Z10-1-a
KE-10-a
KE-10-b
KE-10-c
KE-10-d
KE-10-e
KE-10-f
KE-9
STL-2-a
STL-2-b
STL-2-c
STL-2-d
STL-2-e
STL-2-f
STL-4
KEEYASK
Hydropower Limited Partnership
DATA SOURCE:
Manitoba Hydro; Government of Canada; Manitoba Government
CREATED BY:
Manitoba Hydro - GIS Studies
COORDINATE SYSTEM:
UTM NAD 1983 Z15N
DATE CREATED:
25-MAY-22
REVISION DATE:
VERSION NO:
1.0
QA/QC:
Legend
Monitoring Sites
Total Suspended Solids (TSS); Bedload/Bed Material; Sediment Traps
Turbidity (Tu)
Keeyask Principal Structures
Highway
Access Road
Rail
First Nation Reserve
Keeyask GS
Monitoring Sites
Map A3

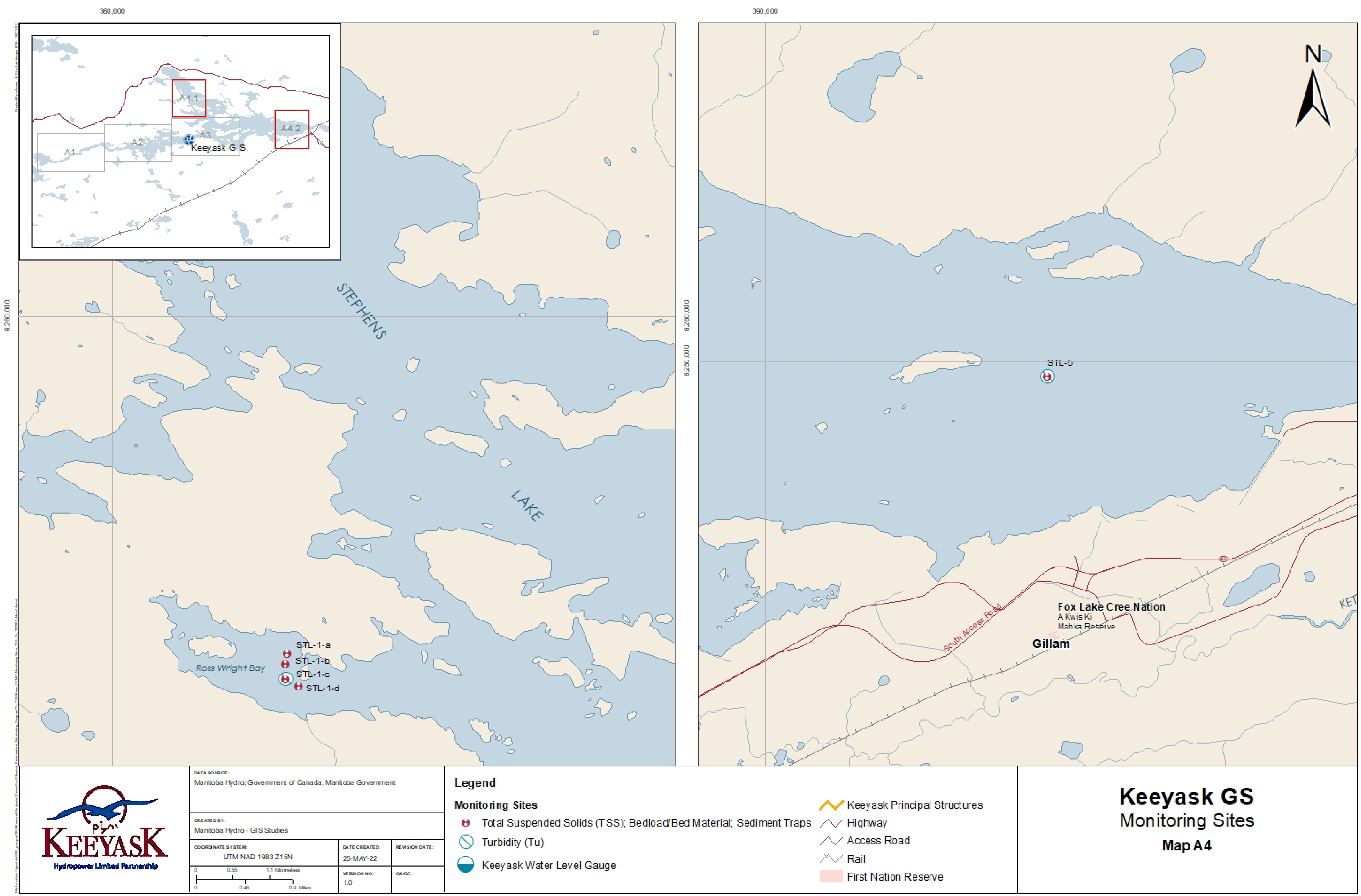
380,000
390,000
6,260,000
6,250,000
A4.1
A4.2
A1
A2
A3
Keeyask G.S.
STEPHENS
LAKE
Ross Wright Bay
STL-1-a
STL-1-b
STL-1-c
STL-1-d
STL-5
N
Fox Lake Cree Nation
A Kwis Ki
Mahka Reserve
Gillam
South Access Road
KEEYASK
Hydropower Limited Partnership
DATA SOURCE:
Manitoba Hydro; Government of Canada; Manitoba Government
CREATED BY:
Manitoba Hydro - GIS Studies
COORDINATE SYSTEM:
UTM NAD 1983 Z15N
DATE CREATED:
25-MAY-22
REVISION DATE:
VERSION NO:
1.0
QA/QC:
0 0.55 1.1 Kilometres
0 0.45 0.9 Miles
Legend
Monitoring Sites
Total Suspended Solids (TSS); Bedload/Bed Material; Sediment Traps
Turbidity (Tu)
Keeyask Water Level Gauge
Keeyask Principal Structures
Highway
Access Road
Rail
First Nation Reserve
Keeyask GS
Monitoring Sites
Map A4

# APPENDIX 2: WINTER DEPTH PROFILE CHARTS OF DISSOLVED OXYGEN CONCENTRATION, PERCENT SATURATION, AND WATER TEMPERATURE

**Site Listing in order of presentation in Appendix 2:**

Note that site names on charts all include the "PE_" prefix that is an internal designation used to identify the monitoring site as part of the physical environment program.

Mainstem sites (upstream to downstream):

- PE_CL-1
- PE_KE-5
- PE_KE-9
- PE_STL-4

North backbay sites:

- PE_KE-Z4-1-a, b, c, d (i.e, PE_KE-Z4-1-a, PE_KE-Z4-1-b, PE_KE-Z4-1-c, PE_KE-Z4-1-d)
- PE_KE-Z5-1-a, b, c, d
- PE_KE-Z7-1-a, b, c, d
- PE_KE-Z7-2-a, b, c, d
- PE_KE-Z8-1, 2, 3, 4
- PE_KE-Z9-1-a, b, c, d
- PE_KE-Z10-1-a, b, c, d

South backbay sites:

- PE_KE-Z11-1-a, b, c, d
- PE_KE-Z12-1-a, b, c, d
- PE_KE-Z12-2-a, b, c, d
- PE_KE-Z13-1-a, b, c, d

Stephens Lake backbay site:

- PE_STL-1-a, b, c, d

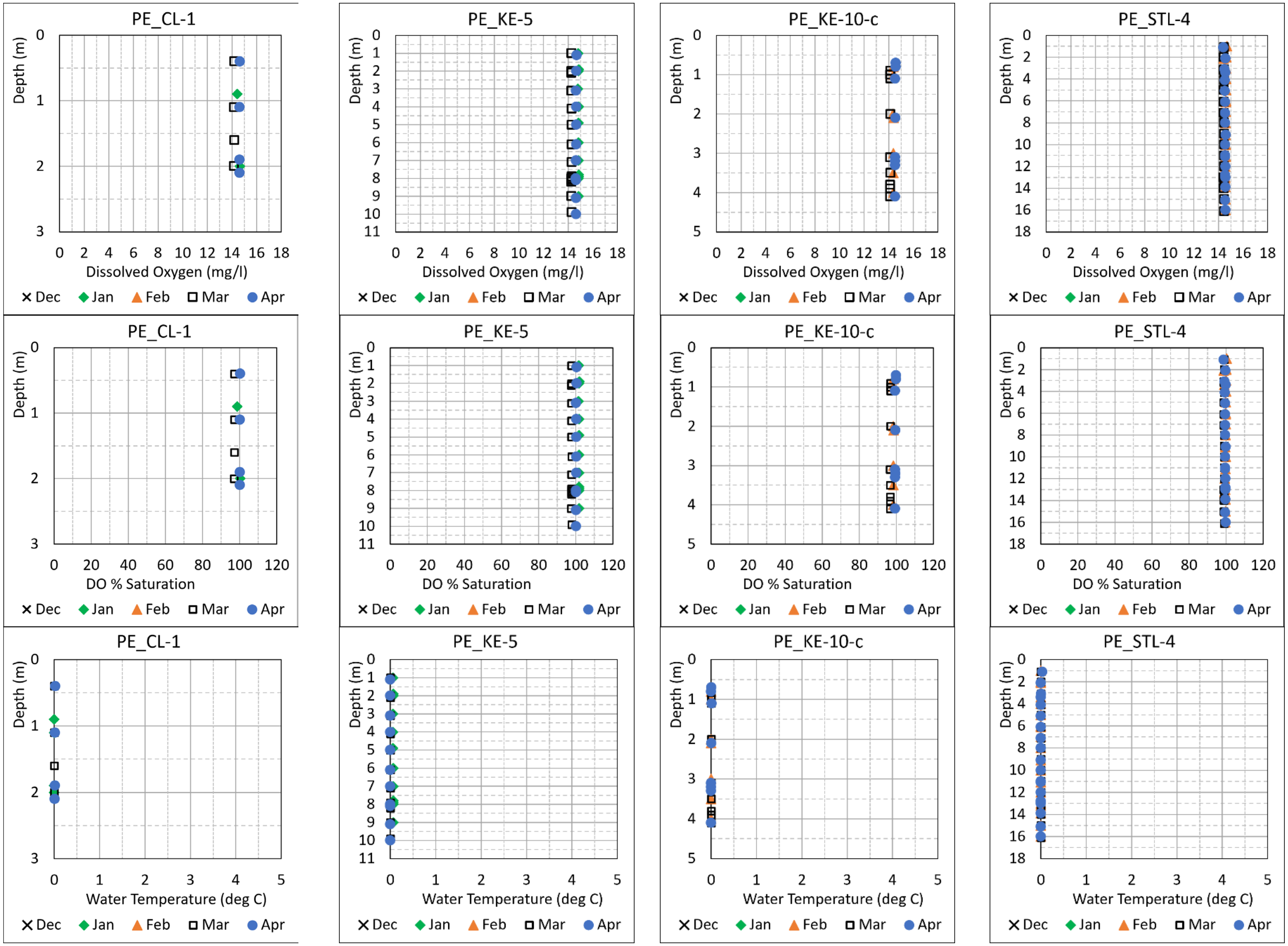
PE_CL-1
Depth (m)
Dissolved Oxygen (mg/l)
× Dec ◆ Jan ▲ Feb □ Mar ● Apr
PE_KE-5
Depth (m)
Dissolved Oxygen (mg/l)
× Dec ◆ Jan ▲ Feb □ Mar ● Apr
PE_KE-10-c
Depth (m)
Dissolved Oxygen (mg/l)
× Dec ◆ Jan ▲ Feb □ Mar ● Apr
PE_STL-4
Depth (m)
Dissolved Oxygen (mg/l)
× Dec ◆ Jan ▲ Feb □ Mar ● Apr
PE_CL-1
Depth (m)
DO % Saturation
× Dec ◆ Jan ▲ Feb □ Mar ● Apr
PE_KE-5
Depth (m)
DO % Saturation
× Dec ◆ Jan ▲ Feb □ Mar ● Apr
PE_KE-10-c
Depth (m)
DO % Saturation
× Dec ◆ Jan ▲ Feb □ Mar ● Apr
PE_STL-4
Depth (m)
DO % Saturation
× Dec ◆ Jan ▲ Feb □ Mar ● Apr
PE_CL-1
Depth (m)
Water Temperature (deg C)
× Dec ◆ Jan ▲ Feb □ Mar ● Apr
PE_KE-5
Depth (m)
Water Temperature (deg C)
× Dec ◆ Jan ▲ Feb □ Mar ● Apr
PE_KE-10-c
Depth (m)
Water Temperature (deg C)
× Dec ◆ Jan ▲ Feb □ Mar ● Apr
PE_STL-4
Depth (m)
Water Temperature (deg C)
× Dec ◆ Jan ▲ Feb □ Mar ● Apr

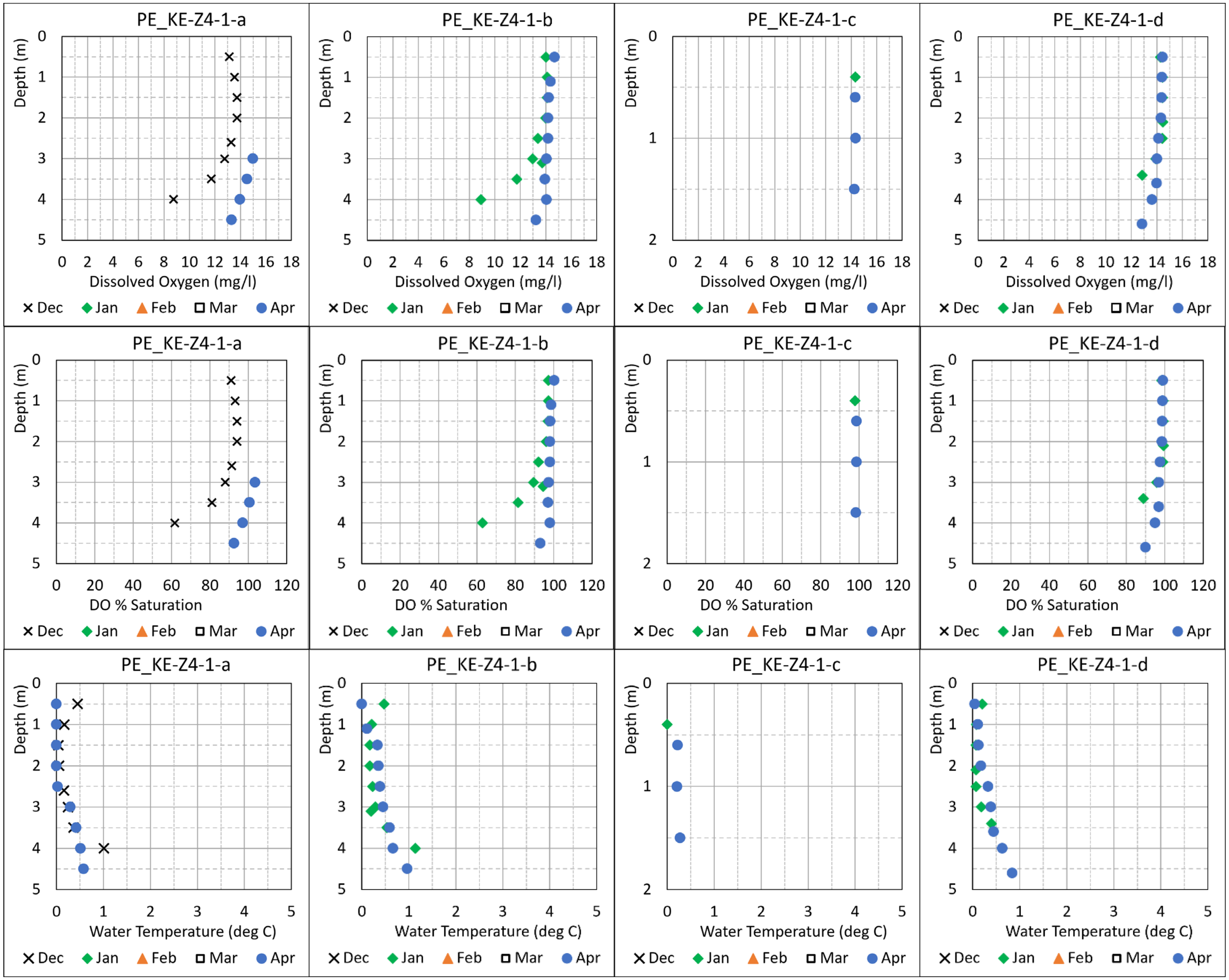
PE_KE-Z4-1-a
PE_KE-Z4-1-b
PE_KE-Z4-1-c
PE_KE-Z4-1-d
Depth (m)
Dissolved Oxygen (mg/l)
DO % Saturation
Water Temperature (deg C)
Dec Jan Feb Mar Apr

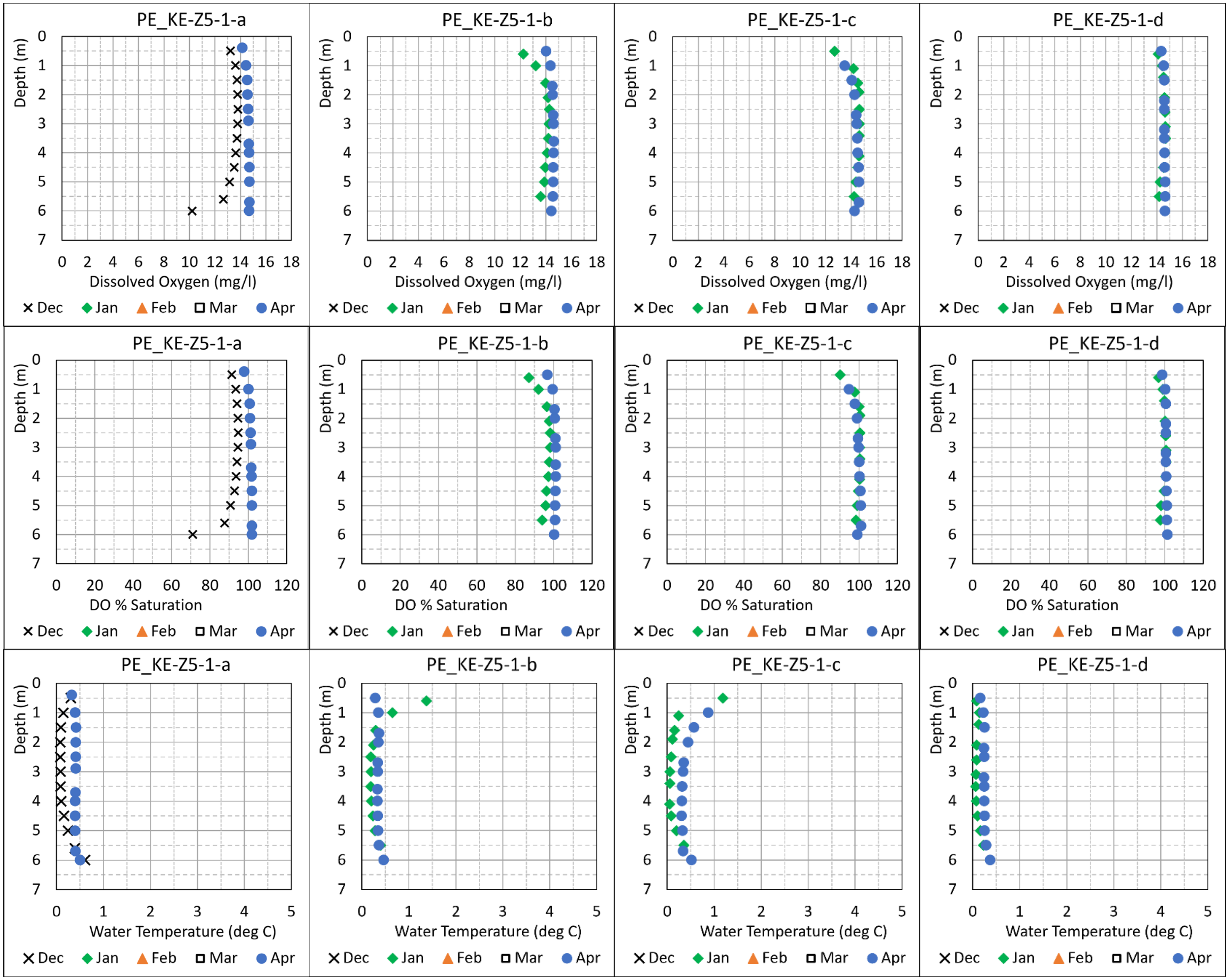
PE_KE-Z5-1-a
PE_KE-Z5-1-b
PE_KE-Z5-1-c
PE_KE-Z5-1-d
Depth (m)
0
1
2
3
4
5
6
7
0 2 4 6 8 10 12 14 16 18
Dissolved Oxygen (mg/l)
Dec Jan Feb Mar Apr
PE_KE-Z5-1-a
PE_KE-Z5-1-b
PE_KE-Z5-1-c
PE_KE-Z5-1-d
Depth (m)
0 20 40 60 80 100 120
DO % Saturation
Dec Jan Feb Mar Apr
PE_KE-Z5-1-a
PE_KE-Z5-1-b
PE_KE-Z5-1-c
PE_KE-Z5-1-d
Depth (m)
0 1 2 3 4 5
Water Temperature (deg C)
Dec Jan Feb Mar Apr

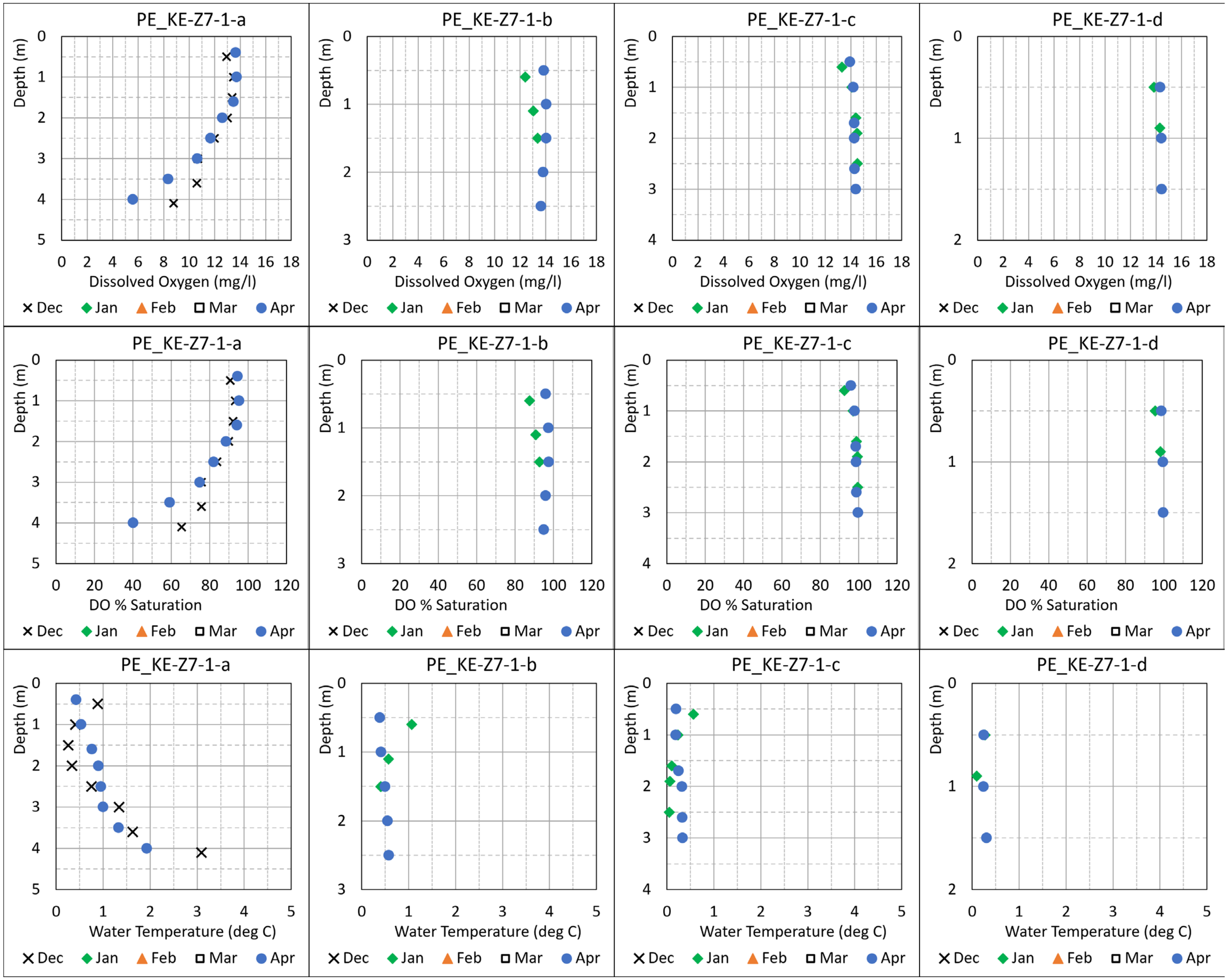
PE_KE-Z7-1-a
Depth (m)
Dissolved Oxygen (mg/l)
× Dec ◆ Jan ▲ Feb □ Mar ● Apr
PE_KE-Z7-1-b
Depth (m)
Dissolved Oxygen (mg/l)
× Dec ◆ Jan ▲ Feb □ Mar ● Apr
PE_KE-Z7-1-c
Depth (m)
Dissolved Oxygen (mg/l)
× Dec ◆ Jan ▲ Feb □ Mar ● Apr
PE_KE-Z7-1-d
Depth (m)
Dissolved Oxygen (mg/l)
× Dec ◆ Jan ▲ Feb □ Mar ● Apr
PE_KE-Z7-1-a
Depth (m)
DO % Saturation
× Dec ◆ Jan ▲ Feb □ Mar ● Apr
PE_KE-Z7-1-b
Depth (m)
DO % Saturation
× Dec ◆ Jan ▲ Feb □ Mar ● Apr
PE_KE-Z7-1-c
Depth (m)
DO % Saturation
× Dec ◆ Jan ▲ Feb □ Mar ● Apr
PE_KE-Z7-1-d
Depth (m)
DO % Saturation
× Dec ◆ Jan ▲ Feb □ Mar ● Apr
PE_KE-Z7-1-a
Depth (m)
Water Temperature (deg C)
× Dec ◆ Jan ▲ Feb □ Mar ● Apr
PE_KE-Z7-1-b
Depth (m)
Water Temperature (deg C)
× Dec ◆ Jan ▲ Feb □ Mar ● Apr
PE_KE-Z7-1-c
Depth (m)
Water Temperature (deg C)
× Dec ◆ Jan ▲ Feb □ Mar ● Apr
PE_KE-Z7-1-d
Depth (m)
Water Temperature (deg C)
× Dec ◆ Jan ▲ Feb □ Mar ● Apr

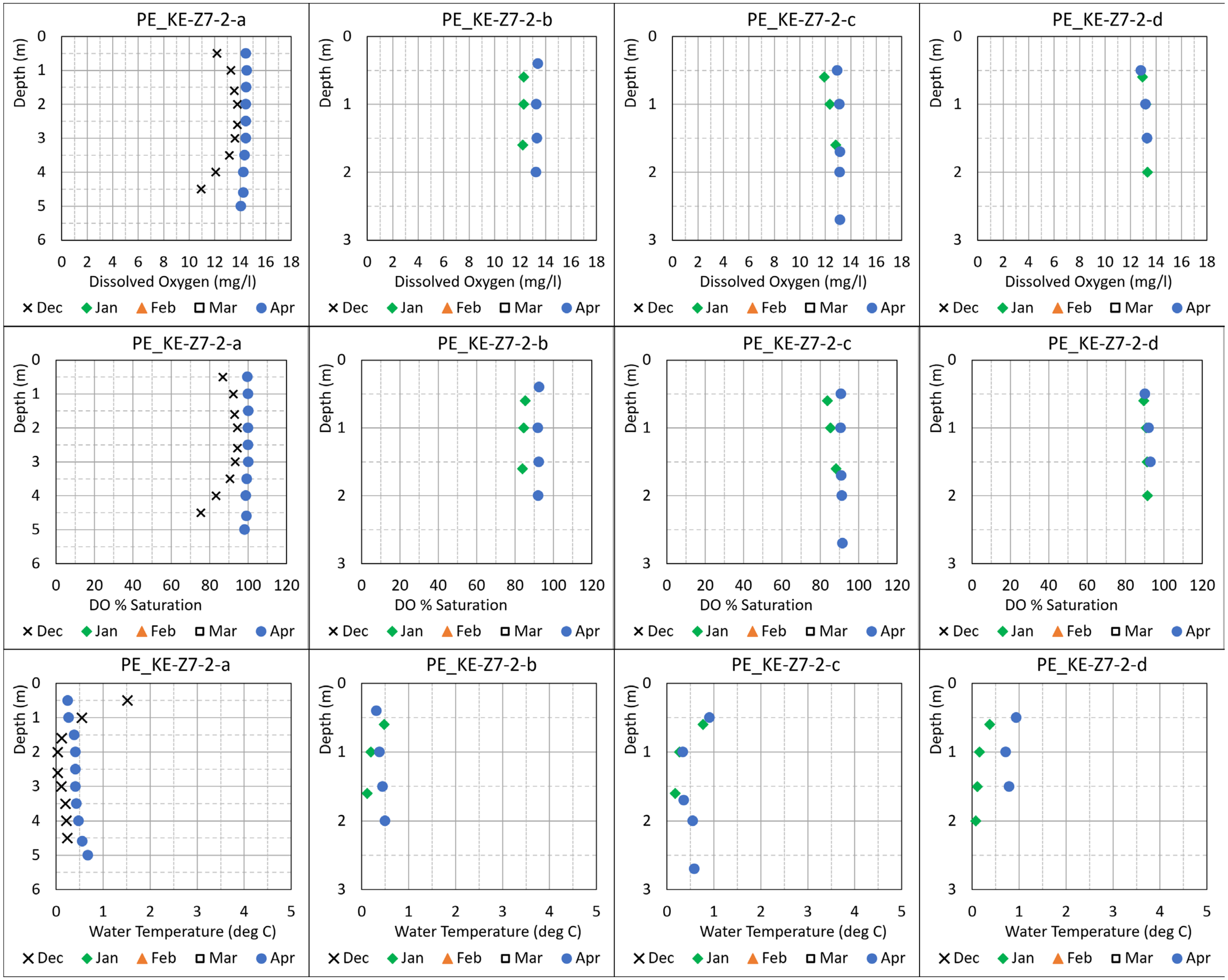
PE_KE-Z7-2-a
PE_KE-Z7-2-b
PE_KE-Z7-2-c
PE_KE-Z7-2-d
Depth (m)
Dissolved Oxygen (mg/l)
DO % Saturation
Water Temperature (deg C)
Dec Jan Feb Mar Apr

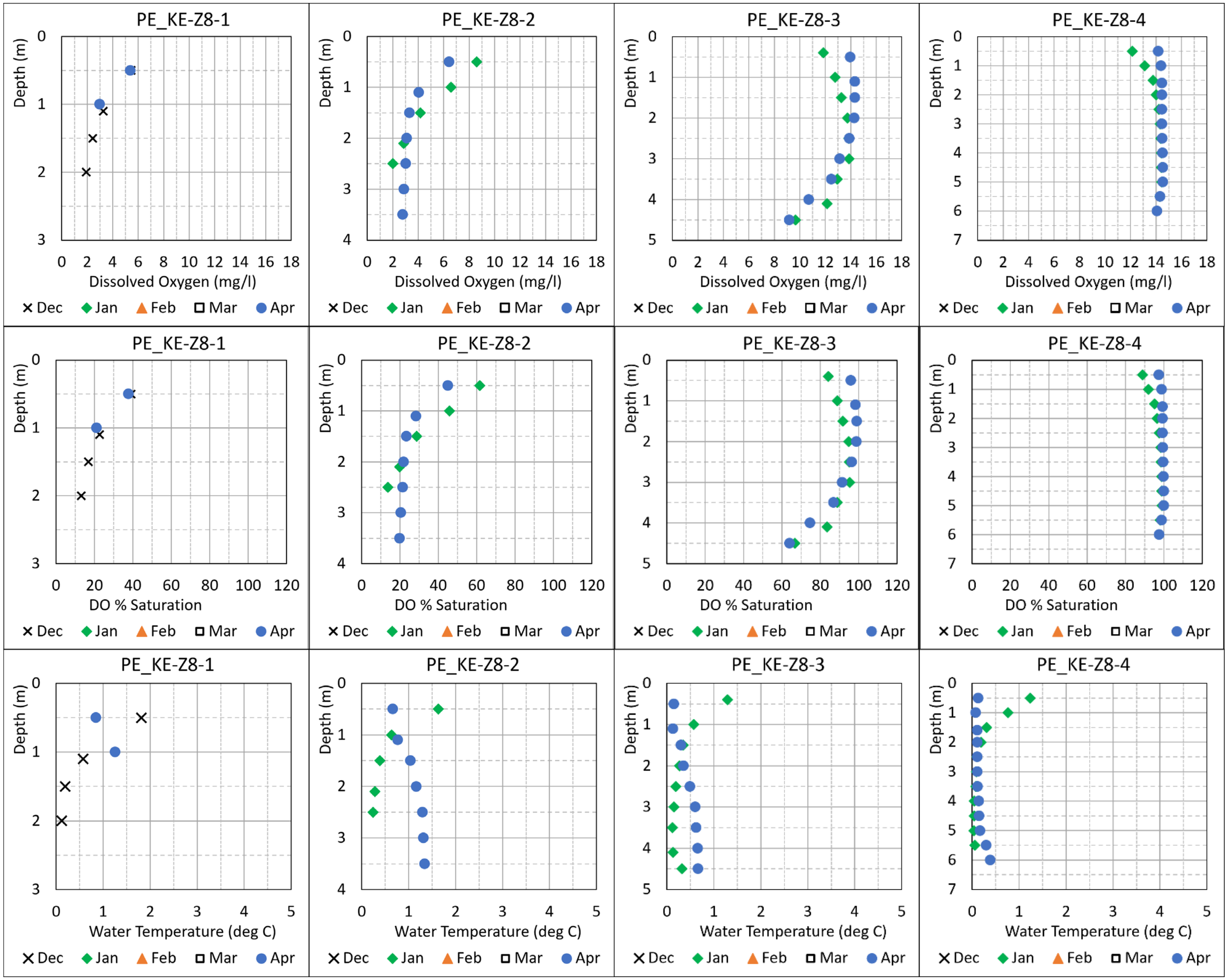
PE_KE-Z8-1
Depth (m)
Dissolved Oxygen (mg/l)
× Dec ◆ Jan ▲ Feb □ Mar ● Apr
PE_KE-Z8-2
Depth (m)
Dissolved Oxygen (mg/l)
× Dec ◆ Jan ▲ Feb □ Mar ● Apr
PE_KE-Z8-3
Depth (m)
Dissolved Oxygen (mg/l)
× Dec ◆ Jan ▲ Feb □ Mar ● Apr
PE_KE-Z8-4
Depth (m)
Dissolved Oxygen (mg/l)
× Dec ◆ Jan ▲ Feb □ Mar ● Apr
PE_KE-Z8-1
Depth (m)
DO % Saturation
× Dec ◆ Jan ▲ Feb □ Mar ● Apr
PE_KE-Z8-2
Depth (m)
DO % Saturation
× Dec ◆ Jan ▲ Feb □ Mar ● Apr
PE_KE-Z8-3
Depth (m)
DO % Saturation
× Dec ◆ Jan ▲ Feb □ Mar ● Apr
PE_KE-Z8-4
Depth (m)
DO % Saturation
× Dec ◆ Jan ▲ Feb □ Mar ● Apr
PE_KE-Z8-1
Depth (m)
Water Temperature (deg C)
× Dec ◆ Jan ▲ Feb □ Mar ● Apr
PE_KE-Z8-2
Depth (m)
Water Temperature (deg C)
× Dec ◆ Jan ▲ Feb □ Mar ● Apr
PE_KE-Z8-3
Depth (m)
Water Temperature (deg C)
× Dec ◆ Jan ▲ Feb □ Mar ● Apr
PE_KE-Z8-4
Depth (m)
Water Temperature (deg C)
× Dec ◆ Jan ▲ Feb □ Mar ● Apr

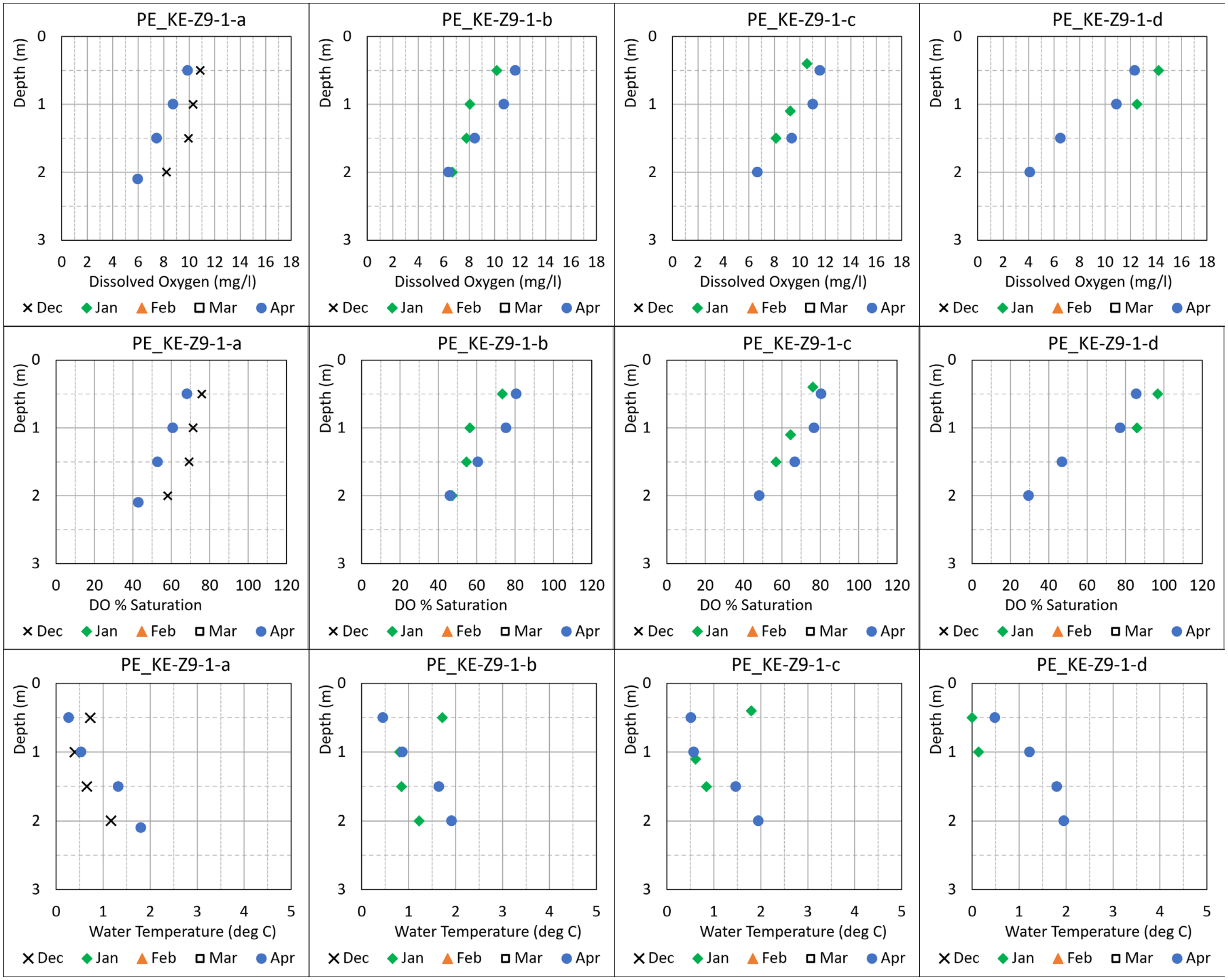
PE_KE-Z9-1-a
PE_KE-Z9-1-b
PE_KE-Z9-1-c
PE_KE-Z9-1-d
Depth (m)
Dissolved Oxygen (mg/l)
DO % Saturation
Water Temperature (deg C)
Dec
Jan
Feb
Mar
Apr

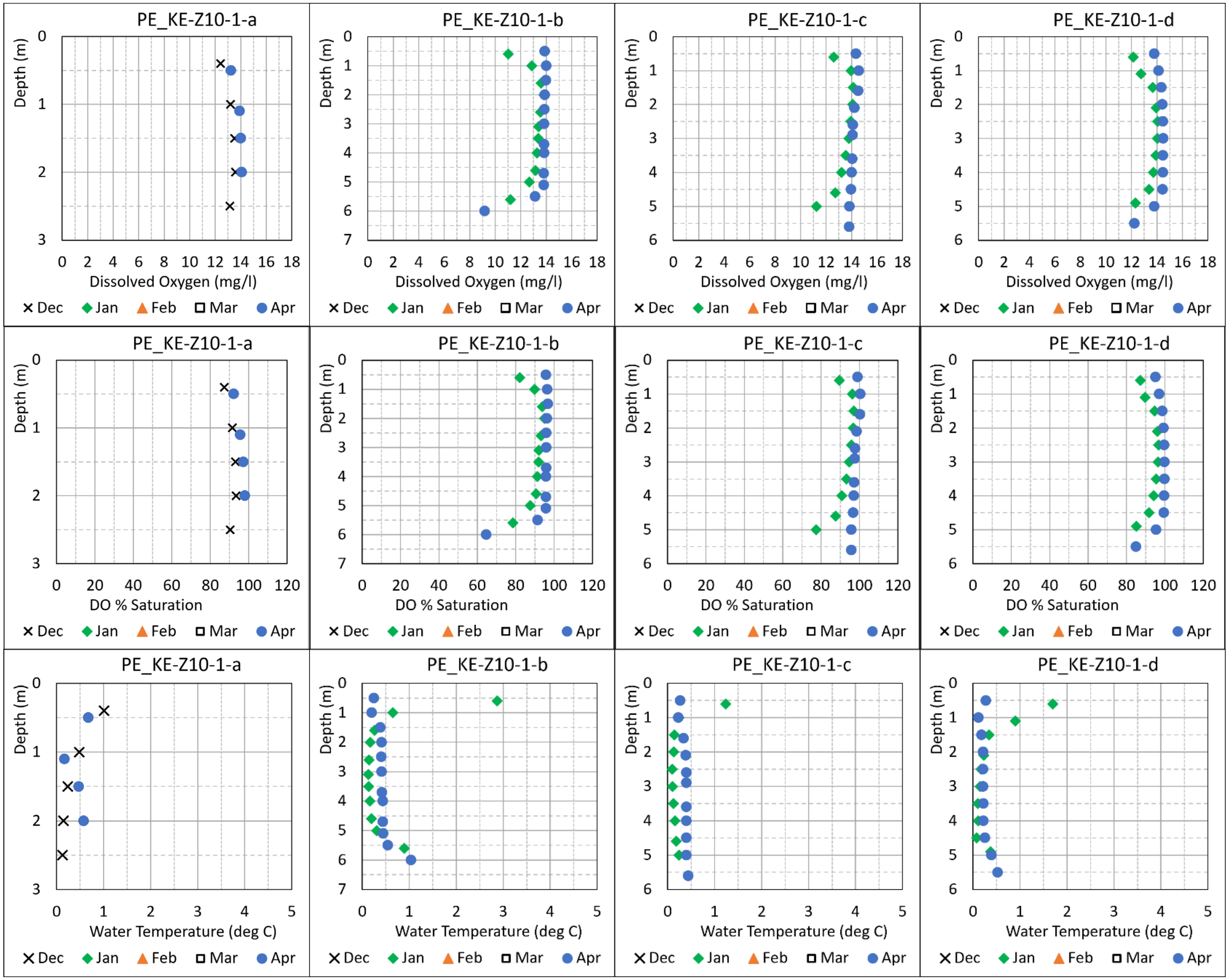
PE_KE-Z10-1-a
PE_KE-Z10-1-b
PE_KE-Z10-1-c
PE_KE-Z10-1-d
Depth (m)
Dissolved Oxygen (mg/l)
DO % Saturation
Water Temperature (deg C)
Dec
Jan
Feb
Mar
Apr

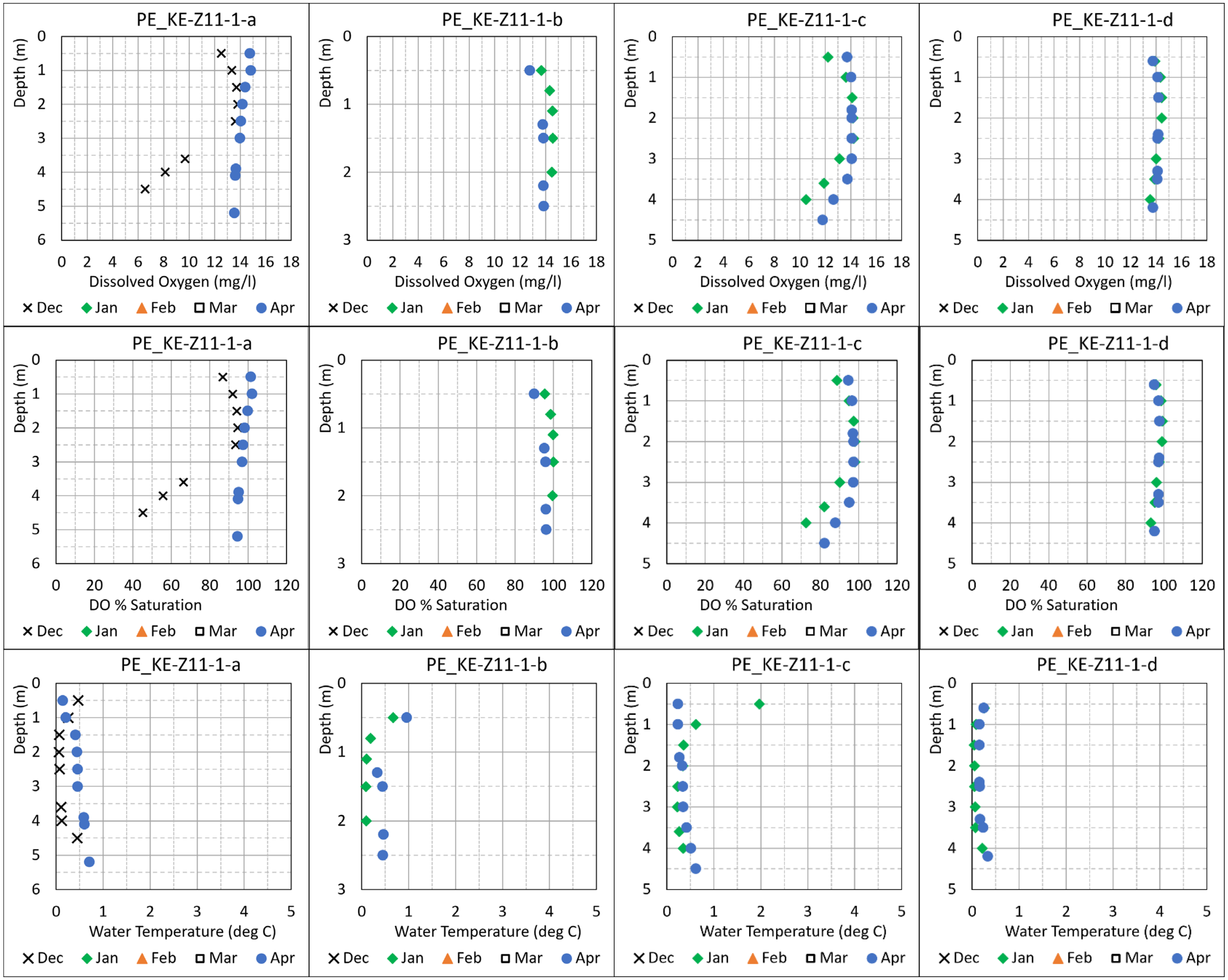
PE_KE-Z11-1-a
PE_KE-Z11-1-b
PE_KE-Z11-1-c
PE_KE-Z11-1-d
Depth (m)
Dissolved Oxygen (mg/l)
DO % Saturation
Water Temperature (deg C)
Dec
Jan
Feb
Mar
Apr

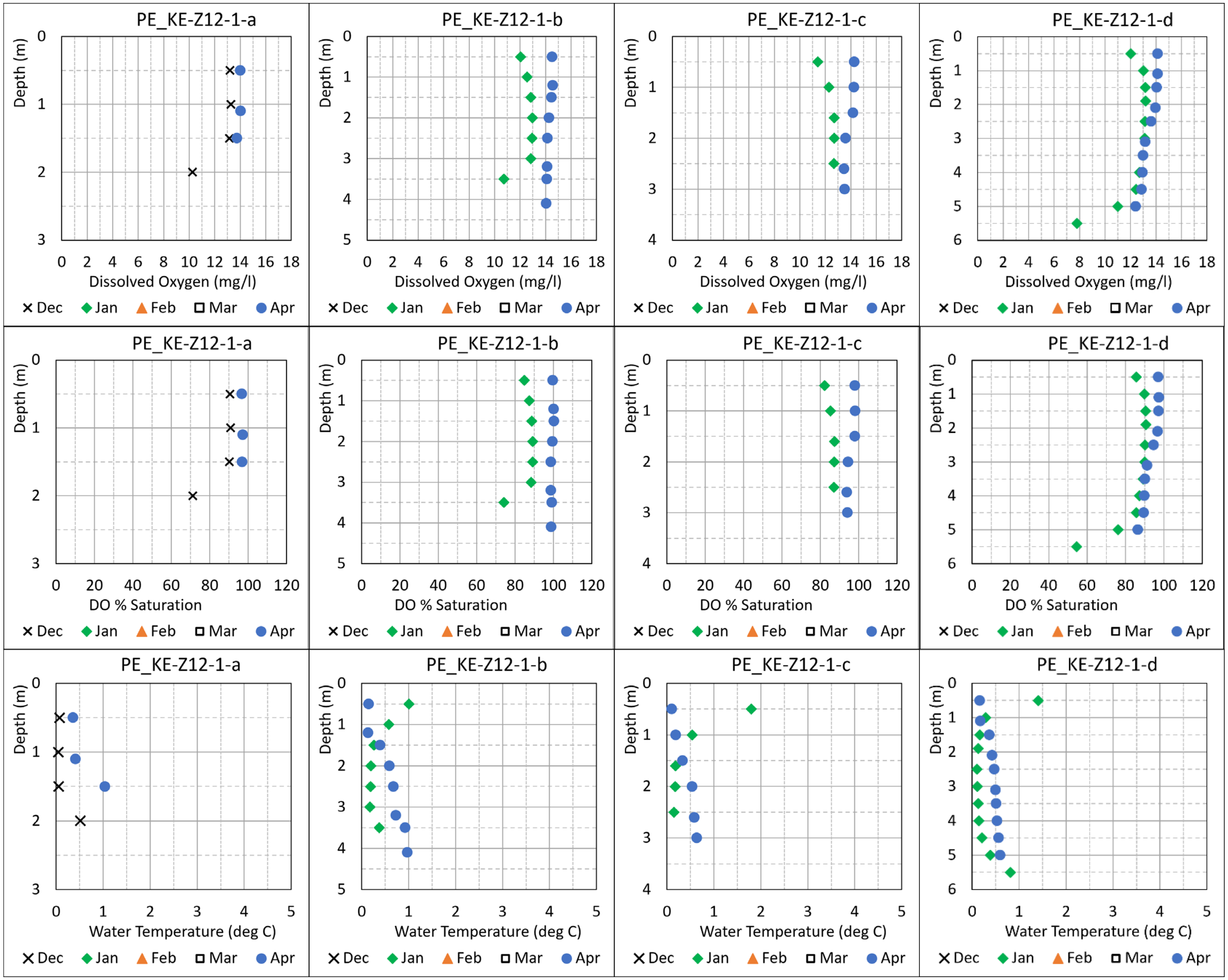
PE_KE-Z12-1-a
PE_KE-Z12-1-b
PE_KE-Z12-1-c
PE_KE-Z12-1-d
Depth (m)
Dissolved Oxygen (mg/l)
DO % Saturation
Water Temperature (deg C)
Dec
Jan
Feb
Mar
Apr

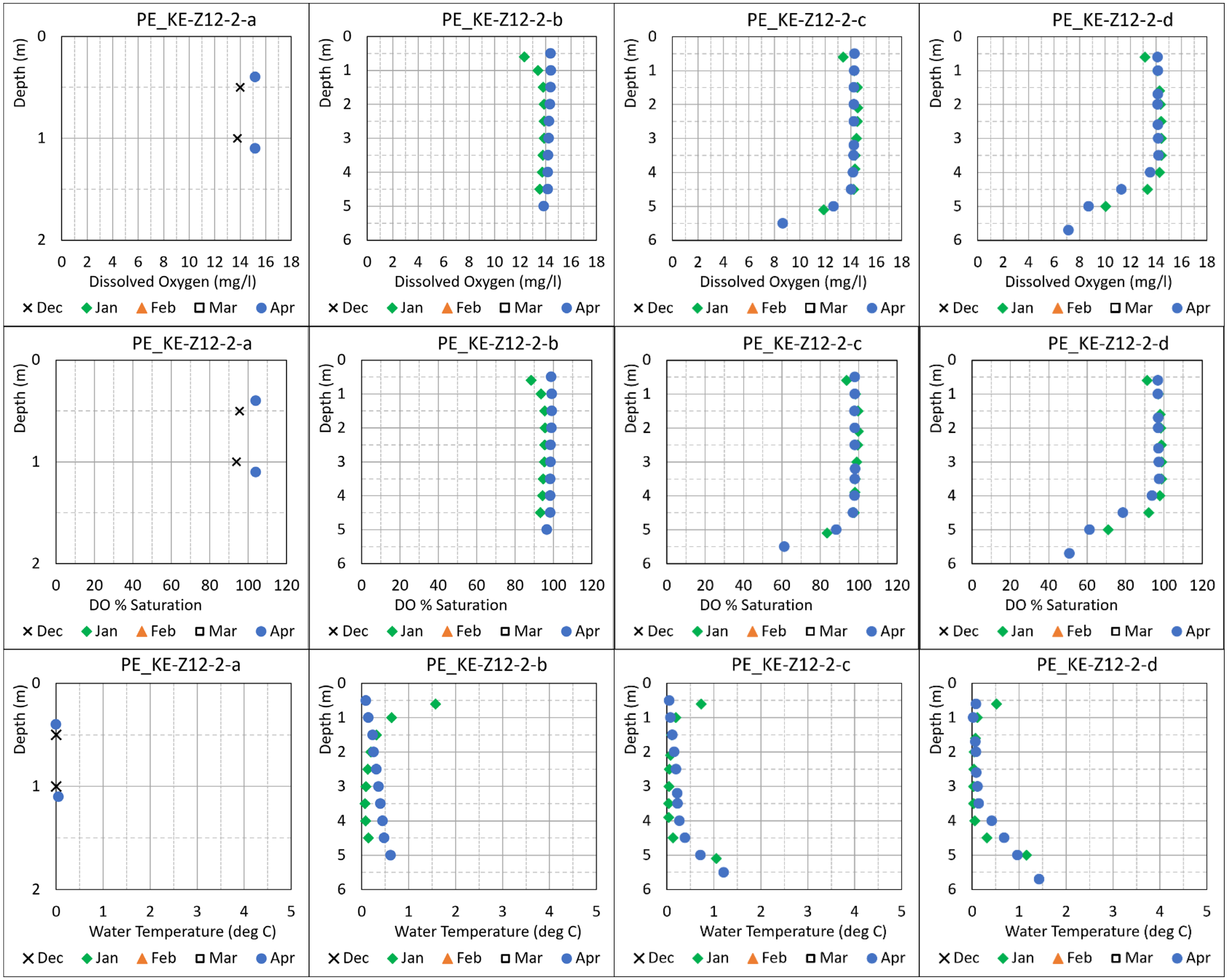
PE_KE-Z12-2-a
PE_KE-Z12-2-b
PE_KE-Z12-2-c
PE_KE-Z12-2-d
Depth (m)
Dissolved Oxygen (mg/l)
DO % Saturation
Water Temperature (deg C)
Dec Jan Feb Mar Apr

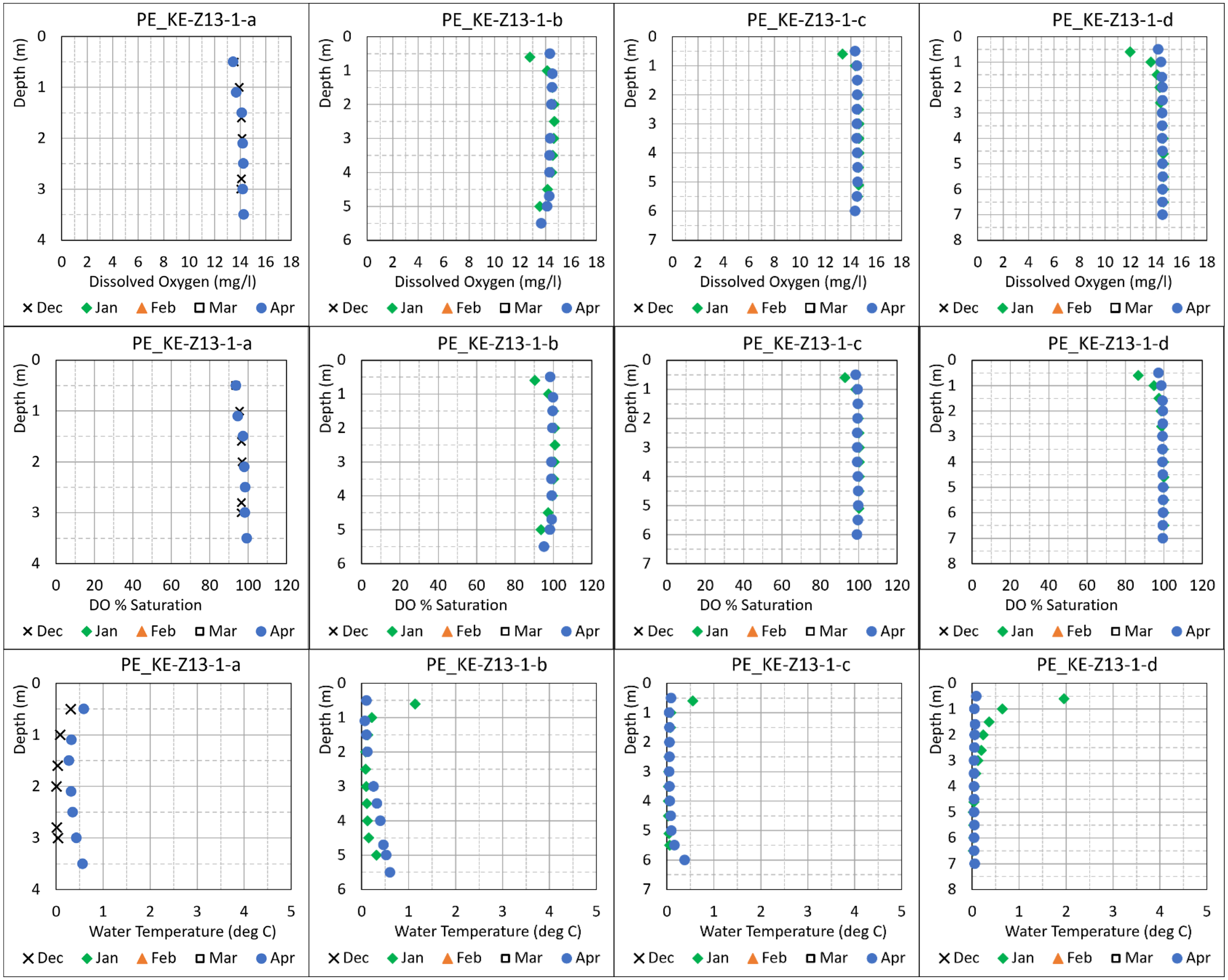
PE_KE-Z13-1-a
PE_KE-Z13-1-b
PE_KE-Z13-1-c
PE_KE-Z13-1-d
Depth (m)
Dissolved Oxygen (mg/l)
DO % Saturation
Water Temperature (deg C)
Dec
Jan
Feb
Mar
Apr

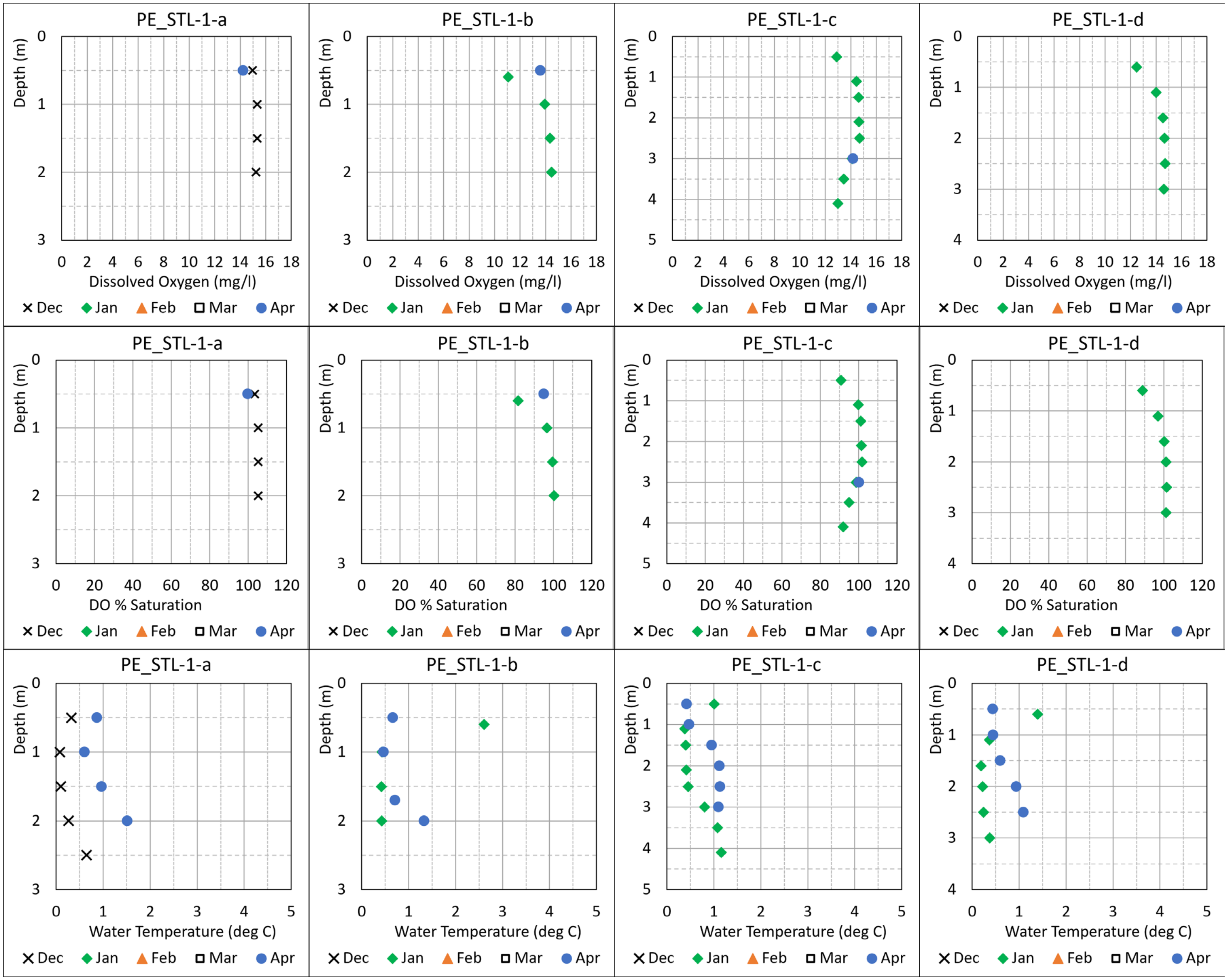
PE_STL-1-a
PE_STL-1-b
PE_STL-1-c
PE_STL-1-d
Depth (m)
Dissolved Oxygen (mg/l)
DO % Saturation
Water Temperature (deg C)
Dec
Jan
Feb
Mar
Apr

# APPENDIX 3:
# SUMMER DEPTH PROFILE CHARTS OF DISSOLVED OXYGEN CONCENTRATION & PERCENT SATURATION, AND WATER TEMPERATURE

**Site Listing in order of presentation in Appendix 3:**

Note that site names on charts all include the "PE_" prefix that is an internal designation used to identify the monitoring site as part of the physical environment program.

Mainstem sites (upstream to downstream):

- PE_CL-2-a, b, c (i.e, PE_CL-2-a, PE_CL-2-b, PE_CL-2-c)
- PE_KE-1- b, c, d
- PE_KE-2-a, b
- PE_KE-3-a, b, c, d, e
- PE_KE-4-a, b
- PE_KE-6-a, b, c, d, e
- PE_KE-7
- PE_KE-8
- PE_KE-10-a, b, c, d, e, f
- PE_STL-2-a, b, c, d, e, f
- PE_STL-5

North backbay sites:

- PE_KE-Z4-1-a, b, c, d
- PE_KE-Z5-1-a, b, c, d
- PE_KE-Z7-1-a, b, c, d
- PE_KE-Z7-2-a, c
- PE_KE-Z8-1, 2, 3, 4
- PE_KE-Z9-1-a, b, c, d
- PE_KE-Z10-1-a, b, c, d

South backbay sites:

- PE_KE-Z11-1-a, b, c, d
- PE_KE-Z12-1-a, b, c, d
- PE_KE-Z12-2-a, b, c, d
- PE_KE-Z13-1-a, b, c, d

Stephens Lake backbay site:

- PE_STL-1-a, b, c, d

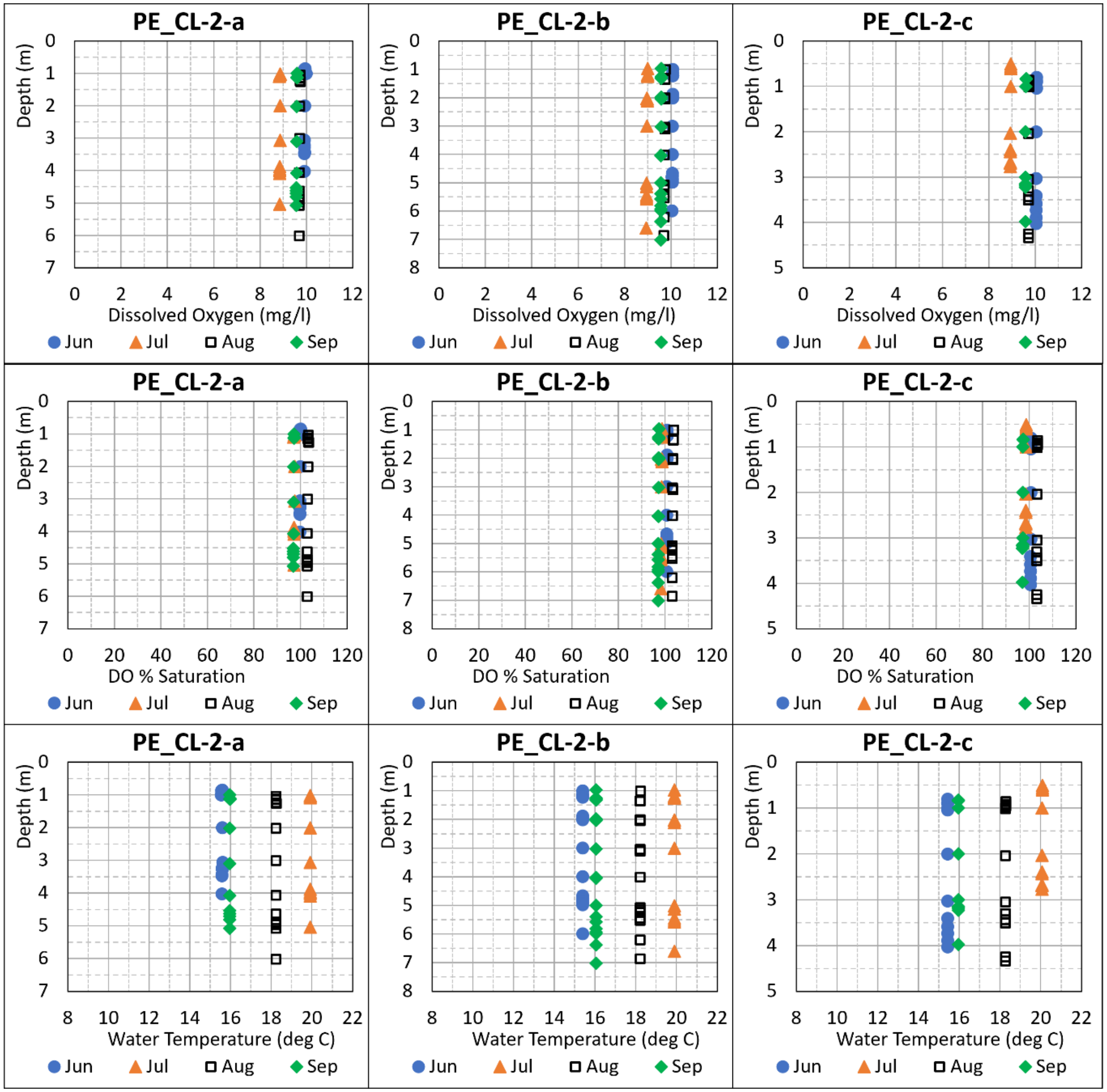
PE_CL-2-a
PE_CL-2-b
PE_CL-2-c
Depth (m)
Dissolved Oxygen (mg/l)
DO % Saturation
Water Temperature (deg C)
Jun Jul Aug Sep

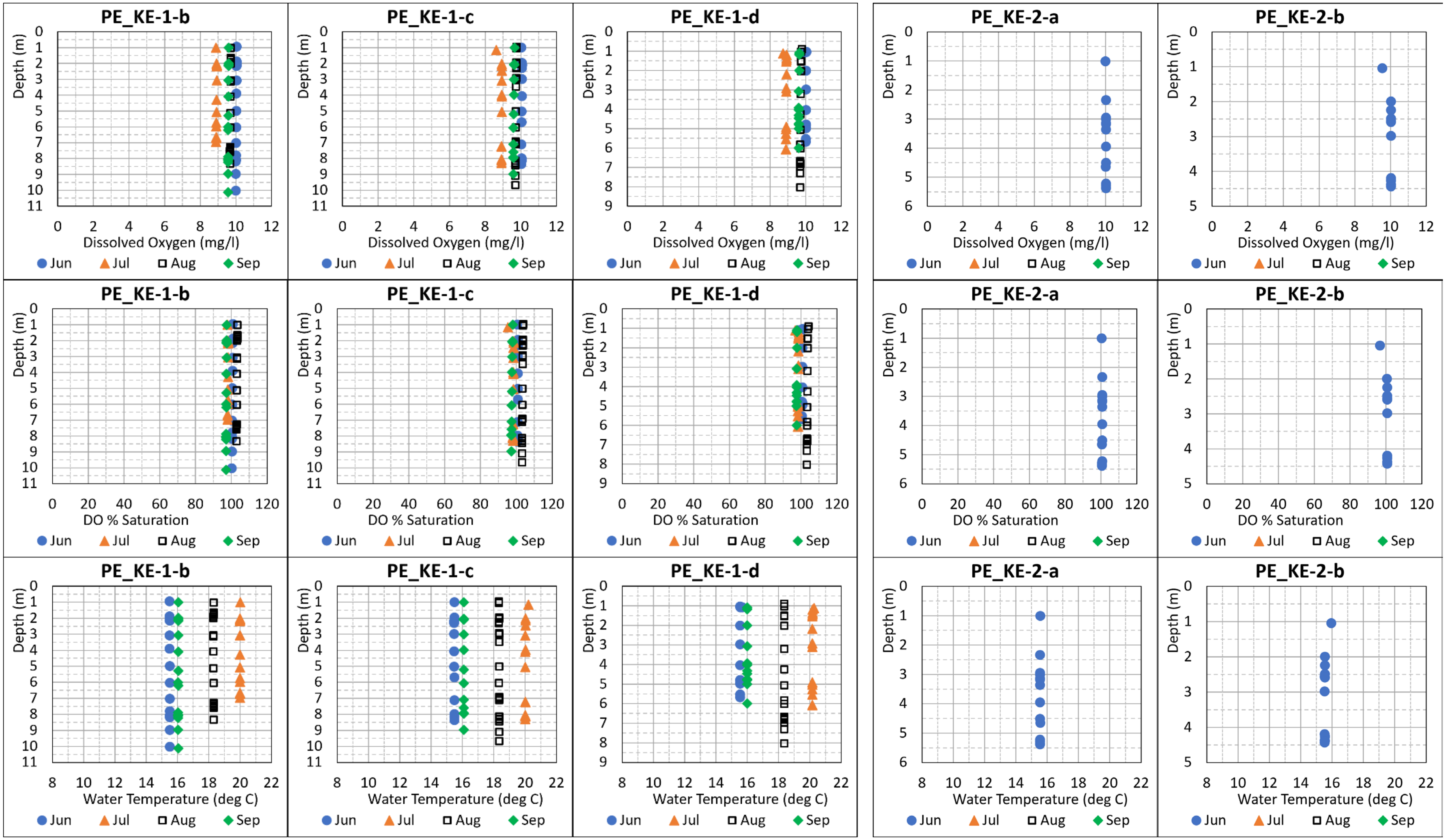
PE_KE-1-b
PE_KE-1-c
PE_KE-1-d
PE_KE-2-a
PE_KE-2-b
Depth (m)
Dissolved Oxygen (mg/l)
DO % Saturation
Water Temperature (deg C)
Jun
Jul
Aug
Sep

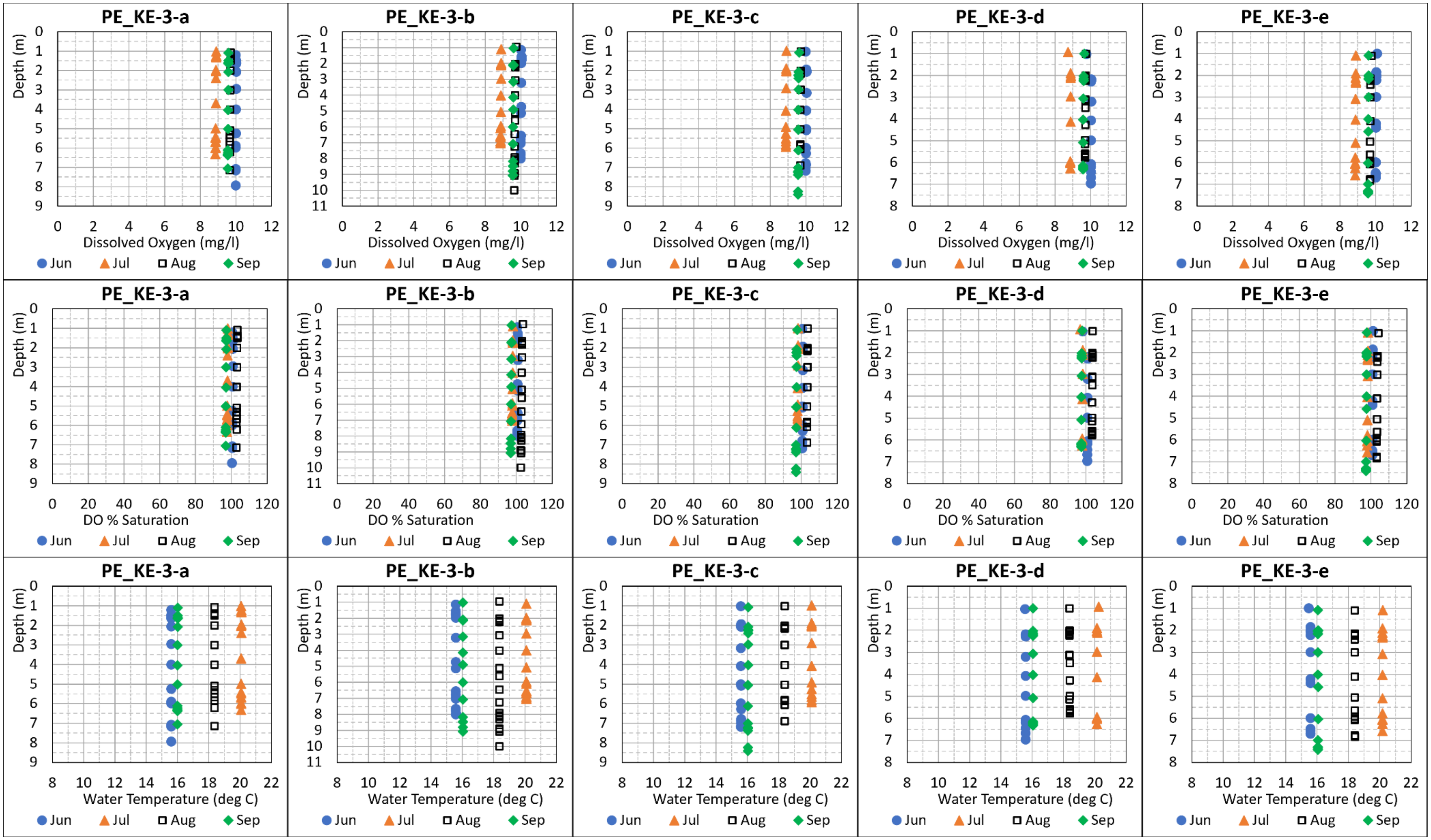
PE_KE-3-a
PE_KE-3-b
PE_KE-3-c
PE_KE-3-d
PE_KE-3-e
Depth (m)
Dissolved Oxygen (mg/l)
DO % Saturation
Water Temperature (deg C)
Jun Jul Aug Sep

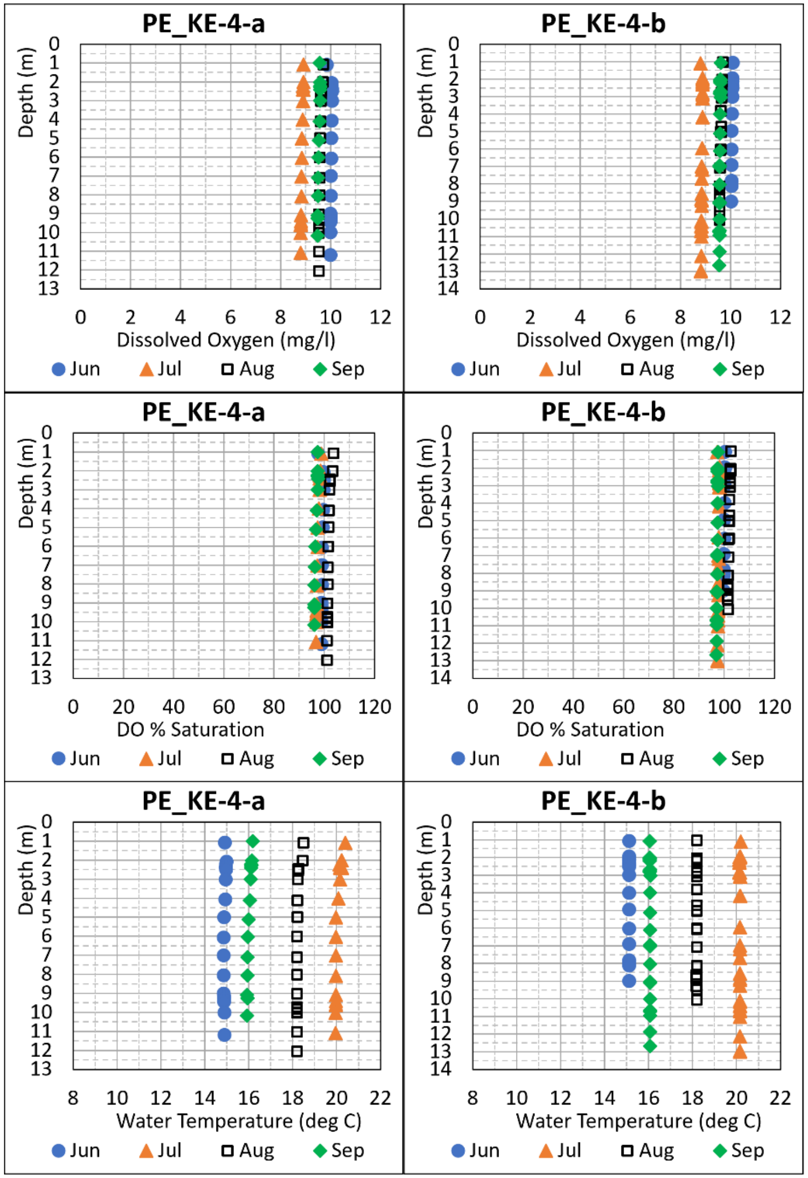
PE_KE-4-a
Depth (m)
Dissolved Oxygen (mg/l)
Jun Jul Aug Sep
PE_KE-4-b
Depth (m)
Dissolved Oxygen (mg/l)
Jun Jul Aug Sep
PE_KE-4-a
Depth (m)
DO % Saturation
Jun Jul Aug Sep
PE_KE-4-b
Depth (m)
DO % Saturation
Jun Jul Aug Sep
PE_KE-4-a
Depth (m)
Water Temperature (deg C)
Jun Jul Aug Sep
PE_KE-4-b
Depth (m)
Water Temperature (deg C)
Jun Jul Aug Sep

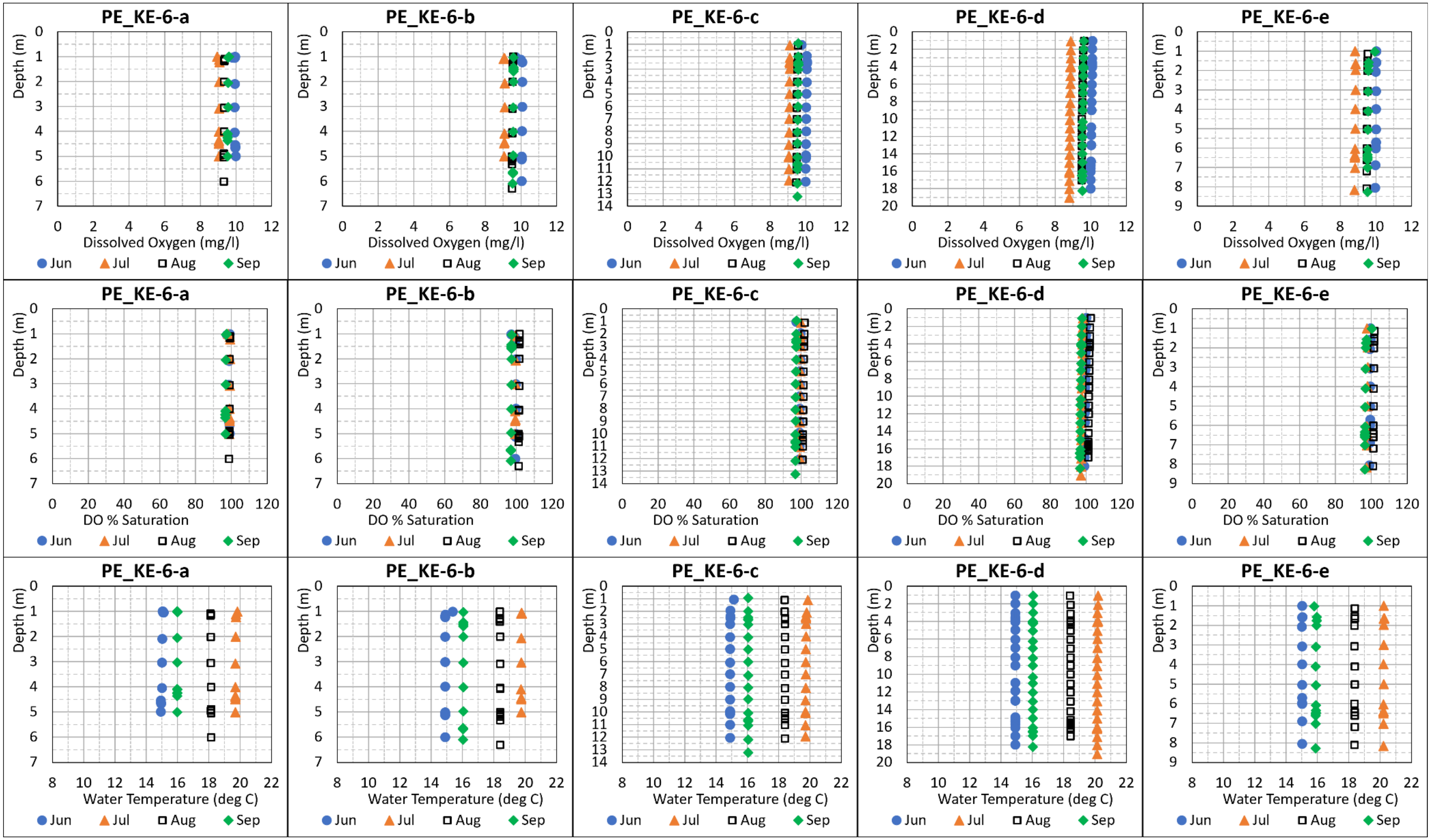
PE_KE-6-a
PE_KE-6-b
PE_KE-6-c
PE_KE-6-d
PE_KE-6-e
Depth (m)
Dissolved Oxygen (mg/l)
DO % Saturation
Water Temperature (deg C)
Jun
Jul
Aug
Sep

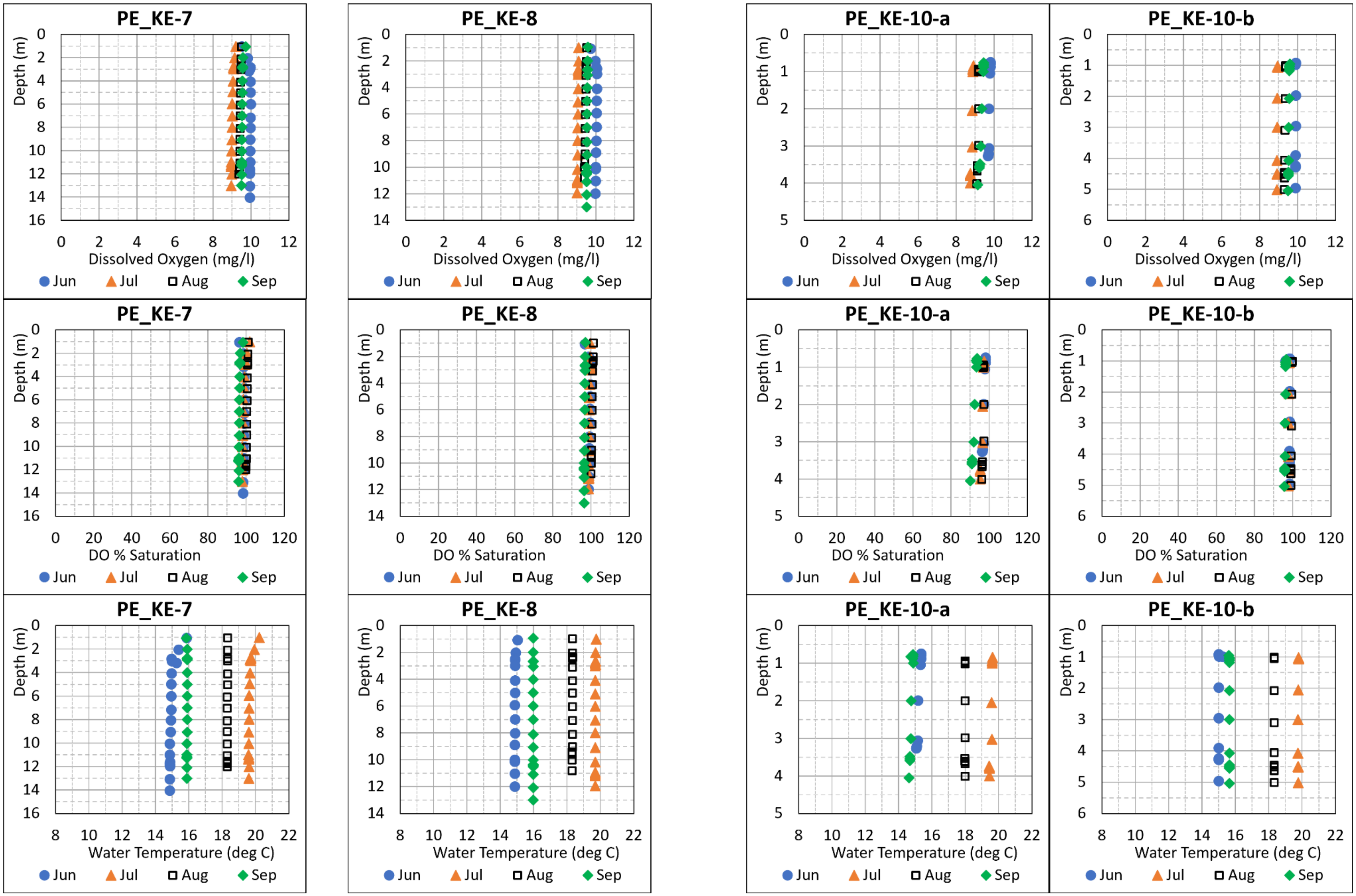
PE_KE-7
PE_KE-8
PE_KE-10-a
PE_KE-10-b
Depth (m)
Dissolved Oxygen (mg/l)
DO % Saturation
Water Temperature (deg C)
Jun
Jul
Aug
Sep

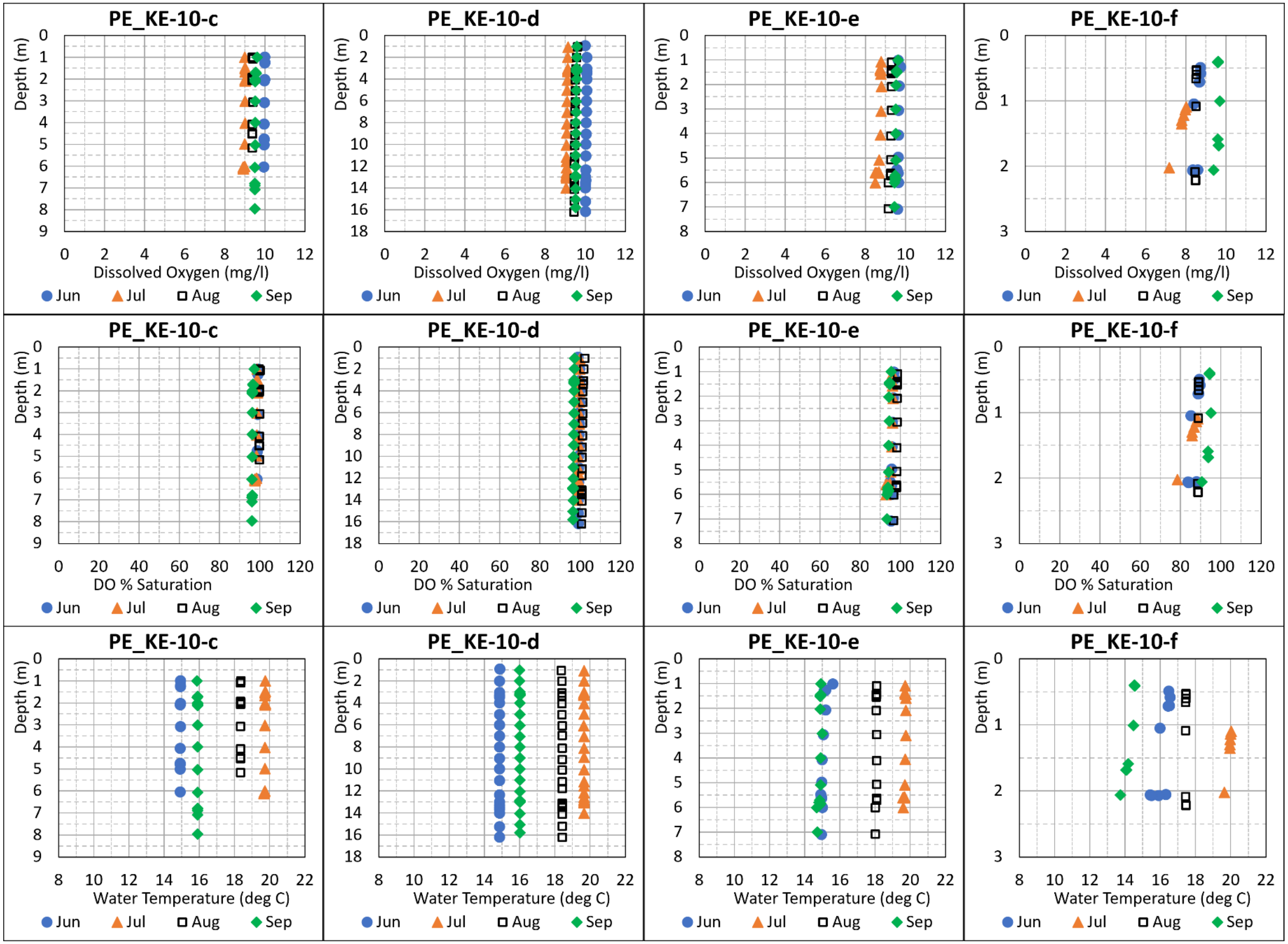
PE_KE-10-c
Depth (m)
Dissolved Oxygen (mg/l)
Jun Jul Aug Sep
PE_KE-10-d
Depth (m)
Dissolved Oxygen (mg/l)
Jun Jul Aug Sep
PE_KE-10-e
Depth (m)
Dissolved Oxygen (mg/l)
Jun Jul Aug Sep
PE_KE-10-f
Depth (m)
Dissolved Oxygen (mg/l)
Jun Jul Aug Sep
PE_KE-10-c
Depth (m)
DO % Saturation
Jun Jul Aug Sep
PE_KE-10-d
Depth (m)
DO % Saturation
Jun Jul Aug Sep
PE_KE-10-e
Depth (m)
DO % Saturation
Jun Jul Aug Sep
PE_KE-10-f
Depth (m)
DO % Saturation
Jun Jul Aug Sep
PE_KE-10-c
Depth (m)
Water Temperature (deg C)
Jun Jul Aug Sep
PE_KE-10-d
Depth (m)
Water Temperature (deg C)
Jun Jul Aug Sep
PE_KE-10-e
Depth (m)
Water Temperature (deg C)
Jun Jul Aug Sep
PE_KE-10-f
Depth (m)
Water Temperature (deg C)
Jun Jul Aug Sep

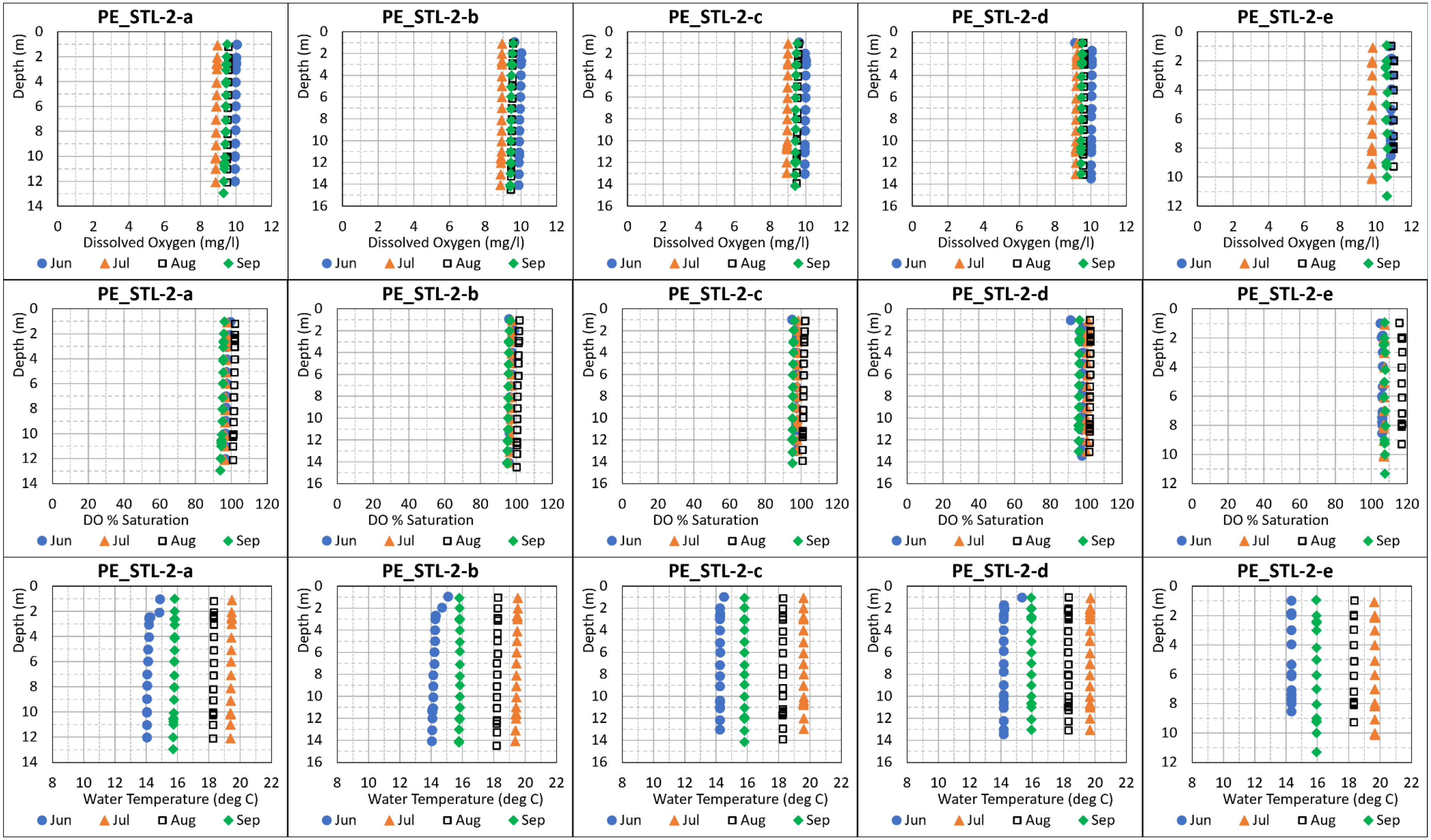
PE_STL-2-a
PE_STL-2-b
PE_STL-2-c
PE_STL-2-d
PE_STL-2-e
Depth (m)
Dissolved Oxygen (mg/l)
DO % Saturation
Water Temperature (deg C)
Jun
Jul
Aug
Sep

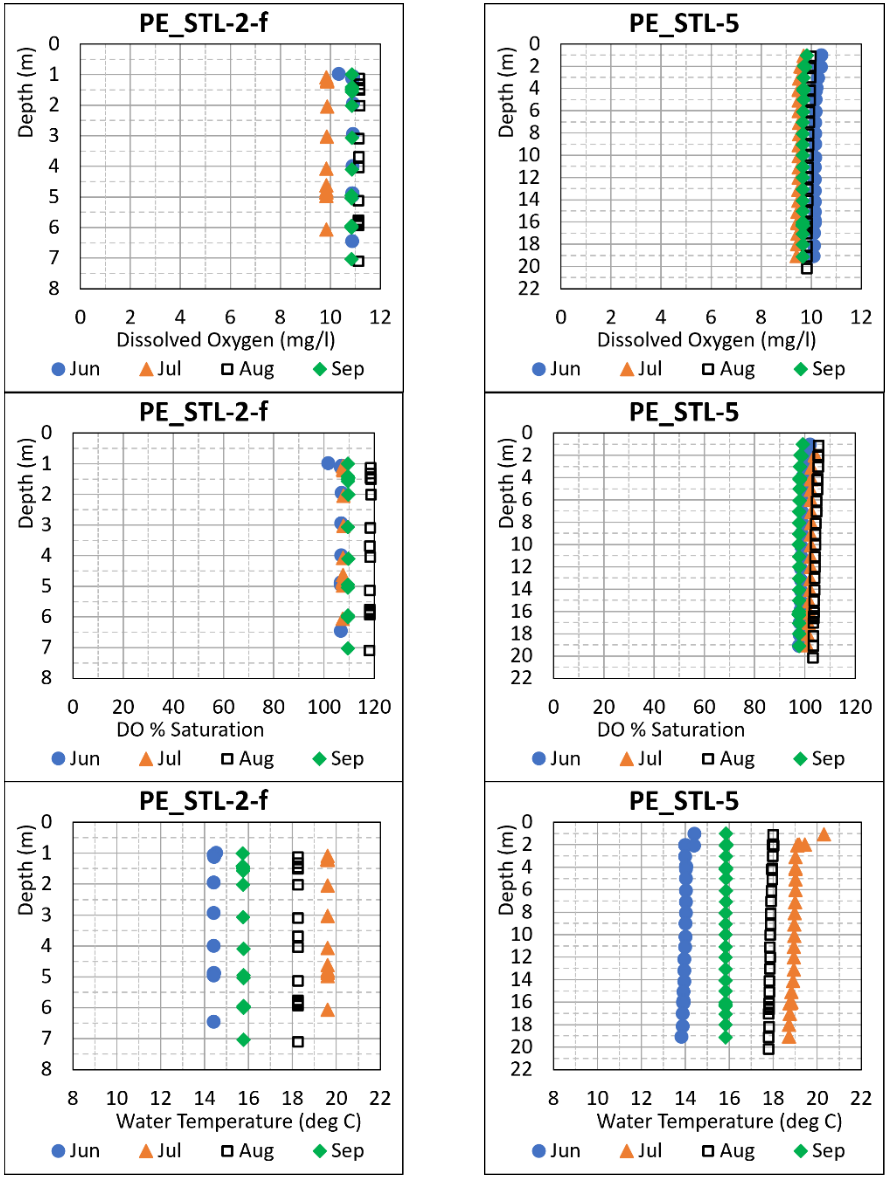
PE_STL-2-f
Depth (m)
Dissolved Oxygen (mg/l)
Jun Jul Aug Sep
PE_STL-5
Depth (m)
Dissolved Oxygen (mg/l)
Jun Jul Aug Sep
PE_STL-2-f
Depth (m)
DO % Saturation
Jun Jul Aug Sep
PE_STL-5
Depth (m)
DO % Saturation
Jun Jul Aug Sep
PE_STL-2-f
Depth (m)
Water Temperature (deg C)
Jun Jul Aug Sep
PE_STL-5
Depth (m)
Water Temperature (deg C)
Jun Jul Aug Sep

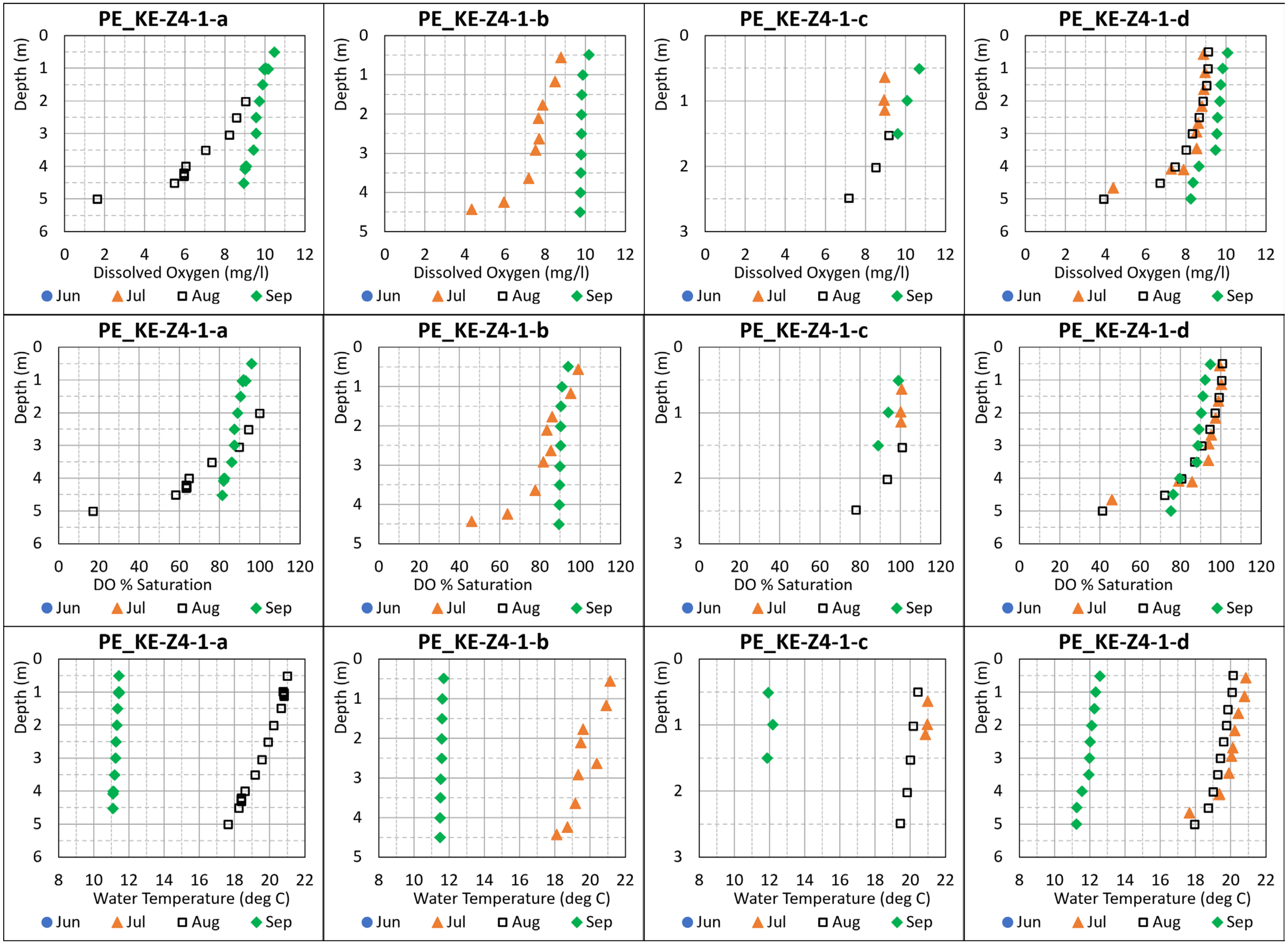
PE_KE-Z4-1-a
PE_KE-Z4-1-b
PE_KE-Z4-1-c
PE_KE-Z4-1-d
Depth (m)
Dissolved Oxygen (mg/l)
DO % Saturation
Water Temperature (deg C)
Jun
Jul
Aug
Sep

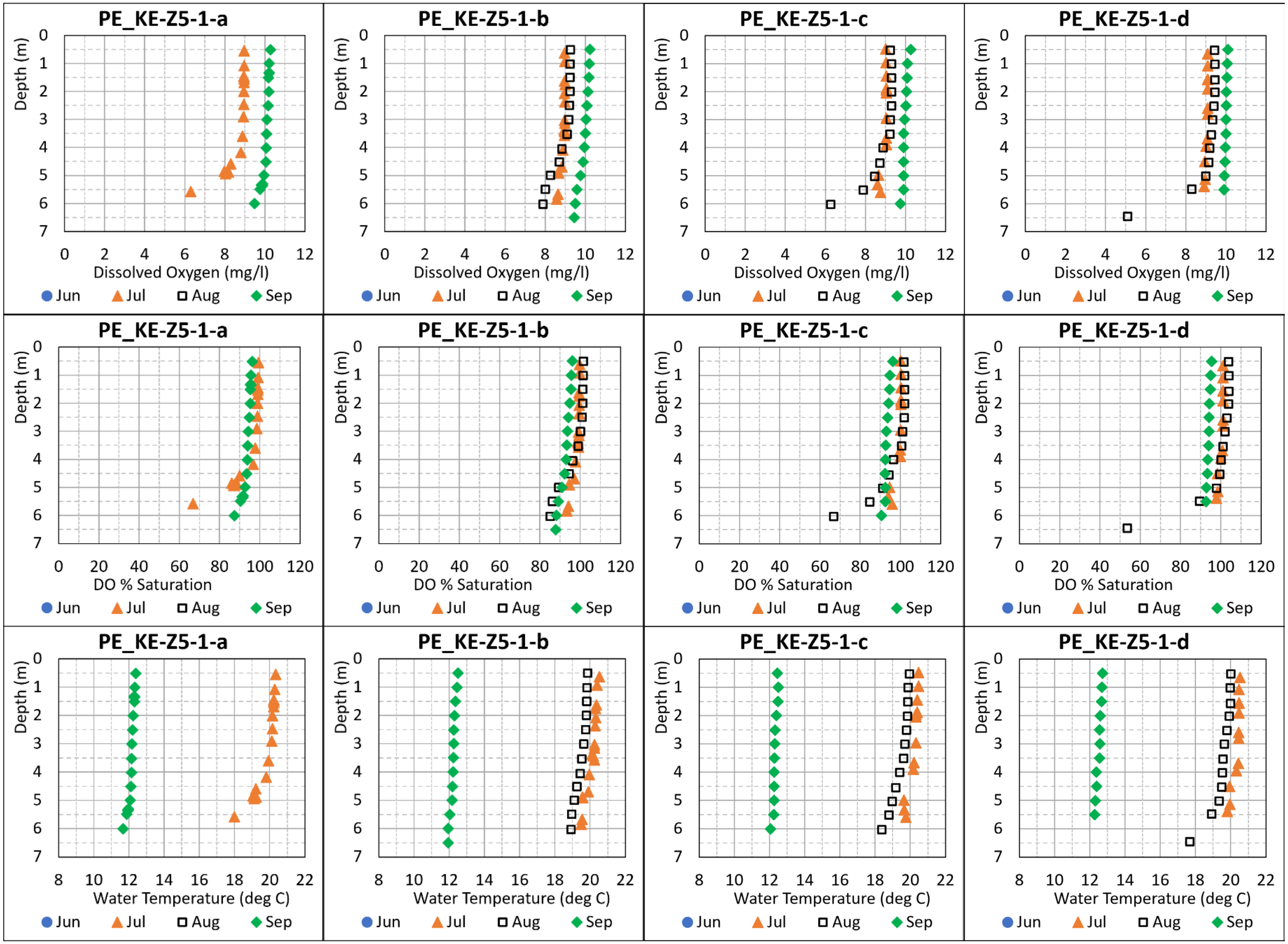
PE_KE-Z5-1-a
PE_KE-Z5-1-b
PE_KE-Z5-1-c
PE_KE-Z5-1-d
Depth (m)
Dissolved Oxygen (mg/l)
DO % Saturation
Water Temperature (deg C)
Jun
Jul
Aug
Sep

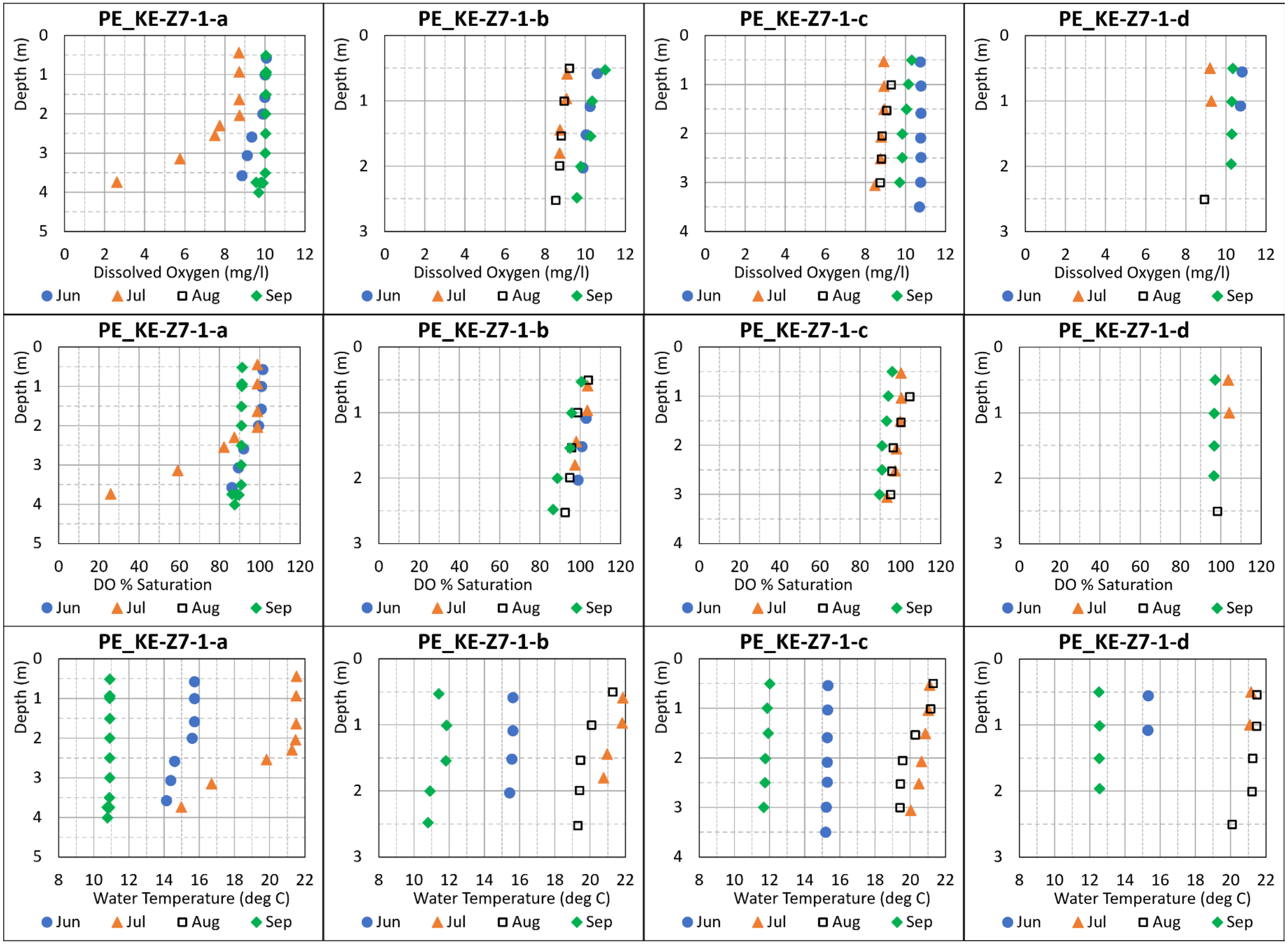
PE_KE-Z7-1-a
PE_KE-Z7-1-b
PE_KE-Z7-1-c
PE_KE-Z7-1-d
Depth (m)
Dissolved Oxygen (mg/l)
DO % Saturation
Water Temperature (deg C)
Jun
Jul
Aug
Sep

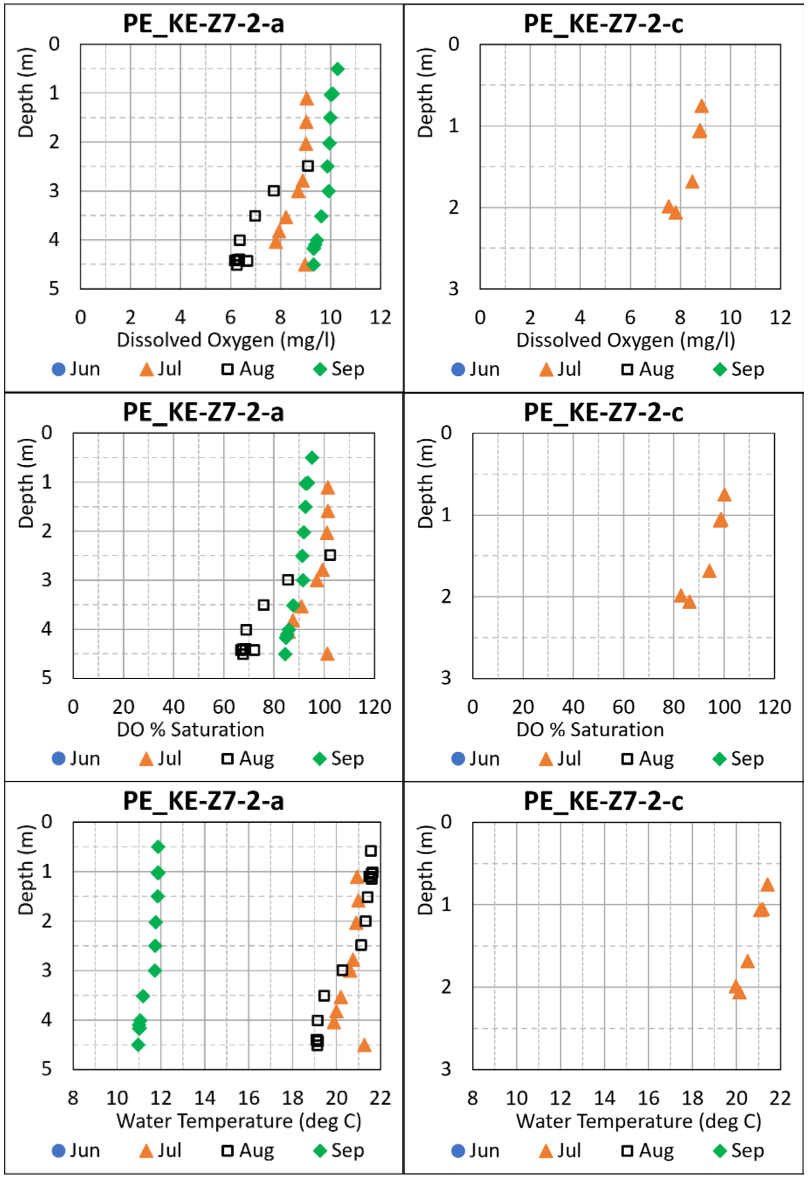
PE_KE-Z7-2-a
Depth (m)
Dissolved Oxygen (mg/l)
Jun Jul Aug Sep
PE_KE-Z7-2-c
Depth (m)
Dissolved Oxygen (mg/l)
Jun Jul Aug Sep
PE_KE-Z7-2-a
Depth (m)
DO % Saturation
Jun Jul Aug Sep
PE_KE-Z7-2-c
Depth (m)
DO % Saturation
Jun Jul Aug Sep
PE_KE-Z7-2-a
Depth (m)
Water Temperature (deg C)
Jun Jul Aug Sep
PE_KE-Z7-2-c
Depth (m)
Water Temperature (deg C)
Jun Jul Aug Sep

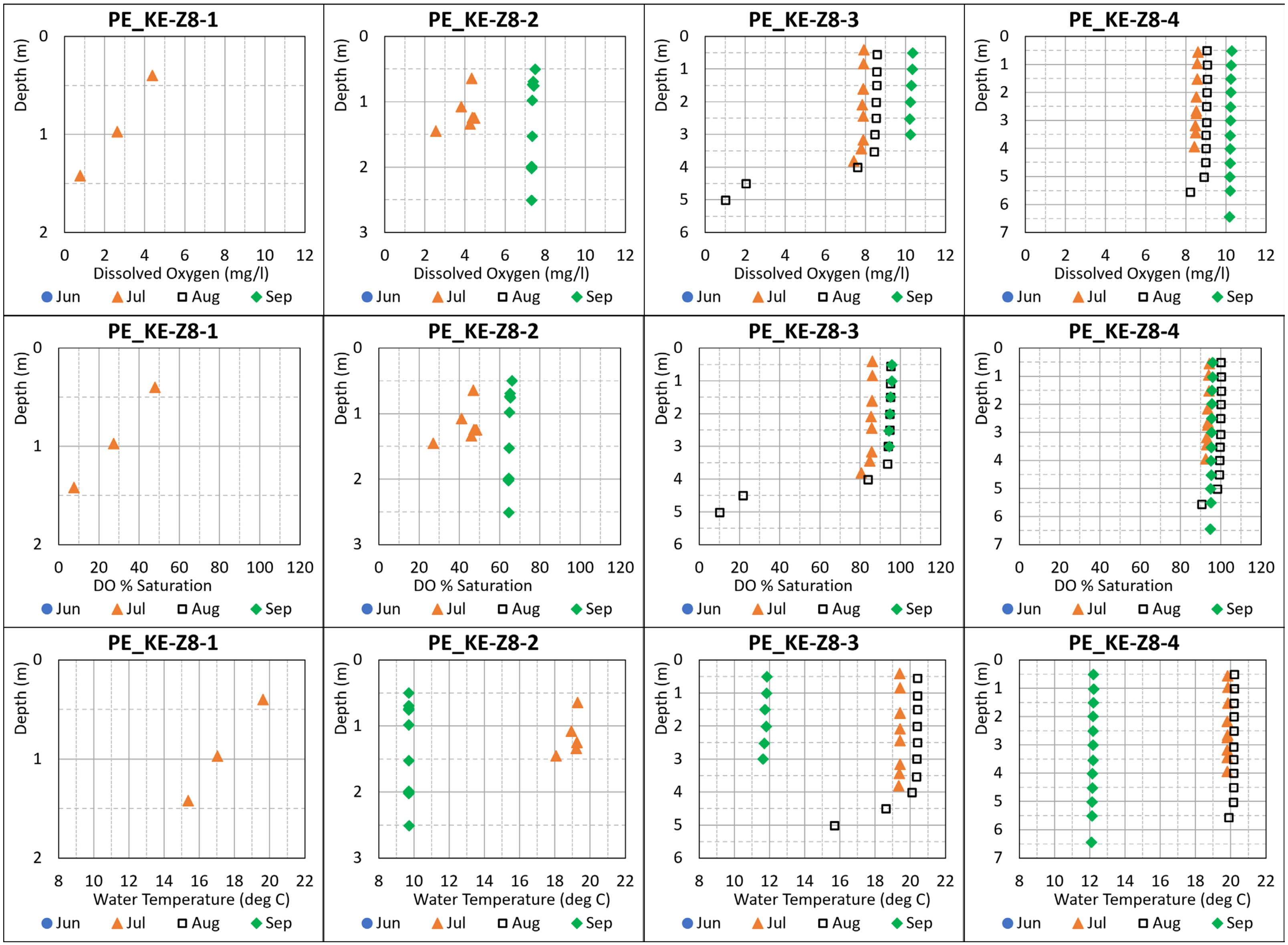
PE_KE-Z8-1
PE_KE-Z8-2
PE_KE-Z8-3
PE_KE-Z8-4
Depth (m)
Dissolved Oxygen (mg/l)
Jun
Jul
Aug
Sep
PE_KE-Z8-1
PE_KE-Z8-2
PE_KE-Z8-3
PE_KE-Z8-4
Depth (m)
DO % Saturation
Jun
Jul
Aug
Sep
PE_KE-Z8-1
PE_KE-Z8-2
PE_KE-Z8-3
PE_KE-Z8-4
Depth (m)
Water Temperature (deg C)
Jun
Jul
Aug
Sep

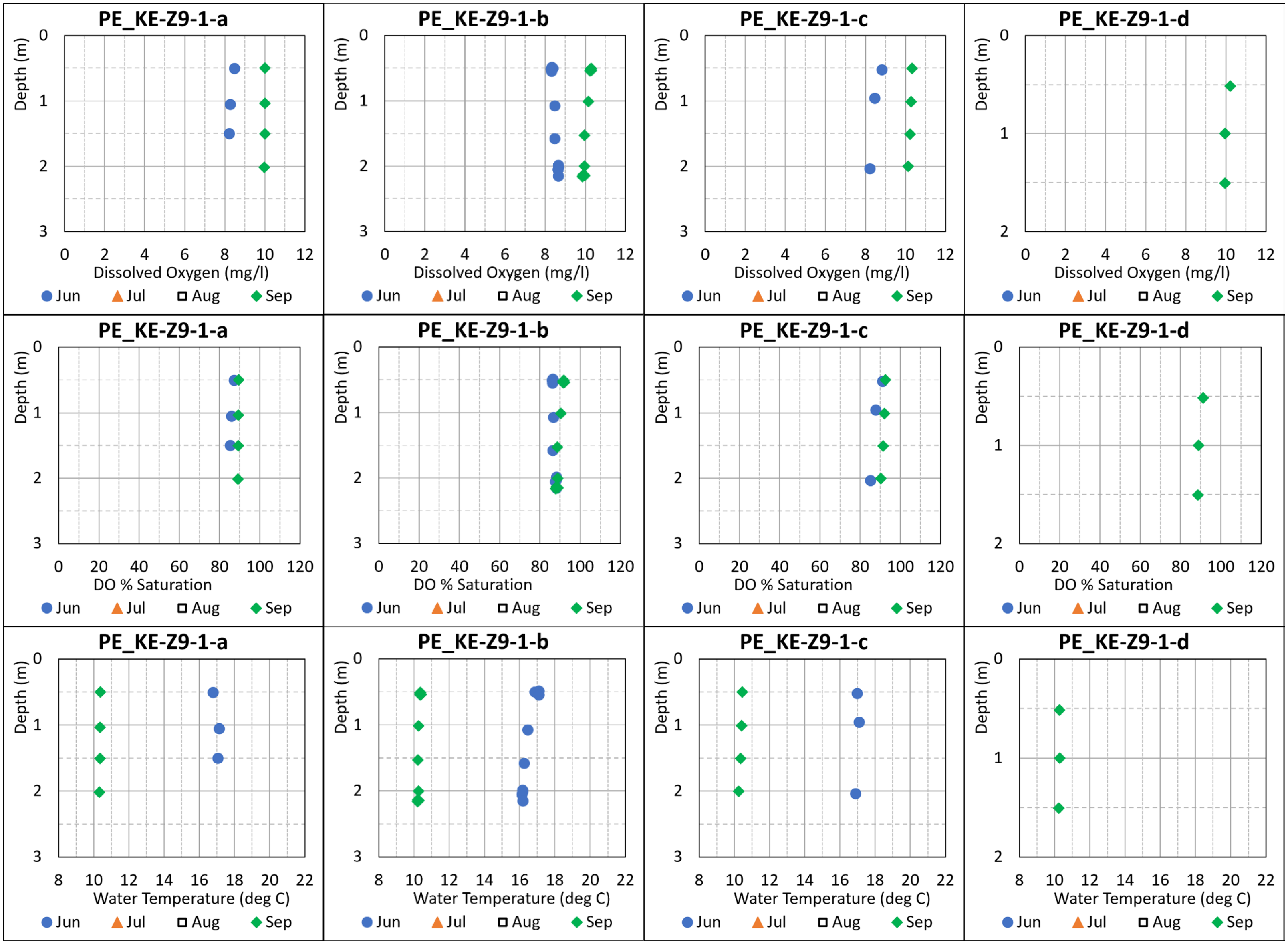

PE_KE-Z9-1-a
PE_KE-Z9-1-b
PE_KE-Z9-1-c
PE_KE-Z9-1-d
Depth (m)
Dissolved Oxygen (mg/l)
DO % Saturation
Water Temperature (deg C)
Jun
Jul
Aug
Sep

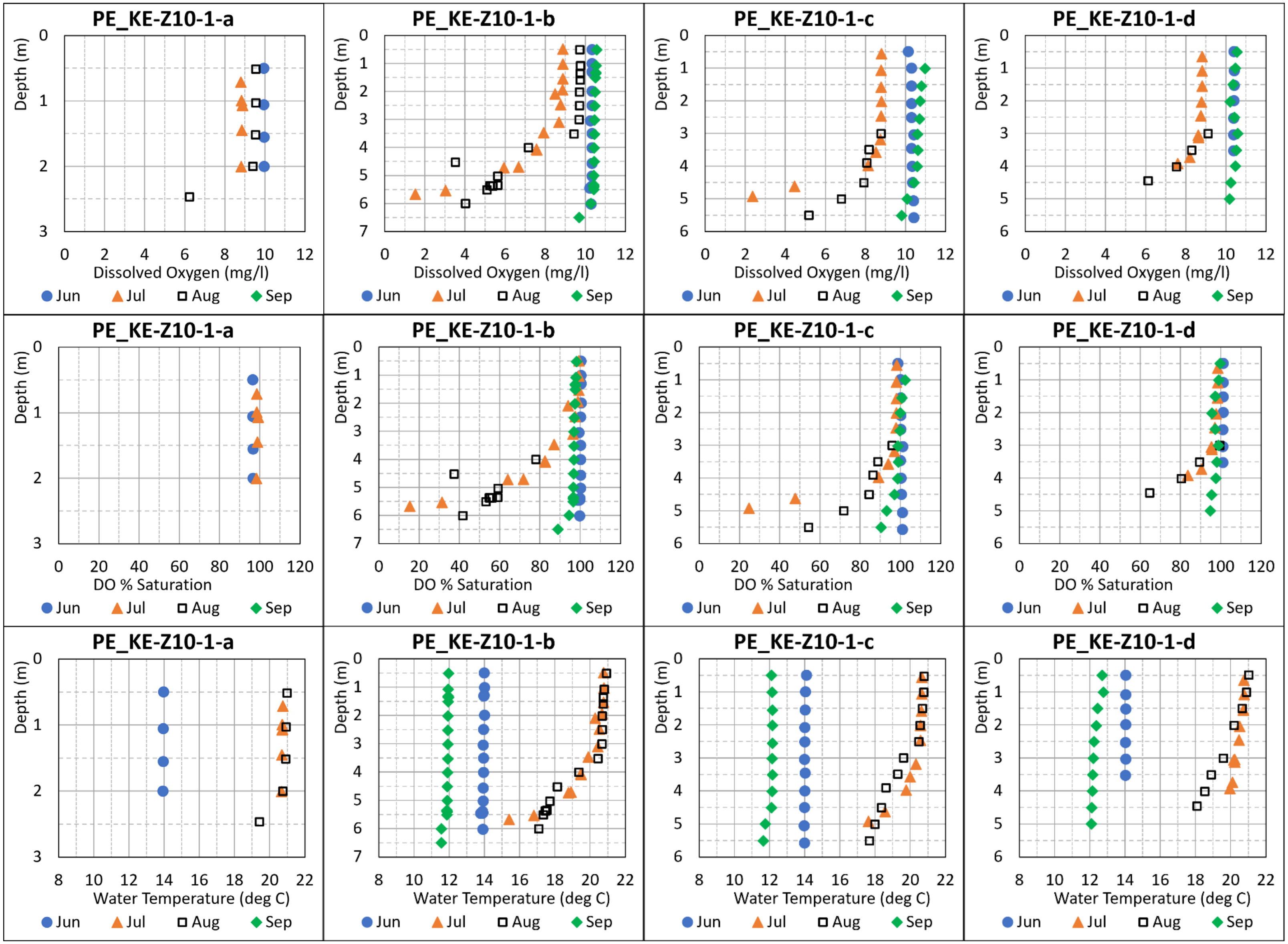
PE_KE-Z10-1-a
PE_KE-Z10-1-b
PE_KE-Z10-1-c
PE_KE-Z10-1-d
Depth (m)
Dissolved Oxygen (mg/l)
DO % Saturation
Water Temperature (deg C)
Jun
Jul
Aug
Sep

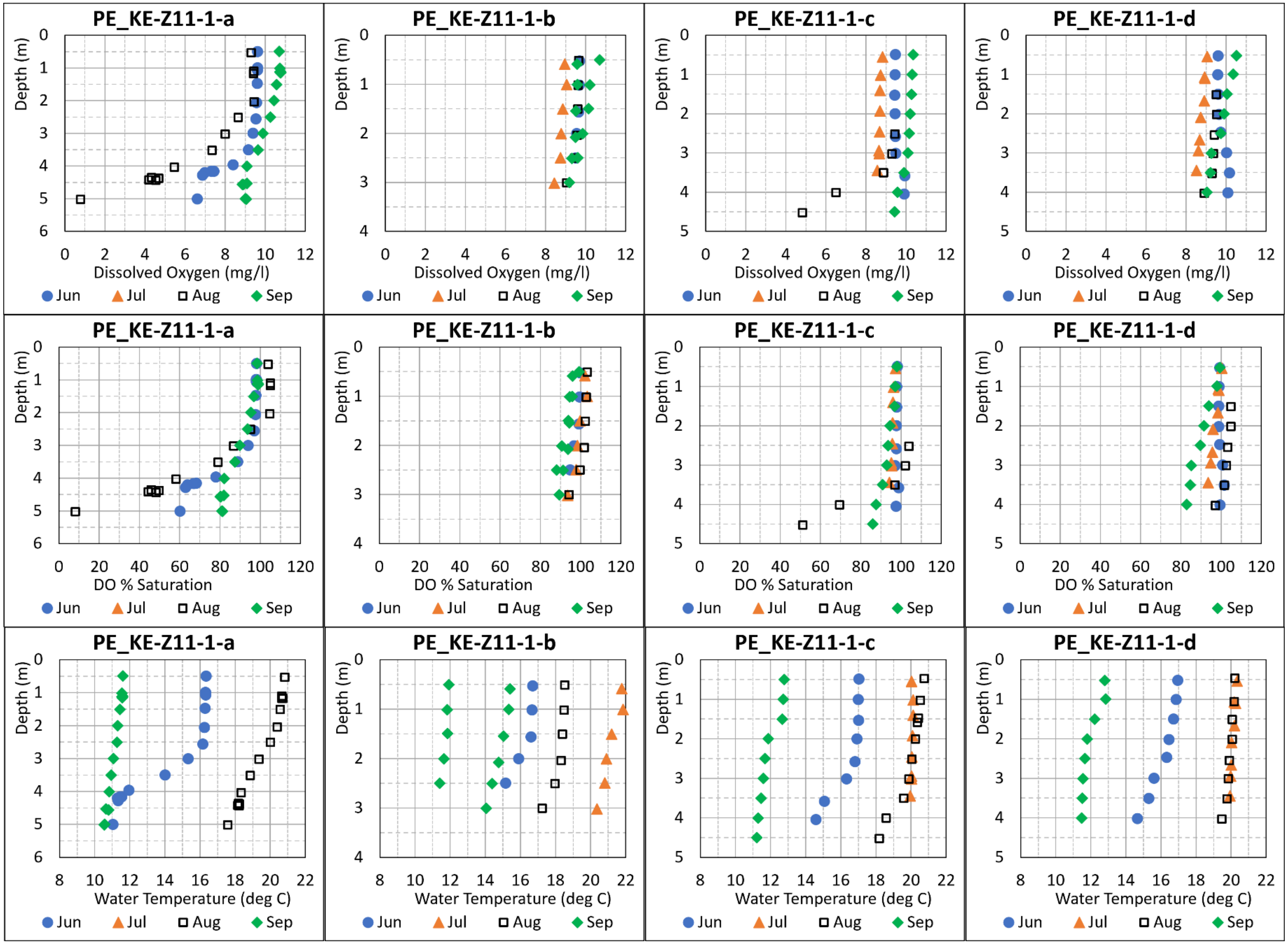
PE_KE-Z11-1-a
PE_KE-Z11-1-b
PE_KE-Z11-1-c
PE_KE-Z11-1-d
Depth (m)
Dissolved Oxygen (mg/l)
DO % Saturation
Water Temperature (deg C)
Jun
Jul
Aug
Sep

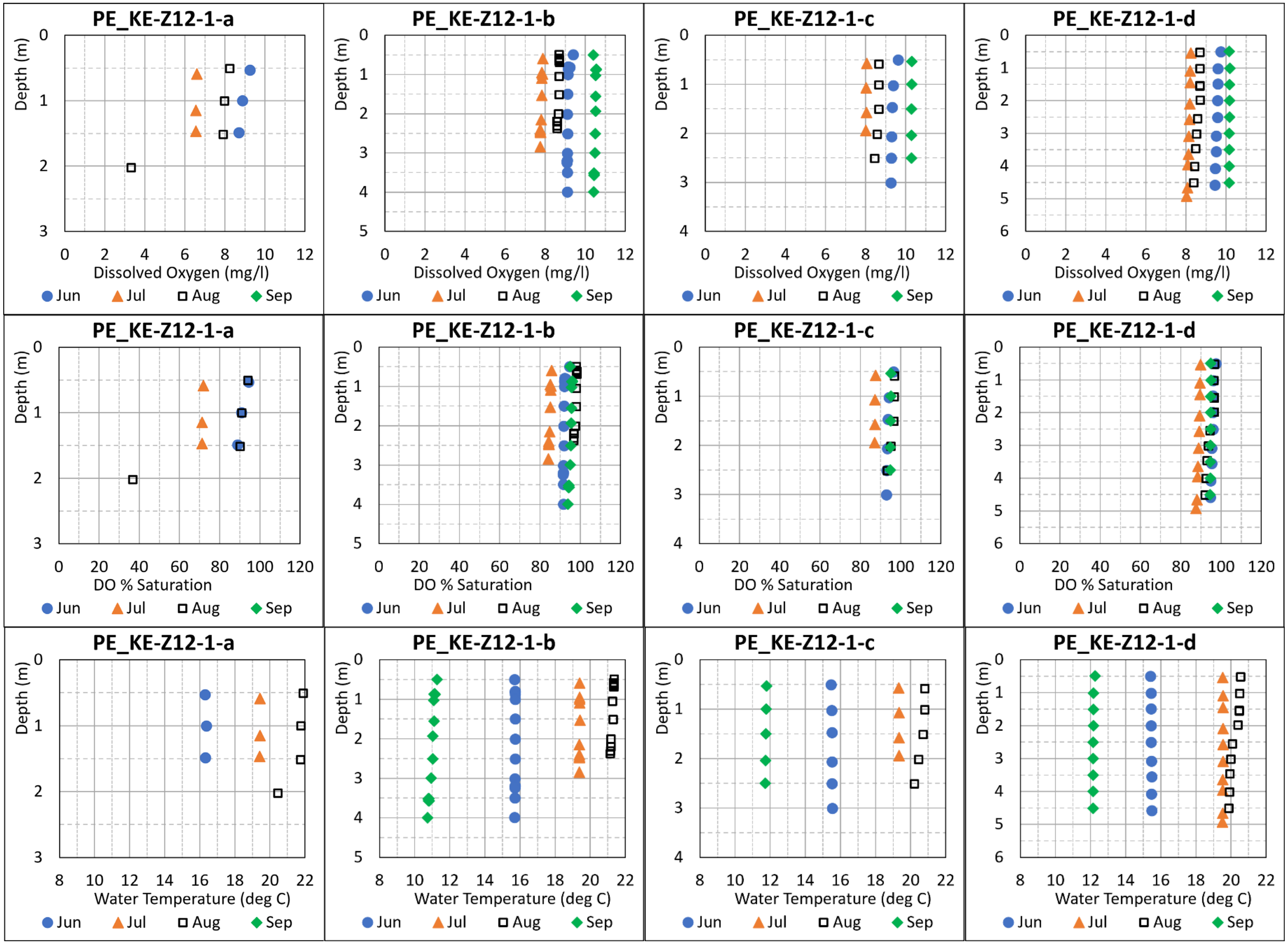
PE_KE-Z12-1-a
PE_KE-Z12-1-b
PE_KE-Z12-1-c
PE_KE-Z12-1-d
Depth (m)
Dissolved Oxygen (mg/l)
DO % Saturation
Water Temperature (deg C)
Jun
Jul
Aug
Sep

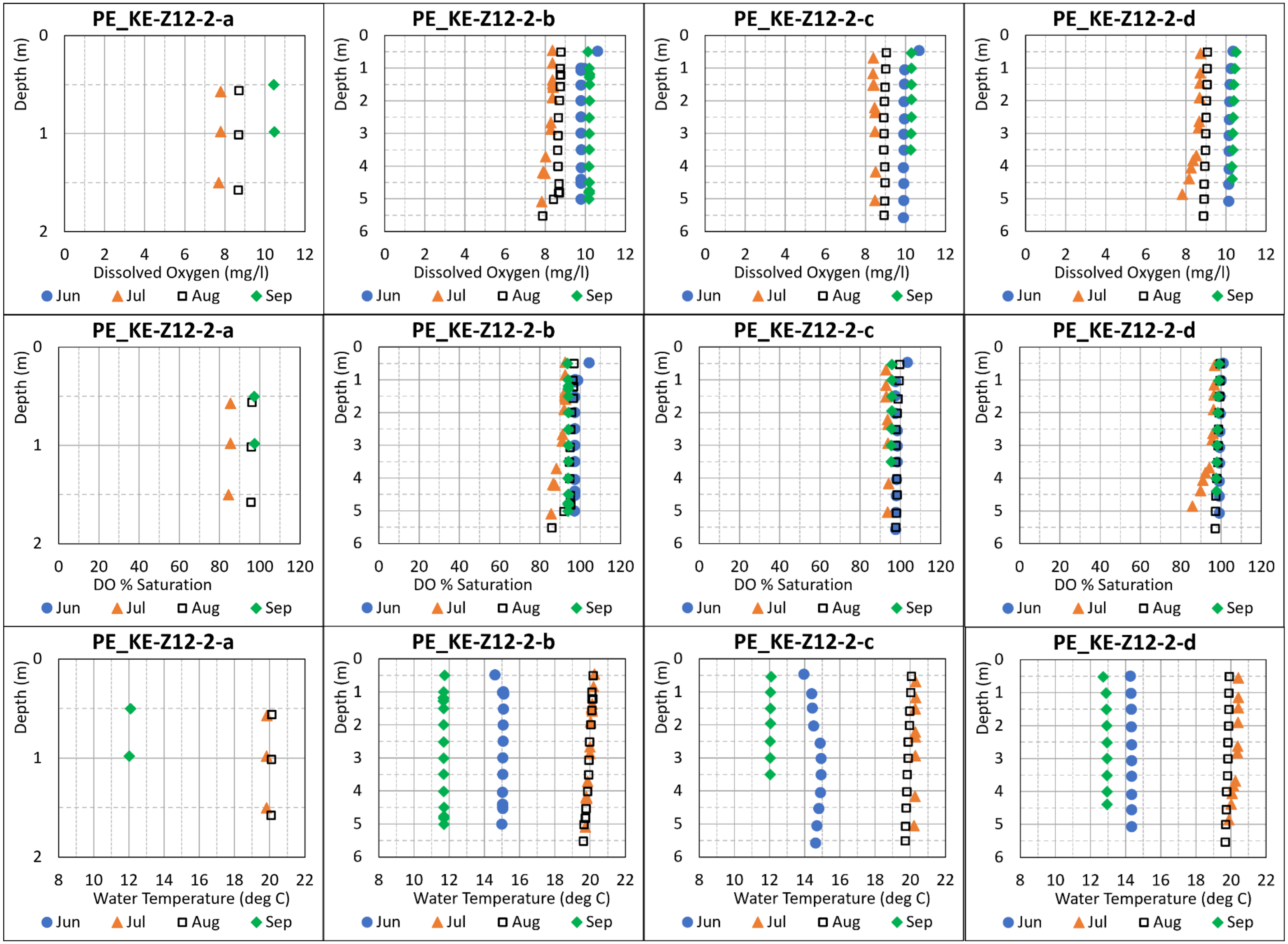
PE_KE-Z12-2-a
PE_KE-Z12-2-b
PE_KE-Z12-2-c
PE_KE-Z12-2-d
Depth (m)
Dissolved Oxygen (mg/l)
DO % Saturation
Water Temperature (deg C)
Jun
Jul
Aug
Sep

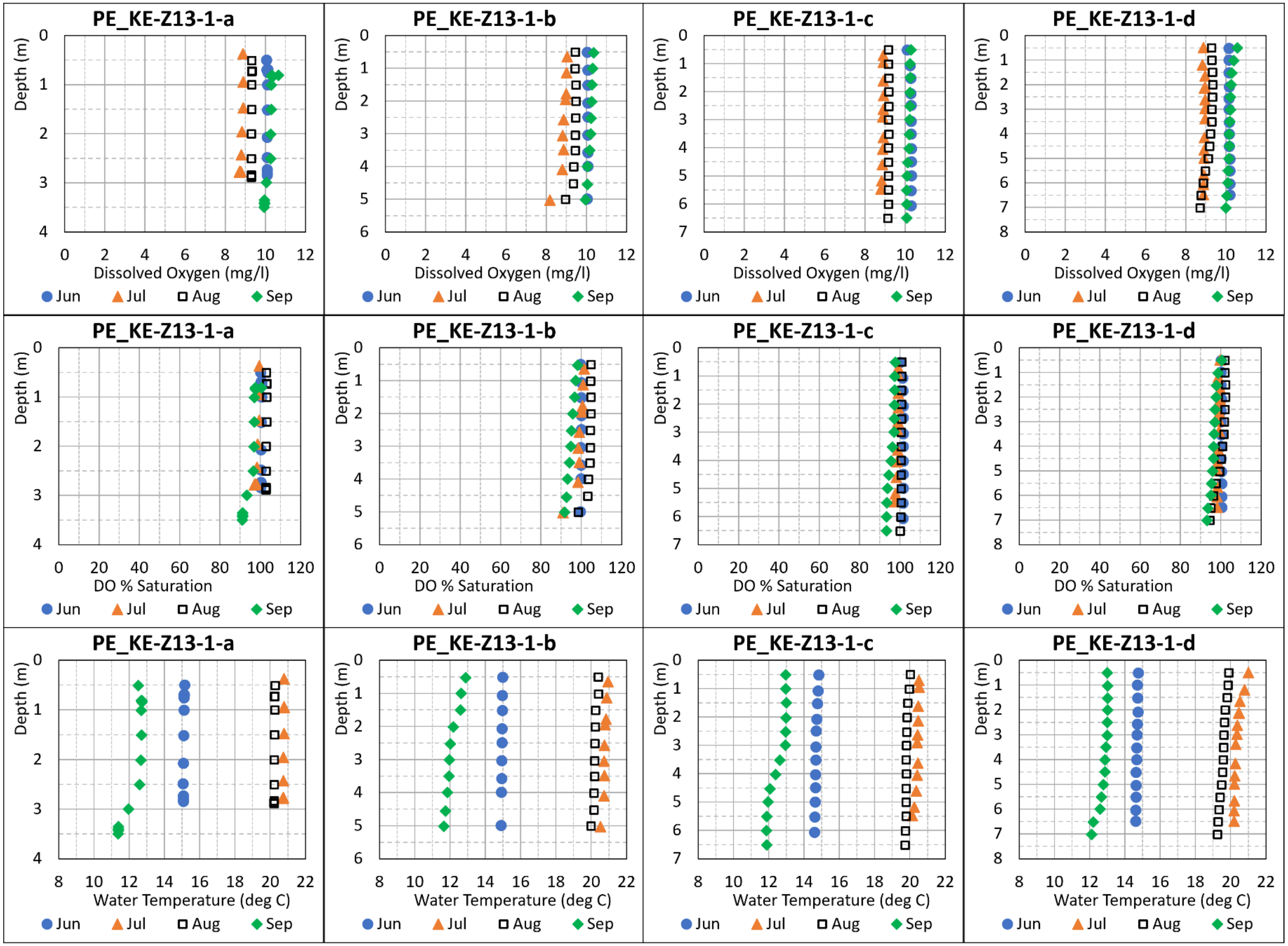
PE_KE-Z13-1-a
PE_KE-Z13-1-b
PE_KE-Z13-1-c
PE_KE-Z13-1-d
Depth (m)
Dissolved Oxygen (mg/l)
DO % Saturation
Water Temperature (deg C)
Jun Jul Aug Sep

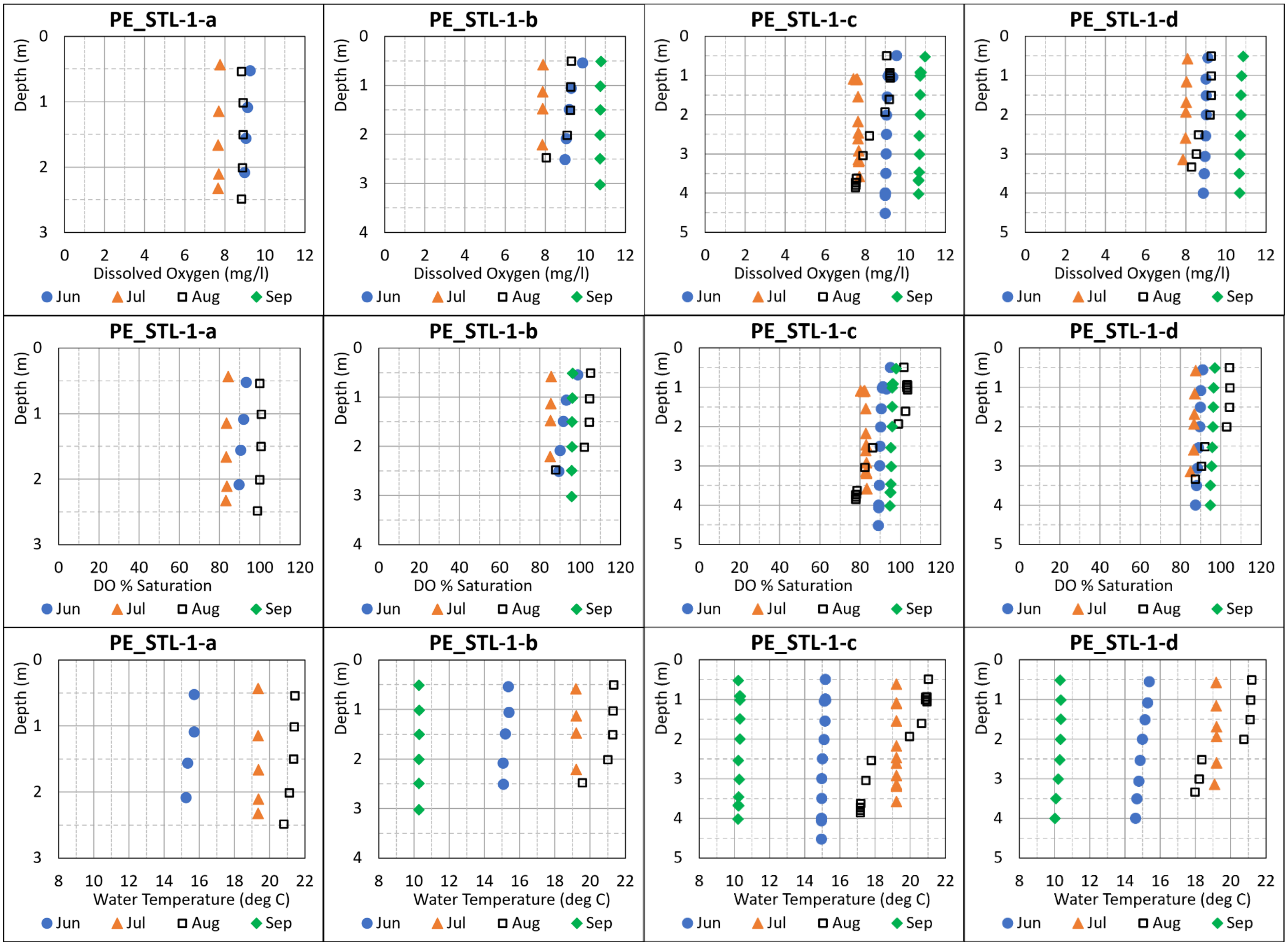
PE_STL-1-a
PE_STL-1-b
PE_STL-1-c
PE_STL-1-d
Depth (m)
Dissolved Oxygen (mg/l)
DO % Saturation
Water Temperature (deg C)
Jun
Jul
Aug
Sep

dsfc

# APPENDIX 4:
# LOCATION OF GREENHOUSE GAS SAMPLING SITES

**Table A4: Site locations for discrete water sampling.**

| Site Name | Latitude | Longitude |
|---|---|---|
| Generating Station | 56.3498 | -95.202 |
| Dike Road Tower | 56.3224 | -95.288 |
| Backbay Tower | 56.2921 | -95.455 |
| PE_CL-1 | 56.2794 | -95.921 |
| PE_CL-2-B | 56.2739 | -95.872 |
| PE_KE-10-C | 56.3416 | -95.263 |
| PE_KE-4-B | 56.3152 | -95.493 |
| PE_KE-6-A | 56.3327 | -95.362 |
| PE_KE-9(-C) | 56.33839 | -95.274 |
| PE_KE_Z11-1-A | 56.30094 | -95.471 |
| PE_KE-Z11-1-B | 56.3039 | -95.47 |
| PE_STL-2-D | 56.3512 | -95.168 |
| PE_STL-3 (PE_STL_4) | 56.3657 | -95.103 |
| PE_STL-5 | 56.3808 | -94.713 |
| PE_KE-5 | 56.3244 | -95.388 |
| Raft | 56.3314 | -95.314 |